Protein Kinase Signalling in *Schistosoma mansoni*

Thesis submitted in fulfilment of the requirement of Kingston University for the degree of Doctor of Philosophy

by

Margarida de Azevedo Gomes de Carvalho Ressurreição

(A project carried out in collaboration with the Natural History Museum, London)

School of Life Sciences
Kingston University
London
2013

IMAGING SERVICES NORTH
Boston Spa, Wetherby
West Yorkshire, LS23 7BQ
www.bl.uk

THESIS CONTAINS

CD

Acknowledgements

Many people helped in the course of the work presented here and contributed to the conclusion of this thesis:

My supervisors Prof. Anthony Walker, Prof. David Rollinson, Dr. Ruth Kirk and Dr. Nigel Page;
My colleagues and friends from the SEC group at Kingston University;
Dr. Aidan Emery, Jayne King and Michael Anderson from the Parasites and Vectors Division of the Natural History Museum;
The NIAID Schistosomiasis Resource Centre;
My friends, parents and brother.

To all I express my deepest gratitude.

Kingston University provided a scholarship for the development of this work.

I dedicate this thesis to my friend Sofia (1987-2009) and to all the neglected people of this world.

Publications and Presentations

Publications

Walker, A.J., **Ressurreição, M.** and Rothermel, R. (2014). Exploring the function of protein kinases in schistosomes: perspectives from the laboratory and from comparative genomics. *Frontiers in Genetics*, (under review)

Ressurreição, M., de Saram, P.S.R., Kirk, R.S., Rollinson, D., Emery, A.M., Page, N.M., Davies, A.J., and Walker, A.J. (2014). Central function for PKC and ERK in movement, attachment, pairing and egg release in the human blood fluke *Schistosoma mansoni*. *PLoS Neglected Tropical Diseases*, (accepted)

de Saram, P.S.R., **Ressurreição, M.**, Davies, A.J., Rollinson, D., Emery, A.M. and Walker, A.J. (2013). Functional mapping of protein kinase A reveals its importance in adult *Schistosoma mansoni* motor activity. *PLoS Neglected Tropical Diseases*, **7** (1), e1988.

Ressurreição, M., Rollinson, D., Emery, A.M. and Walker, A.J. (2011) A role for p38 mitogen-activated protein kinase in early post-embryonic development of *Schistosoma mansoni*. *Molecular and Biochemical Parasitology*, **180**(1), 51-55.

Ressurreição, M., Rollinson, D., Emer, A.M. and Walker, A.J. (2011). A role for p38 MAPK in the regulation of ciliary motion in a eukaryote. *BMC Cell Biology*, **12**(6).

Presentations

British Society of Parasitology Spring meeting, Edinburgh, United Kingdom, April 2009. Protein kinase signalling in *Schistosoma mansoni:* a possible role for p38 MAPK in miracidial swimming. Ressurreição, M., Rollinson, D. and Walker, A.J.

British Society of Parasitology Spring meeting, Nottingham, United Kingdom, April 2011. Protein kinase signalling in *Schistosoma mansoni* during growth and development. Ressurreição, M., Kirk, R.S., Rollinson, D., Page, N.M. and Walker, A.J.

XIth European Multicolloquium of Parasitology (EMOP), Cluj-Napoca, Romania, July 2012. The role of Protein Kinase C and Mitogen-Activated Protein Kinase signalling in host detection, invasion and development of *Schistosoma mansoni.* Ressurreição, M., Kirk, R.S., Rollinson, D., Page, N.M. and Walker, A.J.

Summary

The present study focused on protein kinase C (PKC), extracellular signal-regulated kinase (ERK) and p38 mitogen-activated protein kinase (p38 MAPK) signalling in the human parasite *Schistosoma mansoni*, with a focus on life-stages which are human infective and dependent (cercariae, schistosomules and adult worms). Western blotting with anti-phospho antibodies, detected two phosphorylated PKC (~81 kDa and ~116 kDa) and two phosphorylated ERK (~43 kDa and ~48 kDa) isotypes predicted in the *S. mansoni* genome in addition to the previously identified ~78 kDa PKC and ~42 kDa p38 MAPK (Ludtmann *et al.*, 2009; Ressurreição *et al.*, 2011a,b). Additionally, an unusually large ~132 kDa PKC-like protein was detected that is not predicted in the genome. These proteins possessed enzymatic activities, responded to conventional activators and inhibitors, and their activation profile was dissimilar between life-stages suggesting isotype distinct roles in each developmental stage. *In vitro* challenge with praziquantel stimulated activity of specific PKC and ERK isotypes, showing a putative involvement in the mode of action of this anthelmintic drug. *In situ* localization revealed the activated kinases associated with several regions including tegument, sensory, neuromuscular and reproductive structures; additionally, phosphorylated ERK was associated with the excretory system. PKC, ERK and p38 MAPK function was assessed through pharmacological and environmental assays. PKC and ERK were found to play a role in pairing, motility, ventral sucker attachment and egg output of adult worms and motility of schistosomules. Maintenance of unpaired adult worms in different sex ratio environments resulted in changes in PKC, ERK and p38 MAPK activity (both in male and females) showing importance in transduction of chemotatic and/or thigmotatic stimuli. Light and temperature changes affected kinase activity in cercariae mainly at the cercariae sensory papillae and parasite surface. Moreover, combined linoleic acid (LA) and CFDA-SE based assays developed for induction and monitoring of cercarial gland release showed that PKC, ERK and p38 MAPK are involved in mechanisms that underpin cercariae host detection/penetration and that pharmacological inhibition of these enzymes partially blocked LA induced release, while the PKC activator accelerated it. In schistosomules, epidermal growth factor and insulin stimulated ERK and PKC activity whereas insulin-like growth factor I and mouse red blood cells up-regulated PKC activity only suggesting association with parasite nutrition and host-parasite communication. Internalization of fluorescently labelled transferrin *via* the schistosomule tegument was delayed with PKC inhibitors suggesting a role in transferrin uptake. Taken together, these data contribute significantly to our understanding of cell signalling in schistosomes and how such signalling regulates parasite function, and should open up new avenues of investigation for development of anti-schistosome drugs.

List of Contents

Chapter 1 – General Introduction 1

1.1 - Schistosomiasis, a disease of developing countries 2

1.1.1 - Epidemiology and prevalence 2

1.1.2 - Pathology and control strategies 2

1.1.2.1 – Praziquantel - mechanism of action..... 4

1.1.2.2 – Praziquantel - present problems..... 4

1.1.3 – The future of schistosomiasis control and treatment..... 5

1.2 – The complex life-cycle of *Schistosoma mansoni*..... 7

1.2.1 – Miracidium biology 11

1.2.2 – Sporocyst biology 12

1.2.3 – Cercariae biology 13

1.2.3.1 – Morphological characteristics..... 14

1.2.3.2 – Behavioural characteristics..... 16

1.2.4 –Schistosomule biology..... 17

1.2.5 –Adult worm biology..... 18

1.3– Eukaryotic Protein Kinases (ePKs)..... 21

1.4 – Protein kinases in schistosomes 22

1.5 – Protein Kinase C (PKC) family..... 29

1.5.1 – PKC structure..... 30

1.5.2 – Conventional/classical PKC (cPKC)..... 31

1.5.3 – Novel PKC (nPKC)..... 32

1.5.4 – Atypical PKC (aPKC)..... 32

1.5.5 – PRK..... 32

1.5.6 – Protein kinase D or mouse PKCμ, the not so real PKC..... 32

1.5.7 – PKC maturation/activation..... 33

1.5.8 – Roles for PKCs, particularly in lower organisms..... 35

1.6 – Mitogen-Activated Protein Kinases (MAPKs)..... 37

1.6.1 – Stress-Activated Protein Kinases/c-Jun amino-terminal Kinases (SAPK/JNK) 39

1.6.2 – Extracellular-signal Regulated Kinase (ERK)..... 39

1.6.3– p38 Mitogen-Activated Protein Kinase (p38 MAPK)..... 41

1.7 – Context of this study and aims of the research..... 43

Chapter 2 – General Materials and Methods 45

2.1 – Antibodies and reagents..... 46

2.1.1 - Antibodies 46

2.1.2 – Immunoprecipitation kits and other components..... 46

2.1.3 – Inhibitors and activators..... 46

2.1.4 – Other products and reagents..... 47

2.1.5 – RT-qPCR and siRNA materials..... 47

2.2 – Ethics statement..... 48

2.3 – Maintenance of *S. mansoni* life-cycle..... 48

2.3.1 – Safety procedure for handling of cercariae and other infective material..... 49

2.4 – Isolation of *S. mansoni* for experimentation..... 49

2.4.1 – Adult worm pairs..... 49

2.4.2 – Cercariae..... 50

2.4.3 – Schistosomules..... 50

2.5 – Western blotting..... 51

2.6 – Immunohistochemistry and confocal microscopy..... 52

2.7 – Pharmalogical treatments 53
2.8 – Video imaging and analysis..... 54
2.9 – Statistical methods..... 54
2.10 – Bioinformatics..... 54

Chapter 3 – Initial Immunodetection Studies 56
3.1 – Introduction..... 57
3.2 – Materials and Methods..... 59
3.3 – Results..... 61
3.3.1 – Antibody immunoreactivity profile against *S. mansoni* adult worm protein extracts..... 61
3.3.2 – Putative identities of the detected proteins..... 63
3.3.3 – Detection of phosphorylated ERKs and PKCs in different *S. mansoni* life-stages..... 65
3.4 – Discussion..... 68

Chapter 4 – PKC and ERK Signalling in Adult *Schistosoma mansoni* 74
4.1- Introduction..... 75
4.2 – Materials and Methods..... 76
4.3 – Results..... 79
4.3.1 – *S. mansoni* PKC-like proteins are modulated by a PKC activator and inhibitor and have PKC activity..... 79
4.3.2 –*S. mansoni* ERK-like proteins have ERK activity and are inhibited by a MEK/ERK inhibitor..... 81
4.3.3 – *S. mansoni* ERK and PKC signalling is interconnected..... 82
4.3.4 – *In situ* localization of active PKC and ERK in adult *S. mansoni*..... 83
4.3.5 – Pharmacological modulation of PKC and ERK induces physiological disturbances in adult *S. mansoni* 86
4.3.6 – Praziquantel (PZQ) induces activation of *S. mansoni* PKC and ERK, *in vitro*..... 93
4.4 – Discussion..... 96

Chapter 5 – Insights into PKC, ERK and p38 MAPK signalling during *S. mansoni* female-male interactions 103

5.1 – Introduction..... 104
5.2 – Materials and Methods..... 107
5.3 – Results..... 108
5.3.1 – Effect of different sex ratios on the phosphorylation of PKC, ERK and p38 MAPK in male and female *S. mansoni in vitro*..... 108
5.3.1.1 – Activation of PKC..... 108
5.3.1.2 – Activation of ERK 113
5.3.1.3 – Activation of p38MAPK 115
5.3.2 – Effect of different sex ratios on the phosphorylation status of putative PKC substrates in male and female *S. mansoni in vitro*..... 117
5.4 – Discussion..... 118

Chapter 6 – Insights into PKC, ERK and p38 MAPK signalling during linoleic acid-induced release of cercarial acetabular gland contents 124

6.1 – Introduction..... 125
6.2 – Materials and Methods..... 127
6.3 – Results..... 130
6.3.1 – LA induces release of acetabular gland components labelled with

CFDA-SE..... 130
6.3.2 – Cercarial PKC and ERK activity changes during LA challenge, but not p38 MAPK..... 130
6.3.3 – Cercariae PKC, ERK and p38 MAPK activity is blocked by GF109203X, U0126, and SB203580..... 140
6.3.4 – Modulation of PKC, ERK and p38 MAPK activity affects acetabular gland release..... 140
6.3.5 – Inhibition of PKC, ERK and p38 MAPK affects cercariae behavior..... 143
6.4 – Discussion..... 145

Chapter 7 – Involvement of PKC and MAPK signalling in *S. mansoni* cercariae thermokinesis and photokinesis 152

7.1 – Introduction..... 153
7.2 – Materials and Methods..... 156
7.3 – Results..... 158
7.3.1 – Phosphorylation status of *S. mansoni* cercaria PKC, ERK and p38 MAPK is affected by different light and temperature conditions..... 158
7.3.1.1 – PKC activation..... 160
7.3.1.2 – ERK activation..... 163
7.3.1.3 – p38 MAPK activation..... 166
7.3.2 – Effects of light intensity on the phosphorylation of PKC, ERK and p38 MAPK from the detached tails of cercariae..... 169
7.4 – Discussion..... 173

Chapter 8 – Investigation of PKC and MAPK signalling during *in vitro* development of *S. mansoni* schistosomules 179

8.1 – Introduction..... 180
8.2 – Materials and Methods..... 184
8.3 – Results..... 193
8.3.1 – Phosphorylation of PKC, ERK and p38 MAPK in *S. mansoni* schistosomules..... 193
8.3.2 – Effect of human EGF on schistosomule PKC and ERK phosphorylation..... 200
8.3.3 – Effect of INS on schistosomules PKC and ERK phosphorylation..... 201
8.3.4 – Human IGF-I increases activation of ~116 kDa PKC..... 204
8.3.5 – Addition of erythrocytes to cultured schistosomules increases PKC and p38 MAPK phosphorylation..... 205
8.3.6 – PKC appears to be involved in regulation of transferrin uptake in schistosomules..... 207
8.3.7 – Modulation of PKC, ERK and p38 MAPK activity significantly affects viability, morphology and movement of schistosomules..... 207
8.3.7.1 – Effects of PKC inhibition and activation..... 209
8.3.7.2 – Effects of ERK pharmacological inhibition of activity..... 210
8.3.7.3 – Effects of pharmacological inhibition of p38 MAPK activity... 210
8.3.8 – RNA interference of PKC and ERK expression in cultured schistosomules..... 216
8.3.8.1 – Detection of gene expression..... 217
8.3.8.2 – Knockdown and selection of most effective siRNAs..... 217

8.3.8.3 – Effects of PKC Sm176360 and ERK Sm1047900 knockdown on viability, morphology and movement of schistosomules 219
8.4 – Discussion 220

Chapter 9 – Final Conclusions 228

References 234

Appendix 254
Appendix A
Recipe for Basch's medium 255
Appendix B
Effects on egg output, pairing and ventral sucker attachment observed in *S. mansoni* adult worms after exposure to GF109203X, PMA and U0126 256
Effects on sustained coiling observed in *S. mansoni* adult worms after exposure to GF109203X, PMA and U0126 257
Effects on movement observed in *S. mansoni* adult worms after exposure to GF109203X, PMA and U0126 258
Appendix C
Screen shot of the "wrMTrck" plug-in parameters used for video analysis of *S. mansoni* schistosomules 259
Sequences of siRNAs 260
Sequences of primers used for qPCR 260

List of Figures

Figure 1.1 - The global distribution of schistosomiasis as of 2011 3

Figure 1.2 - Structure of current anti-schistosomal drugs and experimental therapeutics 6

Figure 1.3 - The *S. mansoni* life-cycle 8

Figure 1.4 - Line drawing depicting the morphology of an *S. mansoni* miracidum 12

Figure 1.5 - Schematic diagram depicting the morphology of *S. mansoni* sporocysts 13

Figure 1.6 - Schematic diagram depicting the morphology of *S. mansoni* cercariae 14

Figure 1.7 - Schematic diagram of an *S. mansoni* adult worm and egg 19

Figure 1.8 - The *S. mansoni* MAPK and PKC signalling pathway 25

Figure 1.9 - The primary structure of conventional, normal and atypical PKCs (cPKC, nPKC, aPKC, respectively) 30

Figure 1.10 - PKC activation in mammalian systems 34

Figure 1.11 - The expansion of the PKC family 36

Figure 1.12 - The MAPK signalling cascade 38

Figure 3.1 - Western blot demonstrating the detection profiles of different phospho-specific antibodies screened against *S. mansoni* adult worm total proteins 61

Figure 3.2 - Alignment of antibody recognition sites 64

Figure 3.3 - Phosphorylated PKC- and ERK-like proteins in four different life-stages of *S. mansoni* 66

Figure 4.1 - *In vitro* pharmacological inhibition and activation of *S. mansoni* adult worm PKC-like proteins 80

Figure 4.2 – PKC activity of adult *S. mansoni* proteins immunoprecipitated with anti-phospho PKC antibodies 80

Figure 4.3 - *S. mansoni* ERK-like proteins are phosphorylated (activated) by MEK and possess characteristic ERK activity 81

Figure 4.4 - Phosphorylation of *S. mansoni* ERK and PKCs following treatment with PMA, GF109203X or U0126 82

Figure 4.5 - Representative confocal micrograph of negative control of *S. mansoni* adult worm pair probed without primary antibodies but with Alexa Fluor 488 secondary antibodies 83

Figure 4.6 - Immunolocalization of phosphorylated (activated) PKC and ERK on intact paired adult *S. mansoni* 84

Figure 4.7 - Immunolocalization of phosphorylated (activated) PKC and ERK in PMA treated adult *S. mansoni* 85

Figure 4.8 - Effects of U0126 on adult *S. mansoni* worm uncoupling, egg output and ventral sucker attachment in vitro over 96 h 88

Figure 4.9 - Effects of GF109203X and PMA on adult *S. mansoni* worm uncoupling, egg output and ventral sucker attachment in vitro over 96 h 89

Figure 4.10 – Effects of GF109203X, PMA and U0126 on movement of adult S. mansoni in vitro over 96 h 90

Figure 4.11 - Persistent coiling effect in adult *S. mansoni* pairs exposed *in vitro* for 96 hours to GF109203X or PMA 91

Figure 4.12 - Immunoblot analysis of the phosphorylation status of *S. mansoni* ERK and PKC following challenge with PZQ 94

Figure 4.13 - Immunolocalization of phosphorylated (activated) PKC and ERK in intact adult *S. mansoni* after exposure to PZQ 95

Figure 5.1 - Western blots showing phosphorylated *S. mansoni* PKC, ERK and p38 MAPK of immature male worms and adult male or female worms experiencing different sex ratios, *in vitro*..... 108

Figure 5.2 - Relative changes in *S. mansoni* PKC, ERK and p38 MAPK phosphorylation when experiencing different sex ratios 109

Figure 5.3 - *In situ* localization of phosphorylated PKC detected with anti-phospho PKC (Ser660) antibodies in unpaired adult male and female *S. mansoni* 111

Figure 5.4 - *In situ* localization of phosphorylated PKC detected with anti-phospho PKC (Thr410) antibodies in unpaired adult male and female *S. mansoni* 112

Figure 5.5 - *In situ* localization of phosphorylated ERK detected with anti-phospho ERK 1/2 antibodies in unpaired adult male and female *S. mansoni* 114

Figure 5.6 - *In situ* localization of phosphorylated p38 MAPK detected with anti-phospho p38 MAPK antibodies in unpaired adult male and female *S. mansoni* 116

Figure 5.7 - Western blot showing phosphorylated PKC substrate proteins of adult male and female *S. mansoni* experiencing different sex ratios, *in vitro*..... 117

Figure 6.1 - Detection of acetabular gland components released from CFDA-SE labelled cercariae with or without linoleic acid (LA)..... 131

Figure 6.2 - Visual representation of acetabular gland components remaining inside *S. mansoni* cercariae at different duration after exposure, or not, of linoleic acid 131

Figure 6.3 – Immunodetection of phosphorylated PKC, ERK and p38 MAPK during exposure of *S. mansoni* cercariae to linoleic acid (LA)..... 133

Figure 6.4 - Negative control of *in situ* localization of activated kinases in *S. mansoni* cercariae..... 134

Figure 6.5 - *In situ* localization of phosphorylated PKC using the anti-phospho PKC (Thr410) antibodies during exposure of cercariae to linoleic acid (LA) over time..... 135

Figure 6.6 - *In situ* localization of phosphorylated PKC using the anti-phospho PKC (Ser660) antibodies during exposure of cercariae to linoleic acid (LA) over time..... 136

Figure 6.7 - *In situ* localization of phosphorylated ERK with anti-phospho (ERK 1/2) primary mAb during exposure of cercariae to linoleic acid (LA) over time..... 138

Figure 6.8 - *In situ* localization of phosphorylated p38 MAPK with anti-phospho p38 MAPK antibodies during exposure of cercariae to linoleic acid (LA) over time 139

Figure 6.9 - Immunodetection of phosphorylated PKC, ERK and p38 MAPK following incubation of *S. mansoni* cercariae with GF109203X, U0126, or SB203580 141

Figure 6.10 – Release of acetabular gland components from CFDA-SE labelled cercariae in response to linoleic acid (LA) in the presence of GF109203X, PMA, U0126 or SB 203580..... 141

Figure 6.11 - Detection of CFDA-SE-labelled acetabular gland components remaining in cercariae after 120 minutes exposure to linoleic acid (LA) in the presence GF109203X, U0126, PMA and SB203580 and vehicle control (DMSO)..... 143

Figure 7.1 – Effect of different temperature and light intensity regimes on PKC, ERK and p38 MAPK phosphorylation in *S. mansoni* cercariae..... 158

Figure 7.2 - Relative change in PKC phosphorylation in *S. mansoni* cercariae maintained at different temperature and light intensity regimes..... 159

Figure 7.3 - *In situ* localization of activated PKC (Thr410) in *S. mansoni* cercariae maintained in different temperature and illumination conditions..... 161

Figure 7.4 - *In situ* localization of activated PKC (Ser660) in *S. mansoni* cercariae

maintained in different temperature and illumination conditions..... 162

Figure 7.5 - Relative change in ERK phosphorylation of *S. mansoni* cercariae maintained at different temperature and light intensity regimes..... 164

Figure 7.6 - *In situ* localization of activated ERK in *S. mansoni* cercariae maintained in different temperature and illumination conditions..... 165

Figure 7.7 - Relative change in p38 MAPK phosphorylation of *S. mansoni* cercariae maintained at different temperature and light intensity regimes..... 167

Figure 7.8 - *In situ* localization of activated p38 MAPK in *S. mansoni* cercariae maintained in different temperature and illumination conditions..... 168

Figure 7.9 - Immunodetection of PKC and ERK phosphorylation in cercariae tails maintained in the dark or under intense illumination for 1 min..... 170

Figure 7.10 - *In situ* localization of phosphorylated PKC in detached *S. mansoni* cercariae tails maintained in the dark or under intense illumination for 1 min..... 171

Figure 7.11 - *In situ* localization of phosphorylated ERK in detached *S. mansoni* cercariae tails maintained in the dark or under intense illumination for 1 min..... 172

Figure 8.1 - Phosphorylation of *S. mansoni* schistosomule PKCs, ERKs and p38 MAPK over time in culture..... 194

Figure 8.2 - Representative confocal micrograph of negative control *S. mansoni* schistosomules pored without primary antibodies but with Alexa Fluor 488 secondary antibodies..... 194

Figure 8.3 – *In situ* localization of phosphorylated PKC in intact *S. mansoni* schistosomules during culture detected with anti-phospho PKC (Ser660) antibodies... 195

Figure 8.4 - *In situ* localization of phosphorylated PKC in intact *S. mansoni* schistosomules during culture detected with anti-phospho PKC (Thr410) antibodies... 196

Figure 8.5 - *In situ* localization of phosphorylated ERK in intact *S. mansoni* schistosomules during culture detected with anti-phospho ERK 1/2 antibodies 198

Figure 8.6 - *In situ* localization of phosphorylated p38 MAPK in intact *S. mansoni* schistosomules during culture detected with anti-phospho p38 MAPK antibodies..... 199

Figure 8.7 - Phosphorylation of PKCs, ERKs and p38 MPAK in 72 h *S. mansoni* schistosomules in the presence of human EGF (15ng/ml)..... 200

Figure 8.8 – *In situ* localization of phosphorylated PKC and ERK in 72 h *S. mansoni* schistosomules in the presence of human EGF (15ng/ml)..... 201

Figure 8.9 – Phosphorylation of PKCs, ERKs and p38 MAPK in 72 h *S. mansoni* schistosomules in the presence of human INS (1μM) 202

Figure 8.10 – *In situ* localization of phosphorylated PKC in 72 h *S. mansoni* schistosomules in the presence of human INS (1μM) 203

Figure 8.11 – *In situ* localization of phosphorylated ERK in 72 h *S. mansoni* schistosomules in the presence of human INS (1μM) 203

Figure 8.12 – Effect of human IGF-I (15ng/ml) on ~116 kDa PKC phosphorylation in 72 h *S. mansoni* schistosomules 204

Figure 8.13 – Phosphorylation of PKC, ERK and p38 MAPK in cultured *S. mansoni* schistosomules before and after adding red blood cells 205

Figure 8.13 – Phosphorylation of PKC, ERK and p38 MAPK in cultured *S. mansoni* schistosomules before and after adding red blood cells 205

Figure 8.14 – *In situ* localization of PKC activation in 5 day *S. mansoni* schistosomules in the presence of murine red blood cells 206

Figure 8.15 – Effect of GF109203X on transferrin uptake by *S. mansoni* schistosomules 207

Figure 8.16 – Brightfield micrographs of phenotypes observed in cultured *S. mansoni* schistosomules during pharmacological assays..... 208

Figure 8.17 – Various phenotypes observed in cultured S. mansoni schistosomules under the different pharmacological treatments for 24 h 211

Figure 8.18 – Effects of various concentration of GF109203X on schistosomules standard deviation of perimeter, area and length at 2, 24 and 48 h..... 212

Figure 8.19 – Effects of various concentration of PMA on schistosomules standard deviation of perimeter, area and length at 2, 24 and 48 h..... 213

Figure 8.20 – Effects of various concentration of U0126 on schistosomules standard deviation of perimeter, area and length at 2, 24 and 48 h..... 214

Figure 8.21 – Effects of various concentration of SB203580 on schistosomules standard deviation of perimeter, area and length at 2, 24 and 48 h..... 215

Figure 8.22 – Schistosomule viability at 48 h in various treatments from fluorescent measurement after dual FDA and PI staining..... 216

Figure 8.23 – PKC and ERK gene expression in schistosomules..... 217

Figure 8.24 – Effects of PKC and ERK expression knockdown in schistosomules with siRNA..... 218

List of Tables

Table 1.1 - Key examples of signal transduction protein/receptors identified in *Schistosoma mansoni* list in chronological order..... 24

Table 3.1 – Putative identities of immunodetected proteins..... 64

Table 7.1 – The various temperature and light regiment applied to recently-emerged *S. mansoni* cercariae..... 204

List of Videos

Video 4.1 - Control *S. mansoni* couples *in vitro* over 96 h in RPMI-1640..... 86/CD

Video 4.2 - Effects of U0126 on *S. mansoni* couples *in vitro* over 96 h..... 87/CD

Video 4.3 - Effects of GF109203X on *S. mansoni* couples *in vitro* over 96 h..... 92/CD

Video 4.4 – Effects of PMA on *S. mansoni* couples *in vitro* over 96 h..... 92/CD

Video 4.5 - Effect of 1 h GF109203X in coiling and blood regurgitation on *S. mansoni* couples *in vitro* 93/CD

Video 6.1 - Untreated *S. mansoni* cercariae 143/CD

Video 6.2 - Effect of LA on *S. mansoni* cercariae 143/CD

Video 6.3 - Effects of GF109203X, PMA, U0126 or SB 203580 on *S. mansoni* cercariae 143/CD

Video 6.4 - Effects of GF109203X, PMA, U0126 or SB 203580 on *S. mansoni* cercariae in the presence of LA..... 144/CD

List of Abbreviations

aPKC	aPKC atypical protein kinase C
ATP	adenosine triphosphate
BME	Eagle basal medium
BSA	bovine serum albumin
CaBP	calcium-binding protein
CAMK	calcium/calmodulin regulated kinase
cAMP	3'-5'-cyclic adenosine monophosphate
CFDA-SE	carboxyfluorescein diacetate succinimidyl ester
CK1	cell kinase I
cm, mm, µm	centimeter, millimeter, micrometer
cPKC	conventional protein kinase C
Cy3	fluorochrome , emission in red region
DAG	diacylglycerol
DMSO	dimethyl sulfoxide
EGF	epidermal growth factor
EGFR	epidermal growth factor receptor
ERK	extracellular signal-regulated kinase
EST	expressed sequence tag
FCT	foetal calf serum
FDA	fluorescein diacetate
FTW	filtered tap water
g	gravitational acceleration
g, mg, µg	gram, milligram, microgram
GAP	GTPase-activated protein
GCK	germinal center kinase
GF109203X	bisindolylmaleimide
GPGRs	G-protein coupled receptors
GST	glutathione-S transferase
GTP	guanosine triphosphate
h(rs), min, sec	hour(s), minutes, seconds
HBSS	Hanks' basal salt solution
HMM	hidden Markov model
HRP	horseradish peroxidase
IGF-I	insulin-like growth factor-I
IL-2	interleukin 2
INS	insulin
InsP3	inositol 1,4,5-triphosphate
IR	insulin receptor
JNK	c-Jun amino-terminal kinase
kDa	kilodalton
l, ml, µl	litres, millilitres, microlitres
LA	linoleic acid
M, mM, µM	molar, millimolar, micromolar
MAPK	mitogen-activated protein kinase
MHCs	major histocompatibility complexes
MLCK	myosin light chain kinase
nm	nanometer
nPKC	novel protein kinase C
NRTKs	non-receptor tyrosine kinases
°C	Celsius degree
PBS	phosphate buffered saline
PI	propidium iodide
PIP2	phosphatidyl inositol 4,5-biphosphate
PK	protein kinase
PKA	protein kinase A
PKC	protein kinase C
PKD	protein kinase D
PLC	phospholipase C
PMA	phorbol 12-myristate 13-acetate

PNS	peripheral nervous system
PS	phosphatidylserine
PTK	protein tyrosine kinase
PZQ = Praziquantel	2-(cyclohexycarbonyl)-1,2,3,4,6,7,11b-hexahydro-4H-pyrazino(2,1-alpha) isoquinolin-4-one
Ras	Ras protein
RFUs	relative fluorescence units
RGC	receptor guanylate cyclases
RIPA buffer	radio immunoprecipitation assay buffer
RPMI-1640	Roswell park memorial institute -1640 medium
RTKs	receptor tyrosine kinases
SAPK	stress-activated protein kinases
SB203580	pyridinyl imidazole
SEA	soluble egg antigens
SEM	standard error of the mean
Ser	serine
Smad	Smad protein
Smp	*Schistosoma mansoni* protein
STK	serine/threonine kinase
TBS	Tris-buffered saline
TGF-β	transforming growth factor beta
Thr	threonine
TNFα	tumour necrosis factor α
TPI	triose phosphate isomerase
Tris	tris[hydroximethyl] amino-methane
TRP	transient receptor potential
T-TBS	Tween-20Tris-buffered saline
Tyr	tyrosine
U0126	1,4-diamino-2,3-dicyano-1,4-bis[2-aminophenylthio] butadiene
V	volt
v/v	volume per volume
w/v	weight per volume
WHO	World Health Organization

Chapter 1

General Introduction

1.1 Schistosomiasis, a disease of developing countries

1.1.1 Epidemiology and prevalence

Schistosomiasis, or bilharzia, is an ancient, chronic and debilitating disease caused by parasitic blood flukes (trematode flatworms) of the genus *Schistosoma* (Adamson, 1976). It is one of the 14 neglected tropical diseases (Global Network for Neglected Tropical Disease Control, 2006) that have recently received considerable attention (Hotez *et al.*, 2006). Its prevalence seconds that of malaria with more than 700 million people at risk; 90% of all schistosomiasis cases arise in poverty-stricken areas (Steinmann *et al.*, 2006). More than 200 million people are infected, of which 120 million are symptomatic and 20 million have severe disease (WHO, 2005; Gryseels *et al.*, 2006) resulting in over 250,000 deaths annually (Steinmann *et al.*, 2006; Cardoseo *et al.*, 2006). The principal schistosome species affecting humans are: *Schistosoma haematobium* that causes urinary schistosomiasis, and *S. mansoni*, *S. japonicum*, *S. intercalatum*, and *S. mekongi* which cause intestinal schistosomiasis (Engels *et al.*, 2002). Schistosomiasis is endemic in tropical and sub-tropical regions of Africa, Central America, Brazil, China and South East Asia (Figure 1.1) with children being the principal victims (Steinmann *et al.*, 2006). Increases in the rates of reinfection and disease transmission, especially by *S. mansoni*, are directly related to the extension of endemic areas through increased population. The construction of water schemes to meet agricultural requirements also amplify human exposure to infected areas via bathing, swimming and other water contact (Chitsulo *et al.*, 2000).

1.1.2 Pathology and control strategies

Chronic human schistosomiasis results from granulomatous inflammation in response to schistosome eggs that accumulate in host tissues resulting in extensive tissue damage and loss of function (Ross *et al.*, 2002; Hoffmann *et al.*, 2002). For urinary schistosomiasis there is progressive damage to the bladder, ureters and kidneys that leads to renal failure and sometimes bladder carcinoma. In intestinal schistosomiasis, there is progressive enlargement of the liver and spleen, periportal fibrosis leading to portal hypertension, intestinal damage, and hypertension of the abdominal blood vessels. The infection is associated with anaemia, chronic pain, diarrhoea, exercise intolerance and under-nutrition. Acute schistosomiasis is less

common but is severe and requires hospitalization; if not appropriately treated it can result in severe morbidity or death (King *et al.*, 2006). In acute schistosomiasis, common symptoms are fever, lethargy, myalgia and generalized lymphadenopathy (WHO, 2005). School-age children are at high-risk, likely because of a weaker immune system and higher susceptibility to infection when their increased nutritional needs are not met; they also play in contaminated water (Montresor *et al.*, 2002).

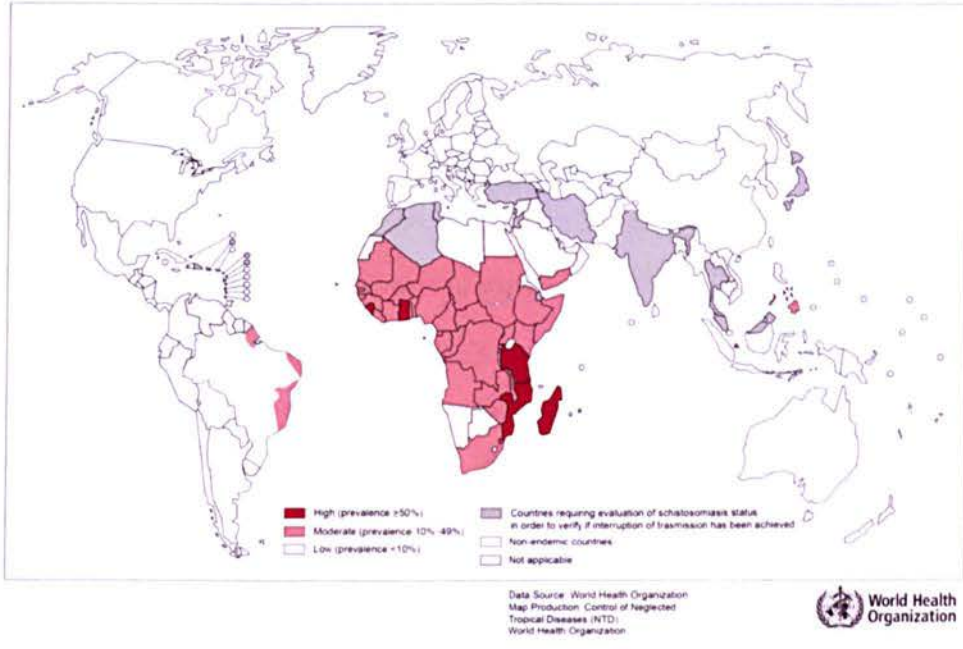

Figure 1.1 - The global distribution of schistosomiasis as of 2011. Image obtained and adapted from the second WHO report on neglected tropical diseases available at: www.who.int/neglected_diseases/9789241564540/en/.

Methods such as control of the intermediate snail host, improved sanitation and health education to change behavioural practices are extremely important as they can potentially interrupt the schistosome life-cycle leading to eradication of the disease. While they are difficult and expensive to implement, programmes aimed at reducing schistosome transmission through concerted control efforts together with economic development have proven effective (Chitsulo *et al.*, 2000). However, population-based chemotherapeutic intervention was also central for success. In Japan and the islands in the Lesser Antilles schistosomiasis has been eradicated while in Brazil, Philippines, and Puerto Rico control programmes considerably reduced morbidity (Chitsulo *et al.*, 2000). Two effective drugs have been available since the 1980s; praziquantel (PZQ) [2-

(cyclohexycarbonyl)-1,2,3,4,6,7,11b-hexahydro-4H-pyrazino(2,1-alpha) isoquinolin-4-one] (or Biltricide; Figure 1.2) used against *S. mansoni, S. japonicum, S. haematobium and S. mekongi* and the more expensive oxamniquine (2-isopropylaminomethyl-6-methyl-nitro-1,2,3,4-tetrahydroquinoline) which is effective in a single dose but only against *S. mansoni* (Fallon and Doenhoff, 1994). Since no alternative compound to PZQ with comparable efficacy and breadth of application is currently available (Meyer *et al.*, 2009), PZQ is the drug of choice in the control and treatment of schistosomiasis and is central to numerous schistosomiasis control programmes (Fenwick *et al.*, 2003; Hagan *et al.*, 2004). In fact, the WHO's strategy for schistosomiasis control (WHO, 2009) aims at reducing morbidity through treatment with PZQ, with a focus on periodic treatment of school-age children and adults considered to be at risk.

1.1.2.1 Praziquantel - mechanism of action

The mechanism of action of PZQ is complex and not yet precisely understood (reviewed by Aragon *et al.*, 2008). It is known that PZQ interrupts Ca^{2+} homeostasis in mature adult worms by increasing Ca^{2+} influx leading to worm paralysis and damage to the tegument membrane, with more extensive damage in the dorsal tegument than the ventral surface. Such membrane disruption releases sub-tegumental proteins and exposes the adult worm to the host's immune system, resulting in worm death (Mehlhorn *et al.*, 1981; Redman *et al.*, 1996; Greenberg, 2005; Braschi and Wilson, 2006). However, recently, Pica-Mattoccia *et al.* (2007, 2008) demonstrated that calcium accumulation by itself, determined using whole parasites *in vitro*, may not represent an exhaustive explanation for the schistosomicidal effects of PZQ. It has further been suggested that PZQ exerts its effect by either altering schistosome membrane fluidity (Harder *et al.*, 1988; Lima *et al.*, 1994), reducing worm glutathione concentrations allowing the host immune system to become more effective (Ribeiro *et al.*, 1998), binding to schistosome actin leading to disruption of the tegument (Tallima and Ridi, 2007), or by inhibiting nucleoside uptake (Angelucci *et al.*, 2007).

1.1.2.2 Praziquantel - present problems

It is important to identify and develop new strategies to combat schistosomiasis since PZQ does not prevent re-infection, especially in children (Kabatereine *et al.*, 1999), only affects the adult egg-laying stage of schistosomes and the poor understanding of its pharmacology limits further development of new drugs with similar

modes of action (Geary *et al.*, 2010). However, the main drawback of PZQ is that it is ineffective against newly acquired and migrating schistosomes (Olds and Dasarathy, 2001). Furthermore, low cure rates ranging from 18 - 38% have been observed in areas of high transmission like Senegal, Egypt and Brazil (Bennett *et al.*, 1997, Olds and Dasarathy, 2001). Treatment failures, especially in areas of elevated transmission of schistosomiasis, could be due to rapid re-infection and PZQ's low efficacy against immature parasites and migrating larvae. Although clinically relevant resistance to PZQ has not yet been reported differences in responses of *S. mansoni* to PZQ treatment have been described (Doenhoff *et al.*, 2002; Cioli and Pica-Mattoccia, 2003) and resistance in the Northern Senegal and Egypt have also been reported (Ismail *et al.*, 1999; Geerts and Gryseels, 2000). This presents concern especially as intensive use of PZQ is recommended as a control method (Ismail *et al.*, 1999; Geerts and Gryseels, 2000; Doenhoff *et al.*, 2002). PZQ is included in the WHO Model List of Essential Drugs (WHO Model Lists of Essential Medicines, 2007) and has been used for over 25 years; relying solely on PZQ is worrying particularly as widespread treatment failure could arise (Caffrey, 2007).

1.1.3 The future of schistosomiasis control and treatment

While the best short-term option for helminthic control involves intelligent, sustainable use of PZQ, the development of new effective drugs is considered necessary to avoid the risk of schistosome resistance to the single chemotherapeutic strategy (Kaplan 2004; Hoste and Torres-Acosta, 2011; McVeigh *et al.*, 2012). Among potential alternatives to PZQ, semi-synthetic derivatives of sesquiterpene lactone, arteminisin, artemether and artesunate have been found to be active against all schistosome species (reviewed by Caffrey, 2007) (Figure 1.2). However, unlike PZQ, these drugs are somewhat variable in efficacy especially for *S. mansoni* and *S. haematobium* while others are not single dose therapies and have to be administered several times a day for extended durations to reduce the number of patent infections (reviewed by Caffrey, 2007). To date anti-schistosomal drugs have originated from industrial and academic "whole organism" discovery programs largely without regard for the molecular target(s) or mode of action. There is therefore a need for target-based drug discovery, which can be a powerful approach. The availability of the *S. mansoni*, *S. japonicum* and *S. haematobium* genome annotations (Berriman *et al.*, 2009; Zhou *et al.*, 2009; Young *et al.*, 2012) and comprehensive EST datasets for both *S. mansoni* and *S. japonicum* will facilitate drug/vaccine target discovery.

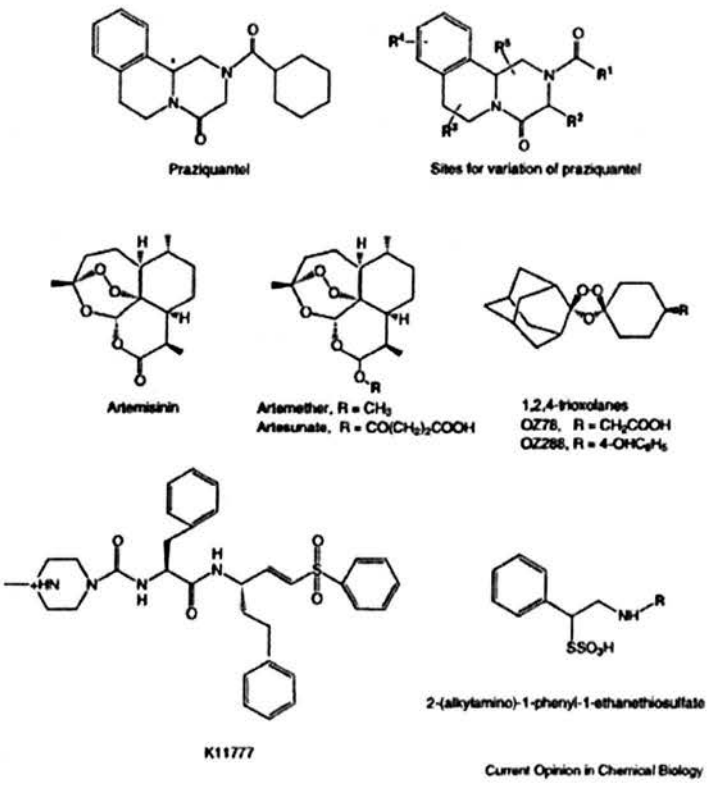

Figure 1.2 - Structure of current anti-schistosomal drugs and experimental therapeutics. Existing drugs which affect schistosome infections. Image obtained from Caffrey (2007).

Research and development of anti-schistosome vaccines has been an active area of research although interest in the use of antigens from schistosomules has so far given disappointing results. Superior results have been obtained with antigens shared between schistosomules and adult worms, such as the 97 kDa paramyosin (Pearce *et al.*, 1988), the 28 kDa triose phosphate isomerase (TPI) (Shoemaker *et al.*, 1992), a 23 kDa integral membrane protein (Sm23) (Koster *et al.*, 1993), and the 26 and 28 kDa glutathione-S-transferases (GSTs) (Olds and Dasarathy, 2001). Recently, the 28 kDa glutathione-S transferase (Sm28GST) candidate (a protein that is expressed in sub-tegumental tissues in most life-stages of the parasite) underwent phase-I and phase-II trials showing safe and good immunogenicity results in human volunteers in France, Niger and Senegal (reviewed by Hotez *et al.*, 2010). Furthermore, vaccination against Sm14, a 14 kDa *S. mansoni* fatty acid-binding protein with cross reactivity in *Fasciola hepatica*, is currently in Phase I clinical trials; Sm14 vaccination provided 67% protection against

challenge with *S. mansoni* cercariae and full protection against *F. hepatica* metacercariae, in mice (Brito *et al.*, 2002; reviewed by Homma *et al.*, 2013; Beaumier *et al.*, 2013). Another approach to vaccination against schistosomiasis has been to target fecundity in order to reduce egg production. Success has been reported in mice and large animal reservoir hosts, including pigs and water buffaloes, using *S. japonicum* 26 kDa GST and paramyosin (reviewed by McManus and Loukas, 2008). Although extensive research efforts have concentrated on the design of vaccines against schistosomes and anti-schistosome vaccine targets (reviewed in McMannus and Loukas, 2008), immune memory seems to be lacking and in trials only ~50% efficacy has been achieved. This could in part be due to variability in vaccine targets at the protein level as shown recently for tetraspanin 23 (Sealey *et al.*, 2013). Thus, there is considerable interest in identifying new anti-schistosome targets including schistosome protein kinases (PKs) that control key cellular events. Being important targets for molecular cancer therapy, PKs offer real potential for the development of novel strategies in chemotherapy of schistosomiasis (Dissous *et al.*, 2007a; Dissous and Grevelding, 2010; Walker, 2011). Understanding schistosome PK-mediated signal transduction pathways is important to such a strategy and would broaden knowledge of the basic biology of schistosomes and of host-parasite interactions. Such knowledge will provide substantial insights into the molecular mechanisms regulating the complex development of schistosome life-stages and will also present opportunities to identify kinase drug targets that block schistosome development.

1.2 The complex life-cycle of *Schistosoma mansoni*

Schistosomes are genetically programmed to develop sequentially within snail intermediate and mammalian definitive hosts. For *S. mansoni*, humans are the main definitive host and *Biomphalaria glabrata*, a hermaphroditic water snail, the main intermediate host. *S. mansoni* has a remarkably complex life-cycle (Figure 1.3) involving multiple life-stages that are morphologically and physiologically distinct from each other with each stage specifically adapted to survive within and during transmission between hosts (Swierczewski and Davies, 2009; Walker, 2011). The life-cycle involves five key life-stages: initial infection of the snail host by the free-swimming *miracidium*, its subsequent transformation to mother and daughter *sporocysts* within the invertebrate host, the formation and release of free-swimming *cercariae*, and

finally infection of the mammalian definitive host where schistosomes transform to *schistosomules* and then mature into *adult worms*.

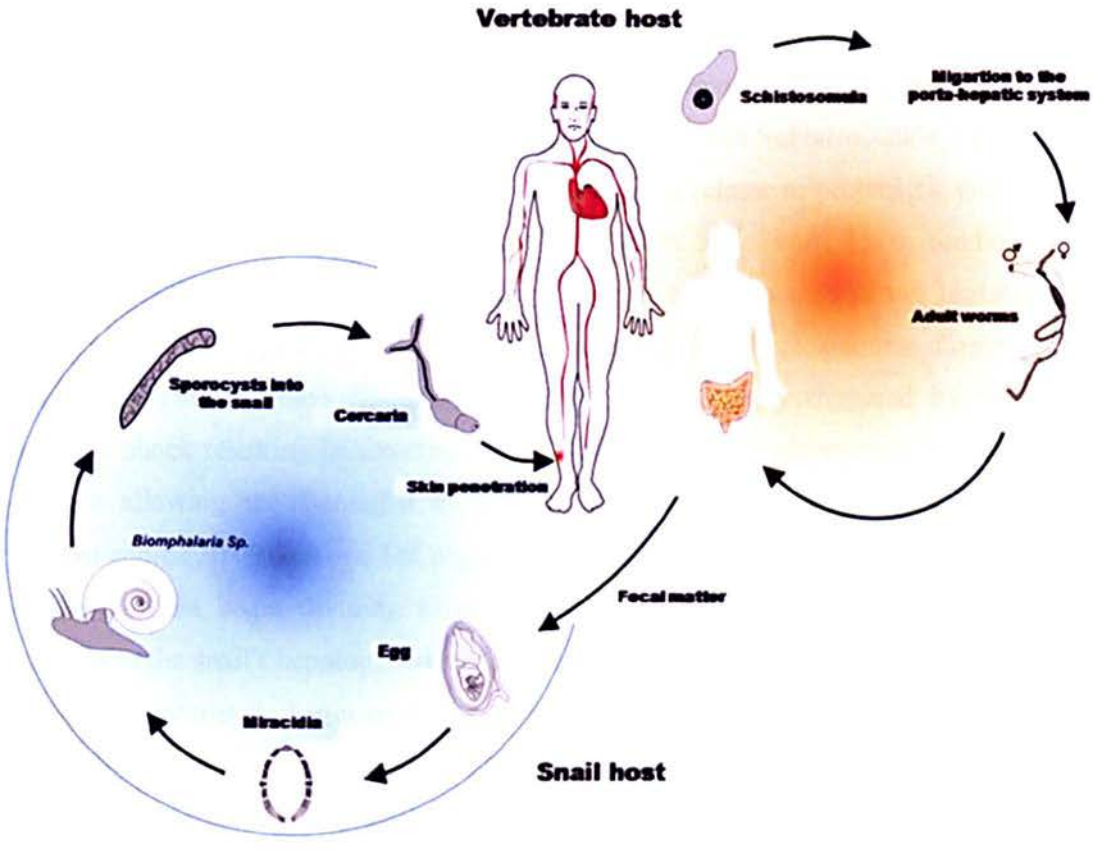

Figure 1.3 - The *S. mansoni* life-cycle. The miracidia are free-living, swimming larvae that infect and then reproduce asexually in freshwater *Biomphalaria* snails; a new larval form, the cercaria, is released from the snail and can swim to find a definitive mammalian host and burrow into its skin. In humans, *S. mansoni* migrate to the hepatic portal vein where they pair and mature into adult worms. They then migrate to the mesenteries surrounding the small intestine and deposit eggs. Eggs produced by the female worm that are released into the environment in faeces hatch into a second larval form, the miracidia, which can then infect the snail. Diagram obtained from Estabile, 2003.

Embryonated eggs produced by paired adult *S. mansoni* in the mesenteric veins of the human host transverse tissues of the intestine and are discharged in the faeces into the environment. Escape through the host tissues is facilitated by the secretion of immunoreactive molecules and the formation of an intense granulomatous host response which acts to push the eggs into the gut lumen (Jones *et al.*, 2008). The eggshell is porous but resistant to degradation by the host and microbes from the environment. Upon contact with fresh water (Pan, 1980) osmotic changes occur that induce the

ciliated miracidium to start moving within the egg which eventually ruptures and the miracidium emerges swimming rapidly (Kusel, 1970; Xu and Dresden, 1986; Gryseels *et al.*, 2006). The molecular cascades leading to hatching are poorly understood. The free-living, non-feeding miracidium survives approximately 24 h during which time it must source a compatible intermediate snail host or die (Gryseels *et al.*, 2006); the miracidium is mainly attracted by light and the presence of snail mucus (especially Ca^{2+} and Mg^{2+}) and actively orientates towards it (Sukhdeo and Sukhdeo, 2004, Gryseels *et al.*, 2006). After, the miracidium uses rotation and the release of proteolytic enzymes to penetrate and enter the snail foot tissue (Sponholtz and Short, 1976; Sukhdeo and Sukhdeo, 2004). Next, close to the site of penetration, the miracidium undergoes a series of morphological, physiological and metabolic changes and transforms into a mother sporocyst. These changes are thought to be mainly triggered by an initial osmotic shock resulting in shedding of the ciliary epidermal plates from the miracidial surface allowing the formation of a new tegumental syncytium of the developing mother sporocyst (Basch and DiConza, 1974; Pan, 1996). Germ cells within the mother sporocyst then begin dividing to produce daughter sporocysts, which subsequently migrate to the snail's hepatopancreas. Once in the hepatopancreas, germ cells within the secondary sporocysts begin to divide asexually, producing thousands of cercariae, the infective human form (Gryseels *et al.*, 2006).

Approximately four weeks post-infection cercariae emerge from the snail in a circadian rhythm, dependent on ambient temperature and light, and search for a definitive mammalian host (Gryseels *et al.*, 2006). The cercariae have a well developed fork-like tail, with longitudinal striated muscles extending underneath the tegument, which they use to swim to find a definitive host (Norton *et al.*, 2008). This non-feeding free-swimming larva can survive in freshwater for up to 72 h, during which time they must attach to human skin or that of another susceptible mammalian host; however, maximal infectivity has been observed to be between one and nine hours post-emergence (Whitfield *et al.*, 2003). Young *S. mansoni* cercariae are highly mobile, alternating between vigorous upward movements and sinking to maintain their position in the water (Haas, 1994). This activity is particularly stimulated by water turbulence, shadows, host body temperature, and chemical host cues such as amino acids including L-arginine, and lipids such as ceramides and acylglycerols which are found on the skin surface (Shiff *et al.*, 1972; Haas, 1979; Haas *et al.*, 1994, 2002; Haeberlein and Haas, 2008). Infection of the definitive host occurs by penetration through pores of the hair follicle during which the cercariae shed their tail. The parasite secretes proteolytic

enzymes from the acetabular glands that break down the host skin enabling penetration and further migration into the blood circulation (Haas *et al.*, 1997).

During skin penetration, the cercariae undergo metamorphosis, shedding their tails and outer glycocalyces while developing a double-lipid bilayer and a heptalaminate tegument that is highly-resistant to the host immune response (Samueleson and Stein, 1989). The larvae, now called schistosomules, incorporate host proteins in their teguments, including major histocompatibility complexes (MHCs) and blood group antigens (Sher *et al.*, 1978; Pearce and MacDonald, 2002). Each 'transformed' schistosomule remains in the skin for 2-3 days before migrating to the lungs (lung-stage schistosomule) where they undergo further developmental changes necessary for subsequent migration to the liver (liver-stage schistosomule). Around 8-10 days after penetration of the skin, the parasite migrates to the portal blood vein where it develops into a mature adult worm (Gryseels *et al.*, 2006). The maturation of female *S. mansoni* is dependent on pairing with a male, which induces mitotic activities in the reproductive organs of the female worm (Schubler, 1997). Therefore, male and female adults pair up; the thin female enters the gynaecophoric canal of the stockier male worm and, in pairs, they migrate to the mesenteric veins where they sexually reproduce (Gryseels *et al.*, 2006). Approximately 35 days after the initial infection, female worms *in copula* start producing up to 300 eggs/day (Moore and Sandground, 1956). Interestingly, the average lifespan of an adult worm is 3-5 years, however it was reported that it can be up to 30 years with an astonishing theoretical reproduction potential of 600 billion schistosomes (Gryseels *et al.*, 2006). Many of the eggs (approximately 50%) pass through the walls of the blood vessels and intestine, to be excreted in the faeces. Only mature eggs are capable of doing this, possibly through the release of proteolytic enzymes (Senft and Maddison, 1975), but also facilitated by the host immune response, which promotes local tissue ulceration (Senft and Maddison, 1975; Gryseels *et al.*, 2006). The remaining eggs become trapped in the mesenteric veins, or are washed back into the liver, where they become lodged. Trapped eggs mature normally, secreting antigens termed soluble egg antigens (SEA) (Pelley *et al.*, 1976; Roberts and Javony, 2000) that elicit a vigorous immune response. The eggs themselves do not cause large tissue damage; rather it is the cellular infiltration resulting from the immune response that causes the pathology classically associated with schistosomiasis (Roberts and Javony, 2000).

It is assumed that as the parasite moves through different environments, both parasitic and free-living, it responds through signal transduction pathways that convey information from the parasite surface to various cells, enabling the parasite to survive

and maintain homeostasis (LoVerde *et al.*, 2007). In addition, signals will also be transduced between cells within the parasite. Together, external and internal signals should regulate development, host- and site-finding behaviour, reproductive activity and immune evasion among other biological activities (reviewed in Bahia *et al.*, 2006). In fact it is clear that maturation of the female worm and the ability of adult worms to survive for decades in the blood-stream of the mammalian host depend on close contact with the male, processes that require molecular communication (Amiri *et al.*, 1992; Schussler *et al.*, 1997; Kunz, 2001; Kapp *et al.*, 2004; Fitzpatrick *et al.*, 2007). So, knowledge gained through studying signal transduction proteins and signalling mechanisms in schistosomes, particularly in the human dependent and infective life-stages, would certainly accelerate our understanding of parasite developmental biology and pathogenesis, and should facilitate development of novel treatments.

1.2.1 Miracidium biology

The miracidium is ~150 μm long (Figure 1.4) and swims rapidly using cilia attached to epidermal plates that cover the surface of the organism (Samuelson *et al.*, 1984). This larval stage is non-feeding and has limited energy resources to find the susceptible host. The miracidium swimming behaviour is mainly positively photokinetic (directed towards increases in light intensity) and chemokinetic (attracted towards factors from the susceptible intermediate snail host). The terebratorium is the sensory organ and is also thought to aid in attachment to the snail surface (reviewed by Walker, 2011). Penetration occurs by release of secretory substances including proteases from the apical and lateral glands and is aided by mechanical movement for burrowing through the snail tissue (Basch and DiConza, 1974). Inside the snail the miracidium sheds its ciliated epidermal plates becoming a post-miracidium and forms a new tegumental syncytium becoming a parasitic mother sporocyst; these, changes are thought to be mainly triggered by an initial osmotic shock and other unknown molecular events (Basch and DiConza, 1974; Pan, 1996). Protein kinase C has recently been shown to negatively affect development of the miracidium to the mother sporocyst (Ludtmann *et al.*, 2008). The miracidium is packed with germinal cells that develop into daughter sporocysts.

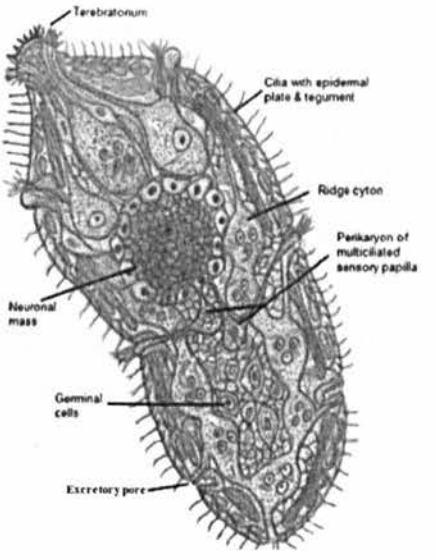

Figure 1.4 - Line drawing depicting the morphology of an *S. mansoni* miracidium. The terebratorium, cilia of the epidermal plate, ridge cyton, sensory papillae, neural mass, germinal cells and excretory pore are indicated. Image obtained from Pan, 1965.

1.2.2 Sporocyst biology

Inside the compatible snail host the post-miracidium differentiates into a mother sporocyst (the second larval form) that absorbs nutrients from the snail plasma across the new syncytial tegument and excretory products are released through the excretory pores *via* the flame cells (Figure 1.5) (Ivanchenko *et al.*, 1999; Walker, 2011). The sporocysts are transported by haemolymph around the body mainly accumulating in the snail hepatopancreas due to the haemolymph circulation (Becker, 1980). They mainly remain bathed in haemolymph in the interfollicular connective tissue of the hepatopancreas providing the best conditions for the sporocysts to develop and multiply (Pan, 1965; Becker, 1980). The tegumental structure of the mother sporocyst (which consists of an outer layer connected to internal nucleated cell bodies) forms extensions that wrap the germinal cells and the parenchyma cells (Meuleman *et al.*, 1980). In the following week after infection, the mother (primary) sporocysts produce first- and second-generation daughter sporocysts *via* asexual replication, which then exit *via* the maternal body wall (Ivanchenko *et al.*, 1999). When the daughter sporocysts develop from the germinal cells they are enveloped by a primitive epithelium which results from expansion of somatic cells located in the periphery of the developing daughter

sporocysts forming the outer layer of the tegument, which contains microvillus-like projections, a surface coat, spines and a basement membrane (Ivanchenko *et al.*, 1999). Further maturation of the daughter sporocysts results in the production of a large number of genetically identical cercariae. The growth and the rapid multiplication of the parasites places a great burden on the host's metabolism (reviewed by Becker, 1980). In fact, at 28°C the developing parasites can increase their mass 150-200 times within six days (Becker, 1980).

When fully developed the cercariae escape through the birth pores of daughter sporocysts, emerging from infected snails ~35 days post infection. How the transforming miracidium and sporocysts evade the immune response of the snail is poorly understood however is likely to be due to a variety of factors including modifications of the snail's immune cell signalling (Walker, 2006; Zahoor *et al.*, 2008, 2009).

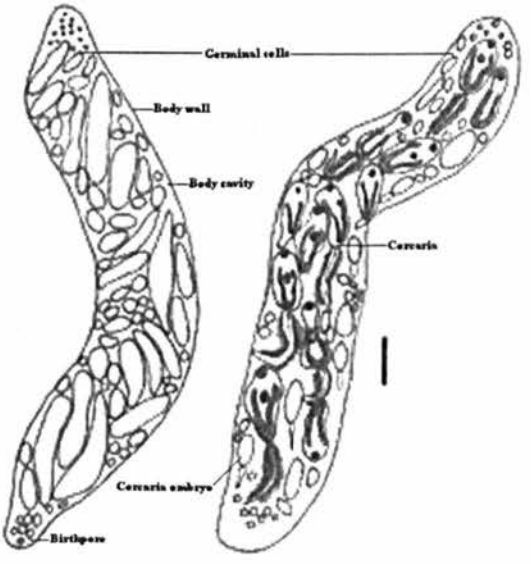

Figure 1.5 - Schematic diagram depicting the morphology of S. *mansoni* sporocysts. The left image represents the first generation (mother/primary) sporocysts and that on the right represents the second generation sporocysts. Image obtained and adapted from http://quizlet.com/20453567/platyhelminthes-lab-practical-lab-7-flash-cards/.Bar = 50 μm

1.2.3 Cercariae biology

Schistosoma mansoni cercariae (Figure 1.6), first identified by Leiper in 1915, are free-living non-feeding organisms programmed for a brief existence in freshwater with limited glycogen stores (Khalil *et al.*, 1922; Walker, 2011). Unless a

cercaria is able to quickly invade a suitable definitive host and resume life as an endoparasitic schistosomule, its stored glycogen resources become exhausted. The host finding behaviour of *S. mansoni* cercariae is complex and cercariae are well adapted to undergo locomotion, host-detection and invasion (Haas 1992; Haas *et al.*, 2008). To maximise chances of successful infection cercariae respond to mechanical, photoreceptive, thermal and chemical stimuli, which trigger specialized behavioural patterns (Haas, 1992; Walker, 2011). Although *S. mansoni* is the most investigated of the schistosome species, little is known about the molecular mechanisms that govern the swimming, host detection and penetration behaviour of cercariae.

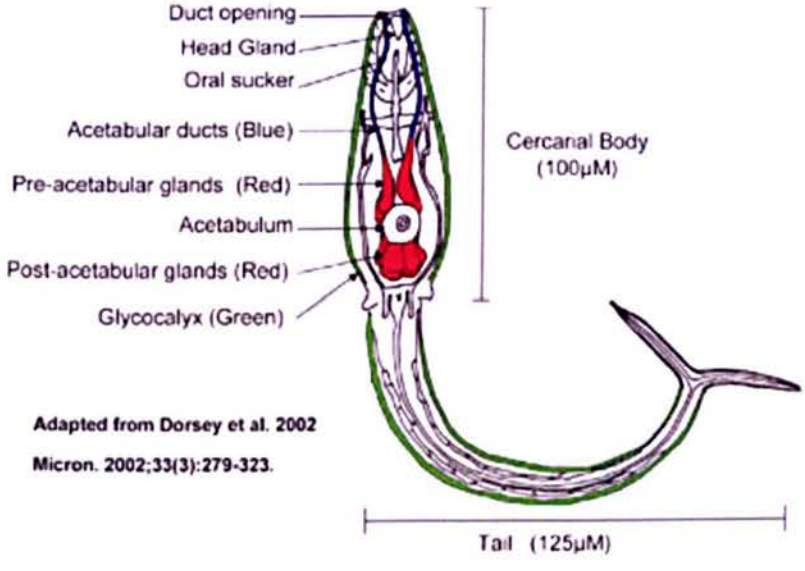

Figure 1.6 - Schematic diagram depicting the morphology of a *S. mansoni* cercaria. Image obtained and adapted from Dorsey *et al.*, 2002.

1.2.3.1 Morphological characteristics

The cercariae (Figure 1.6) are between 225 and 325 µm long and are able to contract and elongate (Brachs and Haas, 2007). The body is covered with a trilaminate layer composed of a single syncytial tegument covered by a carbohydrate-rich glycocalyx with spines; directly beneath the cuticle lay two layers of muscle

fibres (Haas *et al.*, 2008). Ciliated sensory papillae exist and are suspected to play important roles in host detection by sensing temperature, light and/or chemicals (reviewed in Walker, 2011). Anatomically, cercariae can be divided into three main regions; the anterior organ (oral sucker), the body (mid-segment) and the bifurcated fork-like tail (Figure 1.6), which serves as a temporary organ of motility (Dorsey *et al.*, 2002). The attachment of the tail to the body segment is fragile and the tail is cast off upon host penetration. When the tail is separated its movements continue for a short time in water (Khalil *et al.*, 1922). The oral sucker is large almost completely occupying the anterior third of the body, in the anterior organ there is also a head gland (Dorsey *et al.*, 2002). The ventral sucker (acetabulum) is smaller than the oral sucker and is nearer to the posterior end of the mid-segment region and can fix the cercariae securely when water is disturbed or when they have found a suitable substrate. There is also a nervous system, excretory system and germ cells which differentiate into the reproductive system of the adult worm (Dorsey *et al.*, 2002). The excretory system consists of flame cells and excretory tubules leading into a collecting tubule which forms a main excretory duct subsequently joining to make a major excretory vesicle and in the tail, an excretory canal. The cercaria flame cells, which are specialized excretory cells, have a doubly outlined cell wall. They are conical structures visible due to the moving cilia producing a constant flow of fluid (Dorsey *et al.*, 2002). In *S. mansoni* cercariae the number of flame cells is constant, three pairs are found in the body segment and one pair in the tail. The nervous system is distributed throughout the three anatomic segments of the cercariae and is generally organized in a central ganglion from which nerve trunks extend and tegumental sensory papillae emanate (Dorsey *et al.*, 2002; Collins *et al.*, 2011).

The cercaria also contains five pairs of secretory acetabular glands named according to their position with reference to the acetabulum; two pairs are situated anterior to the acetabulum (pre-acetabular) and three pairs posterior to this organ (post-acetabular) (Collins *et al.*, 2011). These glands are essential for host penetration and are produced during cercarial development within the sporocyst. They occupy a large portion of the body segment and each gland consists of an enlarged anucleate area with a long duct opening through the tegument onto the surface of the anterior organ (Dorsey *et al.*, 2002). During phases of creeping and penetration the cercariae secrete pre- and post- acetabular gland contents. Acetabular glands release their contents at the earliest stages of skin invasion and well into the superficial dermis

(Dorsey *et al.*, 2002). Post-acetabular gland contents may function to support cercarial contact with the host skin (Stirewalt and Dorsey, 1974). Furthermore, histochemical analysis of post- and pre-acetabular glands reveals the presence of serine proteases that help in the degradation of host skin macromolecules during penetration, and may also contribute to the removal of the glycocalyx during transformation to schistosomules and for protection or evasion from the host immune response (McKerow *et al.*, 1985; Fishelson *et al.*, 1992; Knudsen *et al.*, 2005). Also phospholipids and various muco-substances, likely assisting in cercarial adhesion to skin surfaces, have been found in post-acetabular glands (Stirewalt and Walters, 1973; Dorsey, 1975; Stirewalt, 1978; Haas *et al.*, 1997).

1.2.3.2 Behavioural characteristics

Schistosoma mansoni cercariae perform an intermittent swimming behaviour; an active phase where the cercariae show upward directed, tail first swimming alternating with a passive phase with the cercariae sinking (Brachs and Haas, 2007). Some cercariae may sink to the bottom and lie quiescent for a moment before resuming swimming activity. Cercariae can also shift to body first swimming, however this is not the normal situation. Enhanced swimming activity is observed in bright light where longer active phases are observed compared to low light intensities (Brachs and Haas, 2007). It is suggested that the active and passive swimming phases are governed by two independent mechanisms, however, which mechanisms are involved is unknown. Swimming behaviour of *S. mansoni* cercariae is also governed by chemical cues with responses to chemical gradients evident, although only when at a close proximity. The effect that such chemical cues have on swimming behaviour is translated into increased rates of changes in swimming direction (considered to be an effective strategy to approach the source of the attractants) (Brachs and Haas, 2007). Interestingly, it is generally accepted that a major stimulus initiating the penetration process of *S. mansoni* cercariae is the presence of unsaturated fatty acids at the skin surface (Shiff *et al.*, 1972) which leads to the release of proteolytic enzymes in the acetabular glands aiding invasion. Overall, the coordinated motility of cercariae is central for the finding and invasion of the definitive host, however the molecular mechanisms that drive such behaviour are unknown.

1.2.4 Schistosomule biology

During penetration into the epidermis, transformation to the schistosomule is initiated. The transformed cercariae undergo several morphological and physiological changes until they reach sexual maturity. Firstly the cercarial tail is shed, a rudimentary gut develops and the tegumental trilaminate membrane is shed along with the glycocalyx and replaced by a heptalaminate tegument (Brachs and Haas, 2007). This differs from the cercarial tegument both biochemically and structurally, displaying a heptalaminate structure with two lipid bilayers (McLaren, 1980). The schistosomule migrates through the body developing in three stages until it reaches maturity as an adult worm: the skin stage, lung stage and liver stage (Haas and Schmidt, 1982).

Cercariae become skin stage schistosomules during penetration through the epidermis, 30 min to 3 h post-infection, when the membrane transformations take place. Schistosomules remain at this stage for 24 h while entering the dermis (Haas and Schmidt, 1982). The parasite burrows and migrates through the deeper layers of the dermis and enters a blood vessel or lymphatic vessel within 2-3 days. Then, the schistosomules are carried by the blood flow to the lungs, *via* the pulmonary artery. At approximately day 6, in the lungs, further developmental changes occur to the intravascular lung stage to enable further migration of the parasite (Haas and Schmidt, 1982). Here the schistosomules become longer and more slender and the parasite begins feeding (Clegg and Smithers, 1972). To develop further, the schistosomules migrate, *via* the blood vessels, through the left side of the heart to reach the hepatic portal vein at day 13-15. Once in the liver (the liver stage) the parasite undergoes considerable growth, with complete development of the gut, and development of the gonads, becoming immature adults (reviewed by Walker 2011). Then the male and female worms search for each other and attempt to pair up.

There are, however, discrepancies in the literature regarding when the different schistosomule stages occur. Clegg and Smithers (1972) concluded that the growth rate of schistosomules *in vitro* is identical to that *in vivo* for at least 12 days. Hockley and McLaren (1972) reported that schistosomules do not start to grow until day 4 at the earliest, although considerable individual variation is always present, and Moser *et al.* (1980) concluded that *S. mansoni* schistosomules reach skin stage after 3 h and lung-stage after 5 days in culture. Keiser *et al.* (2010) concluded that schistosomules survive for at least 96 h in different media (Basch, MEM, DMEM or TC199) regardless of serum supplementation. And Wei and Shu-long (1986) reported that *S. japonicum* begins to ingest blood on day 5 showing dark brown pigment and gut union on day 12,

with the gynaecophoric canal appearing at days 18-21 and pairing first observed on day 41.

The *S. mansoni* life-cycle can be maintained in the laboratory, and it is possible to transform cercariae to schistosomules *in vitro*, that can be kept alive and grown in culture for long durations. However, a vertebrate definitive host is still necessary in order to obtain sexually mature, competent, adult worms, as in culture the paired adults do not produce viable eggs. This *in vitro* culture can be achieved by different techniques using different culture media and the ultrastructure of those parasites transformed and cultured *in vitro* was similar to that of *in vivo* transformed cercariae (Salafsky *et al.*, 1988). Differences in the biochemistry of the resultant *in vitro* transformed organisms have, however, been identified (Salafsky *et al.*, 1988). Nevertheless the only way to obtain high yields of transformed parasites is through *in vitro* culture.

1.2.5 Adult worm biology

Adult *S. mansoni* are acoelomate bilaterally symmetrical worms, which possess a syncytial tegument with tubercles, an oesophagus and gut with one opening, a ventral and oral sucker, a central nervous system and an excretory system (Figure 1.7). Once male and female worms pair, further sexual maturation occurs and the couples migrate against the blood flow back along the hepatic portal vein, to its mesenteric branches around the intestine. There, egg laying commences, approximately 25 to 30 days post-infection.

The excretory system consists of flame cells, which lead into a fine network of tubules lined with epithelial cells and larger tubules that ultimately assemble into ciliated collecting ducts which open to the external environment *via* the nephridiopore (Kusel *et al.*, 2009). The adult male is approximately 1 cm long (Machado-Silva *et al.*, 1995) and 1 mm wide and is more muscular and stockier than females, which are longer (1.2 cm) but more slender (0.2 mm). The anterior of both male and female worms possesses an oral sucker and a more prominent ventral sucker. Spines are present at the anterior and at the bottom of the oral cavity of the oral sucker while sensory papillae line the posterior border (Machado-Silva *et al.*, 1997). Behind the ventral sucker, the male body width increases and folds ventrally to form the gynaecophoric canal where the female resides. The proximal end of the canal possesses fewer tubercles, lacks spines and has a genital pore where the tegument is spineless, porous, and lacks sensory receptors. The dorsal region of the body has a greater number of tubercles and spines

(Machado-Silva *et al.*, 1997). Females possess smaller and fewer tubercles than males. Sensory papillae, ciliated or non-ciliated, are present on the spineless tubercles or are surrounded by spines.

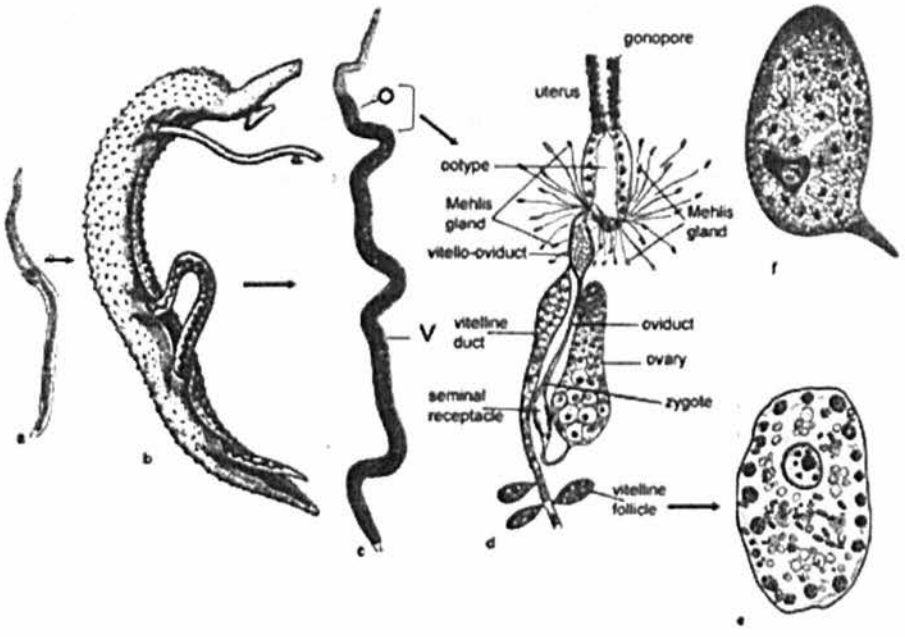

Figure 1.7 - Schematic diagram of an *S. mansoni* adult worm and egg. Showing: a) an immature male worm, b) adult worm pair with female residing in the gynaecophoric canal of the male, c) sexually mature female, d) reproductive organs of the sexually mature female worm, e) a vitelline follicle and f) the fully developed embryonated egg. Images obtained from LoVerde *et al.* (2004).

The schistosome tegument has a complex syncytial organization with an anucleate surface layer connected at intervals *via* cytoplasmic bridges to sub-surface nucleated cell bodies (Halton, 2004). The tegument possesses multiple functions including: host immune evasion/modulation *via* synthesis and secretion of endogenous materials including components of the plasma membrane; absorption of exogenous materials *via* active transport or endocytosis; osmoregulation; excretion *via* ionic pumps; and sensory perception *via* presence of sense organs/receptors that connect with the worm nervous system (Halton, 2004; Walker, 2011).

The nervous system is well developed and is divided into the central nervous system (CNS) comprising the bi-lobed brain and paired main nerve cords and a peripheral nervous system (PNS), consisting of all the minor cords and nerve plexuses

(Brownlee *et al.*, 1995; Halton and Gustafsson, 1996); it also functions as an endocrine system by releasing modulatory substances close to target cells or organs (Halton and Gustafsson, 1996). The central ganglia is located anteriorly and comprises bi-lobed ganglionic structures, with each ganglion consisting of dendrites that are frequently coupled by synaptic contacts and gap junctions, and surrounded by a ring of loosely packed nerve cell bodies (Halton and Gustafsson, 1996; Collins *et al.*, 2011; de Saram *et al.*, 2013). There are various sensory organs found in schistosomes including mechanoreceptors, chemoreceptors, and osmoreceptors. Schistosomes also utilize many neurochemicals and biologically active peptides as neurotransmitters (reviewed by Halton and Gustafsson, 1996; Ribeiro and Geary, 2010; McVeigh *et al.*, 2012).

Schistosome reproductive systems are well developed with the male system being simpler than the female. The testes are posterior and dorsal to the ventral sucker, the genital pore is a muscular structure that opens to the proximal end of the gynaecophoric canal where sperm is released (Machado-Silva *et al.*, 1998). The seminal vesicle is joined to the genital pore through ejaculatory ducts, and at the opposite end is connected with the testes through the deferent duct (*vas deferens*) (Machado-Silva *et al.*, 1998). The female reproductive system (Figure 1.7) comprises a uterus, ootype, Mehlis gland, ovary, ovary duct, vitelline glands and vitelline ducts (Erasmus, 1973). The ootype, located directly in front of the ovary, is where the egg is formed from vitelline cell secretions and secretions from the Mehlis gland that surrounds the ootype. The uterus leads from the ootype to the genital pore, which opens close to the ventral sucker of the female and is believed to be lined with a syncytial layer similar to the outer tegument (Fried and Graczyk, 1997). Oogonia divide forming primary oocytes, which enlarge filling the central and posterior regions of the ovary. As the oocytes mature, they migrate toward the posterior end and enlarge to form germ cells that when mature, are released to the oviduct (Fried and Graczyk, 1997). The area proximal to the ovary is enlarged to form the seminal receptacle where sperm is stored ready for fertilization. Most of the oviduct is non-ciliated but where it joins the vitelline duct to form the vitello-oviduct it becomes ciliated until the ootype. A single non-ciliated vitelline duct collects mature vitelline cells from vitelline follicles in the posterior part of the female body. The additional cells (30-40 cells) produced by vitelline glands are joined with the oocyte into a compound egg but these are degenerated during early cleavage and do not play any role in embryonic development (Kunz, 2001). Vitelline cells are analogous to nurse cells in ovaries in higher organisms, which produce small amounts of vitelline

substance and predominantly eggshell proteins. Paired, sexually mature females can release hundreds of eggs daily (Shaw, 1987; Kunz, 2001).

In virgin females and unisexual infections development of the ovary and vitelline glands is compromised (Shaw, 1987; Shaw and Erasmus, 1981). Thus molecular signalling from the male regulates the multiplication and differentiation of the germ cells committed to become oocytes or vitellocytes after pairing occurs (Kunz, 2001). Hormones, growth factors or lipid molecules have been proposed to be secreted by the male schistosomes to initiate female reproductive development and maintain maturation status (Shaw *et al.*, 1977; Kunz, 2001).

1.3 Eukaryotic Protein Kinases (ePKs)

Signal transduction pathways and the molecules involved are pivotal regulators of cellular functions in the animal kingdom, with their mechanisms of action well understood in mammals and invertebrates such as *Caenorhabditis elegans* and *Drosophila melanogas*ter (Mellor and Parker, 1998). Protein kinases (PKs) are a large family of enzymes that communicate external signals to the cell, triggering cellular responses and controlling many crucial cellular functions such as proliferation and differentiation (McCormick, 1994; Schüβler *et al.*, 1997).

Protein kinases function by catalyzing the transfer of a phosphate group from ATP or GTP by covalent attachment of the catalytic domain to the side-chain carboxyl group of a particular amino acid residue (Cohen, 2002; Bradshaw and Dennis, 2004). For instance, an active protein kinase transfers the terminal phosphate of adenosine triphosphate (ATP) to a hydroxyl group on a protein while a protein phosphatase catalyses removal of the phosphate by hydrolysis. This leads to a conformational change in the target protein that switches its activation status often resulting in signal amplification and activation of transcription factors which influence gene expression (Cohen, 2002; Bradshaw and Dennis, 2004). Many PKs are autophosphorylated or may be phosphorylated by other PKs, an interaction regulated by the accessory protein domains; regulation also occurs by non-protein cellular messengers such as cyclic AMP, Ca^{2+}, diacylglycerol and prostaglandins (Hanks *et al.*, 1988; Andrade *et al.*, 2011).

The catalytic domain of protein kinases normally ranges from 250-300 amino acids (~30 kDa) and is divided into 12 subdomains with highly conserved individual amino

acids and motifs (Hanks, 2003). The location of the catalytic domain within the protein is variable but is usually near to the carboxyl terminus with a regulatory role. According to their substrate recognition sites, in eukaryotes, PKs fall into one of two broad classes; serine/threonine (Ser/Thr) kinases (STKs) and tyrosine (Tyr) kinases (TKs). However, dual specificity kinases, which phosphorylate serine, threonine, and tyrosine, also exist.

Eukaryotic PKs are further classified into eight groups based on sequence similarity of the catalytic domain, the presence or absence of accessory domains and other factors (reviewed by Andrade *et al.*, 2011). According to PKs in the human genome and their homologues in other eukaryotes the eight ePK groups are: AGC (cAMP-dependent protein kinase/protein kinase G/protein kinase C extended), STE (MAP kinase cascade kinases), CAMK (calcium/calmodulin regulated kinases), CK1 (cell kinase I), CMGC (cyclin-dependent kinases), RGC (receptor guanylate cyclases), TK (protein tyrosine kinase) and TKL (tyrosine kinase-like). However several other kinases cannot currently be classified in these families and they form a ninth group called "other" (reviewed by Andrade *et al.*, 2011).

1.4 Protein kinases in schistosomes

Schistosomes, like other multicellular organisms, require permanent processes for cell-to-cell communication. Some of the basic signalling components are likely to have evolved when life became multicellular and can be found in simple metazoans, for example sponges and cnidarians (Freitas and Pearce, 2010). Hence, given the complexity of schistosomes and their different life-stages, it would be surprising not to find several evolutionarily conserved signalling pathways in schistosomes regulating a variety of essential functions. Researchers have been interested in identifying proteins expressed by schistosomes, in the different life-stages, that regulate schistosome growth, cell fate specification, tissue organization and differentiation, body plan establishment, and initiation and maintenance of reproductive function amongst other processes (Amiri *et al.*, 1992; Campbell and Todd, 1995; Schuessler *et al.*, 1997; Sukhdeo and Sukhdeo, 2004; Freitas and Pearce, 2010). For instance, Hernandez *et al.* (2004) found that male worm development is regulated by immune signals derived from the host, and Blank *et al.* (2006) discovered that the host's adaptive immune system provides factors, including the cytokine interleukin 2 (IL-2), that regulate schistosome growth and pairing. Furthermore, it has been shown that the male worm sends

molecular signals to the female worm to regulate maturation and reproductive development (Schüβler *et al.*, 1997). Schüβler *et al.* (1997) explored the role of signalling proteins in co-ordinating the interaction between male and female adult worms and identified the possible involvement of three signalling molecules: mitogen-activated protein kinase (MAPK), GTPase-activated protein (GAP) and Ras. Signalling during snail host-schistosome interactions was explored by Walker and Rollinson (2008) who found that the tyrosine phosphorylation of a 56 kDa protein (p56) might play an important role in the outcome of snail infection; the phosphorylation of p56 on the tegument of *S. mansoni* miracidia increased when parasites were exposed to the haemolymph of schistosome-susceptible but not schistosome-resistant *B. glabrata*.

Although cell signalling in schistosomes has been poorly researched in the past, progress has been recently made in developing databases and modern tools to study these parasites. Schistosomes are the first flatworms to be fully sequenced; a landmark event providing valuable information to study this human pathogen (Berriman *et al.*, 2009; Zhou *et al.*, 2009; Young *et al.*, 2012). The recently-assembled full 363 megabase *S. mansoni* nuclear genome has been analyzed revealing a large number of signalling proteins (e.g. Figure 1.8), including 252 protein kinases (Andrade *et al.*, 2012) giving insights into the biology of the parasite and a better understanding of the signalling pathways involved (Berriman *et al.*, 2009). However, only a fraction of the signalling molecules, including transmembrane and cellular receptors, have been characterized at the biochemical level (Table 1.1).

Table 1.1 - Key examples of signal transduction proteins/receptors identified in *S. mansoni* listed in chronological order.

Identified *S. mansoni* signalling proteins	Reference
S. mansoni Calcium binding proteins (CaBPs)	Siddiqui *et al.*,1991
S. mansoni Heat shock factor (HSF)	Neumann *et al.*,1992
S. mansoni epidermal growth factor receptor (SER)	Ramachandran *et al.*,1996
S. mansoni Mitogen-activated protein kinase (MAP kinase)	Schuessler *et al.*,1997
S. mansoni GTPase activating protein (GAP)	Schuessler *et al.*,1997
S. mansoni Ras	Schuessler *et al.*,1997
S. mansoni receptor kinase (SmRK1)	Davies *et al.*, 1998
S. mansoni retinoid receptor 1 (SmRXR1)	Freebern *et al.*, 1999a
S. mansoni retinoid receptor 2 (SmRXR2)	Freebern *et al.*, 1999b
S. mansoni trispanning orphan receptor (Sh-TOR)	Inal, 1999
S. mansoni stathmin-like protein (SmSLP)	Valle *et al.*, 1999
S. mansoni Smad1 (SmSmad1)	Beall *et al.*, 2000
S. mansoni MK16 (SmMAK16)	Milhon *et al.*, 2000
S. mansoni Smad2 (SmSmad2)	Beall *et al.*, 2000
S. mansoni Smad2 (SmSmad2)	Osman *et al.*, 2001
S. mansoni tyrosine kinase 5 (SmTK5)	Kapp *et al.*, 2001
S. mansoni 14-3-3e (Sm14-3-3e)	McGonigle *et al.*, 2001a
S. mansoni Ca-ATPase (SMA 3)	Da'dara *et al.*, 2001
S. mansoni RK1 interacting protein (SIP)	McGonigle *et al.*, 2001b
S. mansoni Tyrosine kinase 4 (SmTK4)	Knobloch *et al.*, 2002
S. mansoni Fushi Tarazu-factor 1 (SmFTZ-F1)	De Mendonca *et al.*, 2002
S. mansoni Initiation factor subunit 2 α (eIF2α)	McGonigle *et al.*, 2002
S. mansoni GTPase (SmRhol)	Santos *et al.*,2002
S. mansoni receptor tyrosine kinase 1 (SmRTK1)	Vicogne *et al.*, 2003
S. mansoni Smad4 (SmSmad4)	Osman *et al.*, 2004
S. mansoni receptor kinase 2 (SmRK2)	Forrester *et al.*, 2004
S. mansoni FK506-binding protein (SmFKBP12)	Knobloch *et al.*, 2004
S. mansoni P2X receptor (SchP2X)	Agboh *et al.*, 2004
S. mansoni tyrosine kinase 3 (SmTK3)	Kapp *et al.*, 2004
S. mansoni histone acetyltransferase (SmGCN5)	De Moraes Maciel *et al.*, 2004
S. mansoni protein kinase C 1 (SmPKC1)	Bahia *et al.*, 2006
S. mansoni Smad1B (SmSmad1B)	Carlo *et al.*, 2007
S. mansoni cytoplasmic protein-tyrosine kinase (SmFes)	Bahia *et al.*, 2007
S. mansoni insulin receptor 1 and 2 (SmIR1, SmIR2)	Khayath *et al.*, 2007
S. mansoni Ste20-like kinase (SmSLK)	Yan *et al.*, 2007
S. mansoni nuclear receptor R4 (SmNR4A)	Wu and LoVerde., 2008
S. mansoni ecdysone-induced protein 78 (SmE78)	Wu *et al.*, 2008
S. mansoni cAMP-dependent protein kinase (SmPKA-C)	Swierczewsk and Davies, 2009
S. mansoni protein kinase C β(PKC β)	Ludtmann *et al.*, 2009
S. mansoni bone morphogenetic protein (SmBMP)	Freitas *et al.*, 2009
S. mansoni Zinc Finger Protein (SmZF1)	Drummond *et al.*, 2009
S. mansoni glucose transporter 1 and 4 (SGTP1 and SGTP 4)	Krautz-Peterson *et al.*, 2010
S. mansoni p38 mitogen-activated protein kinase (p38MAPK)	Ressurreição *et al.*, 2011a
S. mansoni Tyrosine kinase 6 (SmTK6)	Beckmann *et al.*, 2011
S. mansoni G protein-coupled receptor (SmGPR-3)	El-Shehabi *et al.*, 2012
S. mansoni cAMP-dependent protein kinase (PKA)	de Saram *et al.*, 2013

Reproduced from Bahia *et al.*, 2006, adapted by Ludtmann (2008) and updated.

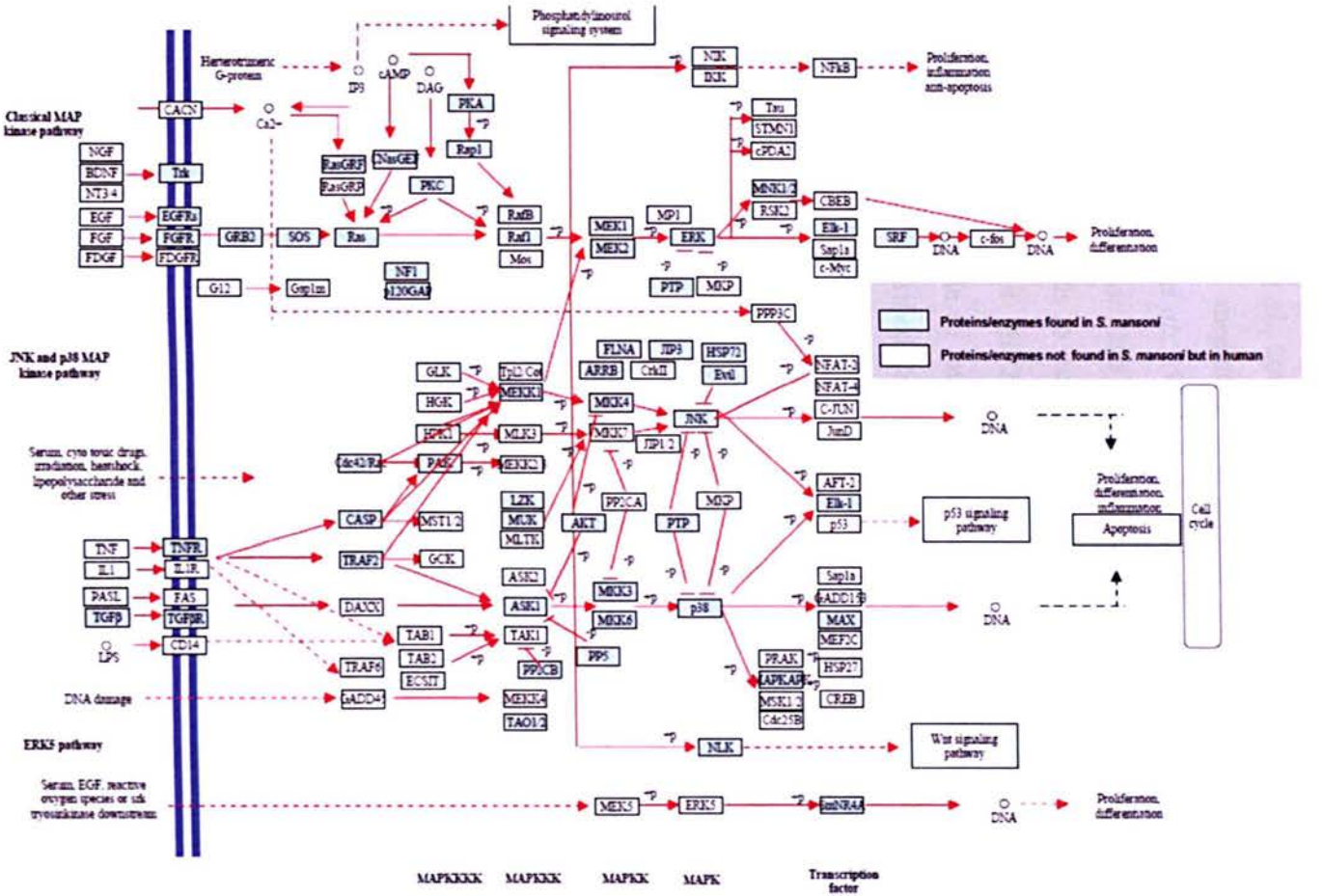

Figure 1.8- The *S. mansoni* MAPK and PKC signalling pathway. Diagram showing the signalling pathways of *S. mansoni* with components found in the schistosome genome shown in blue. The white boxes depict the components present in the human MAPK pathway but not present in the *S. mansoni* pathway. Obtained from Berriman *et al.* (2009), supplementary figure 9

Some characterized kinases in *S. mansoni* seem to be involved with SmRK (*S. mansoni* receptor kinase) signalling, comprising divergent members of the transforming growth factor β (TGF-β) family. SmRKs possibly respond to host growth factors such as those that regulate cell migration, differentiation, adhesion and apoptosis of host cells (reviewed in Osman *et al.*, 2004). SmRK1 is present on the surface of the parasite and may be important in mediating host-parasite interactions associated with parasite development (Davies *et al.*, 1998). Sm14-3-3ε is a cytoplasmic protein associated with TGF-β (McGonigle *et al.*, 2001a) and McGonigle *et al.* (2002) determined that Sm14-3-3ε overexpression leads to increased TGF-β signalling, whereas eukaryotic initiation factor 2 alpha subunit (eIF2α) expression leads to TGF-β inhibition. Smads are signalling proteins able to interact with TGF-β receptor molecules. Both *S. mansoni* Smads originally identified (SmSmad1 and SmSmad2) and SmRK, are found in the same developmental stages (lung stage and adult) of the parasite (Davies *et al.*, 1998; Beall *et al.*, 2000; Osman *et al.*, 2001). SmSmad4 was localized to epithelial tissues surrounding the gut and vitelline lobules in female worms and in the subtegumental tissues and muscle layers of male worms; this protein interacts with schistosome SmSmad1 and SmSmad2 (Osman *et al.*, 2004). These authors showed that the interaction with SmSmad2 was dependent on the receptor-mediated phosphorylation of SmSmad2 and that several phosphorylation sites for extracellular signal-regulated kinase 1/2/ (Erk1/2) kinases were identified in the SmSmad4 linker region.

The *S. mansoni* homologue of the FK506-binding protein called FKBP12 (Sm-FKBP12) is a direct partner of SmRK1 and both are present and interact in the female gonads (Knobloch *et al.* 2004). FKBP12 influences a variety of signal transduction pathways that regulate cell division, differentiation, and ion homeostasis (Chen *et al.*, 1997). Among these, TGF-β signalling and calcineurin phosphatase activity are modulated by FKBP12 *via* binding to TGF-β family type I receptors (TGFβR-I) or to the calcineurin subunit A, respectively (Chen *et al.*, 1997).

However, other signalling proteins identified participate in several different pathways and functions. SMA3 is a Ca^{2+}-ATPase homologue found in the adult tegument that might help control Ca^{2+} homeostasis within this region and play a role in signal transduction at the host-parasite interface (Da'dara *et al.*, 2001). SchP2X is a receptor related to the ATP ionic channel opening (Agboh *et al.*, 2004), whereas SmRhoI (Santos *et al.*, 2002, Vermeire *et al.*, 2003) is a GTPase that possibly

participates in cytoskeletal organization, gene transcription, the cell cycle and membrane transport and is highly expressed in female worms (Vermeire *et al.*, 2003). The SmMAK16 protein contains a nuclear signalling portion and a site for casein kinase 2 phosphorylation; it targets protein transport to the nucleolus and regulates biogenesis of the ribosome 60S subunit as well as regulating the cell cycle and is highly expressed in female worms (Wickner, 1988; Milhon *et al.*, 2000). SmRXR are nuclear receptors and gene transcription activators; the SmRXR gene is constitutively expressed and thus must play multiple roles throughout the schistosome life-cycle (Freebern *et al.*, 1999a, b; Fantappié *et al.*, 2001). SmFTZF1 is another nuclear receptor, with a highly conserved DNA binding domain, thought to be involved in developmental and sexual differentiation (de Mendonça *et al.*, 2002). SmPKC1 is β1-type protein kinase C that was found associated with the ridge cyton and excretory vesicles in sporocysts, while in skin-stage schistosomula SmPKC1 was clearly expressed in the acetabular gland, tegument, and duct (Bahia *et al.*, 2006). Ludtmann *et al.* (2009) identified, for the first time, PKC to be a regulator of *S. mansoni* sporocyst development.

Several protein tyrosine kinases (PTKs) have also been identified and characterized in *S. mansoni*. The PTKs are important molecules for intra- and inter-cellular communication as well as for cell survival in eukaryotes, playing a major role in signal transduction processes (Hanks *et al.*, 1988). SER, SmRTK-1, SmIR-1 and SmIR-2 are receptor tyrosine kinases (RTKs) (Ramanchadran *et al.*, 1996; Vicogne *et al.*, 2003; Ahier *et al.*, 2008) and TK5, TK4, TK3 are non-receptor tyrosine kinases (NRTKs) (reviewed by Bahia *et al.*, 2006). The SER protein is a tyrosine kinase similar to epidermal growth factor receptor (EGFR) family members (Vicogne *et al.*, 2004) and is present predominantly in the muscle of adult male and female worms (Ramachandran *et al.*, 1996); this suggests that it could participate in signal regulated muscle development or function in schistosomes. SmRTK1 is an insulin receptor (IR), probably with a role in male-female communication, and seems to be involved in the recognition of a male pheromone signal necessary for the development of the female ovaries (Vicogne *et al.*, 2003). The preferential localization of SmRTK1 in germinal cells of sporocysts and in oocytes could point to a role for this protein in differentiation. SmIR-1 is also a tyrosine kinase, similar to family members of IR, which might regulate glucose uptake. Immunohistochemical studies have shown that SmIR-1 is mainly expressed at the basal membrane of the tegument in adult worms (Dissous *et al.*, 2007b). Of the NRTKs, SmTK5 and SmTK3 are orthologues of Src family members, and SmTK4 of

Syk family members. SmTK3 is predominantly expressed in the reproductive organs such as testes and ovaries as well as the vitellarium and seems to play a role in signal transduction pathways organizing the cytoskeleton of gonads of schistosomes (Kapp *et al.*, 2004). SmTK5 is also expressed in adult worms and, furthermore, occurs in the free-living larval stages probably with a role in embryogenesis (Kapp *et al.*, 2001). SmTK4, may play a role in germ cell development, and is present in larval stages and adult schistosomes; significant levels of this protein were detected in oocytes and in spermatocytes (Knobloch *et al.*, 2002). A further Src kinase, SmTK6 was recently found to be an upstream interaction partner of SmTK4 and a MAPK-activating protein thought to be involved in the regulation of oogenesis and spermatogenesis (Beckmann *et al.*, 2010).

Genes encoding MAPK signalling molecules are also present in schistosomes but few members of the MAPK pathway have been studied in schistosomes. Schussler *et al.* (1997) identified three putative members of the RAS-ERK signalling pathway, RAS, a MAPK and a GAP protein, implicated in sexual maturation of female schistosomes and egg production. In addition, a MAP4K named SmSLK (*S. mansoni* Ste20-Like Kinase) was identified and found expressed mainly in the tegument of adult worms (Yan *et al.*, 2007). SmSLK has a conserved GCK (germinal center kinases) structure homologous to the mammalian kinase LOK and SLK proteins, which have been demonstrated to possess the capacity to activate the MAPK/Jun N-terminal kinase (JNK) pathway in human embryonic kidney (HEK) cells as well as in *Xenopus* oocytes (Yan *et al.*, 2007). Phylogenetic analysis of these proteins in *S. japonicum*, developed by Wang *et al.* (2006) confirmed the evolutionary conservation of the MAPK signalling pathways and facilitated the *in silico* identification of several MAPK pathway member genes, including ERK, JNK, Sja-DSP, MRAS and RAS. Moreover, studies of the transcriptome and proteome of *S. japonicum* developed by the *Schistosoma japonicum* Genome Sequencing and Functional Analysis Consortium (2009) identified a p38 MAPK, and an intact downstream cascade for ERK-like members composed of the Ras →Raf→ERK signalling pathway, including FGF- and EGF-receptors. These signalling components shared high identity with mammalian orthologues, which means that schistosomes, in addition to using their own pathways, might exploit host growth factors as developmental signals. More recently, active p38 MAPK was biochemically characterized in miracidia and early-sporocysts of *S. mansoni* revealing functions in ciliary beat and in the rate of sporocyst transformation with activity associated with

regions including the tegument, neural mass and germinal cells (Ressurreição *et al.*, 2011a, b). Furthermore, immunodetection of active cyclic AMP (cAMP)-dependent protein kinase/protein kinase A (PKA) in *S. mansoni* adults revealed a role of this protein in motor activity, neuronal communication and possibly interplay between these two systems (de Saram *et al.*, 2013).

Clearly a better understanding of PKs, particularly the evolutionary conserved MAPK and PKC signalling pathways, including their function and activation patterns, in schistosomes would accelerate our understanding the parasite biology.

1.5 Protein Kinase C (PKC) family

The PKC family is part of the AGC subgroup of closely related ePKs. Protein kinase C was the first protein kinase to be discovered in mammals (Inoue *et al.*, 1977). Firstly isolated from rat brain, it required Ca^{2+} for phosphorylation *in vitro* and further research revealed it to be a serine/threonine kinase that could be activated by phosphatidylserine (PS) and diacylglycerol (DAG) in the presence of Ca^{2+} (reviewed by Nishizuka, 1986). Eventually it was shown that the PKC identified was in fact three different isoforms, α, β, and γ (Huang *et al.*, 1989). Several research groups since discovered new PKCs and presently, the PKC family comprises at least 12 mammalian isoenzymes with a broad range of tissue distribution and differential cellular localization; not all cells express all variants, but normally express more than one form (Mellor and Parker, 1998). PKCs are grouped into three classes according to their structure and ability to bind co-factors (the presence or absence of motifs dictate cofactor requirements for optimal catalytic activity); conventional, novel and atypical PKCs (cPKC, nPKC and aPKC, respectively) (Figure 1.9).

Classical and novel PKCs contain two diacylglycerol (DAG)-binding sites (C1 or 'cysteine rich' domains), while atypical isoforms contain only a single C1 domain that cannot bind DAG or phorbol esters (Newton, 2001). Like DAG, the tumour promoting phorbol ester 12-myristate 13-acetate (PMA) can stimulate cPKC/nPKC phosphorylation in various species (Newton, 2001). GF109203X (Bisindolylmaleimide I) is a potent ATP-competitive PKC inhibitor with greater selectivity than staurosporine and commonly used for studying PKC signal transduction pathways (Toullec *et al.*, 1991). It has been suggested that a group of PKC-related kinases (PRK) are also part of

the PKC family (Mellor and Parker, 1998). In addition, another serine/threonine kinase activated by PMA and DAG called protein kinase D (PKD) could be part of the PKC family, however this kinase is 41% homologous with myosin light chain kinase (MLCK) and its catalytic domain is related to the CaMKII-like protein kinases; both its substrate specificity and sensitivity to inhibitors are unlike those of the PKC family (Valverde *et al.*, 1994; Johannes *et al.*, 1995; Newton, 2001).

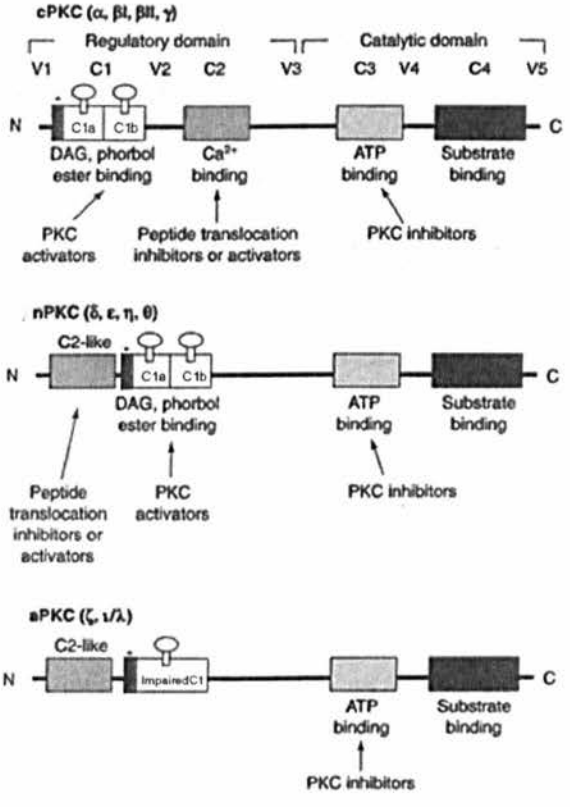

Figure 1.9 – The primary structure of conventional, novel and atypical PKCs (cPKC, nPKC, aPKC, respectively). The catalytic domain of PKC is conserved; the three subgroups have different regulatory domains. The cPKCs share all typical regulatory features: the autoinhibitory pseudosubstrate motif (*), -DAG-binding C1 domains, calcium binding domain C2 and the V5 region in the kinase domain. nPKCs lack the calcium-binding motif but contain an extended N-terminal domain that can receive regulatory signals, they are still regulated by DAG and possess a V5 region in the kinase domain. aPKCs only have a pseudosubstrate, and impaired C1 domain, and a kinase domain containing the V5 motif. The catalytic activity of atypical PKCs is independent of DAG and calcium, mainly regulated through intracellular localization, which is regulated by interaction with regulatory proteins and nuclear localization/nuclear export signals (NLS/NES) in their regulatory domain. Image adapted from Way *et al.*, 2000.

1.5.1 PKC structure

The structure of PKC isozymes includes four conserved domains referred to as C1-C4, which are interrupted by variable regions V1-V5. PKCs are monomeric and

have between 592 and 737 amino acids in mammals, giving molecular weights between 67 kDa and 83 kDa. The C1 domain of cPKCs and nPKCs consists of two cysteine and histidine rich sequences C1a and C1b resembling a zinc-finger motif common to metalloproteins and DNA binding proteins that function in transcriptional regulation, however there is little evidence of PKC DNA-binding proteins that function as transcriptional regulators (Reviewed by Liu and Heckman, 1998). These zinc-finger motifs are responsible for the organization of two Zn^{2+} ions (Bishop *et al.*, 1991; Gschwendt et al., 1991; Quest *et al.*, 1992). Mutational and deletion analysis, revealed a phorbol ester/DAG binding site in the C1 domain (Sharkey and Blumberg, 1985; Kaibuchi *et al.*, 1989). The C2 domain binds anionic lipids (PS) in a Ca^{2+} dependant manner (Shao *et al.*, 1996). This domain is not present in PKD, aPKCs, and only in an impaired version exists in nPKCs. In addition, the receptor for activated PKC 1 (RACK1), which mediates the transport of activated PKC to cellular compartments, can bind the C2 domain of PKCβ (Rodriguez *et al.*, 1999). This suggests a general role for the C2 domain in the regulation of cellular targeting of PKC (Mellor and Parker, 1998). The pseudo-substrate site is found near the N-terminus of the C1 domain in cPKCs, nPKCs and aPKCs; this region interacts with the kinase (catalytic) domain to prevent intramolecular activation of PKC (House and Kemp, 1987; Mellor and Parker, 1998). The V5 region is a very short (~50 amino acid) C-terminal sequence present in all PKCs.

1.5.2 Conventional/classical PKC (cPKC)

Conventional PKCs were the first to be characterized and are the most studied and best understood of all PKC groups. The cPKCs require phosphatidylserine (PS), DAG and Ca^{2+} for activation (Takai *et al.*, 1979). Their structure contains an autoinhibitory pseudosubstrate motif, two repeated zinc-finger motifs C1a and C1b of the DAG domain (C1), a Ca^{2+} binding domain (C2), a catalytic (kinase) domain containing ATP and substrate binding sites, and the V5 region. Four cPKCs have been identified: PKCα, βI, βII and γ (Parker and Murray-Rust, 2004). The different isozymes are encoded by different genes; however, the PKCβ isoforms are derived from alternate splicing of a messenger RNA generating two isoforms (βI and βII) which only vary at the V5 C-terminal region (Coussens *et al.*, 1987). It has been suggested that V5 governs protein-protein interaction and PKC localization since PKCβI and PKCβII are

differently located in human U937 monocytic cells (Kiley and Parker, 1995; Mellor and Parker, 1998). Phorbol esters such as PMA induce the phosphorylation of cPKCs in cells as it mimics DAG in the plasma membrane (Castagna *et al.*, 1982).

1.5.3 Novel PKC (nPKC)

Novel PKCs are Ca^{2+} independent but require DAG/phorbol esters and PS in order to be phosphorylated. Calcium independence is a consequence of nPKCs lacking a functional C2 region (Newton, 2001). The nPKCs contain an autoinhibitory pseudosubstrate motif, two repeated zinc-finger motifs C1a and C1b in the DAG domain (C1), a catalytic (kinase) domain containing ATP and substrate binding sites, and the V5 C-terminal region (Coussens *et al.*, 1987). Four isotypes have been identified, PKCδ, ε, η, and θ.

1.5.4 Atypical PKC (aPKC)

This class was first described from *in vitro* cultured COS-7 cells by Ono *et al.* (1989). These isoforms are $Ca^{2+}$and DAG/phorbol esters insensitive as they lack a fully functioning C1 domain and a complete C2 domain (reviewed by Mellor and Parker, 1998). Two mammalian aPKCs have been identified: ι/λ (human, mouse respectively) and ζ.

1.5.5 PRK

The PRKs are the most recently discovered and define a fourth group consisting of at least three members (PRKs 1-3) (Mellor and Parker, 1998). Like aPKCs, PRKs are insensitive to Ca^{2+} and DAG/phorbol esters (Mukai *et al.*, 1994; Palmer and Parker, 1995). PRK1 (PKN) and PRK2 can be activated by RhoA GTPase, suggesting a general property of this group (reviewed by Mellor and Parker, 1998).

1.5.6 Protein kinase D or mouse PKCμ, the not so real PKC

This serine/threonine kinase is activated by PMA and DAG and was identified by Valverde *et al.* (1994) who at the time could not classify it into the three main PKC subgroups, so it was named PKD. It has since been shown that the mouse isotype for

PKD is PKCμ. It should be noted that many researchers do not refer to a separate PKD subgroup (Newton, 2001). However, other studies revealed that this kinase is 41% homologous with myosin light chain kinase (MLCK) and examination of the PKD catalytic domain shows that it is related to the CaMKII-like protein kinases and both its substrate specificity and sensitivity to inhibitors are unlike those of the PKC family (Valverde *et al.*, 1994; Johannes *et al.*, 1995). Hence the identification of DAG/PMA – responsive proteins raises the need for caution in the interpretation of studies, especially those that solely use phorbol esters as an investigative tool without the use of specific inhibitors and other techniques (Mellor and Parker, 1998).

1.5.7 PKC maturation/activation

For PKC to be catalytically competent, a series of ordered, tightly coupled, and constitutive phosphorylations must occur as only phosphorylated PKCs can transduce signals within the cell (Mellor and Parker, 1998) (Figure 1.10). Recent studies have revealed new players in this maturation process: heat shock protein-90 (Hsp90) which interacts with a specific PKC motif is essential to allow phosphorylations to occur and mTOR complex 2 (mTORC2) whose integrity is required for priming phosphorylations (Newton, 2010). An orthologue of Hsp90 exists in *S. mansoni* (Smp_072900) showing 77% homology to its human counterpart. The earliest identified step in the maturation of conventional and novel PKC is the binding of the chaperone HSP90 and the co-chaperone Cdc37 to a molecular clamp in the kinase domain formed by a conserved PXXP motif (Newton, 2010).

PKC goes through three functional phosphorylations to take on the mature form (Karanen *et al.*, 1995; Newton, 2010). In the absence of stimulation PKCs remain catalytically inactive due to the pseudosubstrate domain and are localized in the cytosol. Upon cell stimulation PKC associates with the membrane where 3-phospho-inositide-dependent kinase-1 (PDK-1) binds and phosphorylates a threonine residue (Thr500 for PKCβII) in the PKC activation loop (Mellor and Parker, 1998). This phosphorylation triggers two autophosphorylation events at the C-terminus when PDK-1 is released; one at Thr641 in the turn motif and one at Ser660 in the hydrophobic motif (for PKCβII) which regulates its subcellular distribution (Dempsey *et al.*, 2000; Newton, 2001). The fully phosphorylated, catalytically competent PKC is then released into the cytosol where it stays inhibited by the pseudo-substrate region. Activation next occurs *via*

hydrolysis of phosphatidylinositol 4,5-biphosphate (PIP_2) by phospholipase C (PLC) which generates DAG and inositol triphosphate (IP_3) (Fig 1.10). DAG fills a broad hydrophilic groove between two hydrophobic beta sheets created by the zinc finger motifs in the C1 domain, and presents a uniform hydrophobic surface to the membrane (Zhang *et al.*, 1995). Then, IP_3 triggers Ca^{2+} release from Ca^{2+} stores into the cytosol. Released Ca^{2+} binds the C2 domain of classical PKCs whereas DAG binds the C1 domain of cPKCs and nPKCs increasing the affinity of membrane PKC to phospholipids. This causes both translocation of PKC to the membrane and conformational changes that displace the pseudosubstrate from the catalytic domain thereby enabling the PKC to phosphorylate protein substrates (Dempsey *et al.*, 2000; Newton, 2001; Newton, 2003; Newton, 2010). PKC is rapidly degraded by membrane bound proteases and chronic activation for over than one hour leads to depletion of PKC in the cell and attenuation of the signal (Gould and Newton, 2008).

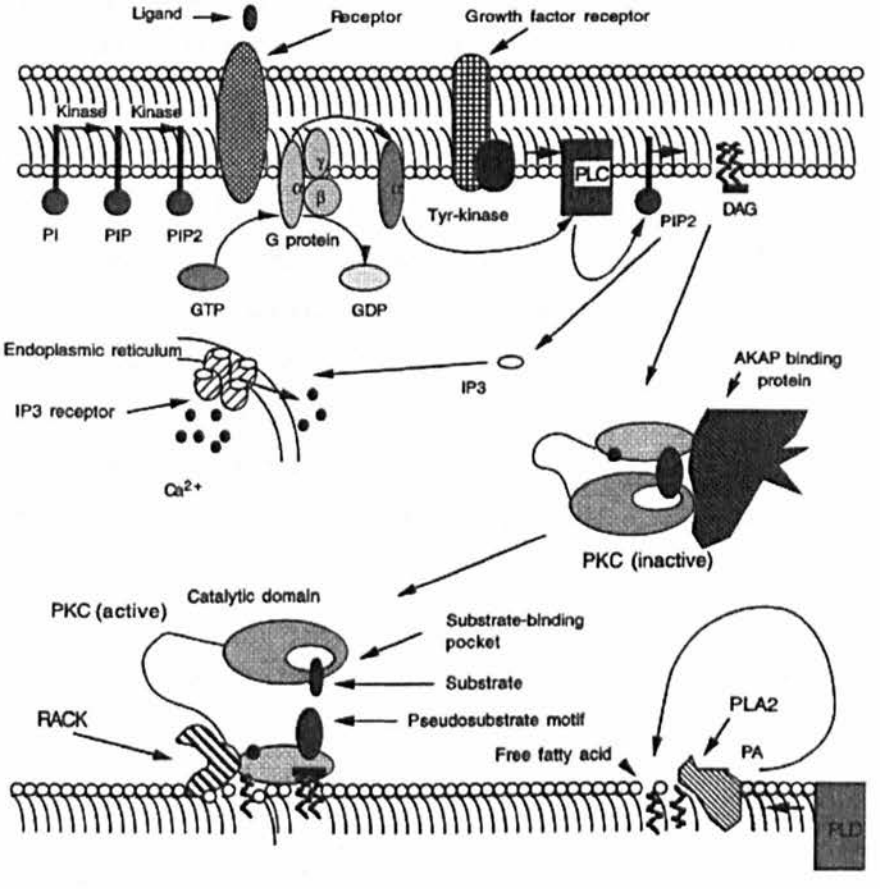

Figure 1.10 - PKC activation in mammalian systems. The fully phosphorylated PKC then released into the cytosol is auto-inhibited by the pseudo-substrate region. Meanwhile DAG is a product of PIP_2 which has been hydrolysed by PLC. PKC is then recruited to the membrane by DAG, PS and Ca^{2+}. The binding of DAG and PS provides energy, which expels the pseudo-substrate and allows a downstream activation of a substrate. Image adapted from Liu and Heckman (1998).

The control of PKC activity especially for the βII isozyme has been broadly studied in detail in eukaryotic cells and is mainly regulated through three distinct phosphorylation events (Karanen *et al.*, 1995). Antibodies specifically recognising the phosphorylated forms of PKCs are available and are employed to individually study the catalytically active form of the different PKCs.

1.5.8 Roles for PKCs, particularly in lower organisms

Protein kinase C has been linked to many cellular functions including growth and development and has been studied in a wide range of organisms (Nishizuka, 1986). In lower organisms, such as the budding yeast *Saccharomyces cerevisiae*, the simplest of all PKCs exists. *S. cerevisiae* contains a sole PKC (Pkc1) which shows all of the elements of the different PKC families in one enzyme demonstrating the age and fundamental importance of this protein kinase (Mellor and Parker, 1998; Parker and Murray-Rust, 2004). At 132 kDa it is much larger than mammalian PKCs due to is extended regulatory domain; in mammalian PKCs the different regulatory domains are differentially distributed between various isotypes, suggesting this protein to be an archetypal PKC (Figure 1.11). The *S. cerevisiae* Pkc1 has many roles in this organism from osmotic and cell cycle regulation to control of the thermal shock response (Levin *et al.*, 1990; Levin and Bartlett-Heubusch, 1992; Kamada *et al.*, 1995). In the freshwater coelenterate *Hydra vulgaris*, pharmacological inhibition of the PKC pathway blocks head regeneration after decapitation (Cardenas *et al.*, 2000) and in the sea urchin, *Strongylocentrotus purpuratus*, PKC activation with PMA induces *in vitro* metamorphosis (Amador-Cano *et al.*, 2006). In vertebrates such as *Xenopus laevis*, insulin signalling mediated *via* PKCζ is important in oocyte development (Dominguez *et al.*, 1992) and in rat (*Rattus norvegicus*) and bovine oocytes pharmacological stimulation of PKC (with PDDβ or PMA) induces rapid nuclear maturation (Aberdam and Dekel, 1985; Rose-Hellekant and Bavister, 1996; Mondadori *et al.*, 2008).

Clues to the evolution of the PKC superfamily come mainly from the study of *C. elegans*, where PKC activation with PMA is known to cause uncoordinated movement and growth arrest. The *C. elegans* PKC-3, which has high homology to mammalian aPKCs, has been shown to play an important role in early embryogenesis (Tabuse, 2002). Furthermore the *C. elegans* nPKC, PKC1, is present in the sensory neurons and interneurons revealing roles in regulation of sensory signalling (Land *et al.*, 1993;

Okochi *et al.*, 2005). In the sea hare, *Aplysia californica*, two PKC isoforms (ApI and ApII) have been found highly expressed in the nervous tissue and under some circumstances 5-HT-dependent learning-related facilitation/synaptic plasticity of sensorimotor synapses requires the activity of protein kinase C (PKC) revealing important roles for PKC in memory and learning (Sossin *et al.*, 1993; Villareal *et al.*, 2009). The simplicity of PKC isoform distribution in *A. californica* makes this mollusc an attractive animal for understanding the differential regulation and physiological activities PKCs (Sossin *et al.*, 1993). Interestingly, in mammals, activation of an nPKC by excess glucose has been implicated in vascular complications; studies by Hiramatsu *et al.* (2002) in embryos of hyperglycaemic diabetic mice during neural tube formation suggests that hyperglycemia just before organogenesis activates the PKC cascade and is correlated with congenital defects. These examples are a selection of studies, which signify the importance of PKC in development, growth and other important functions of multicellular organisms.

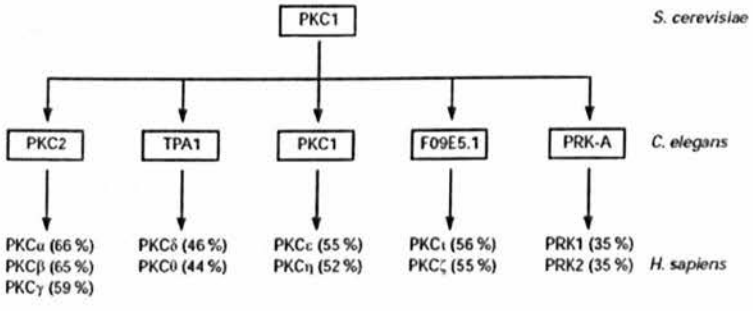

Figure 1.11 - Expansion of the PKC family. Comparison between the PKC gene from the budding yeast *S. cerevisiae* with the five PKC genes from the nematode *C. elegans* and the eleven PKC genes from *Homo sapiens*. Each gene corresponds to a specific subgroup of the PKC superfamily both by overall similarity and protein architecture. The diagram shows the percentage similarity the *C. elegans* PKCs and their corresponding human isotypes. Image from Mellor and Parker, 1998.

Since the early 1990s studies to understand the functional importance of PKC in *S. mansoni* development were attempted. For instance, Wiest *et al.* (1992) examined the changes in PKC enzymatic activity during the *S. mansoni* maturation, showing that the activity of a Ca^{2+} dependent PKC was greater in adult worms than in larval stages. Moreover, PKC activity was detected in the tegument of *S. mansoni* adult worms, and the PKC activator PMA disrupted the tegument integrity (Wiest *et al.*, 1994). Years

later, Bahia *et al.* (2006) identified the first PKC isoform in *S. mansoni* (SmPKC1) and structural analysis revealed its similarity to the classical subfamily showing that SmPKC1 expression was developmentally regulated with higher levels of protein expression in sporocysts. In our laboratory, Ludtmann *et al.* (2009) studied PKC activity during *S. mansoni* miracidia to sporocyst transformation, showing the successful use of an anti-phospho PKC Ser660 polyclonal antibody raised against mammalian PKCβ to detect and localize an *S. mansoni* PKC of ~78 kDa. However, biochemical and functional characterization of *S. mansoni* PKC isoforms especially in human infective and dependent stages has not previously been studied further.

1.6 Mitogen-Activated Protein Kinases (MAPKs)

The MAPKs are a family of proteins that play essential roles in virtually all eukaryotes acting as regulators of gene expression but also cellular function independent of gene expression. They transmit extracellular stimuli, such as growth factors, hormones, cytokines and various environmental stresses (reviewed in Roux and Blenis, 2004; Krens *et al.*, 2006). MAPKs are involved in tissue morphogenesis, cytoskeletal rearrangement, proliferation, differentiation, apoptosis, immune responses, and adaptation/stress-response to name a few (Chang and Karin, 2001; Pearson *et al.*, 2001; Henklova *et al.*, 2008). Virtually all eukaryotic cells possess MAPKs and to-date the microsporidium *Encephalitozoon cuniculi* is the only eukaryote that is apparently lacking any MAPKs (Miranda-Saavedra *et al.*, 2007). The MAPK superfamily, evolved 1.0 - 1.5 billion years ago (Kültz and Berge, 1998) and comprises proline-directed serine/threonine kinases that are classified based on the primary amino acid sequence within the catalytic domains (Hanks, 2003; Coulombe and Meloche, 2007).

The multiple MAPK pathways are neatly organized by scaffolding proteins, which allow cells to respond differently to divergent inputs. All MAPK pathways characterized in higher organisms involve sequential phosphorylation of three component modules consisting of three kinases; MAPK kinase kinases (MAPKKKs, MKKKs, Ste11-like kinases) which activate MAPK kinases (MAPKKs, MKKs, Ste7-like kinases), which in turn activate specific MAPKs (Figure 1.12) (Widmann *et al.*, 1999; Bardwell and Shah, 2006). Many MAPK cascades have been expanded to include a fourth tier involving the MKKKKs (Dan *et al.*, 2001). The existence of this sequential

phosphorylation is important for amplification and tight regulation of the transmitted signal. The MAPKKKs are serine/threonine kinases often activated through phosphorylation and/or as a result of their interaction with small GTP-binding proteins of the Ras/Rho family (Kolch, 2000; Dan, 2001). Active MAPKKKs phosphorylate serine and/or threonine residues in MAPKKs, which in turn phosphorylate tyrosine and/or threonine residues in a conserved 'TXY" motif within the MAPK activation loop (Marshall, 1995, Luo *et al.* 1996, King *et al.* 1998).

Once phosphorylated, MAPKs activate target proteins by phosphorylating them on serine and/or threonine residues followed by a proline; however, substrate selectivity is often conferred by specific binding sites located on physiological substrates (Seger and Krebs, 1995; Kallunki *et al.*, 1996; Yang *et al.*, 1998; Tanoue *et al.* 2000). Known substrates include transcription factors (Kallunki *et al.*, 1994 ; Dickens *et al.*, 1997), membrane and cytoplasmic proteins (Teis *et al.*, 2002), as well as other protein kinases (Tanoue *et al.*, 2000). MAPK signalling can also affect histone modification and have additional epigenetic effects (Yang *et al.*, 2003)

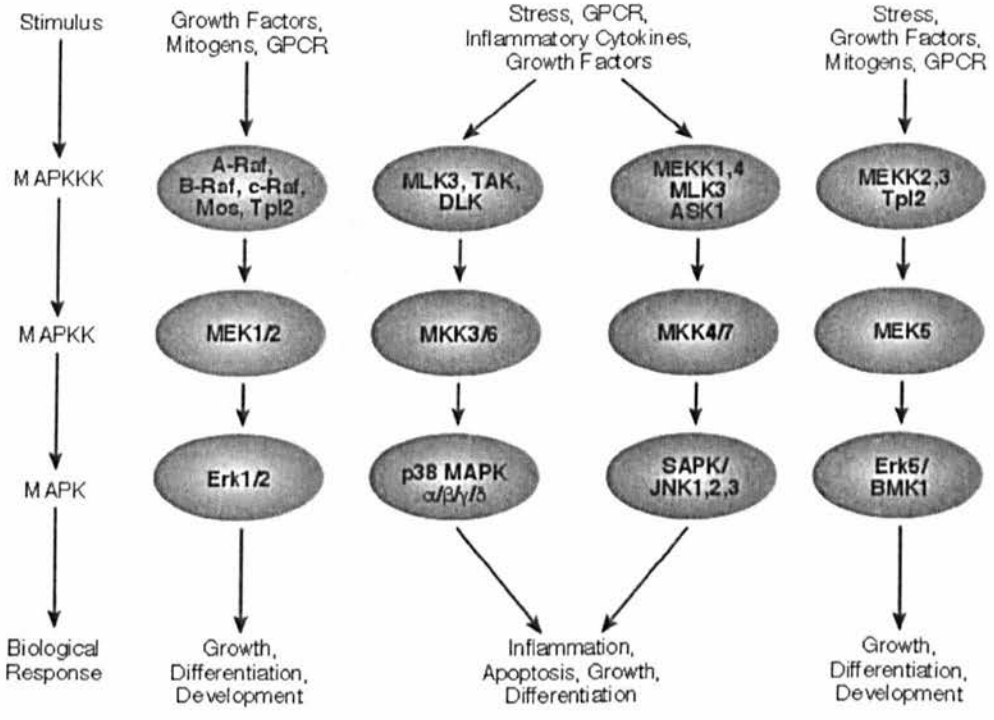

Figure 1.12 - The MAPK signalling cascade. Sequential activation of the three main components of the MAPK signalling pathway; ERK (extracellular signal-regulated kinase), JNK (c-Jun N-terminal kinase) and p38 that mediate functional cellular responses to extracellular stimuli through multiple receptors such as chemoattractant receptors, Toll-like receptors and cytokine receptors. The three-tiered kinase dynamic cascade (represented on the left) leads to activated MAPKs entering the nucleus to trigger immediate

early gene and transcription factor activation for cellular responses such as cytokine production, apoptosis and migration. Image from: http://www.cellsignal.com/reference/pathway/pdfs/ MAPK_Cascades.pdf.

Approximately 18 MAPK genes encompassing four subfamilies have now been identified in mammals (reviewed in Chen *et al.*, 2001). MAPKs are grouped into subfamilies on the basis of amino acid sequence similarity, mechanism of activation, and the type of MAPK cascade to which they belong. Four conventional MAPK subfamilies exist (Coulombe and Meloche, 2007). These conventional MAPK groups include: the extracellular signal-regulated kinases (e.g. mammalian ERK1 and ERK2, possessing a TEY motif at the phosphorylation lip), c-Jun-activated kinases (e.g., mammalian JNK1, JNK2, and JNK3 (TPY motif)), p38 stress response MAPKs (e.g., mammalian p38α, p38β, p38γ, and p38δ (TGY motif)), and the more recently identified larger kinases ERK3 (α and β), ERK4 (ERK1b), ERK5 (big MAPK-1; BMK-1), and ERK8 (TEY motif)) (Kyriakis *et al.*, 1994; Zhou *et al.*, 1995; Dan *et al.*, 2001; Chen *et al.*, 2001; Whitmarsh, 2010;) (Figure 1.12). Various dual-specificity protein phosphatases differentially dephosphorylate and thus deactivate the ERK, JNK or p38 MAPK enzymes. For instance, the phosphatase MKP2 can act on both ERK and JNK, while M3/M6 acts on JNK and p38 MAPK (Neel *et al.*, 1997; Ellinger-Ziegelbauer *et al.*, 1997).

1.6.1 Stress-activated protein kinases/c-Jun amino-terminal kinases (SAPK/JNK)

Stress-activated protein kinases (SAPK)/Jun amino-terminal kinases (JNK) are activated by environmental stresses such as UV-light and osmotic shock, inflammatory cytokines (TNF-α and IL-1β), growth factors and GPCR agonists (Galcheva-Gargova *et al.*, 1994; Hibi *et al.* 1993; Kyriakis *et al.*, 1994; Davis, 1994). As with the other MAPKs, the membrane proximal kinase is a MAPKKK, typically MEKK1–4, or a member of the mixed lineage kinases (MLK). MEKK 1-4 phosphorylates and activates the SAPK/JNK kinases by dual phosphorylation on tyrosine and serine/threonine residues within a conserved Thr-Pro-Tyr (TPY) motif (Kyriakis and Avruch, 1990; Kyriakis *et al.*, 1991). Alternatively, MKK4/7 can be activated by a member of the GCK family in a GTPase-independent manner (Kyriakis *et al.*, 1991). Like ERK1/2 and p38 MAPK, the JNKs may translocate to the nucleus following stimulation and regulate the activity of transcription factors (Mizukami *et al.*, 1997). A well-known substrate for

JNKs is the transcription factor c-Jun, which is phosphorylated on Ser63 and Ser73 (reviewed in Mercer and Pritchard, 2003), but several other transcription factors have been shown to be phosphorylated by the JNKs, such as ATF-2, NF-ATc1, HSF-1, and STAT3 (Chen *et al.*, 2001; Kyriakis and Avruch, 2001).

1.6.2 Extracellular-signal Regulated Kinase (ERK)

The ERK family of MAPKs is crucial for cellular maintenance and proliferation (Chong *et al.*, 2003). It can be activated by growth factors, mitogens, phorbol esters, serum, G-protein coupled receptors (GPCRs), cytokines, osmotic stress and microtubule disorganizers (reviewed in Lewis *et al.*, 1998). Raf (MAP3K or MEKK) once phosphorylated, activates MEK 1 and 2, which in turn phosphorylates ERK1 and ERK 2 (ERK1/2) within a conserved Thr-Glu-Tyr (TEY) motif in the activation loop (Campbell *et al.*, 1998; Roux and Blenis, 2004). Amplification through the ERK cascade is so large that activation of 5% of Ras is sufficient to induce total activation of ERK1/2 (Hallberg *et al.*, 1994). However the exact mechanism of Raf activation is still not characterized fully; it is known to require Ras binding as well as multiple phosphorylation events at the membrane (reviewed in Chong *et al.*, 2003). ERK1 and ERK2 of yeast were the first MAPKs to be identified (reviewed in Levin and Errede, 1995; Herskowitz, 1995). ERKs were also the first MAPKs shown to phosphorylate the transcription factor c-Jun, although later studies proved JNKs to be principally responsible for c-Jun phosphorylation (Pulverer *et al.*, 1991; Karin, 1995). Various studies show that phosphorylated ERK can also regulate activities of targets in the cytosol and then translocate to the nucleus where it phosphorylates a variety of transcription factors that regulate gene expression e.g. Elk-1 and GATA4 transcription factors (Gonzalez *et al.*, 1993; Lenormand *et al.*, 1993; Yang *et al.*, 1998; Babu *et al.*, 2000). A selective non-competitive inhibitor of the Raf/MEK/ERK signalling pathway is U0126, which inhibits MEK1/2 by direct action on its catalytic domain. Due to its unique mode of action, U0126 has been extensively studied in terms of its specificity and its mechanism of action in a variety of diseases including cancer (Zou *et al.*, 2012). Several proteins interact with members of the ERK cascade, including the scaffold proteins MP-1 and KSR and the modulators CNK and RKIP, resulting in stimulation or inhibition of the ERK1/2 cascade (reviewed in Peyssonnaux *et al.*, 2001). ERKs have also been studied in parasites. Two ERKs (ERK1/2) have been characterized in the

intestinal protozoan parasite *Giardia lamblia*, which seem to play distinct roles in encystation suggesting that these kinases play a critical role in trophozoite differentiation into cysts; however functional studies have yet to be performed (Ellis *et al.*, 2003). ERK-like proteins in *Taenia crassiceps* appear to be involved in molecular signalling during the interaction with the host (Escobedo *et al.*, 2010); and in transgenic *Trypanosoma brucei* expression of an ERK mutant that lacks the C-terminal extension produces a slow growth phenotype, associated with the appearance of cells with aberrant karyotype (Ellis *et al.*, 2004). U0126 (Favata *et al.*, 1998) and another compound, PD98059 are noncompetitive inhibitors of MEK1/2/5 and therefore prevent phosphorylation of ERK1/2/5 (reviewed in Ballif and Blenis, 2001); their development has aided ERK pathway research considerably. Because ERK1/2 signalling regulates cell proliferation, inhibitors of the ERK pathway have been explored as potential anticancer agents (Kohno and Pouyssegur, 2003). In addition, ERK is also a downstream target of other kinases including PKC (Goldberg *et al.*, 1997; Ho *et al.*, 1998; Sugden and Clerk 1998; Molkentin and Dorn, 2001).

In *S. mansoni*, Ras GTPase activator protein- (Ras-GAP) and ERK1/2-like proteins have been immunodetected with putative roles suggested in male-female interactions (Schußler et al., 1997; Osman *et al.*, 1999). Furthermore, activation of the *S. mansoni* EGFR, SER, by human EGF leads to ERK2 phosphorylation in *Xenopus* oocytes (Vicogne *et al.*, 2004) and hypothetical ERK pathways for *S. mansoni* and *S. japonicum* have been reconstructed *in silico* (Wang *et al.*, 2006; Berriman *et al.*, 2009; Andrade *et al.*, 2011) supporting that ERK signalling is intact in schistosomes. However, further characterization and functional studies of ERK in schistosomes have not previously been performed.

1.6.3 P38 Mitogen-Activated Protein Kinase (p38 MAPK)

The p38 MAPK pathway can be activated in response to environmental stress such as UV light, ionizing radiation, oxidative stress, temperature, changes in osmolarity, and by the FAS receptor ligand and cytokines (e.g. TNFα) (reviewed in Paul *et al.*, 1997). In mammals there are four different isoforms of p38 MAPK (p38α, p38β, p38γ, and p38δ) where p38α is the most abundant and widely expressed, but it is also the only isoform with a non-redundant function *in vivo* (for review see Kyriakis and Avruch, 2001). Activation of p38 MAPK is associated with phosphorylation at

Thr180/Tyr182 within the active site (Freshney *et al.*, 1994; Rouse *et al.*, 1994). This phosphorylation is mediated primarily by upstream MEK3 and MEK6, although *in vitro,* MEK4 may also contribute to p38 MAPK activation in the absence of MEK3/MEK6 (Chen *et al.*, 2001). It has been shown that p38 MAPK is present in both nucleus and cytoplasm of quiescent cells, but upon cell stimulation, the cellular localization of p38 MAPK can differ, either translocating from the cytoplasm to the nucleus (Quan *et al.*, 1995) or remaining in the cytoplasm (Ben-Levy *et al.*, 1998). Recent research shows that p38 MAPK translocates to the nucleus in response to DNA damage, which is triggered by a conformational change induced by phosphorylation within the active site. This specific nuclear translocation could be important for regulation of the G2/M cell cycle checkpoint and DNA repair (Wood *et al.*, 2009). It is likely that the intracellular distribution of p38 MAPK is associated with its substrate specificity and determined by the nature of the stimuli. P38 MAPK has been shown to phosphorylate several cellular targets depending on the stimulus. These include, transcription factors (ATF-1, ATF-2 and MEF-2), protein kinases (MnK, MAPKAPK2), death/survival molecules (Bcl2, caspases), cell cycle control factors (cyclin D1), cytosolic phospholipase A2, the microtubule-associated protein Tau, MEF2A, Sap-1, Elk-1, NF-κB, Ets-1, and p53 (reviewed in Kyriakis and Avruch, 2001). P38 MAPK also activates several MKs (MAPKAP kinases), including MSK1 and -2, MNK1 and -2, and MK2 and -3 (Tanoue *et al.*, 2000; Kyriakis and Avruch, 2001) These downstream kinases regulate cell growth, differentiation and cell death (Raingeaud *et al.*, 1995; Tanoue *et al.*, 2000; Kyriakis and Avruch, 2001).

Activation of p38 MAPK by dual phosphorylation often leads to cell differentiation. However, activation of p38 MAPK can also mediate cell death or induction of a G2/M cell cycle delay through UV irradiation and p53-dependent and independent mechanisms (Wood *et al.*, 2009). P38 MAPK also regulates cytokine production, playing a role in the production of IL-6 and possibly stabilizing erythropoietin production during hypoxic stress (Jeong *et al.*, 2005). Two relatively specific inhibitors exist for p38α and p38β, SB203580 and SB202190 these work by binding to the p38 MAPK ATP-binding pocket but do not inhibit p38 MAPK phosphorylation by upstream kinases (Lee *et al.*, 1999, 2000). The functional importance of p38 MAPK activation has been studied in several animal models using SB203580 and this compound has been shown to inhibit p38 MAPK *in vivo* (reviewed in Raingeaud *et al.*, 1995). In *S. mansoni* miracidia and sporocysts an active p38

MAPK-like protein was detected using antibodies raised against the phosphorylated form of human p38α and biochemically characterised showing specific p38 MAPK enzymatic activity, activation with anisomycin and inhibition with SB203580 (Ressurreição *et al.*, 2011a,b). Studies revealed that active *S. mansoni* p38 MAPK was mainly associated with cilia of miracidia and germ cells of developing mother sporocysts. Furthermore, p38 MAPK activation reduced miracidial swim speed and increased transformation rate, while pharmacological inhibition had the opposite effect (Ressurreição *et al.*, 2011a, b). No further functional studies on p38 MAPK activity in other schistosome life-stages have previously been performed.

1.7 Context of this study and aims of the research

In the life-cycle of *S. mansoni,* three developmental stages are of great importance for the successful infection, development and survival within the human host: the cercaria, schistosomule and adult worm, respectively. Upon invasion of the human host, schistosomes undergo complex developmental reprogramming processes necessary for survival and growth in a hostile new environment. Notable characteristics of this process include the complete transformation of surface membranes, dependence on haematophagy for energy, selective *de novo* expression of gene products and differentiation into morphologically and transcriptionally distinct adult male and female pairs capable of producing hundreds of eggs each day. Schistosomes can survive in humans for decades, a hallmark of the remarkably well-adapted relationship between these parasites and their hosts.

Although, little is known about the proteins that control the progression of the parasite through the various stages of its life-cycle it is anticipated that improved interventions for the control of schistosomiasis will be realised through a better understanding of how schistosomes exploit host nutrients and neuro-endocrine hormones and use signalling pathways for growth, development and maturation. In light of the potential impact that host molecules have on the developmental biology of schistosomes, the availability of the genomes for *S. mansoni, S. japonicum* and *S. haematobium* provides a rich resource for the identification of parasite molecules which may interact with the host and the identification of molecules with structural similarities

to important eukaryotic regulatory proteins. Hence, understanding the molecular mechanisms that underpin schistosome infection and those that maintain parasite homeostasis is of paramount importance in the search for novel anthelmintic drug targets and strategies.

Therefore, the aims of this study were to:

(i) Identify and detect evolutionarily conserved ePKs predicted in the *S. mansoni* genome with commercially available "smart" anti-phospho antibodies, with special interest in PKC and MAPK signalling proteins.

(ii) Biochemically characterize and localize activity of successfully detected kinases in different *S. mansoni* life-stages, with more attention towards those that are human infective or dependent.

(iii) Determine the functional roles of the detected protein kinases through pharmacological modulation and RNA interference studies.

(iv) Better understand how schistosomes exploit host molecules.

(v) Contribute to the current knowledge on schistosome molecular biology and provide novel methods for the study of signalling in schistosomes.

(vi) Provide important information that constitutes the first steps to catalogue the roles of these protein kinases in search for novel anthelmintic strategies and drug targets.

Chapter 2

General Materials and Methods

2.1 Antibodies and reagents

2.1.1 Antibodies

The primary (anti-rabbit) antibodies used to detect phosphorylated kinases in different *S. mansoni* life-stages were: anti-phospho-PKC (pan) (βII Ser660) polyclonal antibodies (#9371), anti-phospho-PKC (pan) (ζ Thr410) (190D10) monoclonal antibodies (#2060), anti-phospho-p44/42 MAPK (ERK1/2) (Thr202/Tyr204) monoclonal antibodies (#9101), anti-phospho PKC α/βII (Thr638/641) polyclonal antibodies (#9375), anti-phospho-p38 MAPK (Thr180/Tyr182) monoclonal antibodies (#4631) and anti-phospho-SAPK/JNK (Thr183/Tyr185) monoclonal antibodies (#4668) (Cell Signalling Technology, New England Biolabs, Hitchin, UK). The anti-phospho-MAP Kinase Kinase (MEK) 1/2 (Ser217/221) (#M7683) and anti-actin antibodies were purchased from Sigma-Aldrich (Poole, UK). The anti-rabbit horse radish peroxidase (HRP)-conjugated secondary antibodies were also purchased from Cell Signalling Technology. The Cy3 anti-mouse secondary antibodies and anti-rabbit Alexa Fluor 488 secondary antibodies were from Invitrogen (Thermo Fisher Scientific, Loughborough, UK).

2.1.2 Immunoprecipitation kits and other components

The p44/p42 MAPK (ERK1/2) (nonradioactive) immunoprecipitation and kinase assay kit was purchased from Cell Signalling Technology whereas the PKC Omnia kinase assay kit was from Invitrogen. The PKC catalytic subunit from rat brain was purchased from Calbiochem (Merck Chemicals, Nottingham, UK).

2.1.3 Inhibitors and activators

The synthetic PKC activator PMA (phorbol 12-myristate 13-acetate) was purchased from Cell Signalling Technology. The highly selective MEK1/2 inhibitor U0126 (1,4-diamino-2,3-dicyano-1,4-bis[2-aminophenylthio] butadiene), PKC inhibitor GF109203X (bisindolylmaleimide), and p38 MAPK inhibitor SB203580 (pyridinyl imidazole) were purchased from Calbiochem.

2.1.4 Other products and reagents

RPMI-1640 medium (RPMI), foetal bovine serum and streptomycin/penicillin antibiotics were purchased from Invitrogen. Precast Precise 10% Tris-HEPES acrylamide gels, 20x Tris-HEPES running buffer, HALT protease and phosphatase inhibitors, West Pico chemiluminescent substrate kit and Restore western blot stripping buffer were obtained from Pierce (Thermo Fisher Scientific, Loughborough, UK). Hybond nitrocellulose membrane was purchased from GE Healthcare Life Sciences (Amersham, UK); Vectashield mounting medium and the hydrophobic pen were from Vector Laboratories (Peterborough, UK). Page Ruler molecular weight markers were obtained from Fermentas (Fermentas Ltd., UK), whereas dimethyl sulfoxide (DMSO), Tween 20, Ponceau S, bovine serum albumin (BSA), phosphate buffered saline (PBS), SDS-6H molecular weight markers, silane-coated slides, cover slips, rhodamine phalloidin and all other general reagents were obtained from Sigma-Aldrich (Poole, UK). The 10x RIPA buffer and lambda phosphatase were purchased from Cell Signalling Technology and Invitrogen, respectively.

2.1.5 RT-qPCR and siRNA materials

SiRNA duplexes and primer oligonucleotides were obtained from Invitrogen. For the extraction of mRNA, the Dynabeads mRNA Direct Kit from Invitrogen was used due to the fact that it has been previously used to obtain quality mRNA from small quantities of developing *S. mansoni* sporocysts in *B. glabrata* snail tissue (Personal Communication - EMOP 2012 Symposium). Reverse transcriptase and cDNA wipeout were from the Quantitect Reverse Transcription kit and the SYBR Green assay was the Quantitect SYBR Green PCR Kit all obtained from Qiagen (Qiagen, Manshester, UK). The 1.5 ml RNase and Eppendorf DNase treated microfuge tubes were purchased from Fisher, while RNase and DNase treated pipette tips were purchased from VWR (Leicester, UK).

2.2 Ethics statement

Laboratory animal use was within a designated facility at the Natural History Museum (NHM) London, regulated under the terms of the UK Animals (Scientific Procedures) Act, 1986, complying with all requirements therein; regular independent Home Office inspections occurred. The experiments involving mice in this study were approved by the Natural History Museum Ethical Review Board and work was carried out under Home Office project licence 70/6834.

2.3 Maintenance of *S. mansoni* life-cycle

The *S. mansoni* used throughout this research originated from a well established Belo Horizonte strain which had been passaged routinely in *Biomphalaria glabrata* (intermediate host) and albino CD1 female mice (definitive host) at the Wolfson Welcome Biomedical Laboratories at the NHM. Standard procedures were used. To maintain the *S. mansoni* life-cycle, schistosome eggs were recovered from the liver and spleen of infected laboratory mice using standard maceration and sedimentation procedures and hatched, the emergent miracidia were subsequently used to infect *B. glabrata* (Puerto Rico strain, NHM Accession number 1742; 10 miracidia per snail). Snails were maintained at 27°C on a 12 h:12 h light-dark cycle and were fed round lettuce *ad-libitum*. Approximately 4 weeks post-infection, snails were placed in water under a non-heating light source to encourage the shedding of cercariae. Individual mice were then infected by paddling in water containing 200 cercariae, and 45 days post-infection and before mice start to show signs of illness animals were culled in CO_2 chambers and the liver and spleen removed to enable *S. mansoni* eggs to be recovered for continuation of the life-cycle.

For studies involving cercariae and schistosomules, *B. glabrata* infected with the same *S. mansoni* Belo Horizonte strain were obtained monthly from the Schistosomiasis Resource Centre at the National Institutes of Health–National Institute of Allergy and Infectious Diseases (NIH-NIAID), Rockville Biomedical Research Laboratory (USA) (Lewis *et al.*, 2008). Upon arrival the snails were separated in groups of ~50 individuals and kept in individual plastic containers with one litre of filtered tap water (FTW; filtered through a Brimak carbon filtration unit; Silverline, UK) and placed in an

incubator at 26°C with continuous dim light. Snail water was fully changed weekly during the pre-patency period and snails fed twice a week with fresh or air dried round lettuce cut roughly into $1cm^2$ pieces. In our hands, these *S. mansoni* infected *B. glabrata,* reach patency approximately 30 days post miracidial infection. Two days before scheduled shedding of cercariae, containers with snails were placed in opaque black plastic boxes, to reduce emergence of the parasite allowing cercariae numbers to build up within the snail tissues. After two days snails were removed from the dark and using plastic forceps were placed in 100 ml glass beakers with ~40 ml of FTW and left under cold-source light direct light for up to 2 h. Due to the infectious nature of cercariae the beakers were covered with the lid of a Petri dish to avoid snails from escaping during shedding. After cercariae emergence snails were removed from the glass containers with plastic forceps and placed back in their original containers.

2.3.1 Safety procedure for handling of cercariae and other infective material

Due to the infectious nature of *S. mansoni* cercariae several procedures were used in order to avoid contamination. Work surfaces were regularly cleaned with 80% ethanol, any spent snail water was placed in a 20 l plastic buckets with 2% Virkon for disinfection. Disinfected water was then disposed of after one week. Gloves, lab coats and safety spectacles were used all times and gloves were thicker and longer (3/4 length) for extra protection.

2.4 Isolation of *S. mansoni* for experimentation

2.4.1 Adult worm pairs

Adult worms were collected from mice by hepatoportal perfusion with physiological saline. Worm pairs were then carefully collected with tweezers or a small paint brush, gently washed twice with pre-warmed RPMI 1640 and either kept in pre-warmed RMPI 1640 at 37°C for further experimentation, frozen in liquid nitrogen and stored at –80°C for immunoprecipitation and enzyme activity studies, fixed in ice cold absolute acetone and stored at 4°C for immunohistochemistry, or processed for western blotting (Chapters 3, 4 and 5).

2.4.2 Cercariae

Cercariae were left to emerge from ~35-day infected snails in FTW under a cold-source light for 2 h. Next, the cercariae were carefully collected into 15 ml conical tubes with a glass Pasteur pipette and exposed to different treatments (Chapters 3, 6 and 7). Cercariae were then transformed to schistosomules (below), fixed in ice-cold absolute acetone and stored at 4°C for immunohistochemistry, or processed for western blotting.

2.4.3 Schistosomules

Cercariae were transformed mechanically into schistosomules, which were subsequently cultured *in vitro* and used for experiments (Chapter 8). The cercarial suspension (in water) was transferred into 15 ml centrifuge tubes, placed on ice for 15 min, and cercariae pelleted by centrifugation for 5 min at 95 x *g*. The supernatant was then discarded leaving 1 ml water in the tube and Eagles Basal Medium (BME) added to give a total 4 ml; the tube was then capped, gently mixed to re-suspend cercariae and placed at 37°C to encourage cercarial movement. The cercariae in BME were then vortexed for 5 min at maximum speed (at which time the colour of the phenol red indicator in the medium turned pink indicating change in pH due to release of cercarial acetabular gland contents) and tubes observed under a dissecting microscope to confirm successful tail detachment. To remove as many detached tails from the suspension as possible, Hanks Basal Salt Solution (HBSS) was added to a total volume of 7 ml, and tubes left on ice for 7 min before re-centrifuging for 2 min, the supernatant removed and the same process repeated 3 times. Around 10-20% of tails remained; however, this was our procedure of choice as it is the most natural and practical (when compared to Percol gradient separation). After the final HBSS separation, six 5 µl aliquots of the resultant suspension were removed to determine the number of schistosomules per ml using a dissecting microscope. Schistosomules were then left to settle to the bottom of the tubes for 15 min, most of the supernatant was discarded and the schistosomules were re-suspended in 5 ml BME supplemented with antibiotics, and transferred to a new sterile 15 ml tube; after a further 15 min the supernatant was removed and BME with antibiotics added to the desired volume. Finally, depending on the nature of the experiment, cercariae were either placed in wells of 24 well culture plates (Nunc) in BME for 12-24 h, or the medium was replaced with complete Basch's medium (Basch, 1981) (Appendix A) thereafter; this procedure was performed in a laminar flow hood

and schistosomules were maintained at 37°C and 5% CO_2. This protocol was an adaptation of a combination of different procedures (Colley and Wikel, 1974; Cousin *et al.*, 1981; Lazdins *et al*, 1982; Lewis, 1999).

2.5 Western blotting

Western blotting was performed according to our published methods (e.g. Ressurreição *et al.*, 2011a). *Schistosoma mansoni* cercaria, schistosomule or adult worm proteins were extracted in 1.5 ml microfuge tubes by adding an appropriate volume and concentration (1x for schistosomules and adult worms and 5x for cercariae) of RIPA buffer [20mM Tri-HCl (pH 7.5), 150mM NaCl, 1mM Na_2EDTA, 1mM EGTA, 1% NP-40, 1% sodium deoxycholate, 2.5mM sodium pyrophosphate, 1mM β-glycerophosphate, 1mM Na_3VO_4 and 1µl/ml leupeptin] and 1 µl of HALT protease/phosphatase inhibitor cocktail followed by homogenization on ice with a plastic microfuge pestle and motor. When necessary a 2 µl aliquot of the homogenate was removed for protein quantification using Bradford reagent and BSA as the protein standard (Bradford micro assay) and the appropriate volume of 5x SDS–PAGE sample buffer [62.5 mM Tris-HCl (pH 6.8), 2% (w/v) SDS, 2% (v/v) β-mercaptoethanol, 5% (v/v) glycerol and 0.0025% (w/v) bromophenol blue] was added to the remaining homogenate.

Samples were sonicated briefly (10 s), boiled for 5 min, placed on ice, 1 µl protease/phosphatase inhibitors added, and stored at −20 °C prior to electrophoresis. Samples with equal amounts of protein (12 µl) were separated on 10% Precise pre-cast SDS–PAGE gels at 140 V for approximately 50 min (or until the bromophenol blue tracking dye had reached the bottom of the gel) and transferred to nitrocellulose membranes at 20 V using a semi-dry electrotransfer unit (Bio-Rad). In all experiments, protein ladders were used. After transfer, membranes were washed in distilled water and stained with Ponceau S to confirm homogeneous transfer of proteins; they were then washed for 2 min in Tris-buffered saline (TBS) containing 0.1% (v/v) tween-20 (T-TBS) to remove staining. Membranes were blocked for 1 h in 5% (w/v) non-fat dried milk and washed in T-TBS prior to incubation with anti-phospho primary antibodies 1:1000 dilution (v/v) in T-TBS with 1% BSA, rocking overnight at 4°C. The next day, blots were washed with T-TBS (5 x 5 min washes) and incubated for 2 h at room

temperature with HRP-conjugated secondary antibodies (1:3000 in T-TBS) before washing membranes again 5 x 5 min each in T-TBS followed by exposure to West Pico chemiluminescent substrate. Immunoreactive bands were then visualized using a cooled CCD GeneGnome chemiluminescence imaging system (Syngene, Cambridge, UK) and relative band intensities quantified using associated GeneTools software. For all experiments, equal loading of proteins was checked by incubating blots with anti-actin antibodies (1:1000). For most experiments membranes were incubated with various antibodies, and when necessary blots were striped by agitating membranes in 20 ml Restore western blot stripping buffer for 3 h at room temperature prior to washing in T-TBS and incubating in an alternative antibody. In some cases, western blots were incubated in lambda protein phosphatase for 3 h prior to immunodetection to determine the specificity of the anti-phospho antibody. The relative density of the bands was determined by normalizing against the corresponding actin loading control.

2.6 Immunohistochemistry and confocal microscopy

The *S. mansoni* adults and schistosomules were fixed in ice-cold absolute acetone and stored at 4°C. For further preparation, parasites were transferred into 0.5 ml microfuge tubes and acetone was removed after pulse centrifugation, parasites were then washed twice with PBS and were further permeabilized in 0.3% Triton X-100 for 1 h and washed with PBS prior to blocking in 10% goat serum for 1 h. After a further wash in PBS, larvae were incubated with the relevant anti-phospho primary antibody (1:50 in 5% BSA) for 3 days on a microfuge tube rotator. The parasites were then washed twice in PBS for 1 h each and incubated in Alexa Fluor 488 secondary antibodies, and rhodamine phalloidin to stain F-actin (1:500 in 5% BSA) for 24 h in the dark, followed by a further wash in PBS for 1 h. Next, larvae were placed onto microscope slides, left to air dry prior to mounting in Vectashield (Vector Laboratories, Peterborough, UK) anti-bleaching medium, and sealed with transparent nail polish. All incubations were carried out at room temperature and washes were done in 0.5 ml microfuge tubes. Once slides were prepared they were kept in the dark at 4°C. Parasites were visualised on a Leica TCS SP2 AOBS confocal laser scanning microscope using either a 20x dry objective, a 40x or 63x oil immersion objective and images collected with Leica software; digital zoom was used when appropriate. Since *S. mansoni*

autofluoresce, this autofluorescence was quenched in adult worms by incubating worms with 0.1 M glycine before blocking. For all experiments the signal received for the negative controls (i.e. those incubated with secondary but not primary antibodies) was negated from that of the positive samples. This was achieved by reducing the power level of the photomultiplier tube, which was then kept constant for all observations of the same experiment.

Cercariae required a different methodology since their tails easily detach from the body. Cercariae fixed in ice-cold absolute acetone were carefully washed in PBS, pipetted and placed onto silane-treated slides, then heated at 60°C for 30 min. Once cooled, a hydrophobic pen was used to draw a circle around the attached cercariae so that incubations and washes could be done on the slide with small volumes within the circular area. Parasites were further permeabilized for 1 h with 0.3% (v/v) Triton X-100, washed in PBS, blocked for 2 h in 10 % goat serum, washed again in PBS, and incubated with the requisite primary antibodies (1:50 concentration) for 3 days at 4°C in a humidified chamber. After, cercariae were washed in PBS (3 x 1 h each wash), followed by an overnight incubation in Alexa Fluor 488 secondary antibodies (1:500) and rhodamine phalloidin at 4°C in PBS. Slides were then washed with PBS thrice and Vectashield mounting medium added. A cover slip was placed and sealed with transparent nail polish. Cercariae were then visualised on a Leica TCS SP2 AOBS confocal laser scanning microscope using either a 40x or 63x oil immersion objective and images captured with Leica software as detailed above.

2.7 Pharmacological treatments

The pharmacological inhibitors GF109203X, U0126 and SB203580 were used to inhibit PKC, ERK, and p38 MAPK in live schistosomes, respectively; the PKC activator PMA was also employed. Detailed descriptions of the pharmacological treatments are presented in the material and methods sections of Chapters 4, 6 and 8 for adult worms, cercariae and schistosomula, respectively.

2.8 Video imaging and analysis

A detailed description of the videoing and video analysis for each life-stage is described in the material and methods section of Chapters 4, 6 and 8 for adult worms, cercariae and schistosomula, respectively. These videos were firstly converted into uncompressed "old format" AVIs with the VirtualDub software version 1.8.8 (www.virtualdub.com) and analysis performed using the publicly available image analysis software ImageJ (rsbweb.nih.gov/ij/).

2.9 Statistical methods

Statistical differences between means were tested for significance using one-way ANOVA and the Fisher's pair-wise multiple comparison test. The statistical software package used was Minitab (version 16) for windows. All data is expressed as mean ±standard error of the mean (SEM). The p values of 0.001, 0.01, or 0.05 were used to indicate statistical difference.

2.10 Bioinformatics

The *S. mansoni* PKC, ERK, p38 MAPK and JNK/SAPK gene candidates were identified from the *S. mansoni* genome assembly, relying on the existing annotation (http://www.genedb.org/genedb/smansoni). Protein sequence predictions of candidates with matches to PKC, ERK, p38 MAPK and JNK/SAPK were further assessed for similarity with other organisms using the BLAST search tool from the Universal Protein Resource (http://www.uniprot.org/) and also carried out using the NCBI Blast Basic Local Alignment Search Tool (BLAST): http://www.ncbi.nlm.nih.gov. Furthermore, the *S. mansoni* MAPK and PKC sequences identified by Andrade *et al.* (2011) were taken into account. The extent of conservation of the anti-phospho antibodies' detection site available on Cell Signalling Technology Phosphosite (http://www.phosphosite.org)

was also determined towards the putative amino acid sequences for *S. mansoni* PKCs and MAPKs (Chapter 3).

Chapter 3

Initial Immunodetection Studies

3.1 Introduction

As described in Chapter 1, schistosomes are complex multicellular parasites genetically programmed to develop sequentially through different environmental units, from a freshwater environment as a miracidium or cercaria, to an endoparasitic environment of either a poikilotherm invertebrate host or a homeotherm vertebrate host. Schistosomes have thus evolved sophisticated communication systems to ensure that differentiation towards each of the succeeding life-stages is initiated at a proper time and at a suitable site (reviewed in LoVerde *et al.*, 2007, 2009).

Recently, there has been good progress in understanding various aspects of the schistosome neuronal system, particularly in relation to the presence of neurotransmitters (McVeigh et al., 2009; Ribeiro and Geary 2010) and G-protein coupled receptors (El-Sahabi and Ribeiro 2010; Ribeiro and Geary, 2010). Furthermore, considerable research has been conducted into TGFβ signalling and its likely role in female reproductive development and egg embryogenesis (reviewed in LoVerde *et al.*, 2009; Beckmann *et al.*, 2010; see Section 1.3). Other signalling molecules have also been investigated including cytosolic tyrosine kinases such as Syk kinase (Table 1.1). However, our knowledge of PKC and MAPK signalling in schistosomes remains limited.

PKCs, and ERK, p38 MAPK and JNK MAPKs are conserved through evolution and are present across different eukaryotic phyla. As detailed in Chapter 1, these proteins, which are activated by receptors such as RTKs and GPCRs, play a vital role in the co-ordination of diverse and sometimes overlapping cell and tissue functions (reviewed by Kolch, 2005; Parker and Murray-Rust, 2004; Seger and Krebs, 1995; Ventura and Maioli, 2001). Putative PKC and MAPK proteins and their upstream signalling elements are predicted in the genomes of *S. mansoni* (Berriman *et al.*, 2009), *S. japonicum* (Consortium TSjGSaFA, 2009) and *S. haematobium* (Young *et al.*, 2012). In our laboratory a phosphorylated ~78 kDa PKC and a phosphorylated p38 MAPK have previously been detected in miracidia and sporocysts of *S. mansoni* (Ludtmann, *et al.*, 2009; Ressurreição *et al.*, 2011a, b).

The considerable morphological and physiological differences that exist between each of the schistosome life-stages means that certain signalling processes are likely to be different between stages and these might be important to key life-stage transitions in changing environments, within a host and between hosts, and between parasites. For

example, signalling between male and female worms is essential for complete development of the female reproductive apparatus including the ovary and vitellaria, and separation of worm couples reverses maturation (Grevelding *et al.*, 1997; Fitzpatrick and Hoffmann, 2006). Cell communication is also vital to sustain behavioural responses such as muscle contraction (Ribeiro and Geary, 2010), presumably important to pairing of adults and to the migration and swimming of the larval stages. Cercariae behaviours such as light and temperature perception are also vital for the survival of *S. mansoni* cercariae and signal-mediated release of proteolytic acetabular contents is essential for host penetration (Haas *et al.*, 2002; Haeberlein and Haas, 2008; Haas *et al.*, 2008). Overall, knowledge gained through studying genome predicted evolutionary conserved signal transduction mechanisms in different *S. mansoni* life-stages would accelerate our understanding of parasite developmental biology and pathogenesis, and should facilitate development of novel treatments.

Therefore, in this Chapter, several commercially available anti-phospho antibodies were tested that could potentially be used to recognize the catalytically active form of evolutionary conserved PKCs and MAPKs predicted in the *S. mansoni* genome. Selected antibodies were then screened against different *S. mansoni* life-stages to assess the extent of pathway activation/isoform activation during the schistosome life-cycle.

3.2 Materials and Methods

3.2.1 Immunodetection of S. mansoni *phosphorylated protein kinase candidates in adult worms*

To identify *S. mansoni* protein candidates suitable for further study, several commercially available antibodies raised against mammalian phosphorylated PKC, ERK, p38 MAPK, JNK and MEK proteins were initially tested against *S. mansoni* adult worm protein extracts. The phospho-specific antibodies tested were: anti-phospho-PKC (pan) (βII Ser660) polyclonal, anti-phospho-PKC (pan) (ζ Thr410) (190D10) monoclonal, anti-phospho-p44/42 MAPK (Erk1/2) (Thr202/Tyr204) monoclonal, anti-phospho PKCα/βII (Thr638/641) polyclonal, anti-phospho-p38 MAPK (Thr180/Tyr182) monoclonal, anti-phospho-SAPK/JNK (Thr183/Tyr185) monoclonal, anti-phospho MEK monoclonal and anti-phospho-(Ser) PKC substrate polyclonal. These antibodies detect the catalytically active form of each enzyme only. Adult worms were collected and protein extracts prepared and processed for western blotting as described in Sections 2.4.1 and 2.5, respectively.

3.2.2 Sequence identification and bioinformatic characterization of protein candidates that were successfully immunodetected in S. mansoni

Gene candidates were identified from the *S. mansoni* genome assembly relying on the existing annotation (http://www.genedb.org/genedb/smansoni). For proteins that seemed to be specifically detected by the anti-phospho antibodies, protein sequence predictions were further assessed for similarity with other organisms using the Basic Local Alignment Search Tool (BLAST) from the Universal Protein Resource (http://www.uniprot.org/); *S. mansoni* sequences identified by Andrade *et al.* (2011) were also taken into account. The extent of conservation of the detection site of each anti-phospho antibody with the putative amino acid sequence of each predicted *S. mansoni* protein was then determined and the sequences aligned. Immunodetection and bioinformatics were already performed for the protein detected with anti-phospho p38 MAPK antibodies (Ressurreição *et al.*, 2011a) and a ~78 kDa PKC detected with anti-phospho PKC Ser660 antibodies (Ludtmann *et al.*, 2009).

3.2.3 Evaluation of antibody binding

Only those primary antibodies that displayed good results with *S. mansoni* adult worm protein extracts were tested on different *S. mansoni* life-stages. For this evaluation the following parameters were considered: 1) that the antibody used detected a number of proteins that did not exceed the number predicted in the S. *mansoni* genome (for that protein family), and 2) that the molecular weight of the immunoreactive protein(s) closely matched that predicted in the genome (www.genedb.org/Homepage/Smansoni). Apparent molecular weights of immunoreactive bands following SDS-PAGE and western blotting were calculated using the log mass to distance travelled method with the molecular weight markers acting as protein standards.

3.2.4 Detection of phospho-ERK and -PKCs in different S. mansoni *life-stages*

The antibodies displaying good detection profiles against adult worm extracts (i.e. anti-phospho PKC and anti-phospho ERK antibodies) were next screened against different *S. mansoni* life-stages (miracidia, early sporocysts, cercariae and adult male, female or paired worms). The different life-stages were obtained as detailed in Section 2.4 and in Ressurreição *et al.* (2011a, b) and homogenates prepared and processed for western blotting as detailed in Section 2.5. Equal amounts of protein (12 μg) were loaded for each life-stage so that direct comparisons between life-stages could be made.

3.3 Results

3.3.1 Antibody immunoreactivity profile against S. mansoni *adult worm protein extracts*

To detect active PKCs and MAPKs, and PKC substrates, eight different anti-phospho antibodies were screened against *S. mansoni* adult worm protein extracts (Figure 3.1). With exception of the anti-phospho PKCβII (Ser660) and the anti-phospho p38 MAPK antibodies, all antibodies were used for the first time in *S. mansoni*.

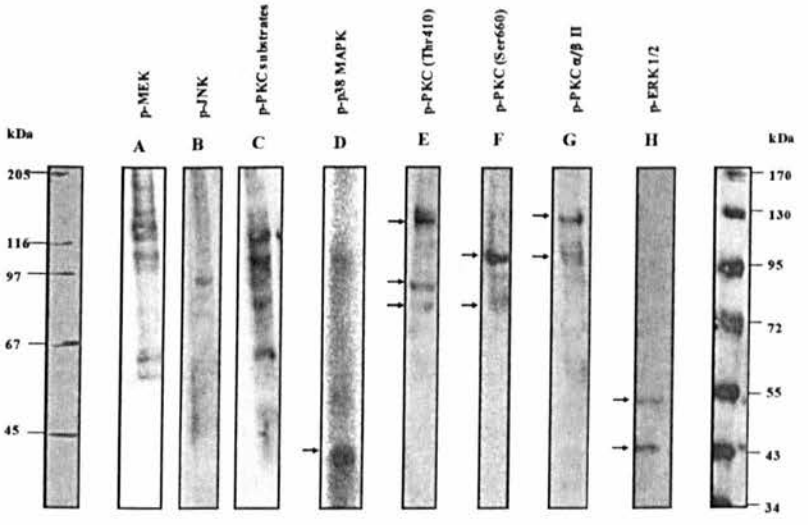

Figure 3.1 - Western blot demonstrating the detection profiles of different phospho-specific antibodies screened against *S. mansoni* adult total proteins. Two different molecular weight ladders were used; on the far left SDS 6H markers and on the far right Page Ruler markers. The panels represent detection with different antibodies as follows: Panel (**A**), immunoreactivity of anti-phospho MEK 1/2 antibodies, showing several immunoreactive bands; Panel (**B**), anti-phospho JNK/SAPK antibodies detecting a high molecular weight protein of ~80 kDa; Panel (**C**), anti-phospho PKC-Ser substrate antibodies used sporadically in this thesis detect several proteins, expected to be PKC substrates; Panel **D**, anti-phospho p38 MAPK antibodies, detecting a protein of ~42 kDa; Panel (**E**), anti-phospho PKC (Thr410) antibodies displaying immunoreactivity towards a total of three proteins; Panel (**F**), anti-phospho PKC (Ser660) antibodies detecting a total of three immunoreactive bands; Panel (**G**), anti-phospho PKC α/βII antibodies reactive towards two proteins; Panel (**H**), anti-phospho ERK1/2 antibodies showing immunoreactivity towards two proteins. Each lane contains total protein from 1 adult worm pair. The blots are representative of data from four independent experiments.

The anti-phospho MEK 1/2 antibody detects proteins when dually phosphorylated at residues homologous to human MEK1/2 Ser218 and Ser222 (VSGQLIDSMANSFVG) but displayed unsatisfactory immunoreactivity against adult worm extracts, detecting several proteins and precluding its further use (Figure 3.1 A). The anti-phospho JNK/SAPK antibody designed to detect active JNK/SAPK when dually phosphorylated at residues homologous to Thr183 and Tyr185

(AGTSFMMTPYVVTRY) was also excluded from further study because it detected a protein of ~80 kDa (Figure 3.1B) which is larger than expected for JNK proteins including that for *S. mansoni* (~44 kDa; Smp_172240). The anti-phospho PKC-Ser substrate antibody reacted with multiple proteins that are likely PKC substrates (Figure 3.1 C), this antibody was used occasionally in this research project.

The anti-phospho p38 MAPK antibody has been previously used to detect phosphorylated p38 MAPK in *S. mansoni* miracidia and sporocysts and the detected p38 MAPK was biochemically characterized in our laboratory (Ressurreição *et al.*, 2011a, b). These antibodies, that detect active p38 MAPK when dually phosphorylated at residues homologous to Thr180 and Tyr 182 (RHTDDEMTGYVATRW), detected in adult worms the same single protein of ~42 kDa similar to that previously characterised in miracidia and sporocysts (Figure 3.1 D).

The anti-phospho PKC (Ser660) antibody has been previously validated for the detection of a ~78 kDa phosphorylated PKC in protein extracts of *S. mansoni* miracida and mother sporocysts by Ludtmann *et al.* (2009). This antibody recognises a sequence homologous to Ser660 of phosphorylated human PKCβ (SEFEGFSFVNSEFL) and in humans detects PKCα, βI, βII, δ, ε, η, and θ. A total of three proteins were detected in *S. mansoni* adult worm protein extracts; two faint bands with molecular weights of ~78 kDa and ~132kDa, and an additional stronger immunoreactive band of ~116 kDa (Figure 3.1 E).

Anti-phospho PKC (Thr410) antibodies detect PKCs only when phosphorylated at a residue homologous to Thr410 of the human PKCζ (PGDTTSTFCGTPNY) and in humans detects PKCα, βI, βII, γ, δ, ε, η, θ, and ι. In *S. mansoni* adult worms three immunoreactive bands were consistently detected, a doublet of ~78 kDa and ~81 kDa and a ~132 kDa band (Figure 3.1 F). This antibody did not detect the PKC like-protein of ~116 kDa detected with the anti-phospho PKC Ser660 but shows strong immunoreactivity against a ~81 kDa PKC.

The anti-phospho PKC α/βII (Thr638/641) antibodies detect PKCα only when phosphorylated at Thr638 (TRGQPVLTPPDQLVI) and PKCβII when phosphorylated at Thr641 (TRHPPVLTPPDQEVI) and also react with PKCγ in humans. This antibody detected two immunoreactive bands in adult worm protein extracts, of ~116 kDa and ~132 kDa (Figure 3.1 G). Although displaying good immunoreactivity, the antibody was mainly used to support the immunospecificity of the other anti-phospho PKC antibodies, particularly as the ~132 kDa PKC-like protein is unusually large.

Anti-phospho ERK antibodies, which detect activated ERK1 and ERK2 when individually or dually phosphorylated at residues homologous to Thr202 and/or Tyr204 (HDHTGFLTEYVATRWYR), detected a total of two immunoreactive bands in protein extracts of *S. mansoni* adults, a ~48 kDa and ~43 kDa (Figure 3.1 H).

3.3.2 Putative identities of the detected proteins

Bioinformatics of the ~42 kDa p38 MAPK, and the ~78 kDa PKC detected with anti-phospho PKC Ser660 antibodies have been previously performed; furthermore, the specific enzymatic activity of the immunoreactive p38 MAPK protein has been confirmed (Ludtmann *et al.*, 2009; Ressurreição *et al.*, 2011a). In summary, only one immunoreactive band of ~42 kDa was detected in *S. mansoni* protein extracts and in the genome only a single putative p38 MAPK was identified although only partial cDNA reads are present (Smp_133020, ~27.2 kDa for the partial sequence). Moreover, only one p38 MAPK was found in the *S. japonicum* genome (Ressurreição *et al.*, 2011a). Based on the partial sequence data (spanning 74 amino acids), and supported by more complete data from *S. japonicum*, the identified *S. mansoni* p38 MAPK is most similar to p38α MAPK (MAPK 14) of humans, the most evolutionarily-conserved and less redundant of the p38 MAPKs (Martin-Blanco, 2000). Pair-wise comparisons of the *S. mansoni* p38 MAPK fragment with corresponding sequences for other organisms revealed ~69-70% similarity with human, *D. melanogaster*, *C. elegans* or *Danio rerio*, and 86.5% with *S. japonicum*.

Using the current version of the *S. mansoni* genome, four putative PKC and five putative ERK proteins were identified from full-length sequences with considerable conservation to mammalian PKC and ERK isoforms. Furthermore the predicted *S. mansoni* proteins had similar amino acid sequences to the antigenic epitopes to which the anti-phospho specific antibodies [anti-phospho PKC (Thr410), anti-phospho PKC (Ser660), and anti-phospho p44/p42 MAPK (ERK1/2)] were raised (Table 3.1; Figure 3.2). Similar levels of sequence homology exist between the schistosome isotypes and mammalian isotypes recognized by these antibodies (Figure 3.2). As in mammals the sequence surrounding the phosphorylated Thr residue within the PDK1 consensus motif was better conserved than that surrounding the serine phosphorylation site in the bulky ring motif (Figure 3.2).

Anti-phospho PKC (Thr410) antibodies detected bands of ~132 kDa, ~81 kDa and ~78 kDa, while the anti-phospho PKC (Ser660) antibodies detected similar ~132

Table 3.1 – Putative identities of immunodetected proteins

S. mansoni protein code	Human sequence and protein description	*S. mansoni* predicted protein length (genome information)	Detected molecular weight in *S. mansoni*	Identity (%)	Domain: alignment position / (position in human)
SmPKC1 Bahia *et al* (2006)	P05571 PKC β type 671 aa 76.9 kDa	662 aa 76.1 kDa	~ 77 kDa	70 80 53.3 75.7 72.8 62.9	C1 C1 C2 S TKc β PKC like Whole alignment
Smp_128480	P05771 PKC β type 671 aa 76.9 kDa	657 aa 75.6 kDa	~ 77 kDa	66 68 36.9 72.6 71.9 58.5	C1 C1 C2 S TKc β PKC like Whole alignment
Smp_096310	P41743 PKC $_{\iota}$ type (iota) 587 aa 67.3 kDa	673 aa 76.7 kDa	~ 83 kDa	43.4 32 69.9 75.5 51.3	PB1 C1 S TKc iota S TKc Whole alignment
Smp_131700	Q02156 PKC epsilon 737 aa 83.7 kDa	860 aa 94.9 kDa	~ 104 kDa	42 66.7 68 68.6 73.9	C2 C1 (1) C1 (1) S TKc epsilon Whole alignment
Smp_176360	Not found in mammals however found in lower organisms (i.e. *Caenorhabditis elegans* 122 kDa)	1052 aa 116.9 kDa	~130kDa		
Smp_133020 (partial sequence)	Q16539 p38 MAPKα 360aa 41.3 kDa	237aa 27.2 kDa	~42 kDa	60.1 86 78	ATP binding site KIM docking site A loop
Smp_142050	P27361 ERK1 379aa 43.1 kDa	379aa 45.3kDa	~48 kDa	73.1 72.6 75.5 70	MAPK CS ATP binding site A loop Whole alignment
Smp_047900	P28482 ERK2 360aa 41.4 kDa	351aa 40.8 kDa	~43 kDa	63.3 76 65.7 69	MAPK CS ATP binding site A loop Whole alignment

Smp – *Schistosoma mansoni* protein

aa – amino acids

kDa and ~78 kDa proteins but also a ~116 kDa protein. In the genome four PKCs are predicted: Smp_128480 (75.61 kDa, with 59% homology to human PKCβ and 91% homology with PKC1 from *Aplysia*), Smp_096310 (76.75 kDa, a PKCι or ζ isotype 99% identical to PKCζ from *D. rerio*), Smp_131700 (94.97 kDa, 52 % homologous to human PKCε) and Smp_176360 (116.9 kDa, a large PKC with 61% homology towards human PKCβ).

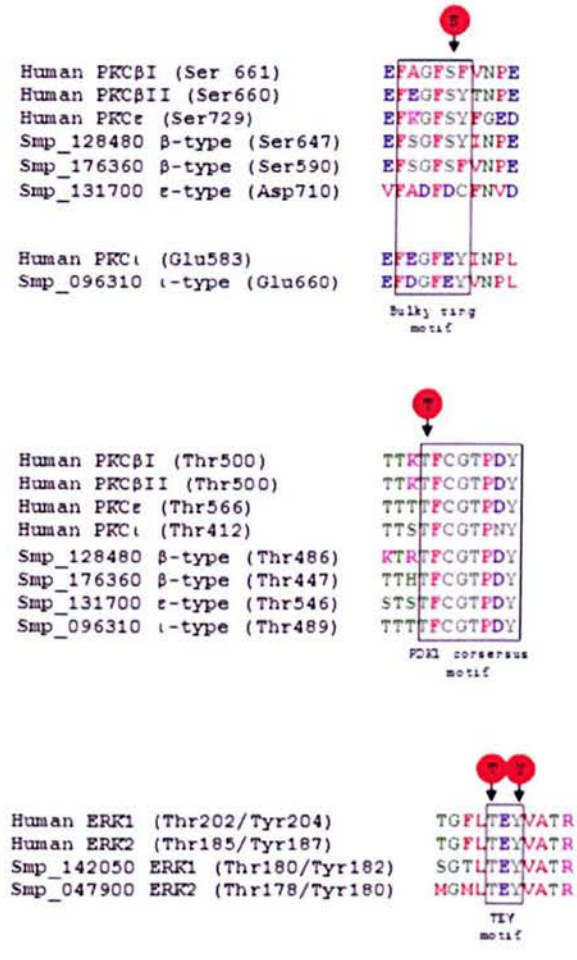

Figure 3.2- Alignment of antibody recognition sites. Comparison of the amino acid recognition sequences, together with the phosphorylated site, for the three anti-phospho antibodies used between *S. mansoni* PKC and ERK predicted protein sequences obtained from the *S. mansoni* genome database and relevant human protein sequences. The anti-phospho PKC (pan) (βII Ser660) antibodies recognize multiple human PKCs including PKCβI, βII and ε; based on sequence similarity these antibodies are predicted to react with Smp_128480 and Smp_176360 (both β-type PKCs) only when phosphorylated on Ser647 and Ser590, respectively within the bulky ring motif. The *S. mansoni* ε-type PKC (Smp_131700) lacks the conserved Ser phosphorylation site, as does ι-type PKC (Smp_096310) in common with human PKCι. The anti-phospho PKC (pan) (ζ Thr410) antibodies also recognize multiple human PKCs including PKCβI, βII, ε and ι; based on sequence similarity these antibodies are predicted to react with all *S. mansoni* PKCs only when phosphorylated on the conserved Thr residue within the PDK1 consensus motif. The anti-phospho p44/42 MAPK antibodies recognize human ERK1 and ERK2 only when phosphorylated on Thr and Tyr within the conserved TEY motif; based on sequence similarity, these antibodies are predicted to detect *S. mansoni* ERK1 and ERK 2 (Smp_142050 and Smp_047900, respectively) when phosphorylated.

The ~78 kDa protein detected with anti-phospho PKC Thr410 and Ser660 antibodies has been identified by Ludtmann *et al.* (2009) and is likely Smp_128480. These results are also in accord with the data here; the detection site for each antibody is well conserved within the predicted amino acid sequence of Smp_128480 (Figure 3.2). The ~81 kDa protein detected only with anti-phospho PKC (Thr410) antibodies seems most similar to Smp_096310 (ι-type PKC) due to molecular weight similarity and also because, as in humans, the consensus Ser phosphorylation site in the bulky ring motif is not conserved in PKCι (Figure 3.2). Interestingly, the ~95 kDa ε-type PKC predicted in the genome (Smp_131700) which has a conserved anti-phospho PKC (Thr401) antibody detection site was not detected (based upon molecular weight) although a faint band of similar weight sometimes appeared in adult worm and cercariae immunoblots (Figure 3.3 A). The ~116 kDa protein detected only with anti-phospho PKC (Ser660) and anti-phospho PKCα/β antibodies is most likely Smp_176360 due to molecular weight similarity and conservation towards the anti-phospho PKC (Ser660) antibody detection site (Figure 3.2) and that of the anti-phospho PKCα/β antibodies (data not shown). Surprisingly, all three anti-phospho PKC antibodies tested in this study also detected a ~132 kDa PKC-like protein not predicted in the genome; however, it could possibly be a PRK member of the PKC family (Mellor and Parker, 1998). This type of protein Smp_160760 (121 kDa) was detected in the *S. mansoni* genome using BLAST although only the anti-phospho PKC (Thr410) detection site seems conserved in this protein; nevertheless the identity of this protein remains unknown. Studies in the following chapter will further elucidate if this large protein has PKC-like characteristics.

The ~43 kDa and ~48 kDa proteins detected with anti-phospho ERK1/2 antibodies are most likely Smp_047900 (40.1 kDa most similar to human ERK2), and Smp_142050 (45.3 kDa with 70% identity towards human ERK1), respectively. Both proteins have a high degree of conservation towards the antibody detection sites and molecular weights are similar between the predicted and observed proteins (Figures 3.1 and 3.2).

3.3.3 Detection of phosphorylated ERKs and PKCs in different S. mansoni *life-stages*

Three different anti-phospho-specific antibodies [PKC (Ser660), PKC (Thr410) and ERK1/2] were next used to detect phosphorylated (activated) PKC and ERK1/2 proteins in homogenates (12 μg protein) of four different life-stages of *S. mansoni*

(miracidium, sporocyst, cercaria and adult worms, including males, females and couples) *via* western immunoblot analysis (Figure 3.3). Although the anti-phospho p38 MAPK antibody was not screened against all these life-stages together, it consistently detected the ~42 kDa protein in adult worm and cercariae homogenates (Chapters 5-8).

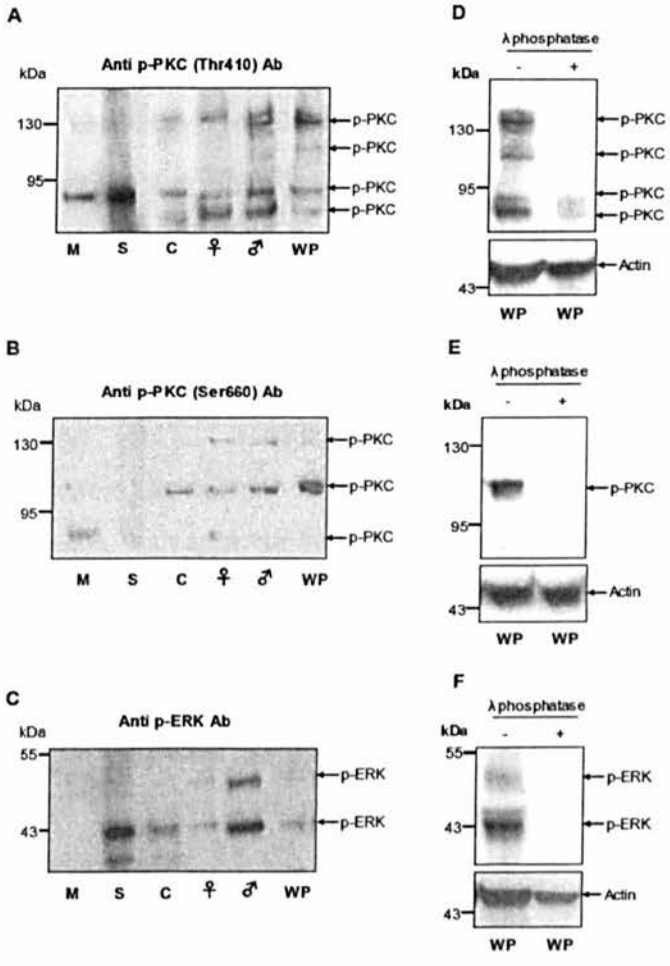

Figure 3.3 – Phosphorylated PKC- and ERK-like proteins detected in four different life-stages of *S. mansoni*. Western blot showing immunoreactive bands detected with **(A)** anti-phospho PKC (pan) (ζ Thr410), **(B)** anti-phospho PKC (pan) (βII Ser660), and **(C)** anti-phospho p44/42 MAPK (Thr202/Tyr204) antibodies (Ab) in miracidia (M), sporocysts (S), cercariae (C), adult female (♀) and male (♂) worms, and coupled worm pairs (WP) (~12 µg for each sample). Results are representative of three independent experiments. Lambda phosphatase was also employed to confirm that the antibodies reacted only with the phosphorylated form of each protein; actin was used a loading control.

Using anti-phospho PKC (Thr410) antibodies the three immunoreactive bands previously detected in adults were consistently detected and cercariae; a doublet with

apparent molecular weights of ~78 kDa and ~81 kDa, and a higher molecular weight protein of ~132 kDa with immunoreactivity stronger in adult males than in cercariae (Figure 3.3 A). In sporocysts and miracidia a single ~81 kDa band was detected which appeared more strong in sporocysts compared to the other life-stages (Figure 3.3 A).

The anti-phospho PKC (Ser660) antibodies detected three immunoreactive bands in protein extracts of *S. mansoni* cercariae and adult worms (Figure 3.3 B). Two faint bands were observed with apparent molecular weights of ~78 kDa and ~132 kDa similar to those detected with anti-phospho PKC (Thr410) antibodies; in addition, a stronger immunoreactive band of ~116 kDa was seen in adult male worms/worm pairs. This ~116 kDa protein was only detected in cercariae and adult worms with greater immunoreactivity generally seen in adult worm pairs (Figure 3.3 B). In sporocysts, no immunoreactive bands were detected with the anti-phospho PKC Ser660 antibody and in miracidia only one band of ~78 kDa was detected which is in accordance with previously published work from our laboratory (Ludtmann *et al.*, 2009) (Figure 3.3 B).

The anti-phospho p44/42 MAPK (ERK1/2) antibodies detected three immunoreactive bands across the different *S. mansoni* life-stages tested (Figure 3.3 C). Two immunoreactive bands, with apparent molecular weights of ~43 kDa and ~48 kDa were detected in adult worm protein extracts, with greater phosphorylation consistently observed in males. In cercariae and sporocysts, these antibodies detected a similar ~43 kDa immunoreactive band and a weaker band of ~35 kDa but not the ~48 kDa protein. Furthermore, the ~43 kDa band was more intense in sporocysts than in cercariae or adult worms (Figure 3.3 C). There were no visible immunoreactive ERK bands in miracidial protein extracts (Figure 3.3 C), when probing equal amounts (12 µg) of protein from each life-stage.

Treatment of western blots containing protein extracts (20 µg) of adult worm pairs with lambda phosphatase for 4 h prior to exposure to each of the anti-phospho PKC or anti-phospho p44/42 MAPK antibodies resulted in either a total loss (Figures 3.3 E, F) or a substantial reduction (Figure 3.3 D) of immunoreactivity demonstrating that the antibodies specifically react with the phosphorylated forms of these proteins.

3.4 Discussion

Overall knowledge of the molecular control of schistosome development, behaviour and reproduction remains poor, including the role of signal transduction enzymes like PKCs and MAPKs. Anti-phospho antibodies which display high degrees of specificity due to their short and well conserved detection site are an important and sometimes overlooked tool for studying these proteins in invertebrates. Hence, one strategy to study signalling proteins in schistosomes is to search commercially available anti-phospho antibodies, which detect catalytically active mammalian isoforms, and test them against active/phosphorylated proteins predicted in the *S. mansoni* genome.

Benefiting from the *S. mansoni* genome project, our research group has previously investigated evolutionarily conserved PKCs, p38 MAPK and PKAs in schistosomes by employing anti-phospho antibodies. It was found that a ~42 kDa p38 MAPK (Ressurreição *et al.*, 2011a, b), a ~78 kDa PKC (Ludtmann *et al.*, 2009) and two ~40 kDa and ~42 kDa PKAs (de Saram *et al.*, 2012) were active in different *S. mansoni* life-stages including miracidia, sporocysts and adult worms using anti-phospho p38 MAPK, anti-phospho PKC (Ser660) and anti-phospho-PKA-C (Thr197) antibodies, respectively. The present study continues efforts to discover useful antibodies; identifying three new antibodies which show good immunoreactive profiles rendering them valuable for studying signalling in *S. mansoni* life-stages.

3.4.1 Four out of the eight tested anti-phospho antibodies used showed specific detection profiles

Two anti-phospho antibodies showed poor immunoreactivity profiles against adult worm proteins. The anti-phospho MEK1/2 antibody detected more proteins than expected based on MEKs in the *S. mansoni* genome and other organisms, and the anti-phospho JNK/SAPK antibody detected a protein of considerably larger molecular weight than expected. Anti-phospho PKC-Ser substrate antibodies were also employed which detected several immunoreactive proteins. Although this study did not involve identifying these putative substrate proteins, this antibody could be a useful tool for future studies aimed at elucidating downstream signalling targets of PKC.

The anti-phospho PKC (Thr410), anti-phospho PKCα/βII (Thr638/641) and anti-phospho p44/p42 MAPK (ERK1/2) antibodies were found suitable for use in *S. mansoni*. From the *S. mansoni* genome database four putative *S. mansoni* PKCs and two

putative ERKs were identified from full-length predicted sequences with considerable conservation to mammalian PKC and ERK isotypes, particularly in the key functional domains. The detection sites (epitopes) of the anti-phospho PKC (Ser660), anti-phospho PKC (Thr410), anti-phospho PKC α/βII (Thr638/641) and anti-phospho p44/p42 MAPK (ERK) antibodies are 13-15 amino acids long and contain a highly conserved phosphorylation site which reduces the chance of non-specific binding. These sites were well conserved in the *S. mansoni* sequences and lambda phosphatase treatment removed reactivity demonstrating specificity. Similar antibodies have been successfully used to detect PKCs and ERKs in a wide range of other invertebrates, reinforcing the conviction that these proteins have been well conserved during metazoan evolution (Widmann *et al.*, 1998). For instance, the anti-phospho PKC (Thr410) antibodies successfully detect phosphorylated PKCs in oocytes of the marine worm *Cerebratulus spp.* (Stricker, 2009) and anti-phospho ERK antibodies have been used extensively for the study ERK phosphorylation (activation) in *C. elegans* and the snails *Lymnaea stagnalis* (Plows *et al.*, 2004) and *B. glabrata* (Zahoor *et al.*, 2008).

Thus searching the *S. mansoni* genome database for conserved signalling proteins with considerable homology towards the epitope of commercially available antibodies (especially those from phospho-antibodies to detect the catalytically active form of the target protein) is a viable way to find new tools for studying schistosome signalling.

3.4.2 Immunodetected proteins display differential PKC and ERK phosphorylation profiles throughout the S. mansoni *life-cycle*

The endogenous activation profiles of the *S. mansoni* PKCs and ERKs were noticeably dissimilar with differential activation evident across four different life-stages studied. Greater PKC and ERK activation were found in male adults compared to females, cercariae, miracidia or sporocysts when similar amounts of protein was used suggesting that PKC and ERK may have distinct physiological roles in *S. mansoni*, allowing them to participate differently at different stages of the life-cycle.

These results are in accord with previous pioneering studies of PKC activity in schistosomes using enzymatic assays by Wiest *et al.* (1992) which examined changes in activity during *S. mansoni* maturation (freshly emerged cercariae and 8 week-old adults); total PKC activity was found to be developmentally regulated (nine-fold higher in adult worms than in larval parasites) (Wiest *et al.*, 1992). In the current study, not

only was the relative phosphorylation (activation) of each detected protein different, but also presence of the activated PKCs differed. For instance, in miracidia only two phosphorylated PKCs of ~78 kDa and ~81 kDa were present and in 48h sporocysts only the ~81 kDa band was seen. While in cercariae and adult worms four immunoreactive PKCs were activated suggesting a more complex role for PKC in human infective and dependent stages that might include reproduction/development. In fact, PKC seems to be a mechanistic regulator of sporocyst development in schistosomes (Ludtmann *et al.*, 2009).

These results are also somewhat in agreement with developmental roles of PKC in growth and differentiation of other organisms. For instance, in *C. elegans*, expression of PKCB1 signalling is variable throughout development and seems to have a more major role in post-embryonic than in pre-embryonic development, with suspected roles in homeostasis and environmental adaptation (Land *et al.*, 1993). Furthermore, differential expression of two PKCs (77 kDa and 78 kDa) in *C. elegans* occurs throughout post-embryonic development with an 81 kDa isoform apparently functioning only in L1 and L2 larvae (Islas-Trejo *et al.*, 1997). PKC isoforms are also known to differ with respect to tissue distribution and subcellular localization, as well as substrate specificity, leading to the speculation of isotype-specific functions in vertebrates and invertebrates, which could also explain the observed differential expression throughout the different *S. mansoni* life-stages.

The activated ERKs (~43kDa and ~48kDa) were only found in the adult worm life-stage, in the miracidium no ERK activation was detected, while in sporocysts and cercariae only one strong immunoreactive band of ~43 kDa was present. These results suggest life-stage specific roles for *S. mansoni* ERKs. The ~43 kDa ERK was found to be highly active in the sporocyst stage which is characterized by extensive asexual replication. In the ascidian *Molgula pacifica* ERK phosphorylation is required for ampulla development morphogenesis (Bates, 2007). Furthermore, the importance of ERK signalling in cellular growth control is reflected by the fact that all the pathway components constitute important oncogenes in mammals (Hilger *et al.*, 2002). The ~48 kDa ERK detected in *S. mansoni* was only active in the adult stage suggesting that this protein plays a heightened role in male/female physiology and/or interactions. Vicogne *et al.* (2004) demonstrated that when expressed in *Xenopus* oocytes SER, the EGF receptor orthologue of *S. mansoni*, binds exogenous human EGF leading to ERK pathways activation; thus it is likely *S. mansoni* adults use host EGF to stimulate growth and development.

Interestingly, in the literature, most parasites possess two or more ERK immunoreactive bands while in lower non-parasitic organisms often only one immunoreactive band is present. Examples of parasites with the two or more ERKs are *Taenia crassiceps* (Escobedo *et al.*, 2010) and *Ascaris lumbricoides* which have ~41 and ~42 kDa ERKs. *Echinococcus multilocularis* has only one ERK-like MAP Kinase encoding gene but this gene encodes for three ERK-like proteins (EmMPK1-1, -2, -3) (Spiliotis *et al.*, 2006). Only one ERK was found phosphorylated in meta-cestode vesicles of *E. multilocularis*, which could indicate developmental stage specificity (Spiliotis *et al.*, 2008).

3.4.3 Putative identities of the newly immunodetected PKC and ERK proteins

The molecular weight similarity between predicted and immunodetected proteins and antibody detection site conservation allowed putative assignment of *S. mansoni* Smp identifiers to protein bands. The ~78 kDa protein detected in adult worms with both anti-phospho PKC (Thr410) and anti-phospho PKC (Ser660) antibodies is likely Smp_128480 using these criteria; this protein was also identified by Ludtmann *et al.* (2009). In addition, SmPKC1 identified by Bahia *et al.*, 2006 which was previously thought to be Smp_128480 is now considered to be the ~116 kDa PKC Smp_176360 (additional information from Andrade *et al.*, 2011). Strangely, SmPKC1 was highly expressed in sporocysts however and in our studies the only PKC phosphorylated in sporocysts was the ~81 kDa form, which according to our studies is most likely an aPKC zeta or iota (Smp_096310). However, in Bahia *et al.* (2006) the age of the mother sporocysts was not stated which could be important for PKC expression; in this study 48 h sporocysts were used. The ~81 kDa band detected only with anti-phospho PKC (Thr410) is likely Smp_096310 as the antibody detection site is conserved in this sequence but the recognition site of the anti-phospho PKC (Ser660) antibodies is not. The ~116 kDa immunoreactive protein only detected with the anti-phospho PKC (Ser660) and anti-phospho PKCα/β antibodies suggests similarity with Smp_176360.

It is important to note that that the *S. mansoni* kinases identified with the HMM model (Andrade *et al.*, 2011) refer to Smp_128480 as a PKCα, Smp_176360 also as a PKCα, Smp_131700 as a PKCη and, finally, Smp_096310 as a PKCι. Our homology studies suggest that Smp_128480 and Smp_176360 are more likely PKCβ isotypes.

Interestingly, the ~132 kDa protein detected with all three anti-phospho PKC antibodies was not found predicted in the *S. mansoni* genome hindering identification.

The closest possibility would be Smp_160760 a PKC-related kinase PRK because the anti-phospho PKC (Thr410) antibody detection site is well conserved within this sequence. However, the detection site of the anti-phospho PKC Ser660, which also detected this protein is not conserved and the molecular weights are slightly different. While our immunoblots show a ~132 kDa protein the Smp_160760 is predicted to have a molecular mass of ~120 kDa however phosphorylation can increase the apparent molecular weight/mass of PKCs (Keranen *et al.*, 1995).

The anti-phospho p44/p42 MAPK (ERK1/2) antibodies detected two proteins in adult worm extracts, which agrees with predicted protein sequences from the S. *mansoni* genome database. The ~48 kDa and ~43 kDa proteins are likely Smp_142050 (45.3 kDa, 70% identity with ERK1) and Smp_047900 (40.8. kDa, 67% identity ERK2), respectively, due to molecular weight similarity and antibody detection site conservation. These ERKs are characteristically found in mammals. The detection site of the anti-phospho ERK antibody was found to be conserved in two other predicted protein sequences (Smp_133500 and Smp_134260) of higher molecular weights (82.67 kDa and 70 kDa, respectively) considered to be MAPK signalling proteins (Andrade *et al.*, 2011). However these bands were not observed on our immunoblots in any of the life-stages tested. On the other hand, an ERK-like protein of ~35 kDa which was detected in cercariae protein extracts was not found in the *S. mansoni* genome database. Such discrepancies could suggest that the *S. mansoni* sequencing results require adjustment/refinement.

3.4.4 Unusually large S. mansoni *PKC-like proteins suggest an ancestral character of PKC in* S. mansoni

Two of the detected PKC-like proteins had unusually high molecular weights (compared to mammals) of ~132 kDa and ~116 kDa. The ~116kDa protein is likely Smp_176360 (predicted size 116.9 kDa). If it is a PKC, the ~132 kDa protein probably is a result of an extended regulatory domain which is common in lower organisms. For example, the 132 kDa Pkc1 that represents the sole PKC in budding yeast *S. cerevisiae* is a much larger protein compared to mammalian PKCs, due to an extended regulatory domain (Mellor and Parker, 1998). While in the mammalian PKC super family, the various regulatory modules are differentially distributed between the different isotypes, in *S. cerevisiae* all of these elements are present together in one enzyme. It has been proposed that a larger PKC protein reflects the ancestral character of the enzyme as an

archetypal PKC (Mellor and Parker, 1998); these might be activated by diacylglycerol but not calcium (Parekh *et al.*, 2000). Such high molecular weight PKCs have also been detected in extracts of a wide range of invertebrates including sea urchin sperm (135-140 kDa) (White *et al.*, 2007) and marine worm oocytes (95-100 kDa) (Stricker, 2009); both were detected with anti-phospho PKC (Ser660) antibodies.

3.4.5 Conclusions

Here, with the use of anti-phospho antibodies raised against mammalian isoforms the successful detection of putative *S. mansoni* ERK and PKC signalling enzymes when in an exclusively active state are reported. PKC and ERK activation were found differentially expressed throughout the different life-stages of the parasite suggesting isoform specific roles at key stages of the parasite development. Collectively, our data is consistent with the information in the *S. mansoni* genome database. Further biochemical characterization of the detected proteins (see Chapter 4) will allow more extensive signalling studies in *S. mansoni* particularly in the context of functional roles in human infective or dependent stages.

Chapter 4

PKC and ERK Signalling in Adult *Schistosoma mansoni*

4.1 Introduction

Adult *S. mansoni* can cause considerable host pathology as eggs released from females living in the hepatic portal vasculature become lodged in tissues resulting in inflammatory granuloma reactions in the spleen, liver, and gut (Burke *et al.*, 2009; see Chapter 1). For this reason, work on cell signalling by protein kinases in schistosomes has largely focused on the adult worm stage.

As reviewed in Chapter 1, evidence for PKC activity in adult *S. mansoni* comes from the work of Blair *et al.* (1998) who discovered a phospholipid dependent and phorbol ester sensitive kinase activity involved in muscular contraction. Additionally, in 1992 Wiest *et al.* demonstrated a DAG and Ca^{2+}-dependent PKC activity in partially purified *S. mansoni* homogenates. More recently, SmPKC1, an *S. mansoni* PKC displaying high sequence homology to human PKCβ was characterized at the molecular level (Bahia *et al.*, 2006), and a phosphorylated PKCβ-like protein was found in miracidia and mother sporocysts (Ludtmann *et al.*, 2009). ERK1/2-like proteins were also detected in *S. mansoni* homogenates by Schüßler *et al.* (1997), and a Ras homologue was characterized at the molecular level two years later (Osman *et al.*, 1999). Activation of the *S. mansoni* EGF receptor (SER) by human EGF has also been shown to phosphorylate ERK2 in *Xenpous* oocytes (Vicogne et al., 2004), indicating conservation of ERK receptor-mediated signalling in schistosomes.

Relying on the current genome assembly and initial immunodetection studies four putative PKC-like and two ERK-like proteins were identified in *S. mansoni* (Chapter 3). Although these proteins appeared to be differentially phosphorylated (activated) in the different life-stages, all six phosphorylated proteins were present in adult worms. In this chapter signalling by these proteins is investigated further and localization of the activated kinase(s) in intact worms is performed together with studies into the effects of PKC and ERK inhibition on worm phenotype. Finally, the effect of the drug PZQ on PKC and ERK signalling is also investigated given that PZQ has been known to interfere with Ca^{2+} dynamics in schistosomes (Cioli and Pica-Mattoccia 2003; Pica-Mattoccia *et al.*, 2007)

4.2 Materials and Methods

4.2.1 Exposure of S. mansoni *to PKC and ERK pharmacological modulators*

The ability of GF109203X and PMA to either block or activate PKC, and U0126 to inhibit ERK phosphorylation was tested in adult *S. mansoni*. Perfused and washed adult worm pairs (Section 2.4.1) were placed in microfuge tubes with RPMI 1640 in a water bath at 37°C for 30 min to equilibrate. Worms were then exposed for various durations (0, 15, 30, 60 and 120 min) to either 20 μM GF109203X, 1 μM PMA, 1 μM U0126, DMSO (0.1% and 0.2%, vehicle) or RPMI 1640 only. As GF109203X competes with the ATP binding site and only non-phosphorylated /catalytically inactive proteins can be inhibited, live adult worms were also incubated for 120 min on ice in 20 μM GF109203X prior to exposure to 1 μM PMA, 0.2% DMSO or RPMI 1640 for 30 min. U0126 inhibits active and inactive MEK1/2 blocking downstream phosphorylation of ERK and therefore lengthy pre-incubation was not required. Immediately after treatment, medium was removed and worms were either homogenized in 30 μl RIPA buffer and processed for western blotting (Section 2.5) or were acetone-fixed for immunohistochemistry (Section 2.6).

4.2.2 PKC and ERK immunoprecipitation and enzymatic activity

Kinase assay kits were employed to detect PKC and ERK activity in immunoprecipitates; the PKC Omnia kinase assay kit with Ser/Thr 8 peptide as the PKC substrate and the p44/p42 MAP Kinase assay kit with Elk-1 as substrate. Perfused adult worm pairs [100 - 200 pairs (PKC assay kit) or 20 (ERK assay kit)] were transferred into 2 ml screw cap tubes and washed twice with pre-warmed RPMI 1640 medium at 37°C. Worm pairs were either left for 15-30 min in 1 ml RPMI 1640 medium at 37°C alone or were exposed to 1 μM PMA or 2 μg/ml PZQ in RPMI 1640. Adult worms were snap frozen in liquid nitrogen and stored at -80°C. The enzyme assay kits were used following the manufacturer's instructions. Briefly, frozen worm pairs were homogenized on ice in a glass homogenizer (100 μl capacity) in 100 μl of 1x cell lysis buffer [20 mM Tris (pH 7.5), 150 mM NaCl, 1 mM EDTA, 1 mM EGTA, 1% Triton X-100, 2.5 mM sodium pyrophosphate, 1 mM β-glycerophosphate, 1 mM sodium orthovanadate, 1 μg/ml leupeptin, and 1 mM PMSF] further supplemented with HALT phosphatase/proteinase inhibitors. The homogenate was transferred to a microfuge tube

and centrifuged for 15 min at 13,400 rpm and 4°C. The supernatant was recovered and the remaining pellet re-homogenized in 50 µl 1x cell lysis buffer and centrifuged at 13,400 rpm for another 10 min at 4°C and the supernatant recovered. The supernatants were combined (total of 150 µl) in a microfuge tube and left rocking overnight at 4°C in anti-phospho PKC (Thr410), anti-phospho PKC (Ser660) or immobilized anti-phospho p44/p42 MAPK (Erk1/2) (Thr202/Tyr204) (D13.14.4E) XP primary antibodies (1/25 dilution). The following day, 50 µl protein A agarose beads were added to homogenates and were rocked for 5 min at 4°C except for the homogenate incubated with the pre-immobilized anti-phospho ERK antibody. Lysates were then centrifuged at 13,400 rpm for 30 s at 4°C and the supernatants discarded, the bead-antibody-protein immunocomplexes were washed twice in 500 µl 1x lysis buffer and twice in 500 µl 1x kinase buffer [25mM Tris (pH7.5), 5mM β-Glycerolphosphate, 2mM DTT, 0.1 mM Na_3VO_4 and 10 mM $MgCl_2$]. A negative control comprising beads only with no primary antibody was also used for the PKC assay.

PKC kinase reactions contained the immunocomplex, 10 mM ATP, 10x peptide substrate Ser/Thr 8, 10 mM DTT, 10x kinase reaction buffer and deionized water. The master mix was assembled in black 96-well plates, according to the manufacturer's recommendations. Accumulation of phosphorylated substrate (relative fluorescence units, RFUs) was monitored every 30 s over 3 h at 30°C by recording fluorescence emissions at 460 nm upon excitation at 355 nm, using a FLUOstar OPTIMA microplate fluorometer. Kinase reactions containing 2 ng recombinant human PKC were included as positive controls. Experiments were done in duplicate. Optimization of the procedure was initially done with rat brain homogenates. For the ERK assay immunocomplexes were each re-suspended in 20 µl kinase buffer supplemented with 200 µM ATP and 2 µg Elk-1-GST fusion protein and incubated for 30 min at 30°C. Reactions were terminated with 10 µl 3x SDS-PAGE sample buffer and samples processed for western blotting (Section 2.5). Experiments included two negative controls, one with homogenate and beads but no antibody and another with assay components but no homogenate.

4.2.3 Phenotypic analysis of adult S. mansoni *cultured in PKC and ERK pharmacological modulators*

To determine the effects of pharmacological PKC inhibition and activation, and ERK inhibition in *S. mansoni* adult worms, parasites were exposed to 1, 5, 20 or 50 µM

GF109203X, U0126, or 1 μM PMA. Untreated control groups were maintained in culture medium only or 0.5% DMSO (vehicle control). The culture medium was changed and inhibitors/activator replenished daily over 4 days. After worms were collected and washed (Section 2.4.1) they were cultured in RPMI-1640 containing phenol red, glutamine, glucose, 1x antibiotic and antimycotic mixture (100U penicillin, 100 μg streptomycin and 0.25 μg amphotericin B/ml) and 10% foetal calf serum (FCS) at 37°C in 5% CO_2 (Bahia *et al.*, 2006). For each treatment, 3 - 6 adult pairs were kept in individual wells of a 24 well plate (Nunc) in 1.5 ml culture medium. Worms were left to equilibrate at 37°C for 1 h prior to adding the pharmacological components and then left to equilibrate for a further hour prior to video imaging and other observations.

Worms were observed at various times over 96 h using an Olympus SZ54045 binocular dissecting microscope and avi-format movies captured using a JVC TK-1481 composite colour video camera linked to Studio Launcher Plus for Windows software. Worm behaviour including pairing status and ventral sucker attachment to the base or sides of the culture plate was determined. Egg release by worms was also enumerated. Detailed analysis of worm movement was done using ImageJ (Rasband, W.S., ImageJ, U. S. National Institutes of Health, Bethesda, Maryland, USA, http://rsb.info.nih.gov/ij/, 1997-2009). The diameter of the well in pixels was calibrated to mm and the distance travelled by the posterior tip of each worm in 10 s was manually tracked and measured enabling translation into speed of movement (velocity) of pixels/s to mm/s. Worm coiling (Figure 4.11) was determined by counting the number of coils that persisted during 10 s visualization. Results are representative of four independent experiments with a minimum of three replicates each; 30 or more parasites per treatment were scored, except for DMSO controls (n=24).

4.2.5 PKC and ERK phosphorylation status after exposure of adult worms to PZQ

A pure preparation of racemic PZQ powder from Shin Poong Pharmaceutical was dispensed from a stock solution in DMSO. Adult worms were exposed to 0.2 μg/ml PZQ in RPMI 1640 or DMSO (vehicle control, 0.1%) at 37°C for 15, 30 and 120 minutes, *in vitro*. Next, adult worms were either processed for western blotting (Section 2.5) or confocal microscopy (Section 2.6). The final concentration of PZQ used in our study follows the studies of Pica-Mattoccia and Cioli (2003), which reports that 0.2 μg/ml PZQ is the lowest concentration, *in vitro,* which induces a typical phenotype of PZQ treated adult *S. mansoni*.

4.3 Results

4.3.1 S. mansoni *PKC-like proteins are modulated by a PKC activator and inhibitor and have PKC activity*

In vitro pharmacological assays were done with adult *S. mansoni* to determine whether the phosphorylation status of the four immunoreactive bands detected with the two anti-phospho-PKC antibodies could be altered using the PKC activator PMA and the PKC inhibitor GF109203X. Phosphorylation of immunoreactive bands detected with both anti-phospho PKC antibodies increased when worms were exposed to 1 μM PMA for 30 min compared to 0.2% DMSO controls (Figure 4.1). The ~116 kDa protein showed the greatest increase (~2.3-fold; $p \leq 0.001$) with the ~78 kDa, ~132 kDa and ~81 kDa immunoreactive bands displaying increases of ~1.4-fold ($p \leq 0.01$), ~1.9-fold ($p \leq 0.001$) and 1.2-fold ($p \leq 005$), respectively (Figure 4.1). The PMA-induced phosphorylation was sustained after 15 and 30 min but after 60 min phosphorylation levels decreased, increasing again at 120 min (results not shown). Adult worms were also exposed to 20 μM GF109203X for 120 min but no significant effect on the phosphorylation of ~81 kDa, ~116 kDa and ~132 kDa bands was observed and only the phosphorylation of the ~78 kDa was reduced ($p \leq 0.05$) (Figure 4.1). GF109203X inhibits PKC activity by competing with the ATP binding site and is therefore unable to directly inhibit active forms of the enzyme. The inhibitory effect of GF109203X on *S. mansoni* PKCs was thus further assessed by pre-incubation of adult worms in GF109203X followed by exposure to 1 μM PMA for 30 min and the PMA-induced increase in phosphorylation was found to be significantly blocked (Figure 4.1).

The enzymatic activity of the immunoreactive bands was confirmed in a PKC immunoprecipitation and kinase assay (Figure 4.2) which demonstrated that *S. mansoni* proteins immunoprecipitated with either anti-phospho PKC antibody phosphorylated the PKC substrate Ser/Thr 8 peptide (Figure 4.2). Higher enzymatic activity was detected with anti-phospho PKC (Thr410) compared to anti-phospho PKC (Ser660) antibodies. Furthermore, the PKC activity increased when live adult worms where exposed *in vitro* for 30 min with PMA (1μM) prior to the immunoprecipitation and kinase assay (Figure 4.2). Thus, both PKC antibodies recognized *S. mansoni* proteins with PKC-like enzymatic activity, which was further stimulated with PMA.

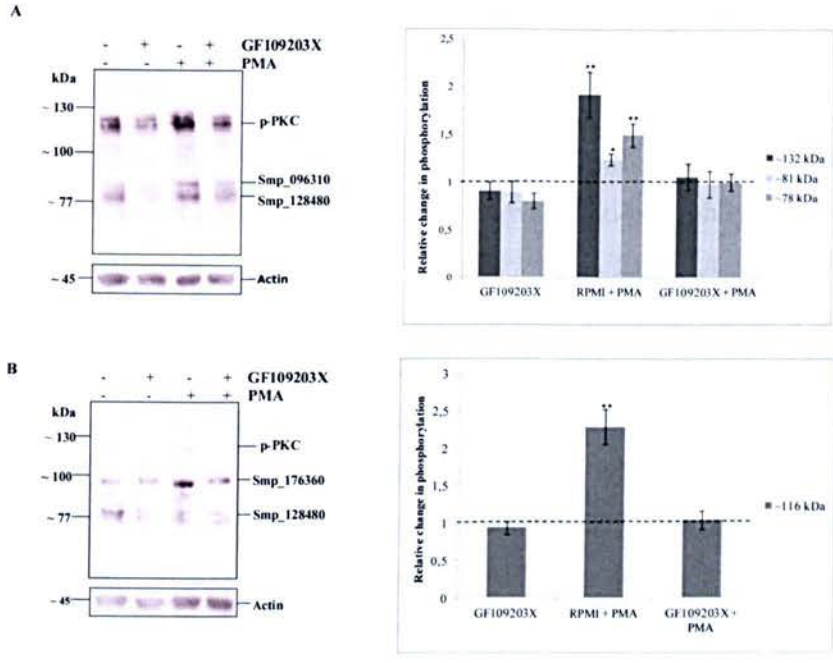

Figure 4.1- *In vitro* pharmacological inhibition and activation of *S. mansoni* adult worm PKC-like proteins. Detection of *S. mansoni* PKC-like proteins after exposure of live adult worm pairs to GF109203X (20 μM; 120 min), GF109203X (20 μM; 120 min) followed by PMA (1 μM; 30 min), or PMA (1 μM; 30 min) only. Protein homogenates of adult worm pairs (12 μg per lane) were probed with anti-phospho-PKC (ζ Thr410) Panel (**A**) or anti-phospho PKC βII (Ser660) antibodies Panel (**B**). An anti-actin antibody was used to confirm equal loading of proteins. Immunoreactive bands were detected and quantified with GeneGnome and GeneTools the mean relative change (± SEM; see graph) in phosphorylation for each protein calculated relative to the phosphorylation levels of untreated (DMSO or RPMI 1640) controls that were assigned a value of 1 (shown as the dotted line). Results are representative of three independent experiments. The dotted line shows control levels of phosphorylation of adult worm couples in RPMI medium with or without DMSO. Statistical analysis of significance was determined with Fishers test, * = ($p \leq 0.05$) and ** = ($p \leq 0.01$).

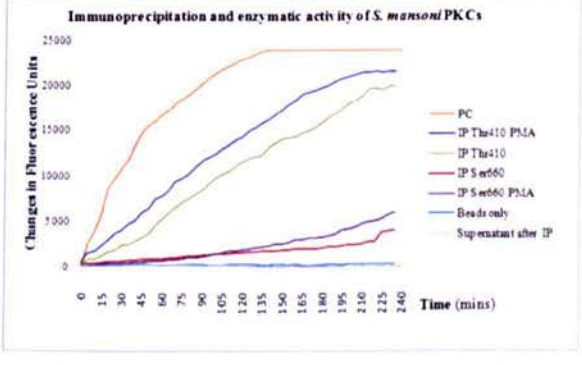

Figure 4.2- PKC activity of adult *S. mansoni* proteins immunoprecipited with anti-phospho PKC antibodies. Line graphs show the PKC activities of immunoprecipitates demonstrating that the proteins recognized by the antibodies used in this study had PKC activity by phosphorylating the PKC substrate peptide Ser/Thr 8. In some cases adult worms were treated with PMA before homogenisation. The immunocomplexes comprising worm protein, agarose beads and anti-phospho PKC antibodies [anti-phospho-PKC (ζ Thr410) or anti-phospho PKC βII (Ser 660), as shown] were assayed with an Omnia PKC kinase kit and enzymatic activity recorded in fluorescence units. Protein homogenates of 100 worm couples challenged with 1μM of PMA for 30 minutes prior to the assay or untreated controls assayed with the two anti-phospho PKC antibodies showing the successful phosphorylation of downstream substrate peptide Ser/Thr 8. Results are representative of the average of 2 independent experiments

4.3.2 S. mansoni *ERK-like proteins have ERK activity and are inhibited by a MEK/ERK inhibitor*

To evaluate the inhibitory effect of the MEK inhibitor U0126 on the phosphorylation status of the proteins detected with anti-phospho ERK antibodies, *S. mansoni* adult worms were exposed, *in vitro,* to 1 μM U0126 for 30, 60 and 120 min. Immunoblotting revealed that U0126 decreased ERK phosphorylation over time when compared to RPMI 1640 and DMSO controls (Figure 4.3 A). After 30 min phosphorylation of ~48 kDa and ~43 kDa proteins was reduced by ~27% and ~72%, respectively ($p \leq 0.01$ and $p \leq 0.001$) (Figure 4.3 B). After 120 min almost no ERK phosphorylation was seen (Figure 4.3 A). Inhibition of ERK phosphorylation with U0126 also demonstrates that *S. mansoni* MEK is sensitive to this compound. Immunoprecipitation and kinase assay with adult protein homogenates showed that the proteins detected by anti-phospho ERK antibodies were capable of phosphorylating the ERK substrate Elk-1 (Figure 4.3 C). The phosphorylation of Elk-1 was detected by western blotting using anti-phospho Elk-1 antibodies (Figure 4.3 C). No Elk-1 phosphorylation was observed in the negative control immunoprecipitations that lacked primary antibody.

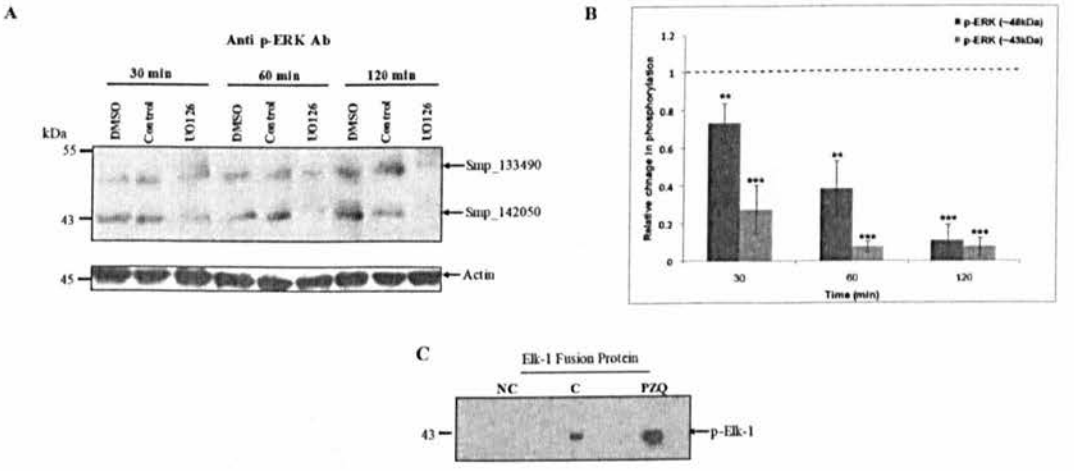

Figure 4.3 - *S. mansoni* ERK-like proteins are phosphorylated (activated) by MEK and possess characteristic ERK activity. Panel (**A**) live adult worm pairs were exposed to 1 μM U0126 or 0.1% DMSO (control) for 30, 60 or 120 min. Protein homogenates (12 μg) were processed for western blotting and blots probed with anti-phospho p44/42 MAPK antibodies. Panel (**B**) immunoreactive bands from three independent experiments were analyzed and the mean relative change (± SEM) in phosphorylation of each protein calculated relative to the phosphorylation levels of controls that were assigned a value of 1 (shown here as the dotted line). **p≤0.01 and ***p≤0.001. Panel (**C**) phosphorylation of Elk-1 fusion protein by immunoprecipitated ERK from adult worm pairs challenged with PZQ (PZQ), untreated controls (C) or with beads only (negative control, NC). Immunocomplexes were then incubated with Elk-1 fusion protein as the ERK substrate and phosphorylated Elk-1 was detected on western blots using anti-phospho Elk-1 antibodies. Results are representative of two independent experiments.

4.3.3 S. mansoni *ERK and PKC signalling is interconnected*

To determine if cross-talk between ERK and PKC exists in *S. mansoni*, the phosphorylation status of ERK proteins was determined after exposure of adult worms *in vitro* with PKC modulators and vice-versa. Exposure to 1μM PMA induced a 1.7-fold increase of the ~43 kDa ERK ($p \leq 0.05$), however phosphorylation of the ~ 48 kDa band was unaffected (Figure 4.4 A). Furthermore, PMA-induced activation of the ~43 kDa ERK was blocked by pre-treatment of adult worms with GF109203X for 120 min prior to 30 min of PMA stimulation, indicating that PMA-induced ERK activation was a consequence of PKC activation. The PKC inhibitor GF109203X alone did not significantly inhibit ERK phosphorylation after 120 minutes incubation. On the other hand, exposure of worms to 1 μM U0126 for 60 or 120 min stimulated the phosphorylation of the ~116 kDa PKC ($p \leq 0.05$; 1.9-fold) (Figure 4.4 B), and of the ~132 kDa PKC after 120 min ($p \leq 0.01$; 2.5-fold) (Figure 4.4 B).

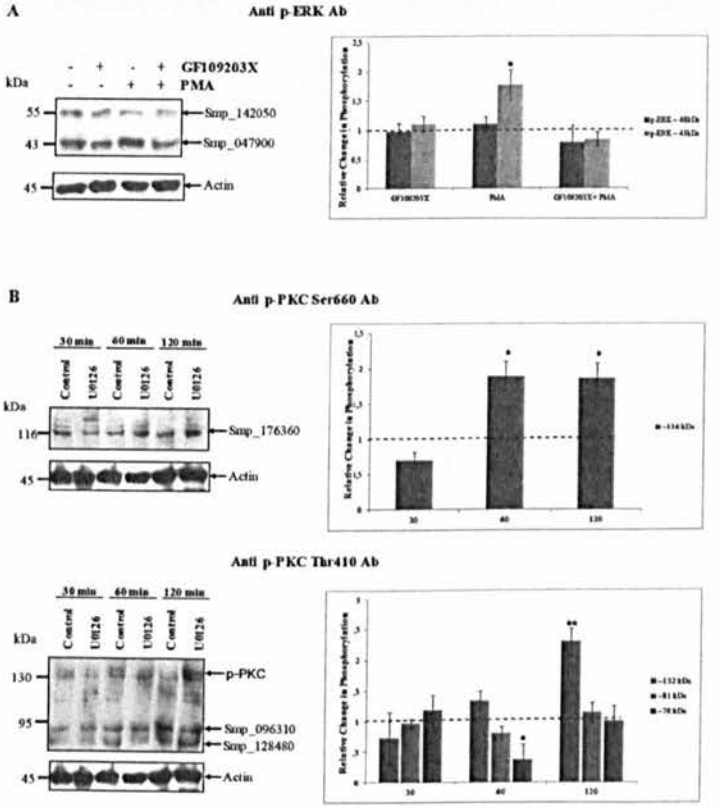

Figure 4.4 - Phosphorylation of *S. mansoni* ERK and PKCs following treatment with PMA, GF109203X or U0126. Panel (**A**) detection of phosphorylated ERKs probed with anti-phospho p44/p42 MAPK antibodies following *in vitro* treatment of adult worms with GF109203X (20 μM) only, GF109203X (20 μM) and PMA (1 μM), or PMA (1 μM) only. Panel (**B**) detection of phosphorylated PKCs probed with anti-phospho PKC (Ser660) or (Thr410) antibodies after challenge of adult worms with 1 μM UO126 for 30, 60 and 120 minutes. An anti-actin antibody was used to confirm equal protein loading and immunoreactive bands quantified. Statistical analysis of significance was determined, ** = ($p \leq 0, 01$) and * = ($p \leq 0, 05$). Results are representative of two independent experiments (12 μg per lane).

4.3.4 In situ *localization of active PKC and ERK in adult* S. mansoni

Activated/phosphorylated PKC and ERK were immunolocalized in whole adult worms fixed immediately after perfusion or after exposure to 1 μM PMA for 15 min. A negative control without primary antibody was included (Figure 4.5).

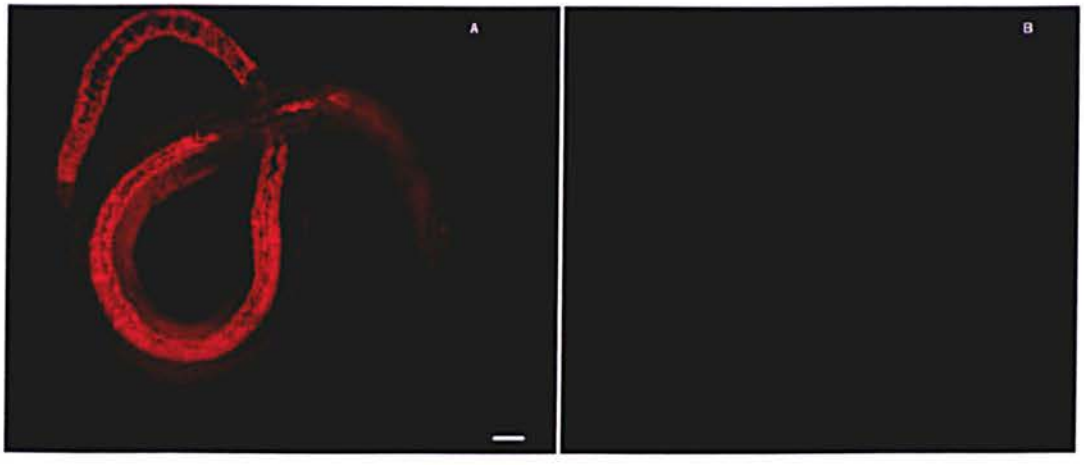

Figure 4.5- Representative confocal micrograph of negative control *S. mansoni* adult worm pair probed without primary antibodies but with Alexa Fluor 488 secondary antibodies. Maximum projection of a worm pair stained only with Alexa Fluor 488 and rhodamine phalloidin which stains F-actin (red). Panel (**A**) shows actin filaments of the worm pair and panel and (**B**) the background green signal from Alexa Fluor 488/autofluorescence which is almost undetectable. Bar=10μm

The activated PKCs detected in control worm pairs with anti-phospho PKC (Thr410) antibodies were consistently associated with regions of the oesophagus, digestive tract, myocytons or neurons, tegumental surface and tubercles of the tegument with higher levels of fluorescence generally observed on the male surface compared to females (Figure 4.6 A). Fluorescence was also sometimes present within subtegumental tissues, the oesophageal gland of males and the female oviduct when an egg was present (Figure 4.6). After PMA challenge an overall increase in fluorescence was observed with the anti-phospho PKC (Thr410) antibodies in the tegument, Mehlis gland and oesophagus compared to control samples (Figure 4.7 A). PMA treatment also revealed a neuron like and ramified-like structure not previously detected in untreated worms in the anterior part of male worms resembling either the excretory or neural system (Figure 4.7 A). Overall, less fluorescence was observed using anti-phospho PKC (Ser660) antibodies; although staining was sometimes associated with the oesophagus and digestive tract and the tubercles of the tegument of male and female worms, it was predominantly associated with the male musculature (Figure 4.6 B).

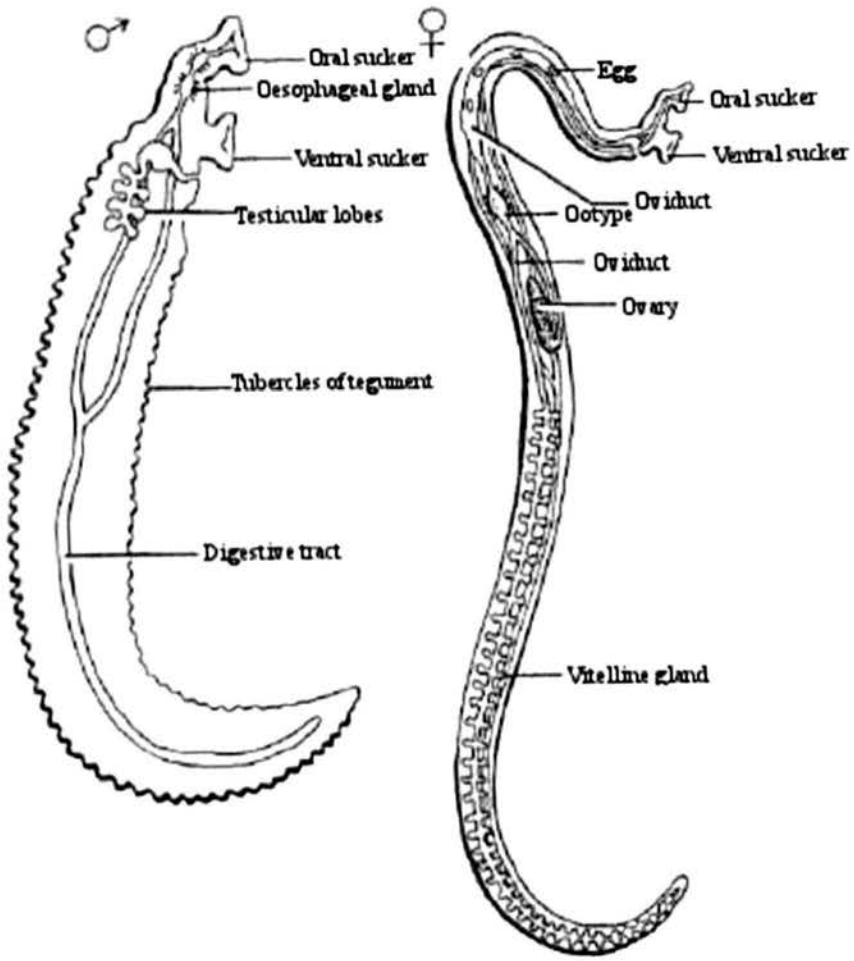
♂
♀
Oral sucker
Oesophageal gland
Ventral sucker
Testicular lobes
Tubercles of tegument
Digestive tract
Egg
Oral sucker
Ventral sucker
Ovi duct
Ootype
Ovi duct
Ovary
Vitelline gland

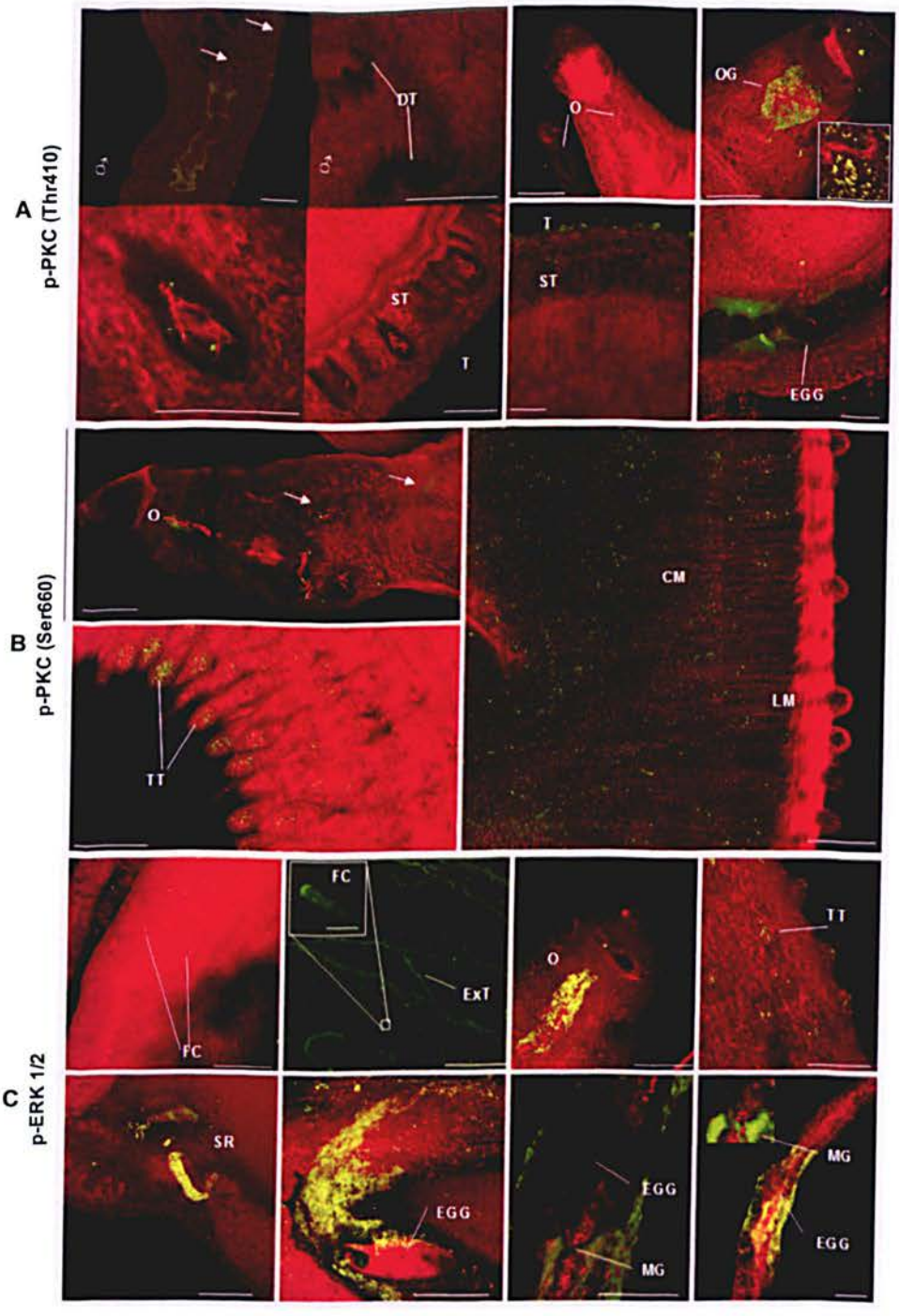

Figure 4.6- Immunolocalization of phosphorylated (activated) PKC and ERK in intact paired adult *S. mansoni*. Untreated adult worms fixed immediately after perfusion were probed with either anti-phospho PKC (Thr410) Panel (**A**), anti-phospho PKC βII (Ser660) Panel (**B**), or anti-phospho p44/p42 MAPK (ERK1/2/) Panel (**C**) primary antibodies and Alexa Fluor 488 secondary antibodies (green signal). Specimens were additionally stained with rhodamine phalloidin, which stains actin filaments (red signal). Panel (**A**) shows activated PKC associated with the digestive tract (DT), oesophagus (O), oesophageal gland (OG), tegument (T), subtegument (ST), oviduct when an egg was present and myocytons or neurons (arrows). Panel (**B**) shows activated PKC associated with the tubercles of the tegument (TT), circular musculature (CM), longitudinal musculature (LM), male oesophagus (O) and unidentified structures in the male head (arrows). Panel (**C**) shows activated ERK associated with ramified-like structures in the male subtegument that resemble excretory tubles (Ext), flame cells (FC), oesophagus of the male (O), tubercles of the tegument (TT), female seminal receptacle (SR), walls of the oviduct when an egg was present, and Mehlis gland (MG). Scale bars = 50 μm

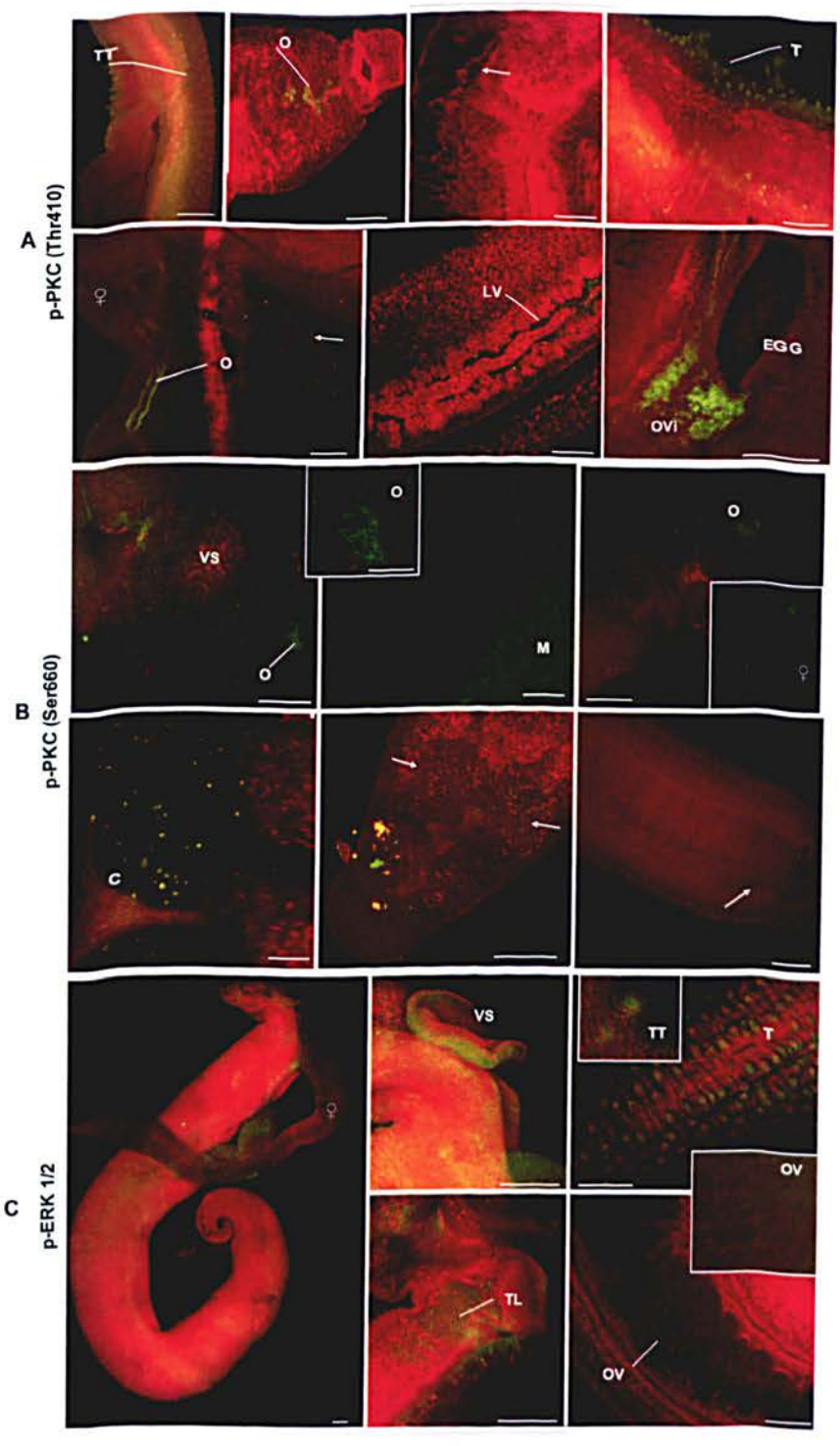

Figure 4.7 - Immunolocalization of phosphorylated (activated) PKC and ERK in intact PMA treated adult *S. mansoni*. Adult worms were probed with either anti-phospho PKC (Thr410) Panel (**A**), anti-phospho PKC (Ser660) Panel (**B**) or anti-phospho p44/p42 MAPK (ERK1/2/) Panel (**C**) primary antibodies and Alexa Fluor 488 secondary antibodies (green signal). Specimens were additionally stained with rhodamine phalloidin, which stains actin filaments (red signal). Worms were treated with 1 μM PMA for 15 min prior to fixing. Panel (**A**) shows worms with activated PKC associated with the tubercles of the tegument (TT), oesophagus (O) of both male and female, the tegument (T) and its disruption, subtegumental structures (arrow), lumen of the vitellaria (LV) and female oviduct (OVi). Panel (**B**) shows worms with activated PKC associated with the musculature (M), ventral sucker (VS), caecum (C) oesophagus (O) and unidentified structures (arrows). Panel (**C**) shows activated ERK associated with the tubercles of the tegument (TT) and structures resembling the ovary (OV), testicular lobes (TL), and ventral sucker (VS). Scale bars = 50 μm.

After PMA treatment, the anti-phospho PKC Ser660 antibodies revealed increased fluorescence associated with the oesophagus, male musculature and subtegumental area (Figure 4.7 B). The *S. mansoni* ERKs were associated with the subtegument, tegument, tubercles (Figure 4.6 C). In male adult worms, fluorescence was associated with ramified structures resembling the excretory system with flame cells at the tips (Figure 4.6 C). In females intense fluorescence was found associated with the walls of the oviduct when an egg was present, in structures resembling the seminal receptacle (SR), the ovary and the Mehlis gland (Figure 4.6 C). Following exposure of adult worms with 1 μM PMA an increase in the overall fluorescence was seen (Figure 4.7 C). In general, higher immunoreactivity was observed in the tegument, ventral sucker, female ovary, in the area where the male fertilizes the female worm and the male testis (Figure 4.7 C).

4.3.5 Pharmacological modulation of PKC and ERK induces physiological disturbances in adult S. mansoni

To ascertain the effects of PKC and ERK inhibition/activation on adult worm phenotype paired worms were cultured with the PKC inhibitor GF109203X or the MEK/ERK inhibitor U0126 at various concentrations (1, 5, 20 and 50 μM), the PKC activator PMA (1μM), DMSO (0.5%), or RPMI 1640 only. Adult worms were videoed at 1, 24, 48, 72 and 96 h (Videos 4.1 – 4.5) and eggs were collected and counted when media/treatments were changed daily. Five observable physiological effects were quantified: decoupling of adult worm pairs, male ventral sucker detachment (in paired and unpaired males), egg output (per couple), speed of movement, and an unusual persistent coiling effect (number of spring-like coils an adult worm had which persisted for more than 10 s).

In untreated control conditions all adult worms remained paired with an average number of ~106 eggs released daily per couple during the first 3 days of the assay with a decrease to ~93 on the fourth day. All worms had their ventral sucker attached during the first 24 h of the assay and only 7% were detached during the following days. The initial average speed of movement was 2.32 mm/s during the first hours of the assay increasing to an average of 3.68 mm/s throughout the remainder of the assay. Sustained coiling was rarely observed. Overall, control worms were elongated and exhibited a slow writhing motion with occasional stronger contractions which is in accordance with observations described elsewhere (Blair *et al.*, 1988) (Video 4.1). The worms exposed

to DMSO (vehicle control) displayed a small transient increase in movement and some temporary loss of attachment returning to the pre-treated status within one hour. The average speed of movement was ~3.4 mm/s and only 2% of the adults showed ventral sucker detachment at the end of the assay. The average of eggs released daily per couple (~122) was similar to RPMI 1640 controls ~112. The quantified physiological effects from DMSO and untreated control groups were not significantly different throughout the length of the assay (Tables 4.1 and 4.2, Appendix).

U0126, which significantly reduced ERK phosphorylation, had a significant effect on adult worm pairing in a time and concentration dependent manner. The highest concentration (50 μM) caused almost instant decoupling of worm pairs and 96% of couples were unpaired after only 1 h ($p \leq 0.001$) (Figure 4.8 A; Video 4.2). After 96 h, 4%, 26% and 35.5% ($p \leq 0.01$) of the adult worms unpaired with 1, 5 and 20 μM U0126, respectively. Ventral sucker attachment was also negatively affected, after 96 h culture 8.3%, 40.7%, 46.9% of worms showed ventral sucker detachment at 1, 5 and 20 μM U0126 respectively ($p \leq 0.001$) (Figure 4.8 C). At 50 μM U0126 all worms detached after 1 h ($p \leq 0.001$). U0126 also affected adult worm movement compared to DMSO controls, and at 1 h a significant stimulatory effect on movement was observed with all concentrations; at 1, 5, 20 and 50 μM worm pairs showed an increase in average speeds of 266% [9.4 mm/s ($p \leq 0.001$)], 215% [7.6 mm/s ($p \leq 0.01$)], 251% [8.9 mm/s ($p \leq 0.001$)] and 302% [10.7 mm/s ($p \leq 0.001$)] respectively, compared to DMSO control speeds of 3.54 mm/s (Figure 4.10 B). However, movement decreased with time and after 96 h a decrease of 52%, 42% and 65% in speed of 1, 5 and 20μM U0126 challenged worms was observed when compared to movement at 1 h (Figure 4.10 B). Because after the first day all adults unpaired with 50 μM U0126, the speed of movement was measured in separated males and females (Figure 4.10). At 1 h both male and females had increased movements with speeds of 9.7 and 8.5 mm/s for males and females respectively (Figure 4.10 D and F; Table 4.3, Appendix). The speed of movement decreased with time and after 96 h culture with 50 μM U0126 male movement reduced by 63% and female movement by 91 %. An interesting behaviour was also observed in adult worms at all U0126 concentrations resembling a jittery-like effect (Video 4.2). U0126 also affected egg output; at 1–20 μM reduced egg output was observed at 24 h although it was slightly higher with 20 μM at 48 h (Figure 4.8 B). At 50 μM U0126 completely blocked egg output after 72 h, with only a few small immature eggs sporadically found at earlier times, likely at least partly a consequence of worm unpairing (Figure 4.8 B).

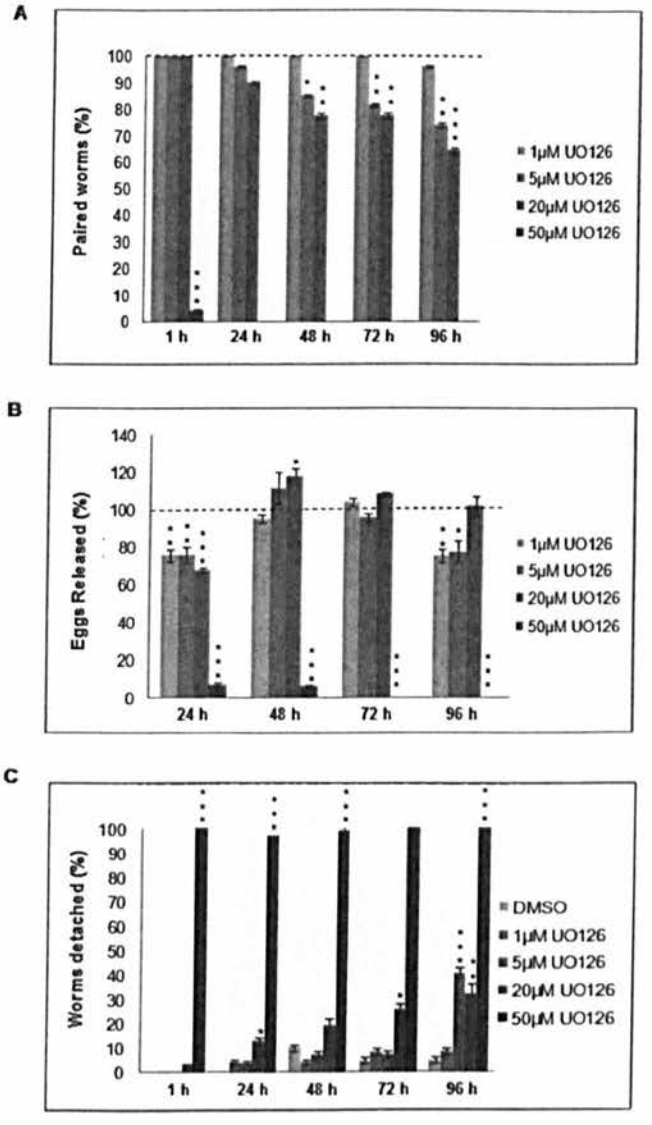

Figure 4.8 - Effects of U0126 on adult *S. mansoni* worm uncoupling, egg output and ventral sucker attachment *in vitro* over 96 h. Worms were treated with either 1, 5, 20 or 50 μM of U0126 or DMSO (vehicle) and movies captured at various time points over 96 h. Panel (**A**) shows the effect on worm pairing; Panel (**B**) shows effect on egg release and (**C**) shows the effect on ventral sucker attachment to the culture dish. Statistical analysis of significance for mean values was determined with Fishers test, *** = ($p \leq 0.001$) ** = ($p \leq 0.01$) and * = ($p \leq 0.05$), when compared to mean values for the DMSO controls. These results are representative of four independent experiments each done with a minimum of two replicates, and containing a minimum of three adult worms pairs per replicate.

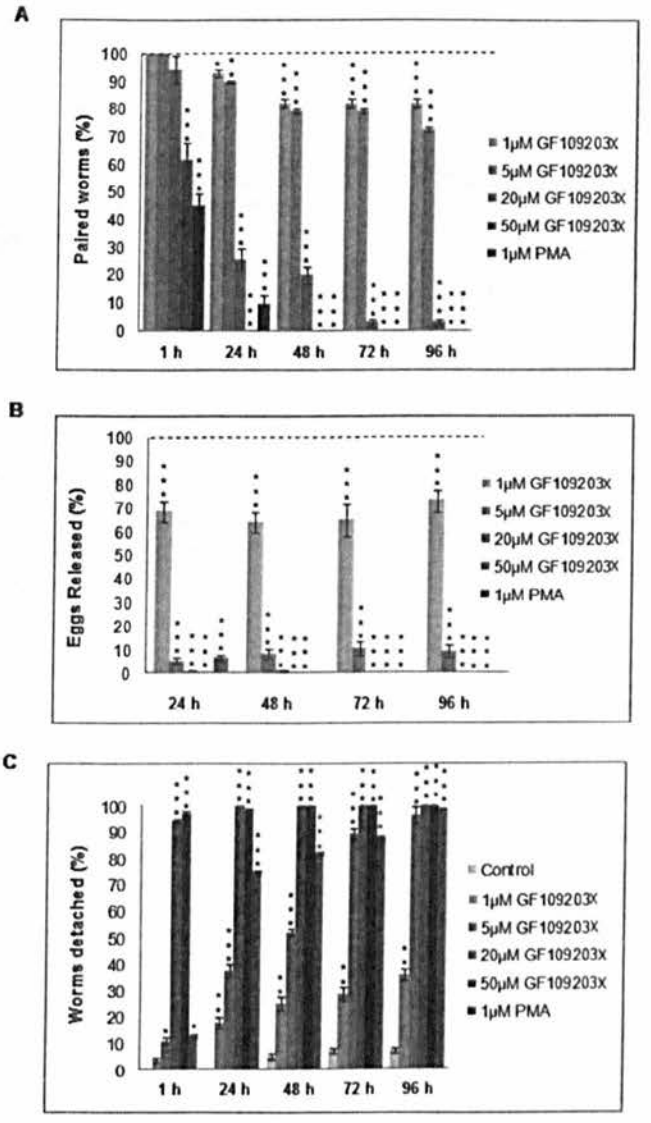

Figure 4.9 – Effects of GF109203X and PMA on adult *S. mansoni* worm uncoupling, egg output and ventral sucker attachment *in vitro* over 96 h. Worms were treated with either 1, 5, 20 or 50 μM of GF109203X, 1 μM of PMA or RPMI 1640 (control) and movies captured at various time points over 96 h. Panel (**A**) shows the effect on worm pairing; Panel (**B**) shows effect on egg release and (**C**) shows the effect on ventral sucker attachment to the culture dish. Statistical analysis of significance for mean values was determined with Fishers test, *** = ($p \leq 0.001$) ** = ($p \leq 0.01$) and * = ($p \leq 0.05$), when compared to mean values for the RPMI controls (for GF109203X treatments) or DMSO controls (for PMA challenge). These results are representative of four independent experiments each done with a minimum of two replicates, and containing a minimum of three adult worms pairs per replicate.

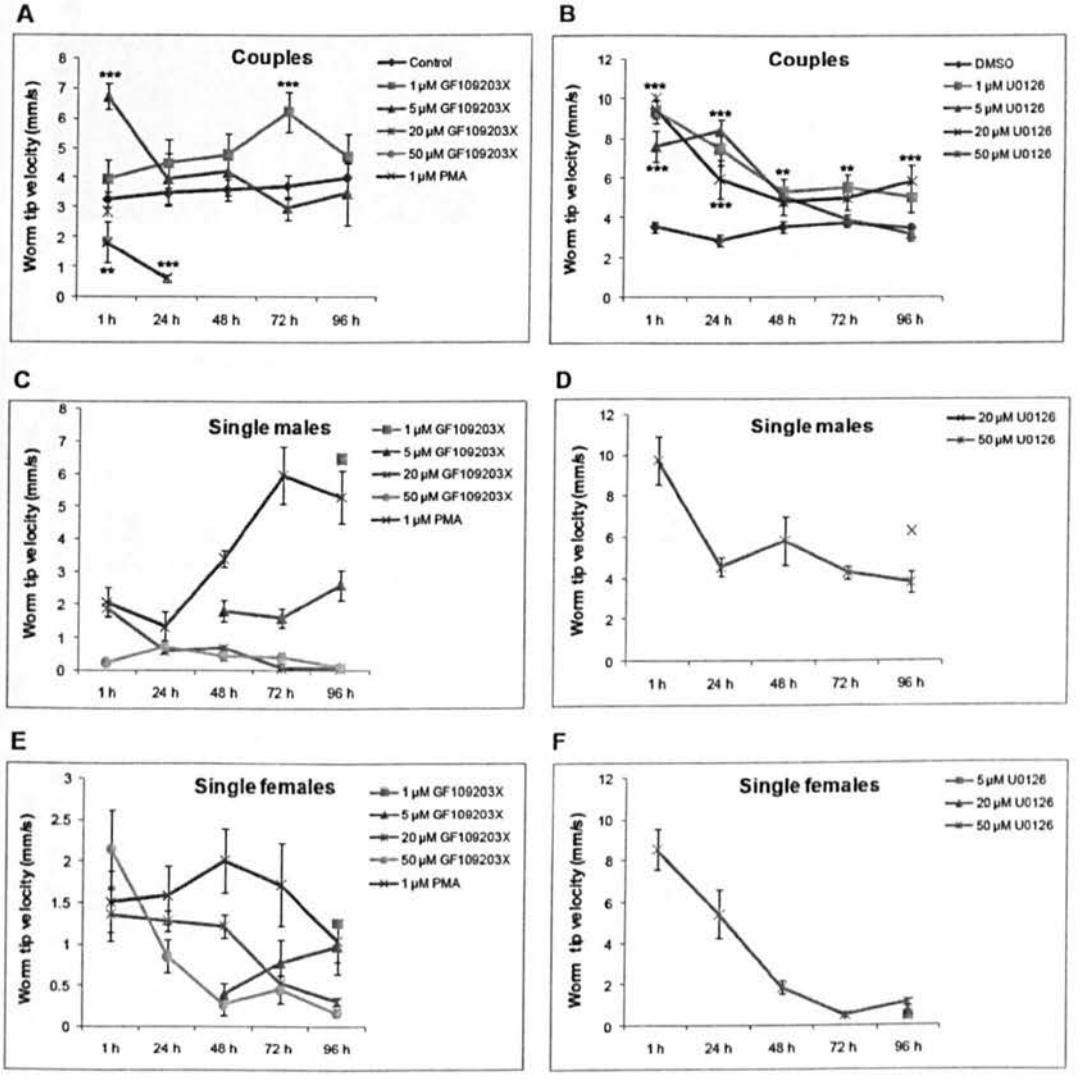

Figure 4.10 - Effects of GF109203X, PMA, and U0126 on movement of adult *S. mansoni in vitro* over 96 h. Panels (**A**) and (**B**) show the effect of pharmacological challenge on worm tip velocity (mm/s) compared to controls in adult worm pairs. Panel (**C**) and (**D**) show effects on separated male worms; these were not directly compared to controls as the controls did not separate. Panels (**E**) and (**F**) show the effects on the movement of separated female adult worms. Statistical analysis of significance was determined with Fishers test, *** = ($p \leq 0.001$), ** = ($p \leq 0.01$) and * = ($p \leq 0.05$). Results are representative of four independent experiments with a minimum of two replicates each, and containing a minimum of three adult worm pairs per replicate.

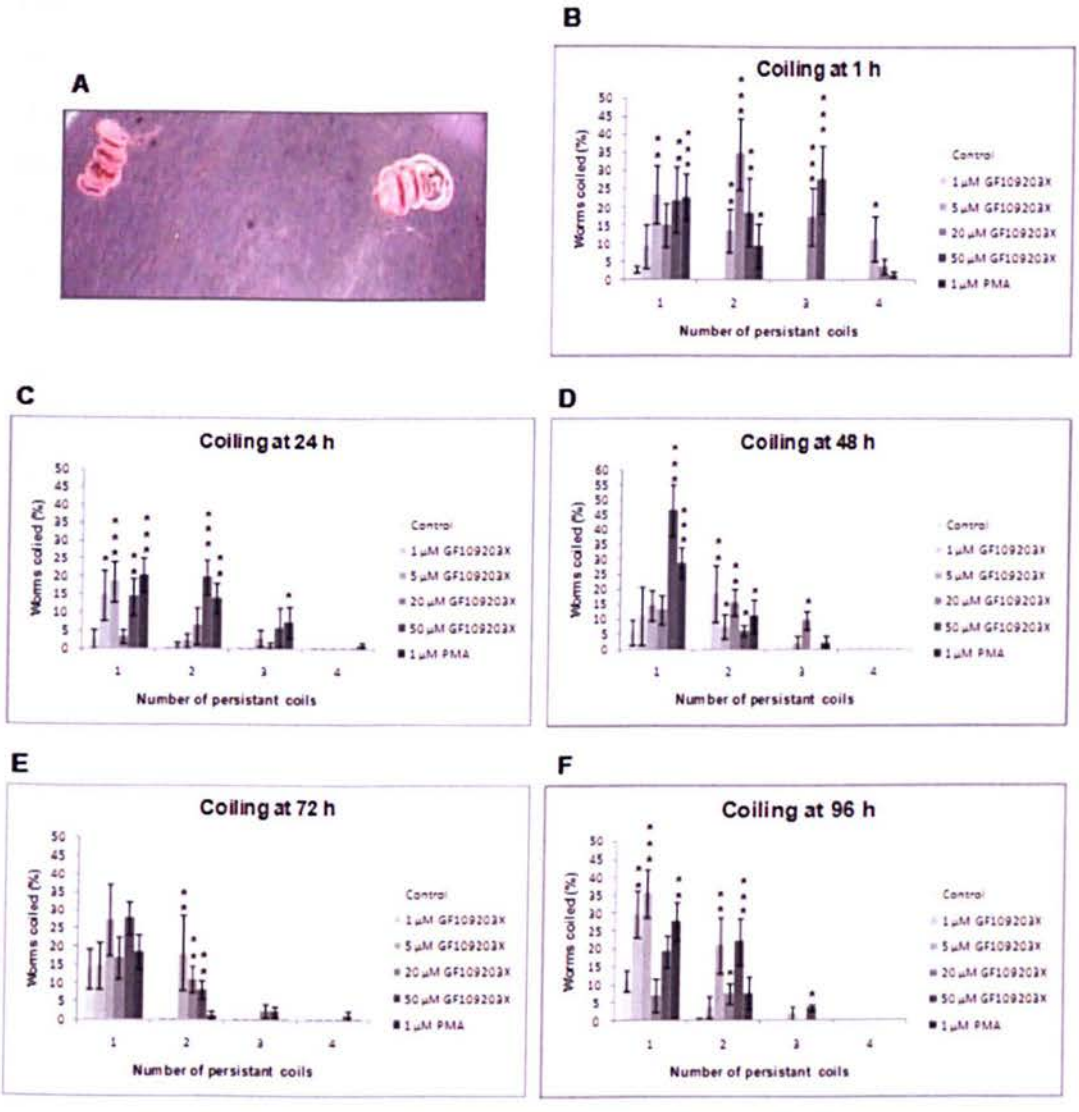

Figure 4.11- Persistent coiling effect in adult *S. mansoni* pairs exposed *in vitro* for 96 h to GF109203X or PMA. Panel (**A**) is a micrograph representing the effect observed, in this case two adult worm pairs displaying a total of four coils each. Panels (**B**), (**C**), (**D**), (**E**) and (**F**) represent the number of adult worm pairs that maintained a persistent coiling effect throughout the assay. The coiling effect was considered persistent if it was maintained for over 10 s. The number of coils was also determined. Statistical analysis of significance was determined with Fishers test, *** = ($p \leq 0.001$) ** = ($p \leq 0.01$) and * = ($p \leq 0.05$). These results are representative of four independent experiments with a minimum of two replicates each and containing a minimum of three adult worm pairs per replicate.

GF109203X, which blocked phosphorylation of the *S. mansoni* PKCs, had an overall negative effect on adult worm pairing, speed of movement and egg output in a time and concentration dependent manner compared to untreated controls (Tables 4.1 and 4.3, Appendix) (Figures 4.9 and 4.10) (Video 4.3). Furthermore, at 5, 20 and 50 μM it induced persistent coiling effects (Table 4.2, Appendix) (Figure 4.11). During the first hour a proportion of worms remained paired across all GF109203X concentrations (Figure 4.9 A) and except at 1 μM pairs exhibited a persistent coiling effect with one and more coils (Figure 4.11); this seemed to be exerted by the males resulting in some cases in release of female gut components (Video 4.4). Furthermore, after 1 h exposure to 20 and 50 μM GF109203X, 93% and 97% of worm pairs showed ventral sucker detachment (Figure 4.9 C). Throughout the following days all adult worm pairs separated with 50 μM GF109203X and a significant reduction in pairing was observed at 1, 5 and 20μM ($p \leq 0.001$) (Figure 4.9 A). Egg output per couple also reduced and no eggs were found in culture with 20 μM or 50 μM GF109203X after the first day ($p \leq 0.001$); after 24 h 1 μM and 5 μM GF109203X reduced oviposition by 31% ($p \leq 0.01$) and 95% ($p \leq 0.001$), respectively (Figure 4.9 B). The sustained spring-like coiling effect was most prominent during the first and second days of the assay (Table 4.2, Appendix; Figure 4.11). For instance, 1 h after culture in 5, 20 or 50 μM GF109203X only 52%, 26% and 30% of worms, respectively, showed a normal behaviour while the remainder displayed sustained coiling with one or more simultaneously sustained coils (Figure 4.11). This effect was persistent with 5 and 20 μM for up to 72 h (Table 4.2, Appendix). At the end of the assay (i.e. at 96 h), GF109203X significantly attenuated pairing with 17.9%, 27.6%, 97.14% and 100% of worms decoupled with 1, 5, 20 and 50 μM respectively ($p \leq 0.001$; Figure 4.9 A). Ventral sucker attachment was also negatively affected, at 20 and 50 μM all worms had detached from the culture plate and at 1 μM and 5 μM 44% ($p \leq 0.01$) and 95% ($p \leq 0.001$) of worms were detached (Figure 4.9 C). Worm movement was also significantly reduced by GF109203X (Figure 4.10). Although lower doses (1μM and 5μM) had little effect, after 1 h exposure to 20 or 50 μM GF109203X speeds of paired worms were 2.8 ($p \leq 0.01$) and 1.9 mm/s ($p \leq 0.001$) compared to an average of 3.2mm/s speeds in control worms (Figure 4.10; Table 4.3, Appendix). This decreased movement was time dependent and a drastic decrease in movement of both unpaired female and male worms was seen at 96 h with males showing speeds of 0.06 ($p \leq 0.001$) and 0.09 mm/s ($p \leq 0.001$), and females 0.3 ($p \leq 0.001$) and 0.17 mm/s ($p \leq 0.001$) for 20 and 50 μM GF109203X, respectively (Table 4.3, Appendix; Figure 4.10). Interestingly, 1 h after challenge with 50 μM GF109203X

separated females had a whip like behaviour followed by curling. The observed physiological effects can be related to the *in situ* localization of phosphorylated PKC in the adult worms in areas with suspected neuromuscular system.

The PKC activator PMA affected worm pairing almost instantly and only 10% of couples remained paired after 24h ($p \leq 0.001$); all worms unpaired thereafter (Video 4.5). Only 1% of worms remained attached to the culture dish after 96 h (Figure 4.9 C). Initially, in PMA males showed very little movement and female movement speeds were similar to control pairs, however, over time male and female speeds of movement increased to 5.3 mm/s and 1.0 mm/s, respectively. Egg output was negligible (Figure 4.9 B) as worms quickly unpaired (Figure 4.9 A). The persistent coiling effect was not significantly observed and worms looked stunted (similar to effect of PZQ *in vitro*), although this became less prominent over time. Converse to that observed with GF109103X, PMA reduced movement on the first day and then increased over time (Figure 4.10).

4.3.6 Praziquantel (PZQ) induces activation of S. mansoni *PKC and ERK,* in vitro

Adult worm pairs were exposed, *in vitro,* to 0.2 µg/ml PZQ to ascertain if the phosphorylation status of the activated PKCs and ERKs could be affected by this drug. This concentration of PZQ was used as it is the lowest concentration known to induce the typical morphological effects of PZQ (Pica-Mattoccia and Cioli, 2004). After 15 min incubation worm pairs became contracted and immobile assuming a shrunken appearance (not shown) and the ~78, ~81 and ~132 kDa PKCs showed increased phosphorylation of 1.7 ($p \leq 0.01$), 1.5 ($p \leq 0.05$) and 2.8-fold ($p \leq 0.001$), respectively when compared to DMSO controls. Although the ~116 kDa immunoreactive band detected with anti-phospho PKC (Ser660) antibodies was not affected at 15 min, after 30 and 120 min it showed a ~1.7 fold and 2.2 fold ($p \leq 0,05$) increase in phosphorylation, respectively (Figures 4.12 A and B). The *S. mansoni* ERKs also showed increased phosphorylation after PZQ treatment compared to controls. The strongest increase was detected after 15 min with the ~43 kDa ERK showing a 2.7 fold increase ($p \leq 0.001$; Figure 4.12 C). The ~48 kDa band was also significantly affected by PZQ and 15, 30 and 120 min there was an increase of 2.2, 2.3 and 2.2 -fold in phosphorylation ($p \leq 0.05$; Figure 4.12 C).

Immunohistochemistry and confocal microscopy corroborated the immunoblotting results, showing an overall increase in the immunofluorescence of

paired worms, however male worms showed higher levels of fluorescence than females (Figure 4.13). Phosphorylated PKC detected with anti-phospho PKC (Thr410) antibodies showed a similar pattern of activation observed with PMA treatments and active PKC was found associated with the musculature and tegument, with structures suggesting excretory functions (Figure 4.13 A). Furthermore, fluorescence associated with the oesophageal gland and oesophagus was present (Figure 4.13 A). With the anti-phospho PKC (Ser660) antibodies a similar pattern of activation to that of PMA challenge but with increased fluorescence associated with the musculature and tegument of the parasite (Figure 4.13 B). After 15 min of PZQ treatment phosphorylated ERK was found to be associated with the tegument of paired male and female worms, male muscular regions, nerve/excretory ramified-like structures and flame cells (Figure 4.13 C).

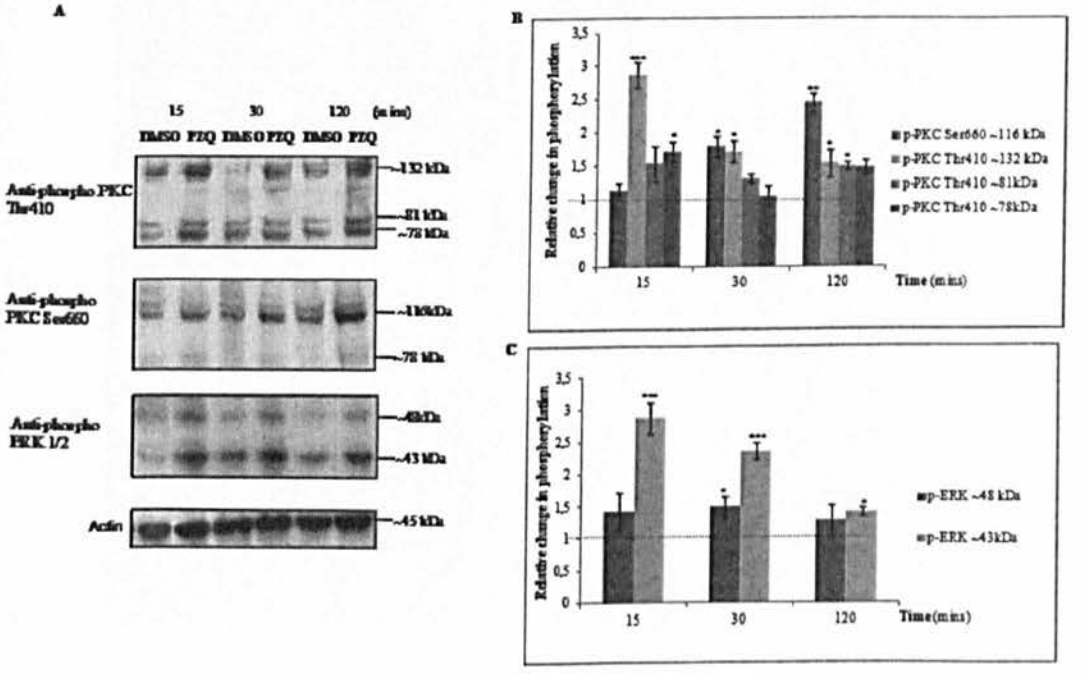

Figure 4.12- Immunoblot analysis of the phosphorylation status of *S. mansoni* ERK and PKC following challenge with PZQ. Adult worms were exposed to either 0.2% DMSO (vehicle control) or 0.02mg/ml PZQ for 15, 30, and 120 min and proteins processed for western blotting. Panel (**A**) protein homogenates were probed with anti-phospho PKC (Thr410), anti-phospho PKC (Ser660) and anti-phospho p44/p42 MAPK antibodies. For each treatment similar amounts of protein were loaded (12 µg) and an anti-actin primary antibody was used to confirm equal loading of proteins. Panel (**B**) immunoreactive bands were detected and quantified with GeneGnome tools and expressed as a proportion of control levels that were assigned a value of 1 (shown as the dotted line). Statistical analysis of significance was determined with Fishers test, *** = ($p \leq 0.001$), ** = ($p \leq 0.01$) and * = ($p \leq 0.05$). These results are representative of three independent experiments each with a minimum of two replicates.

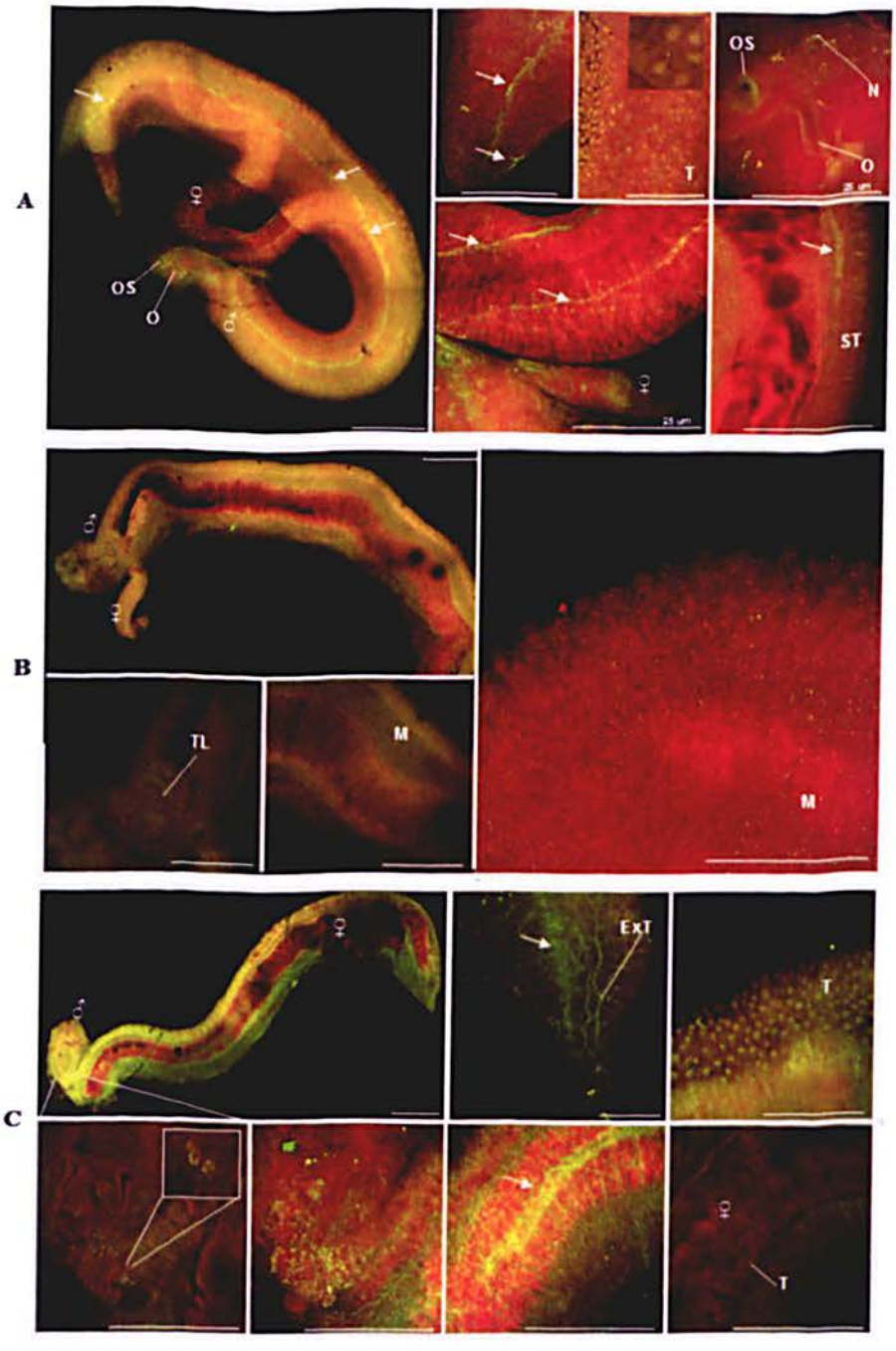

Figure 4.13 – Immunolocalization of phosphorylated (activated) PKC and ERK in intact adult *S. mansoni* after exposure to PZQ. *S. mansoni* adult worms were probed with either anti-phospho (Thr410) (Panel **A**), anti-phospho PKC (Ser660) (Panel **B**) or anti-phospho p44/p42 MAPK (ERK1/2/) (Panel **C**) and Alexa Fluor 488 secondary antibodies (green signal) after 15 min treatment with 0.02 mg/ml PZQ. Specimens were additionally stained with rhodamine phalloidin, which stains actin filaments (red signal). Panel (**A**) shows activated PKC detected with anti-phospho PKC (Thr410) associated with the subtegument (ST), neurons (N), oesophagus (O), oral sucker (OS) and structures in both male and female paired worms resembling the axial muscle of invertebrates (arrows). Panel (**B**) shows activated PKC detected with anti-phospho PKC (Ser660) associated with the male testicular lobes (TL) but predominantly with the musculature (M). Panel (**C**) activated ERK is associated with the male and female tegument (T), tubercles of the tegument, ramified-like structures with possible excretory roles (Ext), structure with possible neuromuscular roles (arrow) and cephalic ganglia (inset). Bar = 200µm.

4.4 Discussion

4.4.1 Immunodetected S. mansoni *proteins have characteristic PKC and ERK properties*

Using immunoprecipitation, the *S. mansoni* immunoreactive proteins detected using the anti-phospho PKC and anti-phospho ERK antibodies have been shown to have PKC and ERK enzymatic activities, with the PKC activity being stimulated with the PKC activator, PMA. Furthermore, by western blotting, the phosphorylation status of the PKCs was stimulated with PMA and the PMA-induced stimulation was blocked with GF109203X, further evidencing that these proteins are PKCs. The large ~116 kDa PKC which is likely to be Smp_160760, a PKCβ-type (Chapter 3), showed the highest increase in phosphorylation after challenge with PMA consistent with it being a classical PKC which are highly responsive to DAG, Ca^{2+} and phorbol esters such as PMA (Newton, 2001). The phosphorylation of the ~81 kDa protein was the least affected by PMA but results indicate it to be Smp_096310 (Chapter 3), an atypical PKC which is not activated with DAG, Ca^{2+} or phorbol esters. Furthermore, the PMA-induced phosphorylation of PKC proteins was transient; this observed biphasic effect in *S. mansoni* is characteristic of PKC signalling in other organisms (Nelson and Alkon, 2009). Phosphorylation of the *S. mansoni* ~48 kDa and ~43 kDa proteins detected with anti-phospho ERK antibodies and shown to possess ERK activity was reduced with U0126, further supporting the presence of MEK protein(s) in S. *mansoni*.

The data are consistent with the immunodetected *S. mansoni* proteins being PKC and ERK homologues. The PKC kinase assay was less sensitive than the ERK enzymatic assay where more adult worms were needed. This is likely to be a consequence of protein expression levels, assay conditions, and antibody binding efficiency in native conditions.

4.4.2 PKC and ERK S. mansoni *signalling pathways are interconnected*

Cross-talk between PKC and ERK, with PKC upstream of ERK, is common in several organisms, from invertebrates like *C. elegans* and *D. melanogaster* to higher organisms such as mammals (Hyde *et al.*, 2011; Mendoza *et al.*, 2011). In this Chapter it is shown that in *S. mansoni*, this signalling interconnection also exists. PMA induced phosphorylation (activation) of the ~43 kDa ERK which was blocked by pre-incubation

with PKC inhibitor GF109203X. Furthermore, 60 minutes exposure to the MEK/ERK inhibitor U0126 increased the phosphorylation status of the ~116 kDa PKC, suggesting the existence of a feedback loop mechanism between *S. mansoni* ERK and PKC proteins.

4.4.3 S. mansoni *PKC and ERK signalling is involved in multiple schistosome functions*

In Chapter 3 the phosphorylation (activation) profiles of *S. mansoni* PKCs and ERKs were found to be noticeably dissimilar across the four life-stages tested (miracidium, sporocyst, cercaria and adult worm) and that more *S. mansoni* PKC isotypes were detected in cercariae and adult worm life-stages compared to miracidium or sporocyst. This suggests a complex role for PKC signalling in the vertebrate host infective and dependent stages. To further elucidate the possible roles/function of these proteins confocal fluorescence microscopy of intact *S. mansoni* adult worms yielded a good resolution analysis of the regional distributions of active PKC and ERK, which combined with the physiological effects of ERK and PKC pharmacological modulation aided identification of roles of these proteins.

4.4.3.1 Strong association of S. mansoni *PKC and ERK activity in the adult tegument surface suggests roles in tegument specific functions*

The tegument of adult schistosomes, especially males, is in constant direct contact with the host environment. It is a dynamic, metabolically active and host-interactive membrane where considerable biochemical, physiological and immunological interplay is expected to take place (Kemp *et al.*, 1980; Saunders *et al.*, 1987; Walker, 2011). It is shown here for the first time that activated/phosphorylated PKC and ERK exist in male and to a lesser extent female tegumental tissues indicating central roles in signal transduction mechanisms regulating schistosome tegument functions. Tegumental immunoreactivity was observed with the anti-phospho ERK and PKC (Thr410) antibodies but less so with anti-phospho PKC (Ser660) antibodies; thus the ~116 kDa PKC detected this latter antibody could have less of a role in tegumental biology. Furthermore, challenge of adult worms with PMA, which is known to induce tegumental disruption (Wiest *et al.*, 1994), increased activity of *S. mansoni* PKC and ERK associated with the adult worm tegument. Synthesis, secretion and transport of proteins and glycoproteins are important mechanisms for maintaining tegument

integrity protecting the schistosome against the host immune responses (Saunders *et al.*, 1987; Jones *et al.*, 2004). PKCs are involved in cell secretion, which may alter transport of cell membrane components to the cell surface (Gil *et al.*, 2001; Sieburth *et al.*, 2006). In schistosomes, PKC signalling might therefore regulate tegumental processes and overstimulation of PKC may affect tegument integrity particularly as PKC is also known to modulate Ca^{2+} channel activity (Nishizuka, 1989) and have disruptive effects for actin microfilaments (Bershadsky *et al.*, 1990). Disruption of the schistosome tegument could lead to its detection by the host immune system, as in optimal conditions the tegument is the key organ for immune evasion by schistosomes (Faghiri *et al.*, 2010). Additionally, the ~43 kDa ERK was the most responsive to PMA and an increase in fluorescence associated with the tegument was observed suggesting a role of this ERK protein at the parasite surface. Interestingly, ERK activation is also associated with the tegument and sub-tegumental tissues of another parasite, *T. crassiceps* (Escobedo *et al.*, 2010).

The tegumental localization of PKC and ERK proteins also suggests potential roles in host endocrine or immune signal exploitation necessary for successful establishment and reproduction of the schistosome in humans. In fact, EGFR (Borisov *et al.*, 2009) and GPCRs which are associated with insulin signalling (Chu *et al.*, 2007), and have ERK and PKC pathways downstream, have already been identified in the surface of schistosomes (Ramachandran *et al.*, 1996; Hamdan *et al.*, 2002; El-Shehabi *et al.*, 2012). PKC activation in the tegument of *S. mansoni* could suggest a role in host immune evasion as analysis of the *S. mansoni* transcriptome suggests that adult worms can protect themselves from immune response-derived oxidative stresses by having several antioxidant enzymes in the tegument including PKC-interacting thioredoxin (Verjovski-Almeida *et al.*, 2003).

Thus active ERK and PKC detected in tegument of schistosomes could have important roles in schistosome survival such as hijacking and exploiting host hormones and growth factors, modifying host immune response, and sustaining tegumental integrity. Indeed, proteins expressed at the surface of the schistosome are considered to be logical targets for vaccine and drug development (Loukas *et al.*, 2007); ERK and PKC might therefore be good candidates for the targeted development of drugs against schistosomiasis.

4.4.3.2 Involvement of PKC and ERK in muscular activity and neuromuscular coordination of S. mansoni

Early reports by Blair *et al.* (1988) first suggested the possible involvement of PKC in *S. mansoni* muscular contraction. Results in this Chapter substantiate this hypothesis and for the first time demonstrate activated PKC in the musculature and ventral sucker of adult worms; they also demonstrate that inhibition of PKC with GF109203X considerably reduced muscular movement and ventral sucker attachment in a time and concentration dependent manner. GF109203X also induced an unusual sustained coiling phenotype, which was not observed in control groups, supporting roles in neuromuscular coordination. Conversely, PKC activation by PMA increased muscular movement and contraction over time with fast contractile whip like movements. Interestingly, PKC activation also had a negative effect on ventral sucker attachment, but the apparently similar effects on this parameter could be due to different/opposite effects in muscular activity, either decreased (GF109023X) or increased (PMA) muscular tension. PKC is known to play important roles in the signal transduction pathway mediating smooth muscle contraction in vertebrates, especially the PKCβ type (Sohn *et al.*, 1997). PKC appears to play a role in neuromuscular functions of other invertebrates. For example, in *A. californica* PKC ApIII is especially enriched in neurons of the central ganglia (Kruger *et al.*, 1991; Sossin *et al.*, 1993), and PMA initially induces contraction of muscle without relaxation similar effects to that observed in our study. Also in *C. elegans* PKCB1 is found exclusively in sensory neurons and PMA treatment causes uncoordinated movement (Land *et al.*, 1993). Exposure to U0126 also significantly increased muscular movement of adult worms and reduced ventral sucker attachment implicating PKC in schistosome neuromuscular function.

Overall, the effects of PKC and ERK pathway modulation on schistosome physiology observed here are strikingly similar to the effects caused by PZQ and neuromodulatory drugs in schistosomes (Ribeiro *et al.*, 2005). The classical consequence of exposure to such neuromodulatory drugs is paralysis of muscles, and alterations of behaviours particularly those involved with locomotion with consequences in elimination of parasite from the host even if the agent is not directly lethal (Ribeiro and Geary, 2010). Therefore, the negative effects of PKC inhibitor GF109203X on adult worm movement and ventral sucker attachment indicate PKC to be a potential target for the control of schistosomiasis, especially as there is a drive to develop more effective and isotype specific inhibitors of PKC (Serova *et al.*, 2006).

4.4.3.3 Activated PKC is associated with S. mansoni *feeding organs*

Activated PKC was also detected in the oesophagus and oesophageal gland of *S. mansoni* adults suggesting a role in feeding of schistosomes. Despite the exact mechanism of schistosome feeding being yet to be unravelled, schistosomes are known to employ proteases to degrade haemoglobin from ingested and lysed erythrocytes, using the released residues for amino acid metabolism (Ernst, 1975; Brindley *et al.*, 1997; Hall *et al.*, 2011); thus a cytolytic digestive function likely exists in the oesophageal region (Ernst, 1975). Here, phosphorylated PKC was observed using both anti phospho PKC antibodies in the oesophagus of both male and female adult worms suggesting that at least the ~116 kDa and/or the ~78 kDa PKCs are present in this region. These findings are in accord with roles for PKC in feeding of the nematode *C. elegans* where feeding occurs when the pharyngeal muscle (smooth muscle) contracts and relaxes (pumps) to take in food (You *et al.*, 2006). This pumping activity of the *C. elegans* pharynx/oesophageal circular muscle has been shown to be dependent of classic and novel PKC activation with contraction antagonized with PKC inhibitors (Sohn *et al.*, 1997). *S. mansoni* PKC(s) could thus have similar roles, inducing pumping of the male and female oesophagus, although the effects on blood ingestion were not assessed in this study.

4.4.3.4 PKC and ERK modulation affects S. mansoni *reproductive functions such as pairing and egg-laying*

Active/phosphorylated ERK and PKC were associated with various structures in both female and male worms associated with reproductive and egg forming functions, namely the Mehlis gland, ootype, vitellaria, ovary, seminal receptacle and testes. Although ERK and PKC proteins were differentially distributed both were noticeably detected in the female Mehlis gland and ootype particularly when an egg was present indicating possible roles in egg formation (including yolk and eggshell) and expulsion. Strikingly, PKC inhibition of *S. mansoni* with GF109203X significantly blocked egg release by more than 90%; with release attenuated while worm pairs remained. This could perhaps be due to an inability to expel or form eggs. Blocking egg release by schistosomes would significantly reduce pathology of the disease and is a possible strategy to control schistosomiasis.

That ERK signalling is also involved in the regulation of *S. mansoni* reproductive function is supported by the localization of phosphorylated ERK in various

organs with sexual functions in adult females and males such as the male testis and the female seminal receptacle, the ovary and ciliated vitelline duct which although not fully active in untreated groups phosphorylation increased after treatments with PMA. ERK seems to also play important reproductive roles in other parasites. For instance, in *Plasmodium berghei* two MAPK homologues, pfmap-1 and pfmap-2, were found to be essential for sexual growth and male gamete formation (Rangarajan *et al.*, 2005) and in *Taenia solium* the ERK inhibitor II (FR180204) decreased 17β-estradiol parasite-induced reproduction (Escobedo *et al.*, 2009).

Pharmacological modulation of PKC and ERK activities also affected the coupling of worm pairs, a state crucial for female maturation and egg production; PKC activation with 1 μM PMA, PKC inhibition with 20 μM, 50 μM GF109203X or ERK inhibition with 50 μM U0126 induced permanent separation of all couples. The observed decoupling effect can be associated with changes in ERK and PKC activity as the phosphorylated proteins were localized to the neuromuscular system and areas of female-male contact. Thus in addition to their roles in muscular contraction that would be needed to sustain coupling these proteins might play a role in chemosensory signalling between worm pairs. Hence, U0126 and more efficient second generation MEK/ERK inhibitors might be useful for the treatment of schistosomiasis, and possibly reduction of egg burden. Second generation MEK/ERK inhibitors are believed to have superior pharmacological and biopharmaceutical properties and are being currently used in anti-cancer treatment clinical trials (Davies *et al.*, 2000; Roberts and Der, 2007).

4.4.4 Praziquantel (PZQ) treatment of adult worms in vitro *increases ERK and PKC phosphorylation mainly associated with the tegument and excretory system*

The effects of PZQ on the ultrastructure of adult schistosomes both *in vivo* and *in vitro* are well described in the literature (Shaw and Eramus, 1983; Pica-Maccottia and Cioli 2004). Adult worms are quickly paralyzed due to muscle contraction and show tegument disruption with loss of tegumental cytoplasm and parenchyma, extensive vacuolization of both tegumental and subtegumental tissues, damage to musculature and changes in vitelline gland structure (Shaw and Eramus, 1983). Worms die/are killed and are washed away by the blood circulation with the extensive tegumental damage eliciting host immune responses. Male worms are more sensitive towards PZQ compared with female worms (Pica-Maccottia and Cioli 2004). It has long been thought that PZQ action was Ca^{2+} dependent through modulation of a specific voltage activated

Ca^{2+} channel (Day *et al.*, 1992; Greenberg, 2005; Jeziorski and Greenberg 2006). However, more recent evidence indicates that actin might be involved as cytochalasin D prevents the overall physiological response of schistosomes to PZQ while the influx of Ca^{2+} is maintained (reviewed by Pica-Mattoccia *et al.*, 2008; Doenhoff *et al.*, 2008). Furthermore, PZQ causes Ca^{2+} influx in immature worms but does not affect the worms significantly (Pica-Mattoccia *et al.*, 2008). Here, evidence is presented that *in vitro* PZQ treatment of adult worms induced activation of PKC and ERK strongly associated with the adult male and female musculature. Therefore, the paralysing effect of PZQ in adult worms could be PKC-dependent. Interestingly tegumental disruption and sustained contraction were observed after treatment with PMA supporting a relation of PKC and perhaps ERK signalling in the not fully understood anti-helminthic action of PZQ. Furthermore, treatment with PZQ appeared to increase ERK activation associated within the excretory system in both male and female worms. Since it is speculated that schistosome excretory system is used to excrete drugs (Kusel *at al.*, 2009), ERK activation might help the parasite to avoid toxicity. Additionally, inhibition of ERK and perhaps PKC could block excretory system function and increase the effectiveness of PZQ and reduce worm resistance. Further studies on ERK and PKC in schistosomula after PZQ treatment will give valuable insights into the biological role of these signalling enzymes in schistosomes and maybe elucidate the unknown mode of action of PZQ against adult schistosomes.

4.4.5 Conclusions

The biochemical characterization of PKCs and ERKs *via* immunoprecipitation of detected proteins and enzymatic activity assays validated the use of anti-phospho PKC and ERK antibodies in schistosomes. Investigation of PKC and ERK signalling in *S. mansoni* adult worm pairs based on immunolocalization and pharmacological studies demonstrated key functional roles for PKCs and ERKs in the maintenance of parasite homeostasis. These signalling proteins therefore appear to be potential targets for chemotherapeutic treatment. Further studies would be of use to decipher the individual roles of each ERK and PKC isotype in schistosomes.

Chapter 5

Insights into PKC, ERK and p38 MAPK signalling during *S. mansoni* female-male interactions

5.1 Introduction

Schistosomes are the only trematodes to have evolved separate sexes (Beckmann *et al.*, 2010) and novel interplay has co-evolved between male and female worms (reviewed in LoVerde *et al.*, 2004). To reproduce, *S. mansoni* depend upon aggregation of the worms in the host, recognition of a partner worm, sexual pairing, maturation of the female, migration of paired worms from the liver to the mesenteric veins, insemination and fertilization (reviewed in LoVerde *et al.*, 2004). Sexual pairing, where the female resides within the male gynaecophoric canal is necessary to direct at the molecular level female growth and reproductive development, with female worms failing to fully develop in the absence of males (Shaw, 1977; Basch and Humbert, 1981; Grevelding *et al.*, 1997; Kunz, 2001). The male also plays a role in passage of metabolites to the female residing in the gynaecophoric canal (LoVerde *et al.*, 2004).

Whether from single-sex or bisexual infections, male schistosomes appear morphologically similar with the exception of the testes, which in paired males have a smaller diameter (LoVerde *et al.*, 2004; Beckmann *et al.*, 2010). Furthermore, in *S. mansoni* male unisexual pairs (achieved by twice infecting mice with male cercariae only) the males residing the gynaecophoric canal show no histological evidence of female reproductive structures, but are stunted with poorly developed testes, and high nuclear density characteristic of mature females (Basch and Gupta, 1988). Female schistosomes from single-sex infections appear stunted with underdeveloped Mehlis' gland and vitellaria but with developed ovary, ootype and uterus (Erasmus, 1973, 1975; Shaw, 1987). When *ex-vivo* paired females are separated from males the unpaired cultured females show a significant loss of mitogenic activity that can be regained upon re-pairing (Knobloch *et al.*, 2006).

Studies on *in vitro* cultured adult *S. mansoni* females have revealed that transcription of female-specific genes is influenced by pairing (Grevelding *et al.*, 1997). Hormones, growth factors and lipids secreted from the male have been proposed to initiate female reproductive development, with the hypothesis that a gynaecophoric canal protein (SmGCP) is involved in male-female interaction (Bostic and Strand, 1996; Kunz, 2001). SmGCP exhibits homology to the cell adhesion molecule fasciclin-I and its expression is regulated by TGFβ; in *S. japonicum* the GCP homologue (SjGCP) is involved in the initial steps of pairing and pairing stability (Osman *et al.*, 2006; Cheng *et al.*, 2009). Further evidence is accumulating that pairing and pairing-dependent

developmental processes such as expression of female-specific genes, proliferation and differentiation of vitelline cells and egg embryogenesis are regulated by the TGFβ pathway and protein tyrosine kinases (LoVerde *et al.*, 2007; Knobloch *et al.*, 2006, 2007; Beckmann *et al.*, 2010). Two *S. mansoni* TGFβ pathway ligands have been identified; an Inhibin/Activin-like molecule (SmInACT) and a bone morphogenic protein (BMP)–like molecule (SmBMP) (Freitas *et al.*, 2007; Freitas *et al.*, 2009). Expression of the SmInACT transcript in vitellaria and eggs of mature (bisexual) female worms but not in immature and mature female worms recovered from infertile infections in lymphopenic IL-7R -/- mice demonstrates the role of TGFβ signalling in egg embryogenesis (Freitas *et al.*, 2007). To further support a role for the TGFβ pathway in female reproductive development, pharmacological inhibition of a TGFβ receptor was shown to reduce female vitelline cell mitotic activity and egg production (Knobloch *et al.*, 2007). It was also demonstrated that pharmacological inhibition of tyrosine kinases, blocks mitotic activity and egg production of paired females suggesting cross-talk between tyrosine kinase and TGFβ pathways for regulation of vitelline cell development and thus egg production (Knobloch *et al.*, 2007; reviewed by LoVerde *et al.*, 2009). Here, ERK localized to the reproductive organs of paired females and inhibition of ERK compromised pairing with the female actively separating from the male, which consequently decreased egg production (Chapter 4). In vertebrates cross-talk between the MAPK pathway and the TGFβ signalling pathway exists, as TGFβ can activate both the MKK4/SAPK and MEK/ERK pathways, through Ras and TGFβ RI and RII (receptors) (Mulder, 2000). Moreover, ERK-mediated phosphorylation of Smad1 in response to TGFβ is critical for regulating Smad1 subcellular localization, which could be determinant in maintaining TGFβ-dependent transcriptional activation (Mulder, 2000). Activated ERK is also able to phosphorylate Smad2, promoting TGFβ-mediated signalling (Hayashida *et al.*, 2003). It is possible that such cross-talk may occur in the vitellarium of schistosome females too (Beckman *et al.*, 2010). Interestingly, in schistosomes, Osman *et al.* (2004) showed that an active mutant of mammalian ERK2 phosphorylated SmSmad4 *in vitro* which significantly inhibited the interaction with the receptor-activated SmSmad2, suggesting that regulation of TGF-β signalling by ERK phosphorylation is exerted through SmSmad4. This process appears to be cell type-specific such that down regulation or stimulation of TGFβ could depend on the cell type (LoVerde *et al.*, 2007). Quantitative RT-PCR analysis of SmRas, showed it to be more expressed in female worms than males (Osman *et al.*, 1999). As the Ras pathway regulates cell proliferation in other organisms, it

might transduce one or more signals for mitogenic proliferation in female reproductive development (LoVerde *et al.*, 2004, for review).

Although, propagation of schistosomes is primarily dependent upon pairing, an important pre-requisite is the ability of them to locate each other for mating. Some studies have shown that chemical mediators secreted by adult worms play an important role in sexual attraction, however, no signalling work has been done in this area. Steroids and lipids secreted by the adult male are thought to play an important role in chemoattraction (Gloer *et al.*, 1986). On the contrary, female worms do not appear to release substances to attract males (Haseeb and Eveland, 1991). *In vivo* experiments have shown that while *S. mansoni* can mate with other species, whenever a choice is available mating occurs preferentially between partners of the same species and heterospecific pairs change partners to form same species pairs (Tchuem Tchuenté *et al.*, 1995, 1996 for review). In *S. mansoni* bisexual populations, single males can displace paired males to mate with females (Pica-Mattoccia *et al.*, 2000). Such competitive mating behaviour implies the involvement of molecular signalling mechanisms that regulate sexual attraction and/or thigmotaction contributing to better fitness of the species by increasing the genetic variability crucial for adaptation to environmental changes (LoVerde *et al.*, 2004). The unknown interactions between males and females appear to be accomplished primarily through chemical communication (Haseeb *et al.*, 2008).

It is possible that adult schistosomes are able to sense the opposite sex through signalling proteins including PKC, ERK and p38 MAPK. Tools to explore these pathways were developed in Chapters 3 and 4, and in Ressurreição *et al.* (2011a) and PKC and ERK were also found in the tegument and gynaecophoric canal (Chapter 4). Hence, in this Chapter attempts were made to understand underlying signalling mechanisms in male-female perception and investigate the association of PKC, ERK and p38 MAPK pathways to this process. Due to the difficulty in recognizing molecular events during schistosome pairing *in vivo*, a set of *in vitro* assays were designed to study spatial and temporal relationships by maintaining adult *S. mansoni* in different sex ratio environments.

5.2 Materials and Methods

5.2.1 Schistosome couple separation and in vitro *sex ratio experiments*

To detect differences in PKC, ERK and p38 MAPK activation in *S. mansoni* adults separated and maintained under different sex ratios, a simple experimental design was developed. Paired adult schistosomes were collected by perfusion of mice as detailed in Section 2.4.1 and were placed in a Petri dish with RPMI-1640 medium on ice and encouraged to unpair by gently easing the female from the male with the aid of a small brush taking care to not damage the worms. Once worms separated, a proportion were either immediately fixed in acetone for immunohistochemistry (Section 2.6) or homogenised in RIPA buffer (20 µl/worm) and processed for western blotting (Section 2.5) as an internal (0 min) control with anti-phospho PKC (βII Ser 660), anti-phospho-PKC (ζ Thr410), anti-phospho p44/42 MAPK (ERK1/2) (Thr202/Tyr204), or anti-phospho p38 MAPK (Thr180/Tyr182) antibodies. Remaining males and females were transferred to 1.5 ml microfuge tubes with 500 µl of RPMI-1640 at 37°C for 90 min in different sex ratios or alone in order to mimic different environments (a single male or female; 3 males and 3 females maintained together to mimic a normal 1:1 bisexual population; or several females or males placed together mimicking a single-sex population). After the 90 min incubation the medium was removed and worms processed for western blotting or immunohistochemistry.

In some cases immature (smaller than usual) male worms were present and were not paired with females on perfusion. These specimens were briefly washed in RPMI-1640 at 37°C and immediately fixed in acetone for immunohistochemistry or processed for western blotting. Sexually immature female worms were not studied as these were very hard to collect and scarcer than immature male worms.

5.3 Results

5.3.1 Effect of different sex ratios on the phosphorylation of PKC, ERK and p38 MAPK in male and female S. mansoni in vitro

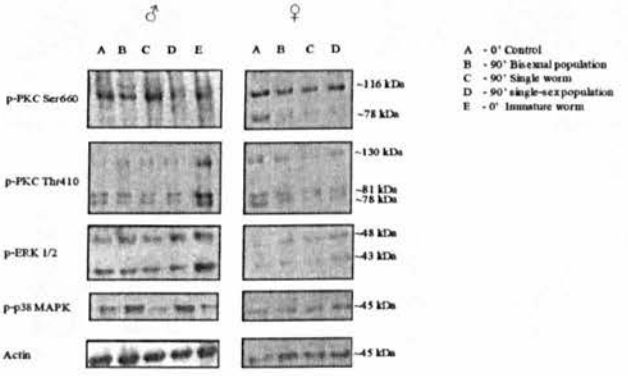

Figure 5.1 - Western blots showing phosphorylated *S. mansoni* PKC, ERK and p38 MAPK of immature male worms and adult male or female worms experiencing different sex ratios, *in vitro*. Representative immunoblots of either male (♂) or female (♀) protein homogenates (12 µg per lane) after separated adult worms were maintained in different sex ratio conditions. The following were used: anti-phospho PKC (βII Ser 660), anti-phospho-PKC (ζ Thr410), anti-phospho-p44/p42 MAPK (ERK 1/2), and anti-phospho p38 MAPK antibodies. *In vitro* treatments were as follows: **(A)** adult worms that once separated were immediately processed (0 min, internal control); **(B)** adult worms in bisexual populations with both males and females together for 90 min; **(C)** single adult worm maintained in isolation for 90 min; **(D)** adult worms maintained in single-sex populations with worms of the same sex; and **(E)** immature unpaired male worm immediately processed after perfusion (0 min). Anti-actin antibodies were used to confirm equal loading of proteins and immunoreactive bands detected with a GeneGnome imaging system. Results are representative of 3 independent experiments with two replicates each.

5.3.1.1 Activation of PKC

The phosphorylation (activation) profile of the *S. mansoni* PKCs detected using anti-phospho PKC antibodies was quantified and localized in adult male and female worms maintained in different sex ratios for 90 min (Figures 5.1 - 5.4). No significant differences in activation of the four immunoreactive PKCs were seen between either control (0 min) male or female adult worms compared to those separated and kept in an bisexual population for 90 min (Figures 5.1, 5.2), revealing that PKC activation was similar in worms separated immediately after perfusion and in bisexual 90 min populations. Control males or males kept in a bisexual population had activated PKC associated with the tegument, musculature and cephalic ganglia, as determined using anti-phospho PKC (Ser660) antibodies (the only antibody to detect the ~116 kDa PKC) (Figure 5.3 A, B). With anti-phospho PKC (Thr410) antibodies activity was found associated with the tegument, oral sucker, sub-tegument and regions that resemble sensory neurons (Figure 5.4 A - D).

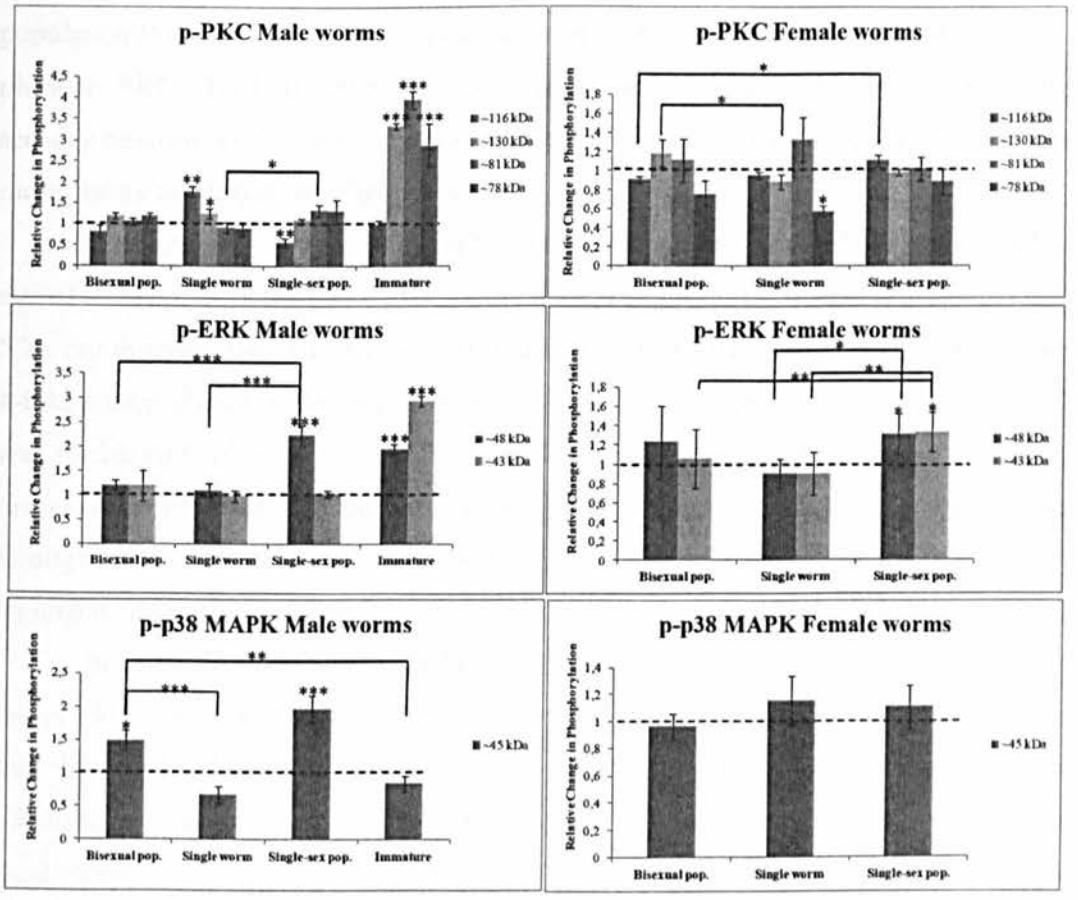

Figure 5.2 - Relative changes in *S. mansoni* PKC, ERK and p38 MAPK phosphorylation when experiencing different sex ratios. Immunoreactive proteins on western blots from 3 independent experiments, each with two replicates (shown and described in Figure 5.1) were quantified using Syngene GeneTools. Phosphorylation levels were normalized against control levels of adult worm couples immediately processed after separation were assigned a value of 1 (shown as the dotted line). Statistical analysis of significance was determined with Fishers test: *= ($p \leq 0.05$), **= ($p \leq 0.01$) and *** = ($p \leq 0.001$).

In single adult male worms, activation of the ~116 kDa and ~132 kDa PKC proteins significantly increased 1.7–fold ($p \leq 0.01$) and 1.3–fold ($p \leq 0.05$), respectively when compared to the internal (0 min) control (Figure 5.2). PKC activity detected with anti-phospho PKC (Ser660) antibodies was evident in the tegument and in previously unseen areas including the head region and testicular lobes (Figure 5.3 C - E). Anti-phospho PKC (Thr410) antibodies detected PKC activity in the same regions as the control including the sensory neurons, ventral and oral suckers, tegument, tegument tubercles and sub-tegument (Figure 5.4 E - J).

Male worms from the single-sex population displayed a significant reduction in the phosphorylation status of the ~116 kDa PKC ($p \leq 0.01$) and an increase in

phosphorylation of the ~81 kDa PKC ($p \leq 0.05$) compared to males from a bisexual population (Figure 5.2 A). *In situ* localization revealed PKC activity detected with anti-phospho PKC (Thr410) antibodies to be associated with the oesophagus, tegument, sensory neurons and in new anterior and posterior areas, which extend through the musculature and tegument (Figure 5.4 K - N).

Interestingly, the smaller sexually immature male worms displayed considerably more PKC activity compared with sexually mature control male worms (Figures 5.1 and 5.2). For instance, the ~81 kDa, ~78 kDa and ~132 kDa PKCs displayed between 3 and 4-fold greater phosphorylation ($p \leq 0.001$), while phosphorylation of the ~116 kDa band was unchanged (Figures 5.1 and 5.2). In these immature worms *in situ* localization revealed that PKC activity detected with either anti-phospho PKC antibody was diffuse throughout the whole worm (Figures 5.3 F, 5.4 O) with some specific staining in tegument and testicular lobes (Figure 5.4 O).

In single females a ~40% reduction in phosphorylation ($p \leq 0.05$) was seen for the ~78 kDa PKC when compared to female 0 min control worms; the ~132 kDa protein also displayed reduced activation ($p \leq 0,05$) when compared to females from bisexual populations (Figure 5.2). With anti-phospho PKC (Thr410) antibodies *in situ* localization in control females revealed PKC activity generally localized to the tegument, sub-tegument, and structures with reproductive function such as the ovary, oviduct and uterus (Figure 5.4 P-X). Using anti-phospho PKC (Ser660) antibodies PKC activation was also found associated with the female tegument and structures with reproductive function e.g. surrounding the egg, female oviduct (panels H-J), lumen of the vitelline glands and oocytes (panel L) (Figure 5.3 panels G-M). In single females activated PKC localized with anti-phospho PKC (Thr410) antibodies was mostly associated with tegument, sub-tegumental regions surrounding the vitellaria and the egg; intense activity was associated with the oesophagus (Figure 5.4 panels Y-Ab).

In females from single-sex populations no significant changes in PKC activity were observed with the exception of the ~116 kDa PKC which showed a 1.4–fold increase in phosphorylation when compared with females from bisexual population ($p \leq 0.05$; Figure 5.2). No changes in localization were observed compared to internal control and females from bisexual populations.

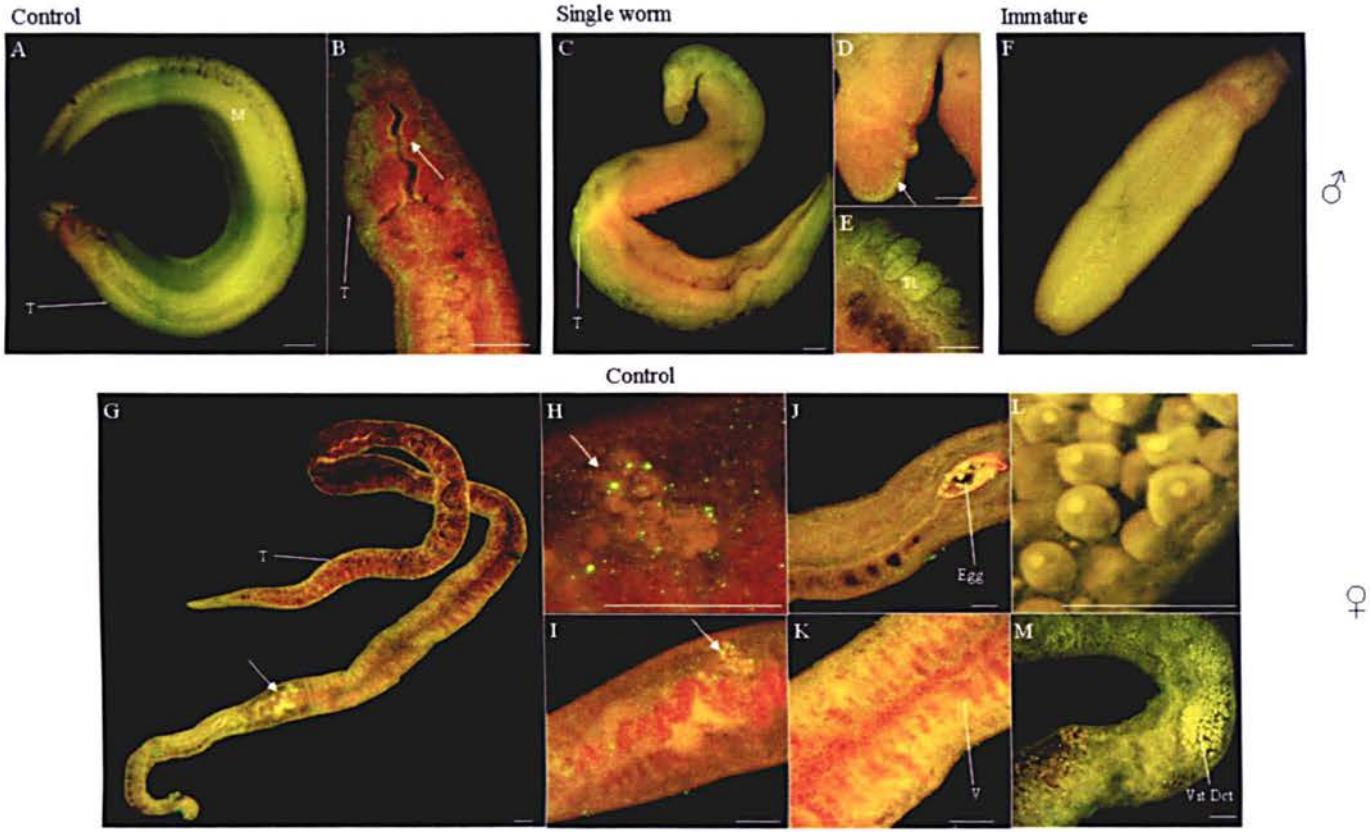

Figure 5.3 - *In situ* localization of phosphorylated PKC detected with anti-phospho PKC (Ser660) antibodies in unpaired adult male (♂) and female (♀) *S. mansoni*. Male single worms were either (A-B) fixed immediately after separation on ice, or, (C-E) fixed after 90 min isolation as individual worms; (F) sexually immature male worm immediately fixed after perfusion. (G – M) Female worms were fixed after being kept in a bisexual population for 90 min. All panels are maximum projections of at least 50 z-sections with exception of panel B which is a projection of 3 z-sections. Worms were incubated in anti-phospho PKC (Ser660) antibodies and Alexa Fluor 488 secondary antibodies (green); specimens were additionally stained with rhodamine phalloidin to stain actin filaments (red). Under normal conditions activated PKC was generally found in the tegument (T), musculature (M) and cephalic ganglia (arrow Panel B), when maintained in isolation males showed increased fluorescence associated with the tegument (T), testicular lobes (TL) and new regions of unknown identity (arrow Panel D). Female worms showed similar regions of PKC activity between treatments with localizations associated with regions of the tegument (Te), surrounding the vitelline duct (Vit Dct), oocytes (arrows and panel L) and vitellaria (V). Bars = 100 μm.

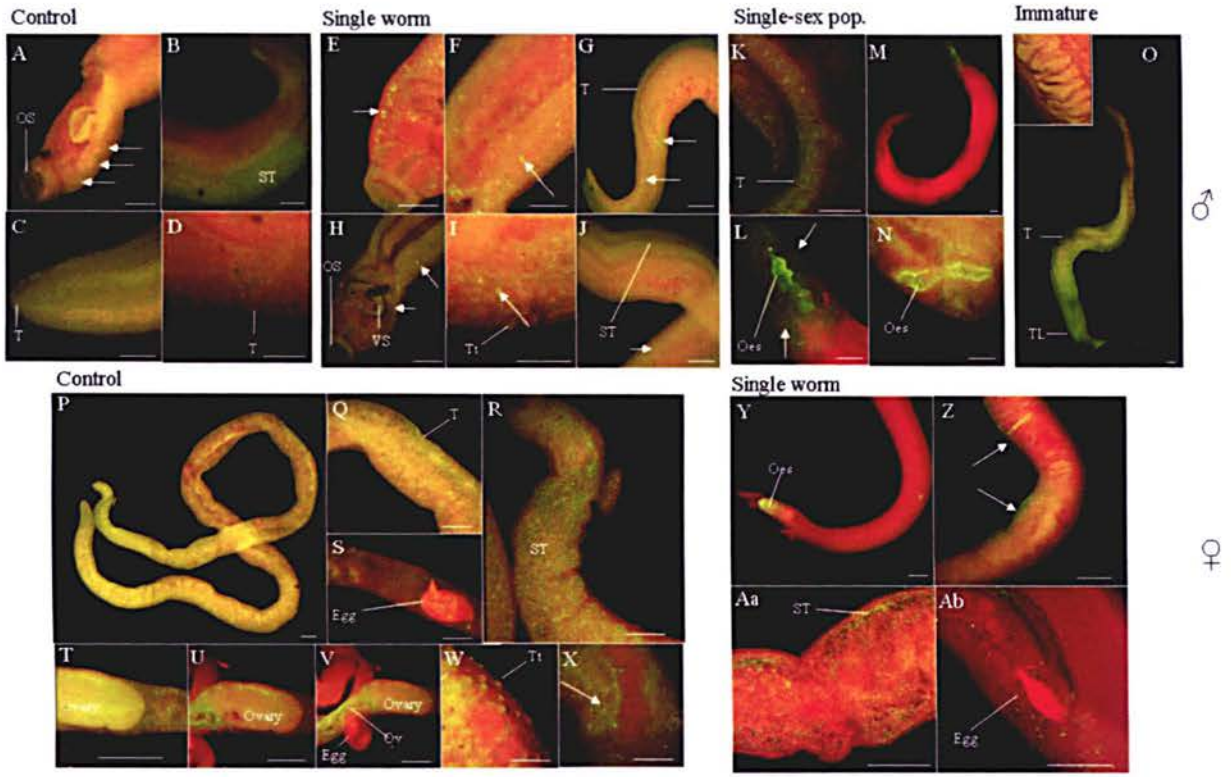

Figure 5.4 - *In situ* localization of phosphorylated PKC detected with anti-phospho PKC (Thr410) antibodies in unpaired adult male (♂) and female (♀) *S. mansoni* worms. Male worms were either (A-D) immediately fixed after separation on ice (control), (E-J) fixed after 90 min in isolation as individual worms, or (K-N) maintained for 90 min in a single-sex population prior to fixing; (O) sexually immature male worm immediately fixed after perfusion. Female worms were (P-X) fixed immediately after separation, or (Y-Ab) fixed after isolated as individuals for 90 min. Worms were incubated in anti-phospho PKC (Thr410) antibodies and Alexa Fluor 488 secondary antibodies (green); specimens were additionally stained with rhodamine phalloidin to stain actin filaments (red). Under normal conditions activated PKC was generally found in the tegument (T), oral sucker (Os), sensory neurons (arrows) and sub-tegument (ST). When males were maintained in isolation PKC activity was found associated with the ventral sucker (Vs) tegument (T), tubercles of the tegument (Tt), sub-tegument (ST) and sensory neurons (arrows). Males maintained in single-sex populations show fluorescence associated with the tegument (T) sensory neurons (arrows) and oesophagus (Oes). Immature male worms showed fluorescence associated mainly with the tegument (T), musculature and testicular lobes (TL). Control females showed fluorescence associated with the tegument (T), sub-tegument (ST), surrounding the uterus (arrow), ovary and oviduct (Ov). A reduction in fluorescence was observed in female worms kept in isolation showing fluorescence mostly associated with the tegument (arrows), sub-tegument (ST) and oesophagus (Oes) and musculature sorrowing and egg. Bar = 100 μm.

5.3.1.2 Activation of ERK

Western blotting of phosphorylated *S. mansoni* ERKs using anti-phospho ERK antibodies revealed changes in activity of these proteins when adult male and female worms experienced different sex ratios (Figure 5.1 and 5.2). No significant changes in phosphorylation were observed for the ~43 or ~48 kDa ERKs in single worms or worms from bisexual populations when compared to both control (0 min) males/females (Figures 5.2). *In situ* localization of 0 min control males showed ERK activity associated with the tegument and gynaecophoric canal (Figure 5.5 A).

Unpaired adult males maintained in a single-sex population possessed increased phosphorylation of the ~48 kDa ERK (~2-fold, $p \leq 0.001$) compared to control males (Figure 5.5 A). *In situ* localization revealed similar regions of ERK activity to that of control males in areas such as the gynaecophoric canal, oral sucker, ventral sucker, sub-tegument, excretory system and flame cells (Figure 5.5 B - F). Interestingly, ERK activity also localized within a previously unseen circular region in the posterior side of the worm (Figure 5.5 B, D).

Sexually immature male worms had higher ERK phosphorylation compared to sexually mature males with 1.8- and 2.9-fold ($p < 0.001$) greater phosphorylation for the ~48 kDa and ~43 kDa ERKs, respectively (Figure 5.2). This increased activity could not be localized as diffuse staining appeared throughout the worm musculature; however, the tegument was highly immunoreactive and stained with definition (Figure 5.5 G, H).

In control females (Figure 5.5 I-M) ERK activity was associated with the tegument especially near the vitellaria (Figure 5.5 K, L), the anterior end (Figure 5.5 M) and nervous or excretory tissues (Figure 5.5 J, M). No significant differences in distribution of activated ERK were observed in single females and females from bisexual populations. In females from single-sex populations both ERKs showed increases in phosphorylation of 1.4-fold ($p \leq 0.05$) when compared to controls (Figure 5.2). ERK activity (Figure 5.5 N-T) was associated with the tegument, tegument tubercles, female head (panel Q), previously described nervous or excretory tissues (panels O, P and T) and musculature surrounding ovary and egg (Figures 5 S, R).

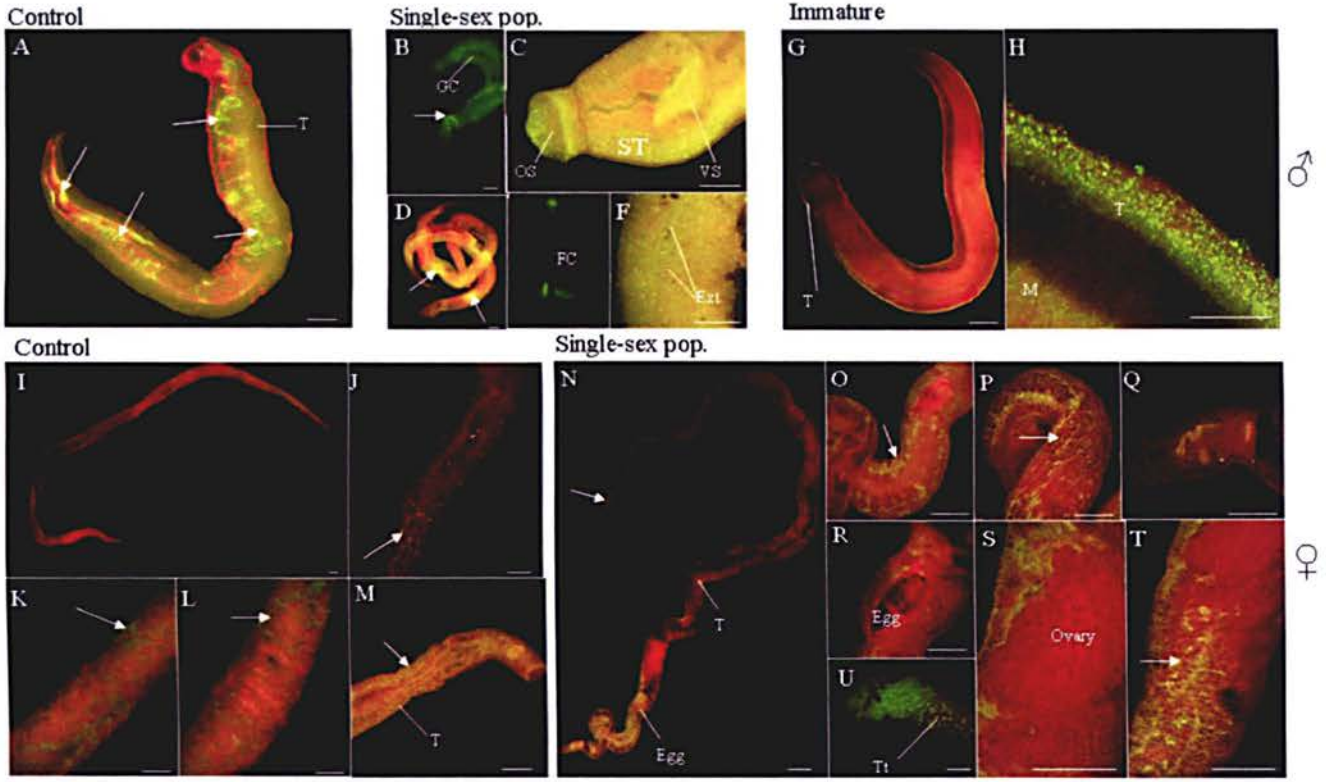

Figure 5.5 - *In situ* localization of phosphorylated ERK detected with anti-phospho ERK 1/2 antibodies in unpaired adult male (♂) and female (♀) *S. mansoni* worms. Male worms were either (A) fixed immediately after separation on ice, or (B-F) fixed after 90 min experiencing a single-sex population; (G and H) sexually immature male worm immediately fixed after perfusion. Female worms were fixed immediately after (I-M) separation on ice, or (N – T) when maintained in a single-sex population for 90 min. All panels are maximum projections of at least 50 z-sections. Worms were incubated in anti-phospho ERK 1/2 antibodies and Alexa Fluor 488 secondary antibodies (green); specimens were additionally stained with rhodamine phalloidin to stain actin filaments (red). In control males phosphorylated ERK associated with the tegument and gynaecophoric canal (arrows). Males kept in single-sex populations showed activity in distinct areas throughout the worm (arrows), oral and ventral suckers (OS and VS), sub-tegument (ST), and flame cells (FC). Immature males showed activity associated with the tegument (T) and musculature (M). Control females showed activity mostly associated with the tegument surrounding the vitellaria (arrows panels K and L), tegument and structures resembling excretory tubules (Ext) at the anterior end (panel M) and surrounding the uterus (arrow, panel J). When females were maintained in a single population fluorescence was associated with the tegument (T), tubercles of the tegument (Tt), head region (panel Q), surrounding eggs (panels N, O and R), surrounding the ovary and structures of suspected nervous function (arrows). Scale bar = 100 μm.

5.3.1.3 Activation of p38MAPK

Western blotting revealed changes in the phosphorylation of p38 MAPK in unpaired *S. mansoni* adult male worms when experiencing different sex ratios (Figures 5.1 and 5.2). There was a significant increase in p38 MAPK activation in unpaired adult male worms kept in a bisexual population compared to unpaired control (0 min) adult males ($p \leq 0.05$) or those kept alone for 90 min ($p \leq 0.001$) (Figure 5.2). Confocal microscopy of control males revealed p38 MAPK activity associated with the tegument, testicular lobes, tubercles of the tegument and the head region (panel C) (Figure 5.6 A - E). Adult male worms that were kept in a bisexual population showed activity also in the tubercles of the tegument but also within the gynaecophoric canal, ventral sucker and distinct circular areas throughout the male body (Figure 5.6 F - I).

Single adult males showed significantly reduced p38 MAPK phosphorylation compared to adult male worms maintained in a bisexual population showing a decrease in 70% of p38 MAPK activity ($p \leq 0.001$) (Figure 5.2). On the other hand, unpaired adult male worms that were kept in single-sex populations showed an increase in p38 MAPK phosphorylation of 1.9-fold ($p \leq 0.001$) compared to control (0 min) adult males (Figure 5.2). Interestingly, increased activity appeared to be associated with the gynaecophoric canal, tubercles of the tegument and with the circular regions throughout the body (Figure 5.6 J, K).

Interestingly no differences in p38 MAPK phosphorylation were seen between immature and mature (control) adult males (Figure 5.2). In immature male worms p38 MAPK associated fluorescence was generally localized within the tegument and ventral sucker (Figure 5.6 L - N).

No significant changes in the p38 MAPK activity of female worms from the different sex ratios were observed (Figure 5.2). In control females *in situ* localization revealed p38 MAPK activity associated with the tegument and strongly associated in general with the reproductive region including the ootype when an egg was present and surrounding the oocyte (Figure 5.6 O, P).

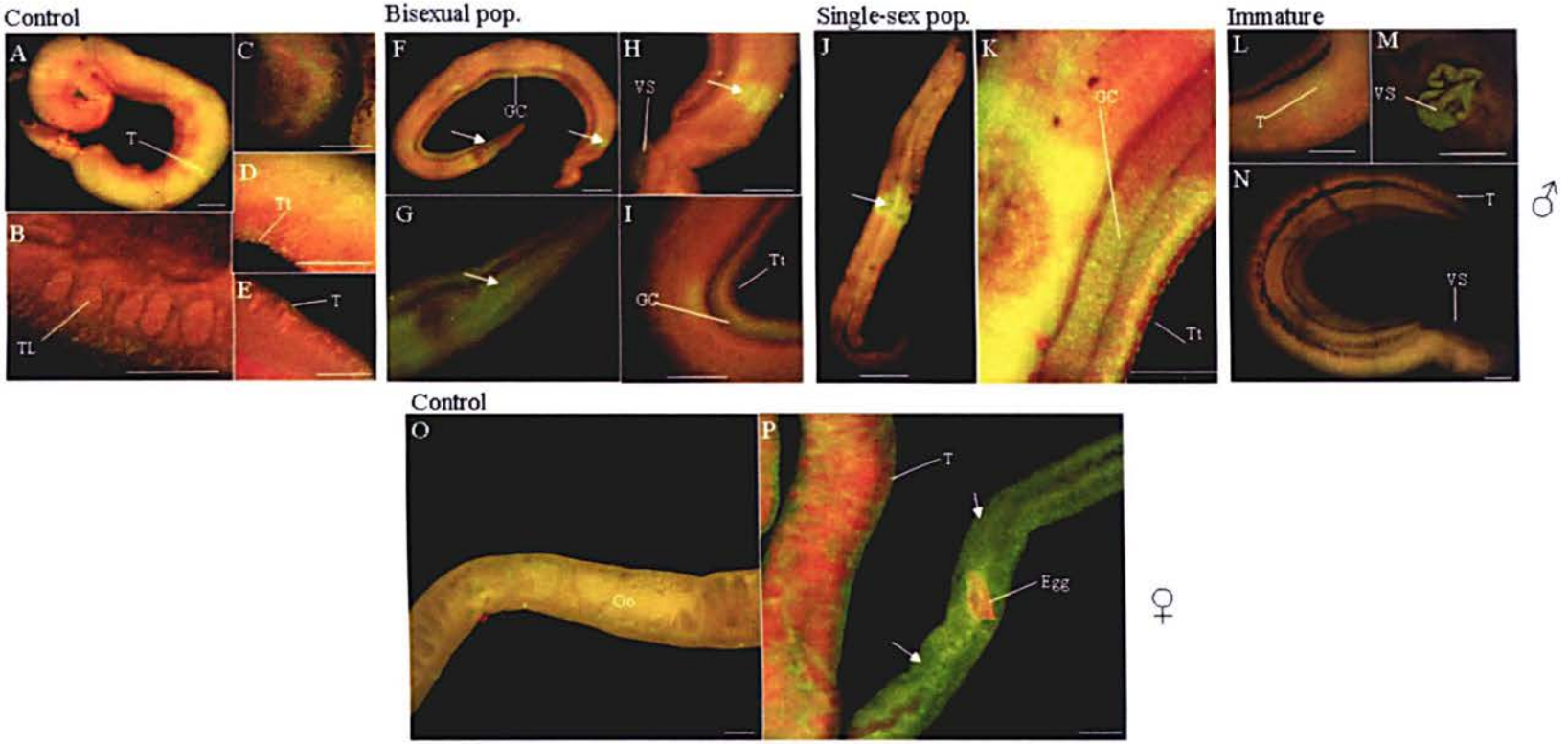

Figure 5.6 - *In situ* localization of phosphorylated p38 MAPK detected with anti-phospho p38 MAPK antibodies in unpaired adult male (♂) and female (♀) *S. mansoni*. Male worms were either (A-E) fixed immediately after separation on ice, or (F – I) fixed after 90 min in a bisexual population, or (J and K) a single-sex population; (L – N) sexually immature male worm immediately fixed after perfusion. Female worms were (O-P) fixed immediately after separation on ice. Worms were then incubated in anti-phospho p38 MAPK antibodies and Alexa Fluor 488 secondary antibodies (green); specimens were additionally stained with rhodamine phalloidin to stain actin filaments (red). In males fixed after separation p38 MAPK was apparent in the tegument (T), tubercles of tegument (Tt), testicular lobes (TL) and head region (panel C). Males from bisexual populations showed activity in distinct areas throughout the male (arrows), tubercles of the tegument (Tt), gynophorical canal (GC) and ventral sucker (VS). In males from single-sex populations p38 MAPK was apparent in the gynophorical canal (GC), tubercles of the tegument (Tt) and distinct areas throughout the male (arrow). Immature males showed activity associated with the tegument (T) and ventral sucker (VS). Control females showed activity mostly associated tegument (T) and surrounding the egg (arrows) but also surrounding the ootype (Oo). All panels are maximum projections of at least 50 z-sections, scale bar = 100 μm.

5.3.2 Effect of different sex ratios on the phosphorylation status of putative PKC substrates in male and female S. mansoni in vitro

The phosphorylation status of putative *S. mansoni* PKC substrates detected with anti-phospho PKC substrate antibodies was also assessed by western blotting. Although some changes in immunoreactivity were observed these were not assessed by confocal microscopy. Results show that the greatest differences in substrate phosphorylation occurred when both male and female worms were either maintained as separate individual worms or single-sex populations when compared to controls (0 min).

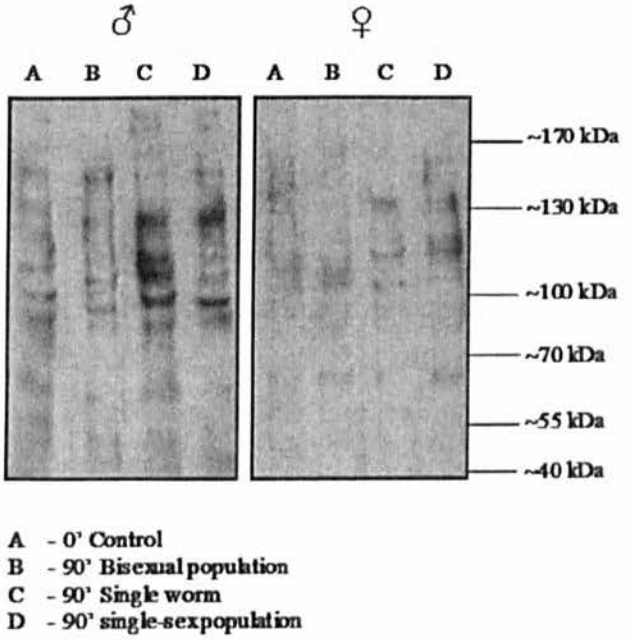

Figure 5.7 - Western blot showing phosphorylated PKC substrate proteins of adult male (♂) and female (♀) *S. mansoni* experiencing different sex ratios, *in vitro*. Protein homogenates (12 µg per lane) of adult worms probed with anti-phospho-(Ser) PKC substrate antibodies. *In vitro* treatments as follows: A – adult worms separated on ice (0 min control); B – adult worms in bisexual populations with both males and females together for 90 min; C - single adult worm maintained in isolation for 90 min; and D adult worms maintained in single-sex populations with worms of the same sex. Blots were imaged using a GeneGnome imaging system.

5.4 Discussion

The sexual maturation of schistosomes is unique in nature, characterized by a continuous intimate association where the female resides in the gynaecophoric canal of the male. This close contact is necessary for female growth, development, maturation and maintenance of the sexually mature state indispensable for the continuous production of fertile eggs (Popiel and Basch, 1984; Gupta and Basch, 1987; reviewed by Kunz, 2001; LoVerde *et al.*, 2004). Complex interplay occurs where the male appears to actively release substances to the environment for female recognition (Vogel, 1941; Michaels, 1969; Kunz, 2001; LoVerde *et al.*, 2004) and subsequently emits 'signals' that regulate female gene expression in a stage-, tissue-, and temporally-specific manner. A number of female-specific genes have been identified, along with signalling pathways and nuclear receptors that play a role in female reproductive development. In addition, host factors such as cytokines affect adult male and female development and egg production (reviewed by LoVerde *et al.*, 2004). Despite this knowledge, little is known about molecular mechanisms involved in mate attraction, mate choice and mating behaviours.

5.4.1 Male S. mansoni *have more PKC, ERK and p38 MAPK activity than females*

Interestingly, male schistosomes had more phosphorylated PKC, ERK, and p38 MAPK compared to females (when equal amounts of protein were loaded). While some of this is likely due to the males being more muscular to sustain pairing (Haseeb and Eveland, 1991; Kunz, 2001), higher levels in males could be related to roles in female attraction, and perhaps maintenance of post-pairing functions such as preservation of female homeostatic processes and the mature state, *via* complementation of female signalling referred to by LoVerde *et al.* (2004). That PKC, ERK and/or p38 MAPK signalling might play such roles is supported by the fact that activated forms of these kinases were detected in male structures crucial for pairing including the male neuromuscular system the gynaecophoric canal and tegument a structure involved in secretion and absorption. As PKC and MAPK influence secretion in other systems (Arkhammar *et al.*, 1994; Farhan *et al.*, 2010) in schistosomes these proteins might play a role in passage of metabolites to the female residing in the gynaecophoric canal.

Moreover, active PKC and ERK in the tegument might play a role in sensory processes; association of PKA with tegument sensory nerve endings has recently been reported by our group (De Saram *et al.*, 2013) and bulbous sensory structures are known to exist at the surface of S. *mansoni* males (Morris and Threadgold, 1967).

5.4.2 Possible role for ERK and p38 MAPK in partner attraction and maintenance of pairing

The localization of activated ERK and p38 MAPK in control males (fixed immediately after unpairing) within the gynaecophoric canal supports the involvement of MAPK signalling in schistosome pairing processes as the gynaecophoric canal is the region in which direct male-female contact occurs (Kunz, 2001). Additionally in immature males, neither ERK or p38 MAPK activity was detected in the gynaecophoric canal; studies have also shown that juvenile *S. mansoni* worms do not attract each other *in vitro* (Eveland and Haseeb, 1989). Interestingly, the *S. mansoni* gynaecophoric canal protein SmGCP plays a key role in maintenance of worm pairing and is directly mediated through the TGFβ receptor (SmTGFβRII) as RNA knockdown of this receptor reduces the expression of SmGCP (Bostic and Strand, 1996; Kunz, 2001; Osman *et al.*, 2006). Regulation of *S. mansoni* TGF-β signalling by ERK phosphorylation has been demonstrated by Osman *et al.* (2004), and it is shown here (Chapter 4) that ERK inhibition reduces schistosome pairing. Overall these findings suggest that ERK activity in the gynaecophoric canal might be linked to SmGCP regulation of gynaecophoric canal function.

In different sex ratio environments, the phosphorylation status/localization of p38 MAPK and ERK altered. Activation of p38 MAPK increased in adult males maintained for 90 minutes in a bisexual population; ring-shaped areas of activation were seen particularly on the ventral side where the gynaecophoric canal is located. Furthermore, similar ring-shaped activation patterns were present in males maintained in single-sex populations, for both p38 MAPK and ERK, but not in males kept alone (single male) or in 0 minute control males. The similar association of activated p38 MAPK and ERK with these circular-shaped regions suggests a role for MAPK signalling in partner attraction; that they were localized towards the gynaecophoric canal is important as they might represent important "points of contact" specialised in partner recognition, triggered in the presence of other schistosomes regardless of sex, as males are known to pair with other males (reviewed by Kunz, 2001).

Although mating signalling is an intricate process that is poorly understood, in yeast it is well established that pheromones activate GPCRs (G protein-coupled receptors) initiating a signal transduction cascade that includes a MAPK pathway (Sprague, 1998; Xue *et al.*, 2008; reviewed by Jones and Bennett, 2011). In fact, GPCRs exist in the surface of schistosomes (Ramachandran *et al.*, 1996; Hamdan *et al.*, 2002; El-Shehabi *et al.*, 2012). Thus male schistosomes might have specific regions for partner recognition "telesensing" molecules such as pheromones used for mating regulation and that ERK and p38 MAPK signalling might be involved in this process.

5.4.3 Possible roles for PKC in male neuronal processes involved in partner recognition and pairing

In control males and those maintained in a bisexual population, PKC activation was similar and was mainly associated with the neurons and tegument, indicating the involvement of PKC in neurosensation. Furthermore, male worms maintained isolated (single worm) or in single-sex populations also showed PKC activation in the neurons at the anterior of the worm; such neurons are thought to have a sensory function and sensory bulbous receptors exist at the tegument surface of males (Morris and Threadgold, 1967). This is interesting, as PKC signalling plays pivotal roles regulating various neuronal functions in invertebrates. For instance, in *C. elegans*, rescue experiments demonstrated that after restoring pkc-1 function in the ASH sensory neurons, defects in osmolarity sensing were ameliorated (reviewed by Hyde *et al.*, 2011). In addition pkc-1 in sensory neurons is required for nose touch response in adult *C. elegans* and other sensory responses including olfaction and thermotaxis (Okochi *et al.*, 2005; Hyde *et al.*, 2011). In mammals, gene knockout studies have identified roles for cPKCs and nPKCs in the nervous system including roles for PKCγ in spatial learning (Abeliovich *et al.*, 1993), and PKCγ and PKCε in pain sensation and sensitivity (Aley *et al.*, 2000; Cesare *et al.*, 1999; Khasar *et al.*, 1999; Malmberg *et al.*, 1997). Interestingly, PKC activity associated with *S. mansoni* male neurons was only detected with the anti-phospho PKC (Thr410) antibodies and not anti-phospho PKC (Ser660) antibodies, suggesting that the ~81 kDa PKC (suspected to be Smp_096310, atypical PKC ζ/ι) has a specialized role in neuronal processes.

In unpaired male worms kept in different sex ratios PKC activity detected with the anti-phospho PKC (Thr410) antibodies was associated with the anterior and sometimes posterior ends. It is thought that both schistosome female and male worms

have highly differentiated linear receptors at their anterior and posterior ends to determine mating position (Michaels, 1969); meeting of complementary receptors results in a normal mating position "anterior end to anterior end and posterior end to posterior end" (Michaels, 1969). This finding suggests that PKC signalling could be implicated in transduction of signals that regulate suitable pair recognition and pairing orientation processes.

5.4.4 Involvement of PKC and p38 MAPK signalling in male reproductive function

Single male worms, maintained isolated for 90 minutes, showed increased activation of the ~116 kDa β-type PKC by western blotting and activated PKC (presumably from this isoform) was detected in the testicular lobes. However, neither the control males nor those from single-sex or bisexual populations showed PKC activity in the testis. Therefore, activation of PKC in the testes seems to occur only in the absence of potential partners. Such signalling could serve to keep sperm release or other functions on "standby" until mates are detected. Interestingly, classical PKCs have been associated with sperm capacitation, activation and spermatogenesis in a variety of organisms. For instance, in mammals, sperm capacitation and acrosome reaction is dependent of PKC activation (Breitbart *et al.*, 1993; Breitbart, 2003) while in boar spermatozoa PKC activity is required for hyperactivation (Harayama and Miyake, 2006). It is not known to what extent mature adult worms once unpaired and maintained in isolation for long periods revert to an immature state. However, physiologically, the male testes are different when development has taken place in a single-sex population (infection) suggesting that male maturation is somewhat dependent on a female; nevertheless there is not yet a consensus on this in the literature. In immature male worms probed with the anti-phospho PKC (Thr410) antibody, PKC activity was found associated with the male testes, thus PKC dependent events likely play a role in the development of this organ.

Conversely, p38 MAPK activation in the testes was only found in males from bisexual populations and from single sex populations. And no p38 MAPK activity was detected in the testicular lobes of control males or single (isolated) adult males. This finding shows that testicular p38 MAPK activity only occurs in unpaired sexually mature males in the presence of potential partners, independent of the sex. This phenomenon might be a response to detection of a stimulus (e.g. pheromones) from a possible partner. In the absence of a partner stimulus or when already paired, down

regulation of p38 MAPK activity in the testes might affect testicular function/sperm maturation. Support for this comes with the fact that MAPK has an important role in signalling male reproductive function in various systems. In the mammalian testis, it is involved in cell-cycle progression, differentiation of germ cells and germ cell apoptosis (reviewed by Li *et al.*, 2009). Moreover the MAPK-activating protein, PM20/PM21, has been identified in the gonads of male *S. mansoni* (Beckmann *et al.*, 2010).

Overall, the data suggest that PKC and p38 MAPK are involved in different testicular functions, which are strikingly influenced by an external stimuli from a possible partner.

5.4.5 PKC, ERK and p38 MAPK signalling in female reproductive organs

The most controversial and at the same time fascinating aspect of the sexual development of female schistosomes lies on the nature of the stimulus produced by the male that triggers and controls this process. Although the precise nature of the stimulus (physical or chemical) is unknown, there is agreement that pairing is a necessary requirement for maturation and for migration of the female to the final site of residence in the vascular system of the vertebrate host (reviewed by LoVerde *et al.*, 2004; Knobloch *et al.*, 2006). Observations regarding pairing/development include stimulation of reproductive morphogenesis in females by lipid extracts of male worms (reviewed by Kunz, 2001; Haseeb and Eveland, 1991), increased tyrosine uptake by females stimulated with male extracts (Popiel and Erasmus, 1981), transfer of reserves and an increase in DNA synthesis in paired versus unpaired female worms (Kunz, 2001).

Results here show that in control females activated PKC, ERK and p38 MAPK were associated with reproductive organs and/or with regions of the tegument or musculature surrounding female reproductive organs. PKC activity was mainly associated with the oocytes, oviduct, ovary and tegument mostly surrounding the ovary; ERK activity was mostly associated with the ovary and vitelline glands; and p38 MAPK activity associated with the vitellaria region and the oviduct when an egg was present. These observations show the likely involvement of these signalling proteins in the regulation of female reproductive processes during mating. Interestingly, PKC, ERK and p38 MAPK activity in reproductive structures was independent of stimulation through male contact. In unpaired females from bisexual populations no changes were observed relative to control females (representing paired females as they were processed immediately after separation). This shows that for periods of up to 90 minutes, the male

presence is sufficient to maintain PKC, ERK and p38 MAPK signalling activity in the female reproductive structures.

No significant differences in ERK activation/distribution were observed in single females and females from bisexual populations. Although, in females from single-sex populations new regions of ERK activity increased and were also detected in reproductive structures including the ootype and oviduct suggesting that additional signalling to reproductive structures might occur when females do not receive male specific signals. The PKC and p38 MAPK activity also did not increase with the different sex ratio environments, and distribution was similar to controls. Interestingly, the MAPK-activating protein, PM20/PM21 has been identified in the ovary of *S. mansoni* (Beckmann *et al.*, 2010). Moreover, inhibitor studies in oocytes of the marine worm *Cerebratulus sp.*, with Piceatannol provided evidence for a role in MAPK activity in oocyte maturation (Stricker and Smythe, 2006). Interestingly, these results are similar to those obtained by Beckmann *et al.* (2010) who observed Piceatannol- induced dysfunctions in maturation of schistosome oocytes. That ERK and p38 MAPK activity were found associated with the vitelline cells further corroborates the likelihood that the TGFβ and MAPK signalling pathways are interrelated and that cross-talk exists in the vitellaria as suggested by LoVerde *et al.* (2007). The MAPKs likely control major cell fate decisions such as proliferation, differentiation and apoptosis, mainly by inducing alterations in gene expression in schistosomes as they do in other organisms (Bluthgenand and Legewie, 2008).

5.4.6 Conclusions

The dioecious state of schistosomes results in an interesting interplay between the sexes where the male, by an unknown mechanism, transduces a signal that regulates female gene expression in a stage-, tissue-, and temporal-specific manner. The data in this Chapter show that it is possible to study the signalling mechanisms of sex perception in schistosomes *in vitro*. It is shown that PKC and MAPK signalling pathways are prime candidates for transduction of stimuli from partners of both male and female worms. Although this Chapter reveals for the first time novel signal based molecular interactions between worms in different sex ratios, further studies with longer and shorter exposure times would provide a more detailed insight into the role and relevance of MAPKs and PKCs and other signalling pathways in perception and pairing between worms.

Chapter 6

Insights into PKC, ERK and p38 MAPK signalling during linoleic acid-induced release of cercarial acetabular gland contents

6.1 Introduction

As described in Chapter 1 (Section 1.2.3) the *S. mansoni* cercaria is morphologically and behaviourally well adapted to quickly locate and penetrate a suitable definitive mammalian host, essential for survival. Strategies and adaptations such as chronobiological emergence from the snail, sensitivity to mechanical, light, and thermal stimuli, and chemical stimuli from the host facilitate this (Haas, 1992; Walker, 2011; Section 1.2.3). However, *S. mansoni* cercariae are suspected to be primarily sensitive towards host chemicals (Haas and Haberl 1997; Haas *et al.*, 2008) and it is accepted that an important stimulant initiating penetration of host skin is the presence of unsaturated fatty acids at the skin surface (Shiff *et al.*, 1972; Shiff and Graczyk, 1994). During phases of creeping and penetration, these chemicals influence the release of enzymes from the pre- and post- acetabular glands including serine proteases, which play key roles in facilitating skin invasion and evasion of the host immune response (reviewed by Walker, 2011). Such proteases might also contribute to the removal of glycocalyx during transformation of cercariae to schistosomules (McKerow *et al.*, 1985; Fishelson *et al.*, 1992). Phospholipids and mucosubstances found in the post-acetabular glands likely assist in cercarial adhesion to skin surfaces (Stirewalt and Walters 1973; Dorsey 1975; Stirewalt 1978; Haas *et al.*, 1997).

Although the behavioural responses of cercariae towards stimulants are well reported in the literature, the molecular mechanisms involved have been scarcely studied. *Schistosoma mansoni* acetabular gland release is selectively stimulated by skin surface lipids, and free fatty acids, ceramides, glucoceramides, phospholipids, phosphatidylcholines, L-arginine, and acylglycerols induce the invasion behaviour of cercariae (MacInnis, 1969; Shiff *et al.*, 1972; Granzer and Haas, 1986; Shiff and Graczyk, 1994; Haas *et al.*, 1997). Linoleic acid (LA or linoleate) is an essential polyunsaturated fatty acid found in mammalian skin (at less than 1%) and the cell membrane; it is known to stimulate host seeking, cercarial attachment to skin, and acetabular gland secretion (Stirewalt, 1978; De Luca and Valacchi, 2010).

Some members of the PKC family can be activated by fatty acids (Murakami and Routtenberg, 1985). Interestingly, PKA and PKC have been suggested to play important roles in the transmission of extracellular signals to the intracellular systems of cercariae (Hara *et al.*, 1993). In fact, Matsumura *et al.* (1991) showed that phorbol

esters induce *S. mansoni* cercarial penetration behaviour and protease release, and PKC inhibitors abolish this response. Furthermore, calcium mobilization seems to be involved in gland secretion as incubation of cercariae in calcium and calcium inophores increases proteolytic enzyme release, while this effect is reduced by calcium chelators (Fusco *et al.*, 1991; Matsumura *et al.*, 1991). Gene expression studies on *S. mansoni* cercariae revealed that the most abundant gene encodes an 8 kDa calcium-binding protein (Santos *et al.*, 1999); clearly this might play a role in gland release.

Other studies support the view that cercarial penetration behaviour and enzyme release from the glands are mediated *via* chemoreceptors and the nervous system. For instance, King and Higashi (1992) reversibly inhibited *S. mansoni* cercarial penetration behaviour and protease release by blocking the argentophilic papillae sensory organs with silver nitrate treatment.

Therefore, in light of this information and given that activated PKC, ERK and p38 MAPK were detected in cercariae (Chapter 3), it was decided to investigate the involvement of these kinases in the release of cercarial acetabular gland contents. To induce and track the release of cercarial acetabular gland contents, the skin component LA and the cell permeable amine reactive tracer carboxyfluorescein diacetate succinimidyl ester (CFDA-SE) were used. LA not only induces acetabular gland release but also stimulates other infective behaviours such as directed creeping and initiation of transformation of cercariae to schistosomules. The CFDA-SE specifically reacts with proteases and thus stains the acetabular glands of cercariae, shifting from its non-fluorescent to fluorescent form, facilitating detection. The novel method used here of combining LA and CFDA-SE was informed by the methodology of four publications (Stirewalt, 1978; Harrop and Wilson, 1993; Jenkins and Mountford, 2005; Paveley *et al.*, 2009).

6.2 Materials and Methods

6.2.1 Labelling of acetabular gland enzymes with CFDA-SE

Cercariae were obtained and handled as detailed in Sections 2.3 and 2.4.2 and were enumerated by counting the number present in 20 µl aliquots after adding Lugol's solution. They were then incubated with 20 µM CFDA-SE (Molecular Probes, Invitrogen) for 45 min in 15 ml tubes at room temperature to allow CFDA-SE to penetrate. CFDA-SE specifically reacts with the proteolytic enzymes within the acetabular glands to produce a fluorescent green signal. This concentration of CFDA-SE was used by Paveley *et al.* (2009) who found it to give optimal labelling while being non-toxic to cercariae. Next the tubes were placed on ice for 15 min and cercariae concentrated by centrifugation at 200 x *g* for 30 s. Supernatant containing excess dye was discarded and the cercariae were re-suspended in filtered tap water (FTW) to the desired volume. Although ~20% of the original cercariae population was lost, which could be reduced by longer incubation on ice and centrifugation periods, it was decided to perform rapid washing and centrifugation to reduce stress to the parasite. Paveley *et al.* (2009) also reported that short periods of ice incubation and centrifugation did not affect the infective behaviour of cercariae. Cercariae in water without CFDA-SE were manipulated similarly. Cercariae were then immediately used in experiments.

6.2.2 Linoleic acid (LA) experiments

When exposed to air, LA oxidizes producing a hard glossy surface, enabling it to be applied to the base of culture dishes. The release of acetabular gland contents can vary with different LA concentrations (Stirewalt, 1978). As concentrations of 3.5 - 20 µg/cm^2 seemed ideal (Stirewalt, 1978), 7 µg/cm^2 were used here. Wells of non-treated 24-well tissue culture plates were therefore coated with 500 µl of 14 µg/ml LA (in 100 % methanol) and allowed to air dry at 4°C overnight; this gave 7µg/cm^2 based on a well area of 1.9 cm^2.

Plates containing wells previously coated with LA or not, were left for 1 h at room temperature to equilibrate. Aliquots of non-labelled cercariae (700–1000 cercariae in 1 ml FTW) were then applied to individual wells of the plates with or without LA and were incubated for different durations (0-120 min). Next, parasites were either processed for western blotting, or were fixed in 80% acetone for confocal microscopy

(Section 2.6). For western blotting, cercariae were pipetted into 1.5 ml microfuge tubes, left on ice for 1 min and pulse centrifuged; the supernatant was removed leaving 30 µl then 6 µl of 5x RIPA buffer with HALT protease and phosphatase inhibitors were added and cercariae homogenised with a plastic motorized pestle. From each sample 2 µl was removed and kept at -20°C for protein quantification (Section 2.5). Further processing for western blotting was as detailed in Section 2.5. Anti-phospho-(Ser) PKC substrate, anti-phospho-PKC (pan) (βII Ser660), anti-phospho-PKC (pan) (ζ Thr410) (190D10), anti-phospho-p44/42 MAPK (ERK1/2) (Thr202/Tyr204), and anti-phospho-p38 MAPK (Thr180/Tyr182) antibodies were employed.

The CFDA-SE labelled cercariae (700–1000 cercariae in 1 ml FTW) were also incubated in wells with or without LA for different durations (0–120 min) at room temperature. At the appropriate times cercariae were pipetted into 1.5 ml microfuge tubes, left on ice for 1 min, pulse centrifuged and the supernatant collected in 25 µl aliquots for fluorescence quantification of released gland contents. The aliquots were placed into black-walled 96 well microtitre plates (Nunc) and wells quickly visualized under a microscope to ensure that no cercariae were present that would otherwise interfere with the fluorescence readings. Two negative controls were also used; an aliquot of water from cercarial suspension without CFDA-SE and an aliquot of water from a CFDA-SE labelled cercarial suspension at 0 min. Fluorescence was measured in a FluoStar Optima microplate reader using 492 nm excitation and 520 nm emission. Gain adjustment was performed on the well expected to have the greatest fluorescence (120 min in LA). Data obtained was expressed in relative fluorescent units (RFU).

To corroborate the results of the fluorescence assay, confocal microscopy was performed on cercariae labelled with CFDA-SE and exposed to LA obtained from the above experiment to ascertain the amount of fluorescence remaining in the glands at each time point. Thus, aliquots containing cercariae were also removed from the wells and were fixed in 2% methanol-free paraformaldehyde for visualization on the Leica laser scanning confocal microscope detailed in Section 2.6. These cercariae had to be visualized within 4 h as the CFDA-SE dye diffused out to the other regions of the parasite over time even when fixed.

6.2.3 Effects of kinase inhibition/activation on release of gland contents

Cercariae (1000 per treatment) were incubated in 1 µM or 10 µM GF109203X, 1 µM U0126, 1 µM SB203580, 1 µM PMA, and 0.1% DMSO (vehicle for PMA and

U0126) for various durations (15, 30 and 60 min) and processed for western blotting (as detailed above in Section 6.2.2) to ascertain their inhibitory effects on PKC, ERK, and p38 MAPK phosphorylation and stimulatory effect on PKC phosphorylation, respectively. In subsequent experiments, the CFDA-SE labelled cercariae were pre-incubated in 10 μM GF109203X, 1 μM U0126, 1 μM SB203580, 1 μM PMA, and 0.1% DMSO for the optimal time points (maximum inhibition or activation of phosphorylation) prior to adding them to wells coated with LA (Section 6.2.1.). The effects of pathway inhibition/activation on acetabular gland release were then determined as detailed in Section 6.2.2. Temperature, light intensity, CFDA-SE and LA concentrations were kept constant for all observations.

6.2.7 Effects of kinase inhibition/activation on cercarial behaviour in the presence or absence of LA

The effect of 1 μM SB203580, 10 μM GF109203X, 1 μM U0126, 1 μM PMA, DMSO (0.1 %, vehicle control), or water (internal control) on cercarial behaviour in the presence of absence of LA was determined. Cercariae (~30) in 400 μl FTW were pre-incubated with the pharmacological inhibitors/activator or DMSO for 30 min at room temperature and were then transferred to wells with or without LA for up to 1 h. Exposing one sample at a time to each treatment, cercariae were filmed 1, 15, 30, and 60 min post-exposure using a 2.0 Mega Pixels Motic Moticam USB camera attached to an inverted microscope and movies captured with Motic Images Plus (version 2.0) for Windows. A total of two independent experiments were done. Categories of behaviour were adapted from Norton *et al.* (2008) and Brachs and Haas (2008) and included: 1) frequency of resting periods while swimming; 2) swimming orientation (i.e. tail first or head first); 3) peculiar behaviour e.g. increased change in direction or spinning around; 4) number of cercariae that sank to the bottom without resuming swimming; 5) creeping behaviour; 6) head contraction; and 7) tail contraction/activity without swimming. As light considerably affects the cercariae swimming behaviour, light intensity and positioning remained constant for all experiments. To better analyse the behaviour of cercariae ImageJ for windows was employed (Rasband, W.S., ImageJ, U. S. National Institutes of Health, Bethesda, Maryland, USA, http://rsb.info.nih.gov/ij/, 1997-2009).

6.3 Results

6.3.1 LA induces release of acetabular gland components labelled with CFDA-SE

To study release of acetabular gland components, CFDA-SE (to label the acetabular gland contents of cercariae) and LA (to induce the release of these acetabular contents) were employed. CFDA-SE-labelled cercariae exposed to LA released fluorescent acetabular gland contents into the water throughout the assay whereas those not exposed to LA (control) did not (Figure 6.1). With LA a significant and gradual increase in release of acetabular gland contents was observed between 15 and 120 min when compared to the same time points without LA ($p \leq 0.05$; Figure 6.1 B); at 15 min fluorescence was 359 % greater than without LA ($p \leq 0.05$) increasing to 532 % greater by 120 min ($p \leq 0.001$). As it was intended to also assess the effect of pathway inhibitors/activators that are soluble in DMSO on the release of acetabular gland contents, the effect of 0.1% DMSO on release was also assessed. Results showed that 0.1% DMSO alone did not significantly affect the release of acetabular gland contents when cercariae were in wells with or without LA. The effects of LA on the release of fluorescently labelled acetabular gland components were also analyzed using confocal microscopy at all time points studied (Figure 6.2). As the LA exposure time increases, fluorescence associated with the acetabular glands and ducts in the cercaria head decrease and is almost absent at 120 min. These results are in accord with the quantitative fluorescence readings obtained here and also with effects observed in studies exploring acetabular gland release with skin (Paveley *et al.*, 2009). Interestingly, on some occasions after 120 min in control (no LA) conditions a proportion (~50%) of the cercariae showed early signs of release characterized by fluorescence in the gland ducts although high levels of fluorescence remained within the acetabular glands.

6.3.2 Cercarial PKC and ERK activity changes during LA exposure, but not p38 MAPK

Next the phosphorylation profiles of PKC, ERK and p38 MAPK were assessed during cercariae exposure to LA to study the activities of these signalling proteins during LA-induced release of gland contents over 120 min.

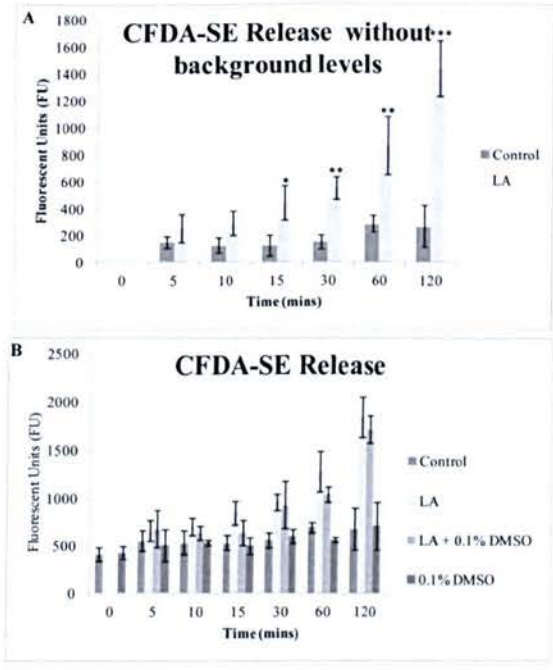

Figure 6.1 - Detection of acetabular gland components released from CFDA-SE labelled cercariae with or without linoleic acid (LA). Cercariae were incubated with CFDA-SE and then added to wells of a tissue culture plate either containing LA or not (control). The fluorescence (fluorescence units, FU) of the released gland components was then measured at defined time points (0–120 min) using a Fluostar Optima microtitre plate reader. Panel (**A**) fluorescence of the over time release of acetabular contents with or without LA when the 0 min background levels were removed; Panel (**B**) Release of gland components of cercariae when exposed to LA or not (control) with or without 0.1% DMSO. Mean values are shown (+/- SD), based on data from 3 independent experiments. * = $p \leq 0.05$, ** = $p \leq 0.01$ and *** = $p \leq 0.001$.

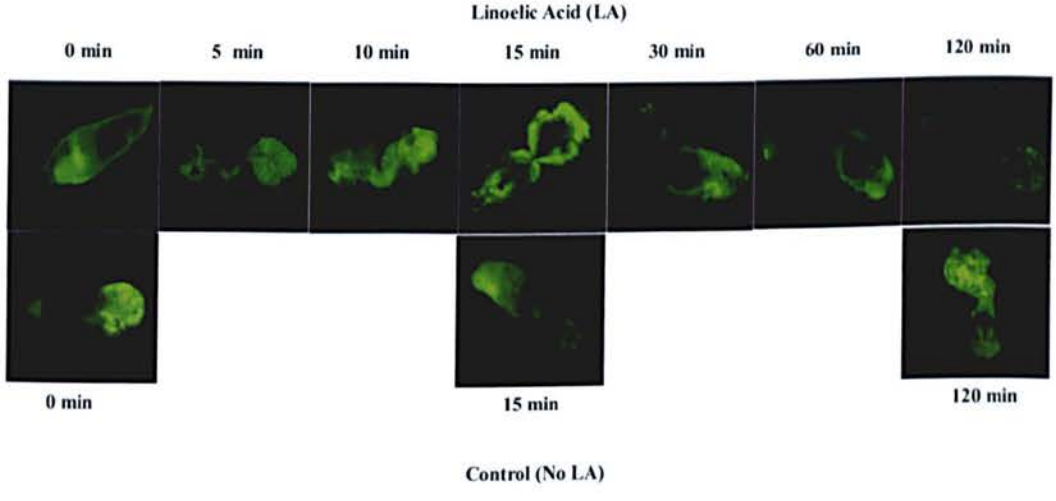

Figure 6.2 - Visual representation of acetabular gland components remaining inside *S. mansoni* cercariae at different durations after exposure, or not, to linoleic acid (LA). Maximum projections of 20 confocal z-sections of fixed *S. mansoni* cercariae demonstrating remaining CFDA-SE labelled gland components at 0, 5, 10, 15, 30, 60 and 120 min in the presence of LA or 0, 15 and 120 min without LA (control). Green signal represents CFDA-SE cleaved by the acetabular gland contents. Results are representative of those seen in cercariae populations obtained from two independent experiments.

Western blotting revealed that when *S. mansoni* cercariae experienced LA significant changes were seen, when compared to control conditions, in the phosphorylation of PKC and ERK, but not p38 MAPK (Figure 6.3). Furthermore, for the controls no significant changes in phosphorylation were observed for all proteins studied over 120 min. Phosphorylation of the ~81 kDa PKC, detected with anti-phospho PKC (Thr410) antibody, significantly increased after 10, 15 and 30 min in LA with increases of 1.6–fold ($p \leq 0.01$), 2–fold ($p \leq 0.001$) and 1.3–fold ($p \leq 0.05$), respectively, peaking at 15 min (Figure 6.3 A). Furthermore, ERK activation increased at 10, 15 and 30 min in LA, similarly to the ~81 kDa PKC however less intensely ($p \leq 0.05$; Figure 6.3 B); the maximum increase, 1.5-fold, occurred at 15 min (Figure 6.3 B). The ~45 kDa p38 MAPK detected with anti-phospho p38 MAPK antibodies did not show significant change.

In situ localization studies were next performed. In Figure 6.4 a representative negative control image of a cercaria incubated without primary antibody is shown demonstrating that the Alexa Fluor 488 secondary antibody does not bind cercariae proteins. Staining with anti-phospho PKC (Thr410) antibodies revealed PKC activity associated with several structures. Control cercariae not exposed to LA at 0 and 120 min (Figures 6.5 A and B, respectively) showed phosphorylated PKC mainly associated with the head/tail junction, nerves of the acetabulum, acetabular gland tubule (duct), sensory papillae/sensory neurons and the dorsal nerve cords (Figure 6.5 A and B). After 5 min in LA, PKC activation was still found in the acetabular tubules and the dorsal nerve cords as in control cercariae, but was also detected in regions including nerve-like ramified structures in the tail and the acetabular gland region (Figure 6.5 C). At 10 min LA exposure a shift in PKC activation pattern was observed in the head region mostly associated with the acetabular nerves and acetabular tubules; activity in the longitudinal nerve cord was maintained with activity also detected at the surface of the tail which could be sensory papillae/sensory nerves (Figure 6.5 D). When cercariae were exposed for 15 minutes in LA PKC activity in the head region was similar to that seen at 10 min (Figure 6.5 E). PKC activity was also found associated with the longitudinal nerve cord of the tail and conical like structures of the longitudinal nerve cord which could be nerve receptors (Figure 6.5 E, arrowed). After 30 minutes in LA PKC activity in cercariae was similar to that at 15 min (Figure 6.5 F). Following 60 min exposure to LA PKC activity generally decreased (Figure 6.5 G) and after 120 min in LA, PKC activity was only observed in unknown structures of the head region and some areas of the tegument (Figure 6.5 H).

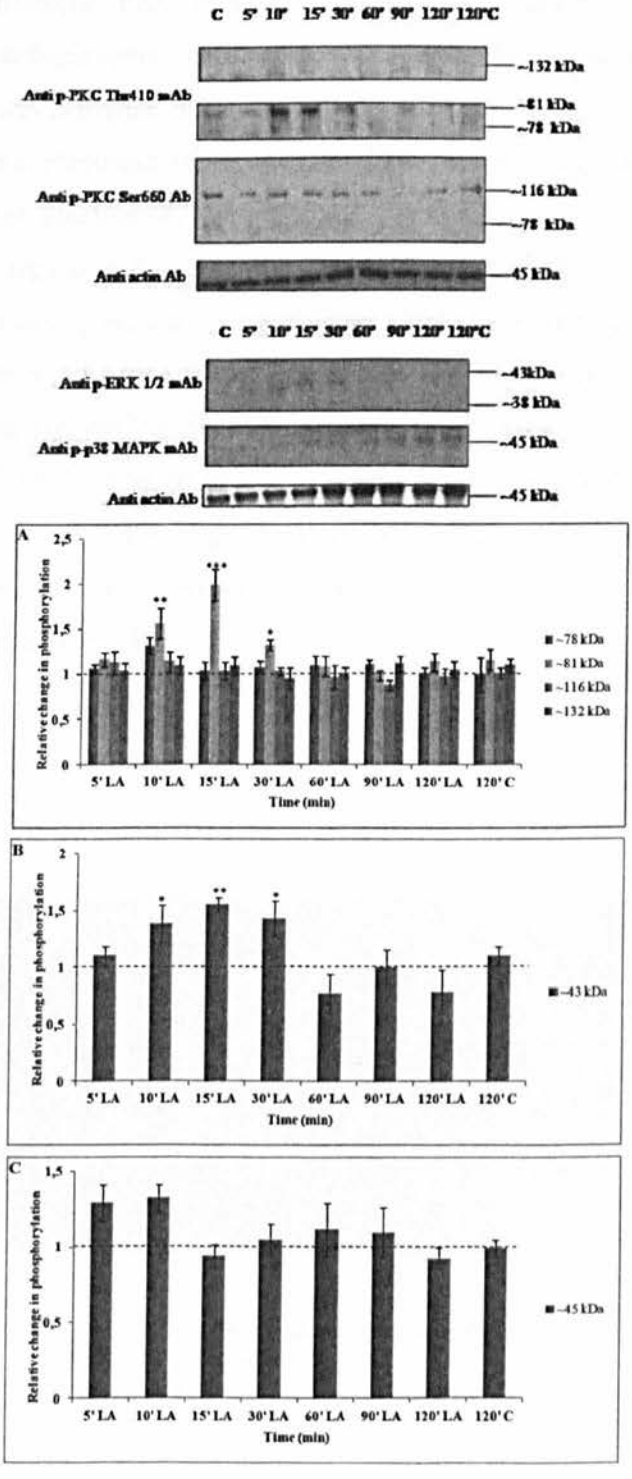

Figure 6.3 - Immunodetection of phosphorylated PKC, ERK and p38 MAPK during exposure of *S. mansoni* cercariae to linoleic acid (LA). Representative western blots showing active *S. mansoni* PKC, ERK and p38 MAPK detected with anti-phospho PKC (Thr410), anti-phospho PKC (Ser660), anti-phospho p44/p42 MAPK (ERK1/2), and anti-phospho p38 MAPK antibodies. Cercariae (700 per treatment) were maintained for 5, 10, 15, 30, 60, 90 and 120 min in LA, or 0 (C) and 120 min (120'C) without LA. To confirm equal loading of proteins and for semi-quantitative analysis, anti-actin antibodies were used. Immunoreactive bands from either three (**B**, **C**) or four (**A**) independent experiments were analysed and normalized according to 0 min controls assigned and value of 1 (shown as the dotted line), with adjustment for actin. Four immunodetected PKCs ~78 kDa, ~81 kDa and ~116 kDa and ~132 kDa, one ERK and one p38 MAPK were analysed. *= $p \leq 0.05$, **= $p \leq 0.01$ and ***= $p \leq 0.001$.

With anti-phospho PKC (Ser660) antibodies less intense staining was seen compared with anti-phospho PKC (Thr410) antibodies (Figure 6.6 and 6.5, respectively). Control cercariae maintained without LA for 0 min showed PKC activity associated with the acetabulum and acetabular nerve region, dorsal nerve cord, sensory papillae and head/tail junction (Figure 6.6 A); at 120 min PKC activity was only evident in the acetabulum region and acetabular nerves (Figure 6.6 B). During LA exposure new areas of PKC activity became evident (Figures 6.6 C-H). At 5 min activity was still detected in the sensory papillae and dorsal nerve cords, however a new activity was detected in a region resembling the ventral nerve cords (Figure 6.6 C). PKC activity decreased after 10, 15, 30 and 60 min in LA with activity associated mainly with the sensory papillae and acetabulum region and acetabular nerves (Figure 6.6 D-G). After 120 min in LA, strong PKC activation appeared in the region of the acetabulum and acetabular nerves (Figure 6.6 H).

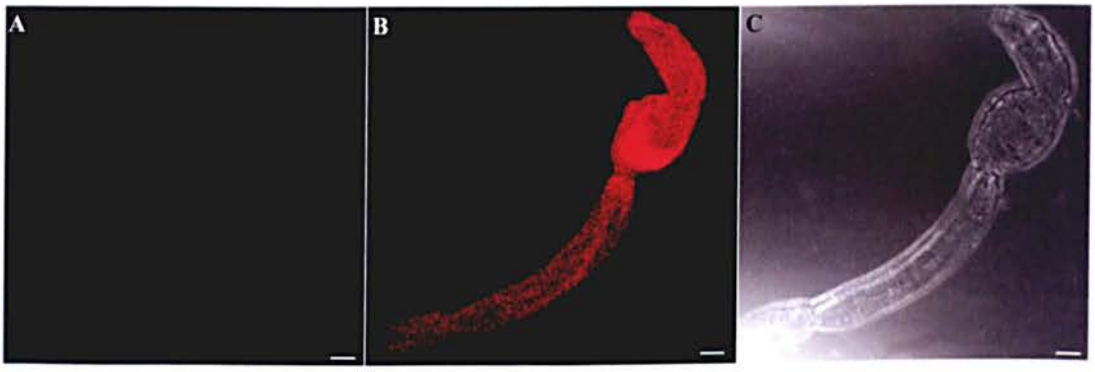

Figure 6.4 - Negative control for *in situ* localization of activated kinases in *S. mansoni* cercariae. Panel (**A**) cercaria not incubated with a primary antibody showing absence of green signal from secondary Alexa Fluor 488 antibodies and hence non-specific immunofluorescence. Panel (**B**) red signal from rhodamine phalloidin which stains actin filaments. Panel (**C**) reflection micrograph of the same specimen. Bar = 10 μm

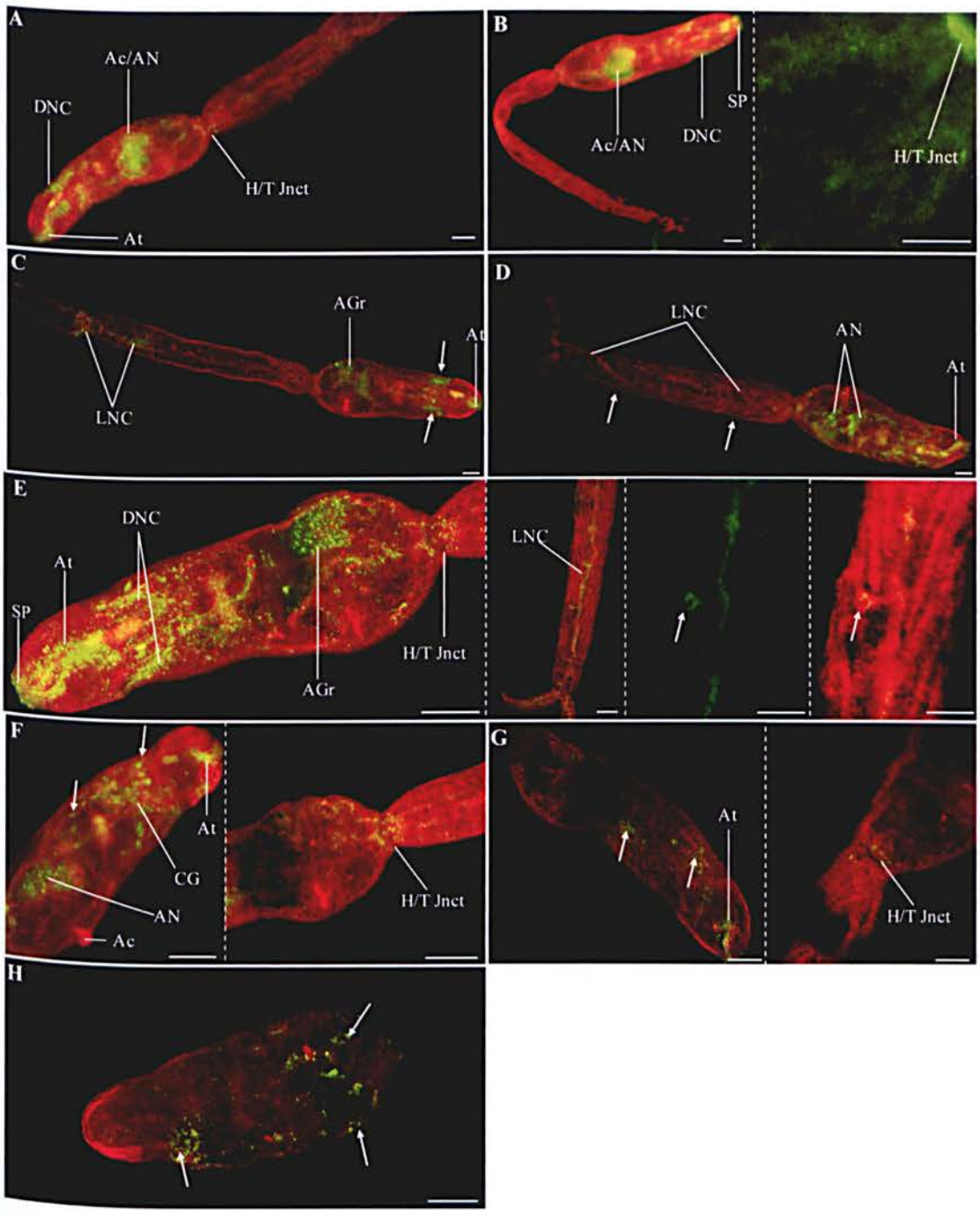

Figure 6.5 - *In situ* localization of phosphorylated PKC using anti-phospho PKC (Thr410) antibodies during exposure of cercariae to linoleic acid (LA) over time. Images show maximum projections of confocal z-sections and green signal represents phosphorylated PKC detected by anti-phospho PKC (Thr410) antibodies, whereas red shows filamentous actin. Panels (**A** and **B**) phosphorylated PKC in control cercariae not exposed to LA at 0 min and 120 min, respectively. Panels (**C** - **H**) phosphorylated PKC in cercariae exposed to LA for 5, 10, 15, 30 and 60 min respectively. Arrows show PKC activation in/at: (**C**) dorsal nerve cords; (**D**) tail surface; (**E**) sensory receptors at the tail surface; (**F** and **G**) sub-tegumental regions; (**H**) unidentified structures. Labels: (DNC), dorsal nerve cord; (LNC), longitudinal nerve cord; (AGr), acetabular gland region; (At), acetabular tubule (duct); (AN), acetabular nerves, (SP), sensory papillae; (H/T Jnct), head/tail junction; (Ac), Acetabulum; (CG), cephalic ganglia. Bar = 20 μm.

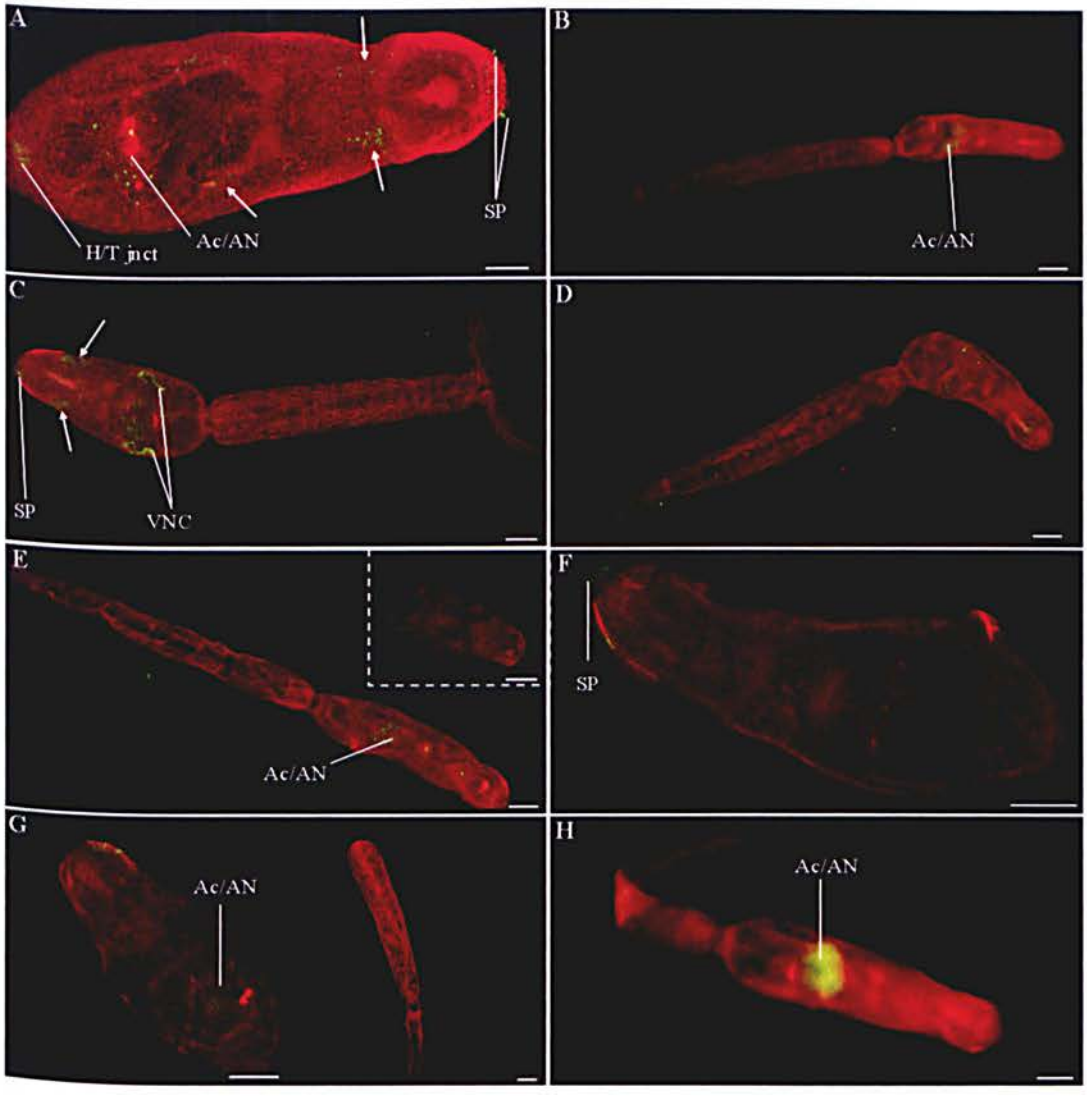

Figure 6.6 - *In situ* localization of phosphorylated PKC using the anti-phospho PKC Ser660 antibodies during exposure of cercariae to linoleic acid (LA) over time. Images show maximum projections of confocal z-sections and green signal represents phosphorylated PKC detected by anti-phospho PKC (Ser660) antibodies, whereas red shows filamentous actin. Panels (**A** and **B**) phosphorylated PKC in control cercariae not exposed to LA at 0 min and 120 min, respectively. Panels (**C - H**) phosphorylated PKC in cercariae exposed to LA for 5, 10, 15, 30 and 60 min respectively. Arrows show PKC activation in/at: (**A** and **C**) dorsal nerve cords. Labels: (H/T Jnct), head/tail junction; (Ac/AN), acetabulum/acetabular nerves; (SP), sensory papillae; (VNC), ventral nerve cords. Bar = 20 µm.

The anti-phospho ERK antibody revealed ERK activation mainly associated with structures of the sensory and excretory systems (Figure 6.7). In cercariae maintained without LA for 0 or 120 min ERK activity was mainly associated with the acetabular region and acetabular nerves, flame cells, head/tail junction and sensory papillae (Figures 6.7 A and B). When cercariae experienced LA for 5 or 10 min an overall increase in the number of regions with ERK activity was observed (Figures 6.7 C and D). Phosphorylated ERK appeared in all regions observed with the controls and was also detected in all flame cells and new regions in the tail which resemble the excretory tubules and sensory papillae (Figures 6.7 C and D). After 15 min in LA, activated ERK was found associated with the surface/glycocalyx, flame cells, acetabulum and sensory papillae (Figure 6.7 E). Afterwards (30, 60 and 120 min in LA) it appeared reduced, but was mostly associated with flame cells, sensory papillae and the acetabulum and acetabular gland region (Figure 6.7 F-H). Interestingly, as with adult worms, (Chapter 4) active ERK was always found in the sensory papillae and flame cells.

Finally, immunolocalization with anti-phospho p38 MAPK antibodies revealed ap38 MAPK activity mainly associated with structures of suspected sensory and neural function (Figure 6.8). Activated p38 MAPK was discretely associated with the acetabulum and the acetabular nerve region in control cercariae at 0 and 120 min (Figures 6.8 A and B). After exposure to LA for 5 min p38 MAPK activity was associated with the cephalic ganglia, region of the acetabulum where the acetabular nerves are located and also with the anterior region of the head (Figure 6.8 C). After 10 min activated p38 MAPK activity was found in additional areas such as the head gland, the longitudinal nerve cord and the surface of the tail were sensory neurons are known to be located (Figure 6.8 D). After 15 min activated p38 MAPK was found in the cephalic ganglia, the region of the acetabulum and putative sensory neurons at the surface of the tail (Figure 6.8 E). After experiencing LA for 30, 60 or 120 min cercariae showed negligible p38 MAPK activation (Figures 6.8 F-H).

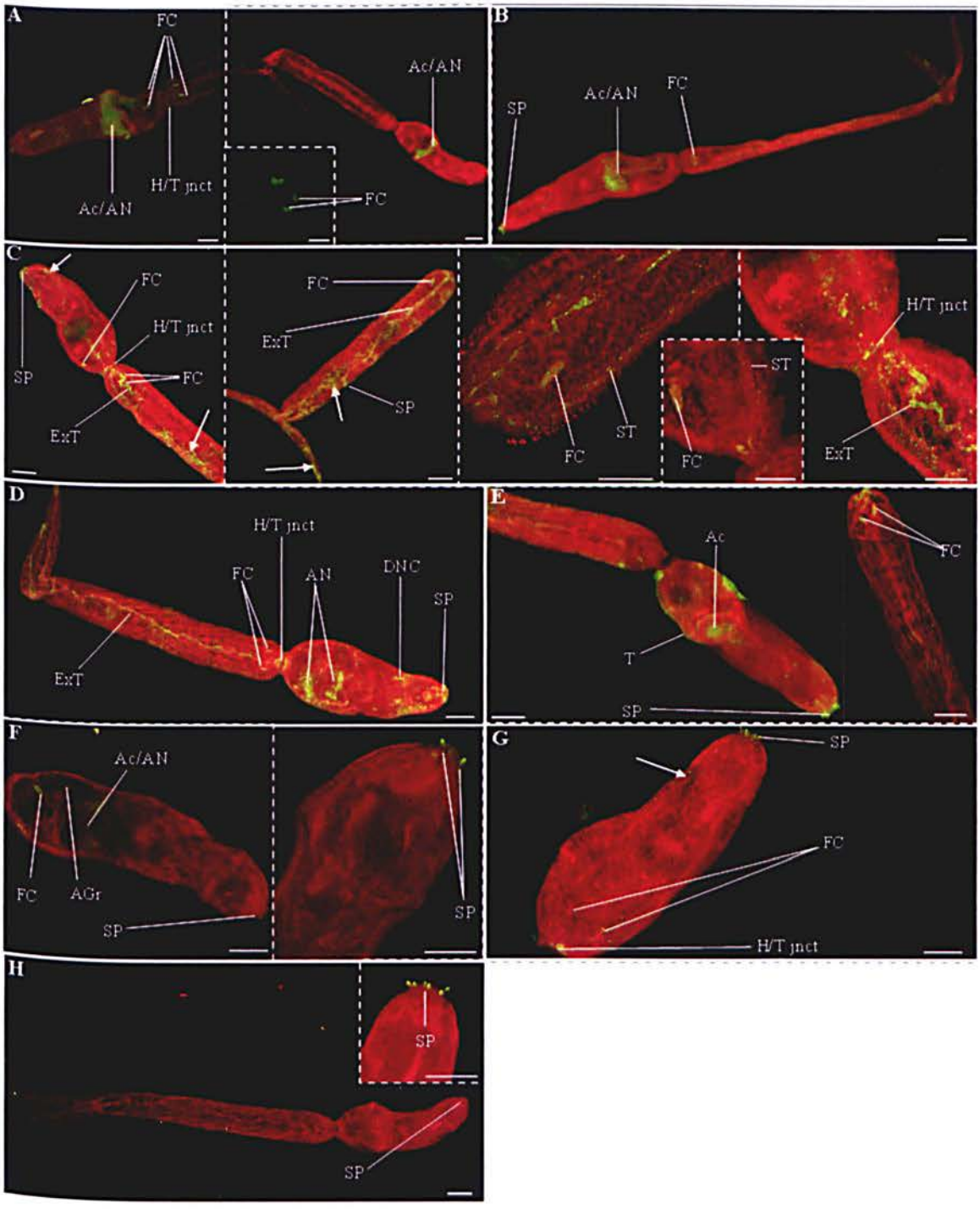

Figure 6.7 - *In situ* localization of phosphorylated ERK using anti-phospho p44/p42 MAPK (ERK 1/2) antibodies during exposure of cercariae to linoleic acid (LA) over time. Images show maximum projections of confocal z-sections and green signal represents phosphorylated ERK detected by anti-phospho ERK (1/2) antibodies, whereas red shows filamentous actin. Panels (**A** and **B**) phosphorylated PKC in control cercariae not exposed to LA at 0 min and 120 min, respectively. Panels (**C** - **H**) phosphorylated PKC in cercariae exposed to LA for 5, 10, 15, 30 and 60 min respectively. Arrows show ERK activation in/at: (**C**) ramified-like structures at the tail of suspected excretory or neural roles; (**G**) dorsal nerve cord. Labels: (FC), flame cell; (Ac/AN), acetabulum/acetabular nerves; (H/T Jnct) – head/tail junction; (SP), sensory papillae; (ExT), excretory tubule; (ST), sub-tegument; (AN), acetabular nerves; (DNC), dorsal nerve cord; (T), tegument; (Ac), acetabulum; (AGr), acetabular gland region. Bar = 20 μm.

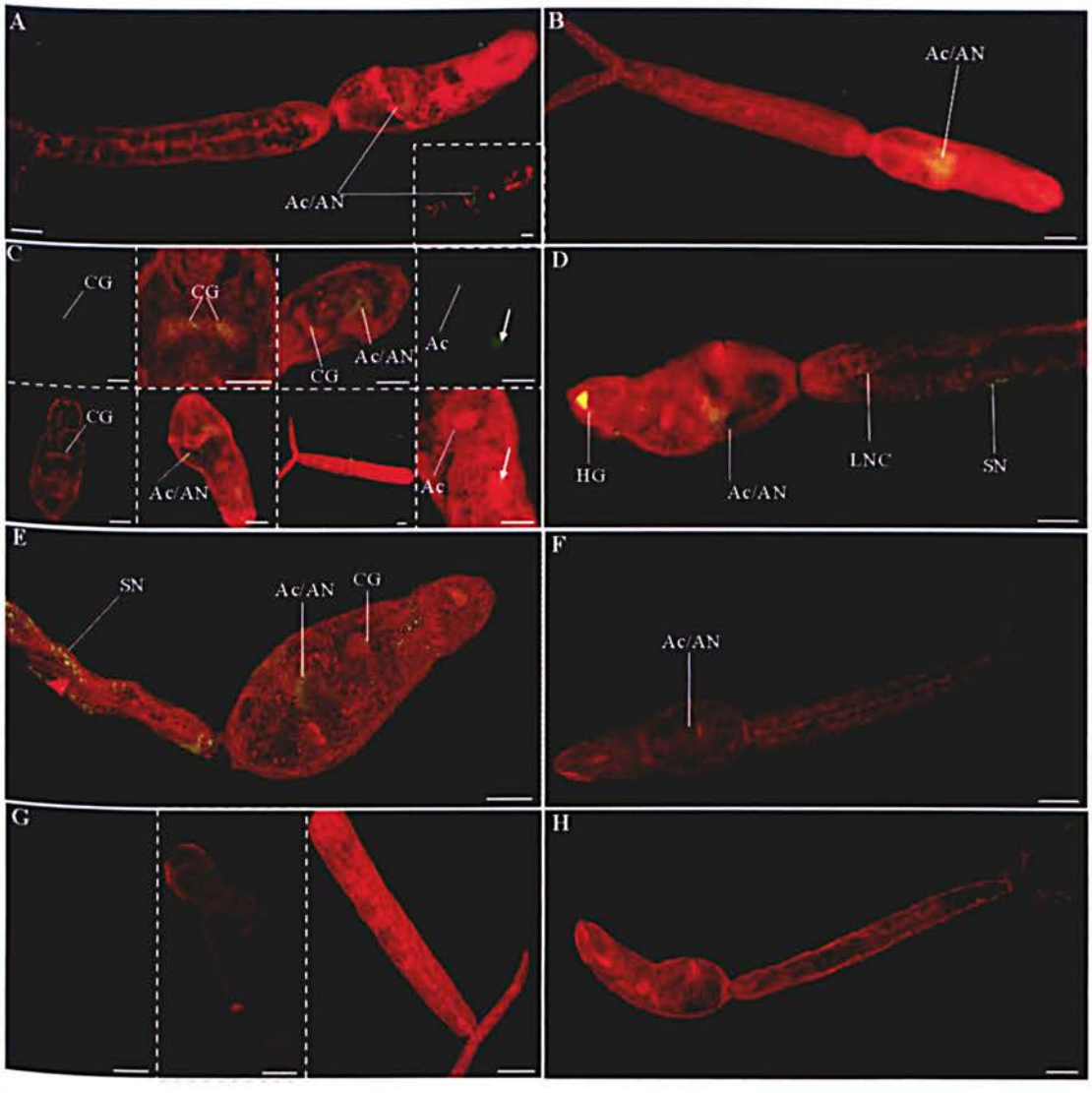

Figure 6.8 - *In situ* localization of phosphorylated p38 MAPK with anti-phospho p38 MAPK antibodies during exposure of cercariae to linoleic acid (LA) over time. Images show maximum projections of confocal z-sections and green signal represents phosphorylated p38 MAPK, whereas red shows filamentous actin. Panels (**A** and **B**) phosphorylated PKC in control cercariae not exposed to LA at 0 min and 120 min, respectively. Panels (**C** - **H**) phosphorylated PKC in cercariae exposed to LA for 5, 10, 15, 30 and 60 min respectively. Arrows show p38 MAPK activation in/at: (**C**) head gland. Labels: (Ac/AN), acetabulum/acetabular nerves; (CG), cephalic ganglia; (Ac), acetabulum; (HG), head gland; (LNC), longitudinal nerve cord; (SN), sensory nerves. Bar = 20 μm.

6.3.3 Cercariae PKC, ERK and p38 MAPK activation is blocked by GF109203X, U0126, and SB203580

The inhibitors GF109203X, U0126, and SB203580 have been previously used by us to specifically block the activity of PKC, ERK, and p38 MAPK in adult *S. mansoni* and miracidia (Chapter 4 and Ressurreição *et al.*, 2011a). Nonetheless, to decipher whether these inhibitors could block signalling in cercariae, 700-1000 cercariae (per treatment), were incubated with 1 μM and 10 μM GF109203X, and 1μM U0126 or SB203580 for 15, 30 and 60 min. Immunoblots show that 10 μM GF109203X was more effective at blocking the phosphorylation of all immunodetected PKCs (~132, ~116, ~81, and ~78 kDa) compared to 1 μM with inhibition of phosphorylation visible after 15 min (Figures 6.9 A and B). At the lower concentration (1 μM), GF109203X also reduced the phosphorylation of the ~116 kDa PKC detected with anti-phospho PKC (Ser 660) antibodies after 60 min (Figure 6.9 B). The MEK/ERK inhibitor U0126 (1 μM) inhibited the phosphorylation of ERK at in a time dependent manner, although inhibition was visible after 15 min (Figure 6.9 C). The p38 MAPK inhibitor SB203580 inhibited the phosphorylation of p38 MAPK at 1 μM after 30 min with little phosphorylation remaining at 60 min (Figure 6.9 D). The cPKC activator PMA (1 μM) was also tested revealing increased PKC phosphorylation at 15 min (data not shown). Overall, these results confirmed that PKC, ERK and p38 MAPK could be inhibited in cercariae permitting investigation into the role of these kinases in LA-induced acetabular gland component release.

6.3.4 Modulation of PKC, ERK and p38 MAPK activity affects acetabular gland release

Next the effect of PKC, ERK and p38 MAPK inhibition, or PKC activation, on the release of CFDA-SE labelled acetabular gland contents with or without LA was investigated using spectrofluorimetry and confocal microscopy. Cercariae were pre-incubated in 10 μM GF109203X or 1 μM U0126 for 15 min, or 1 μM SB203580 for 30 min (Figure 6.9), prior to adding them to LA coated plates; the release of acetabular gland contents was then determined over 120 min in the presence of these inhibitors. The effect of PMA was also assessed but pre-incubation was not necessary.

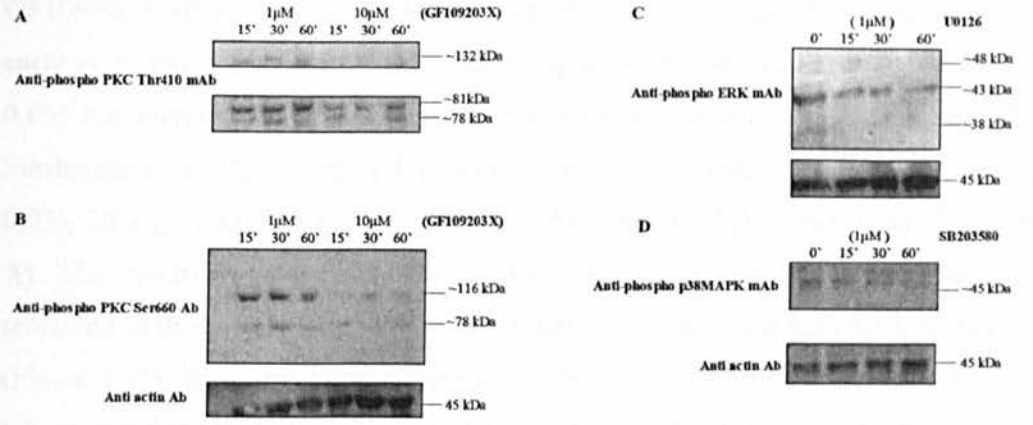

Figure 6.9 - Immunodetection of phosphorylated PKC, ERK and p38 MAPK following incubation of *S. mansoni* cercariae with GF109203X, U0126, or SB203580. Live cercariae (1000 per treatment for A-C; 700 per treatment for D) were exposed to either (A, B) 1 μM or 10 μM GF109203X, (C) 1 μM U0126, or (D) 1 μM SB203580 for 15, 30 and 60 min. Protein homogenates were then processed for western blotting with anti-phospho PKC (Thr410), anti-phospho PKC (Ser660) anti-phospho p44/p42 MAPK (ERK1/2), or anti-phospho p38 MAPK antibodies as shown; blots were also probed with anti-actin antibodies to detect actin as a loading control. Results are representative of two independent experiments.

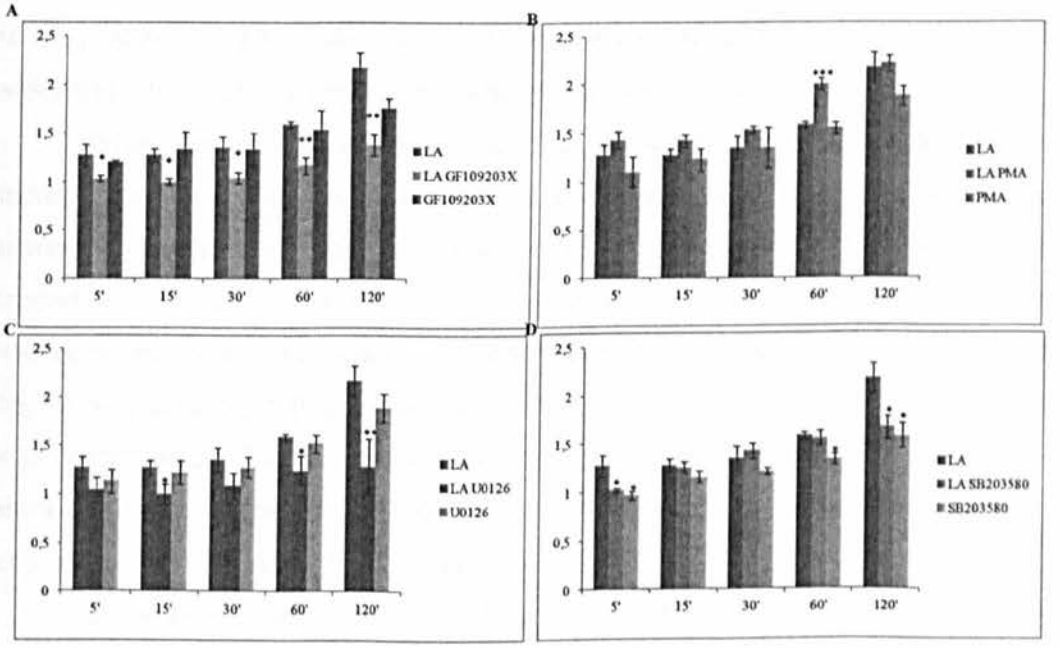

Figure 6.10 - Release of acetabular gland components from CFDA-SE labelled cercariae in response to linoleic acid (LA) in the presence of GF109203X, PMA, U0126 or SB203580. Cercariae were incubated with CFDA-SE in the presence of (**A**) 10 μM GF109203X, (**C**) 1 μM U0126, or (**D**) 1 μM SB203580 and then added to wells of tissue culture plates containing LA, keeping the inhibitors present. (**B**) 1 μM PMA was added at the time of adding cercariae to the wells. Release by cercariae without inhibitors/PMA was also determined (shown as LA). As a further control, release of gland components was also monitored in cercariae which were not exposed to LA but with the pharmacological modulators. The relative fluorescence of the released gland components was measured at defined time points (0–120 min) using a FluoStar Optima microtitre plate reader and the values for 0 min (control with no linoleic) were given a value of 1 Results are representative of 3 independent experiments and display mean change (+/- SEM). * = $p \leq 0.05$, ** = $p \leq 0.01$ and *** = $p \leq 0.001$.

In the presence of LA, inhibition of PKC phosphorylation with 10 μM GF109203X attenuated the release of acetabular contents; this effect was observed as early as 5 min when GF109203X-treated cercariae exposed to LA released 85% ($p \leq 0.05$) less contents compared to untreated cercariae exposed to LA (Figure 6.10 A). Furthermore, at 15, 30, 60 and 120 min, GF109203X reduced release by 96% ($p \leq 0.05$), 86% ($p \leq 0.05$), 80% ($p \leq 0.01$) and 67% ($p \leq 0.001$), respectively (Figure 6.10 A). The results were corroborated by fluorescence microscopy; green fluorescence remained in the acetabular glands of GF109203X treated cercariae after 120 min in LA (Figure 6.11). Interestingly, treatment of cercariae with GF109203X but not exposed to LA appeared to induce the release acetabular gland contents (Figure 6.10 A).

Incubation of cercariae with 1 μM PMA also stimulated the release of acetabular gland contents in the absence of LA and levels of release were similar to those obtained with LA exposed cercariae (Figure 6.10 B). However, when cercariae were exposed to LA in the presence of PMA, after 60 min the amount of contents released was significantly increased by ~2-fold ($p \leq 0.001$) when compared to LA only. At 120 min the levels of release were similar between PMA treated and untreated cercariae exposed to LA (Figure 6.10 B). Observation of cercariae demonstrated the lack of contents in the acetabular glands of PMA treated cercariae exposed to LA for 120 min.

Incubation of cercariae with 1 μM of the MEK inhibitor U0126 without LA also induced acetabular gland release to levels somewhat similar to those obtained from untreated cercariae exposed to LA (Figure 6.10 C). However, when cercariae were treated with U0126 and then exposed to LA a significant inhibitory effect on release was observed as early as 15 min with 96% reduction ($p \leq 0.05$); at 60 min there was a 58.7% reduction ($p \leq 0.05$), and at 120 min a striking 76% reduction ($p \leq 0.01$), which was confirmed by fluorescent microscopy (Figures 6.10 C and 6.11). These results show that in the presence of U0126 the LA induced release is substantially blocked, an effect also observed by the PKC inhibitor GF109203X.

Cercariae treated with 1 μM of the p38 MAPK inhibitor SB203580 but not exposed to LA displayed attenuated release of acetabular gland contents when compared LA exposed cercariae, particularly at 60 min and thereafter ($p \leq 0.05$; Figure 6.10 D). Furthermore, cercariae pre-treated with SB203580 and then exposed to LA also showed a significantly reduced gland release at 5 min and 120 min, inhibited by 90.4% ($p \leq 0,05$) and 42.6% ($p \leq 0,05$), respectively (Figure 6.10 D). This effect was also confirmed by microscopy, that revealed remnants of CFDA-SE fluorescence in the acetabular glands of SB203580 treated cercariae exposed to LA for 120 min (Figure

6.11). Thus SB203580 inhibits the release of cercariae acetabular gland contents, but unlike GF109203X and U0126 does not induce release in the absence of LA.

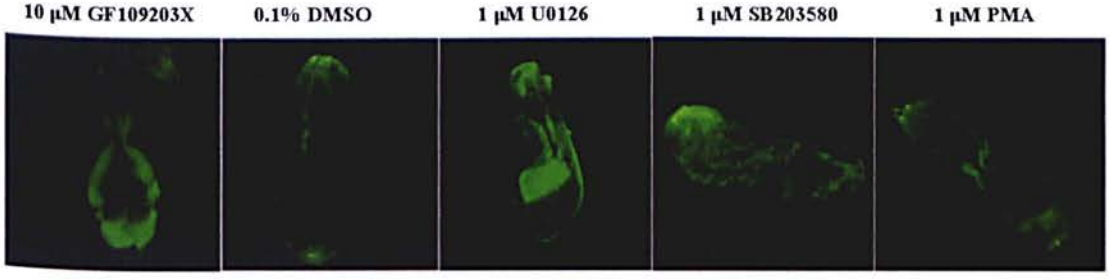

Figure 6.11 - Detection of CFDA-SE-labelled acetabular gland components remaining in cercariae after 120 min exposure to linoleic acid (LA) in the presence of GF109203X, U0126, PMA, SB203580 and vehicle control (DMSO). Maximum projections of 20 confocal z-sections of fixed *S. mansoni* cercariae demonstrating remaining CFDA-SE labelled gland components with treatment Green signal represents CFDA-SE cleaved by the acetabular gland contents. Results are representative of those seen in cercariae populations obtained from three independent experiments.

6.3.5 Inhibition of PKC, ERK and p38 MAPK affects cercariae behaviour

The behaviour of cercariae is complex with swimming enabled by the fork-like tail, and behaviours such as attachment and creeping governed by the acetabulum and musculature. Control cercariae maintained in wells containing water (without LA) swam normally, tail first and with longer active than resting phases (Video 6.1). Cercariae that experienced LA but were not exposed to kinase inhibitors/activators also swam mostly tail first but stopped often on the bottom of the wells covered with LA for brief moments and displayed head contractions in the first 15 min. After this most sank to the bottom of the wells and showed head contraction movements (Video 6.2). The vehicle (DMSO) did not alter cercariae behaviour with or without LA when compared to the respective controls.

Without LA, GF109023X affected the behaviour of cercariae with a higher proportion visibly sinking to the bottom of the wells for longer periods (longer resting phases) compared to control untreated cercariae; after 1 h) most cercariae had sank to the bottom and did not resume swimming (Video 6.3). The PKC activator PMA induced exploratory behaviour and release of proteolytic enzymes. The majority of PMA-treated cercariae sank to the bottom and displayed both head and tail contractions, sometimes

short tail-first bursts of swimming with shifting direction were observed (Video 6.3). Cercariae treated with U0126, showed less active phases than resting (Video 6.3). Cercariae treated with SB203580 behaved similarly to control cercariae however were visibly slightly more active with less resting phases and sometimes changing from tail first to head first swimming (Video 6.3).

In cercariae treated with the various pharmacological compounds and exposed to LA behavioural differences were observed relative to LA controls. The differences largely concerned tail movement, head contraction, swimming orientation and the proportion of cercariae that sunk to the bottom of wells that did not resume swimming. Cercariae treated with PMA (Video 6.4) were visibly more active compared to LA controls displaying increased tail and head movements. Conversely, cercariae treated with the GF109203X sank but did not attach to the LA coated base, however the majority of cercariae still showed characteristic head contractile movements (Video 6.4). When treated with SB203580 only few cercariae migrated towards the LA and these showed fast head contractions in the substrate and sporadic tail first swimming stopping often in the substrate (Video 6.4). When treated with U0126, cercariae were seen to be mostly immobile (tails did not move or moved very slowly) however showing head contractions (Video 6.4).

6.4 Discussion

Host finding and invasion by schistosome cercariae are examples of biological adaptation, which have been studied in several *Schistosoma* spp. (McKerrow and Salter, 2002). A major part of cercariae infective behaviour is the release of acetabular gland contents (packed with proteolytic enzymes), which aid in attachment to and degradation of host skin (reviewed by Walker, 2011). This mechanism is thought to be complex involving both sensory and neuromuscular actions in which signalling is suspected to have an important role (Haas *et al.*, 1997). Work in this Chapter focused on the involvement of PKC, ERK and p38 MAPK in host detection and penetration mechanisms using novel LA/CFDA-SE and pharmacological assays.

6.4.1 Combination of LA and CFDA-SE allows the reliable induction and tracking of release of S. mansoni *cercaria acetabular gland contents*

The combination of LA and CFDA-SE in assays enabled the release of acetabular gland contents from *S. mansoni* cercariae to be reliably tracked. Significant and gradual increases in gland release in response to LA were observed as early as 15 min while control cercariae not exposed to LA showed no gland release. The kinetics of release are in accord with that observed when *S. mansoni* cercariae experience mammalian skin where release was seen within 10 min extending until 120 min (Paveley *et al.*, 2009). At 120 min without LA, some variability in fluorescence readings was detected, suggesting low (but insignificant) levels of release. Such release of acetabular contents without the appropriate stimulus might be an innate emergency response of the parasite for a "last attempt" to successfully infect, as cercariae have limited glycogen stores (Norton *et al.*, 2008).

6.4.2 Putative role for PKC and ERK in triggering cercariae acetabular gland content release induced by LA

The initiation of cercariae acetabular gland content release in response to LA was concomitant with a significant increase in PKC and ERK phosphorylation at 15 min. In the presence of LA phosphorylation of the ~81 kDa PKC and ~43 kDa ERK was transient, with significant stimulation at 10, 15 and 30 min, decreasing to basal levels thereafter. This strongly suggests an underlying involvement of these enzymes in

triggering the mechanism of cercariae acetabular gland content release as increases in phosphorylation correspond with the initial phase of release. Additional support for this is provided by the fact that inhibition of cercarial PKC and ERK with GF109203X and U0126, respectively, drastically reduced LA-induced acetabular gland content release as early as 15 min. The PKC activator PMA also induced acetabular gland content release on its own and induced additional release with LA at 60 min. This extends considerably the work by Matsumura *et al.* (1991) who showed that PKC activators induce *S. mansoni* cercariae penetration behaviour and protease release.

In mammalian systems there are differences in the ability of fatty acids to activate PKCs (Naor *et al.*, 1988). For instance, arachidonic acid and LA are effective PKC activators while nonessential fatty acids (i.e. oleic acid, palmitic acid, stearic acid and elaidic acid) are less effective. Surprisingly, arachidonic acid and LA are potent stimulants of cercariae penetration response whilst nonessential fatty acids are less potent (Haas and Schimitt, 1982; Salafsky *et al.*, 1984). Therefore, it is attractive to hypothesize that essential fatty acids play a role as second messengers by intercalating with cercarial membranes (either at the surface of the parasite or after ingestion) and activate cercarial PKC. However, the similar timing of PKC activation with initiation of acetabular gland release and the reduction of release when PKC is inhibited supports the participation of PKC in this important cercarial infection mechanism. In general, our results suggest that both PKC and ERK signalling proteins are directly involved in the initial mechanisms of cercarial acetabular gland release. Whether ERK is activated downstream as a direct response of PKC activation (as was shown in Chapter 4) during this process remains to be elucidated.

6.4.3 Putative role for PKC in LA-induced cercariae acetabular gland content release via regulation of neuromuscular and sensory mechanisms

In the presence of LA, only the activity of the ~81 kDa PKC was significantly increased. However, changes in distribution pattern of PKC activation in cercariae were detected with both anti-phospho PKC antibodies [anti-phospho PKC (Thr410) and anti-phospho PKC (Ser660)]. During the first 30 min of LA exposure, activated PKC was detected in previously unseen regions of the central nervous system, such as longitudinal and dorsal nerve cords, the acetabular nerves (surrounding the acetabulum), acetabular gland region, and also in regions where sensory papillae are known to exist in the anterior tip of the head region (Dorsey, 2002; Collins *et al.*, 2011).

The acetabular nerves have suspected roles in the neuromuscular function of the acetabulum for the success of attachment and creeping on host skin (Dorsey, 2002). As activated PKC was associated with this structure, during the initial phases of exposure to LA, PKC likely plays a part in enabling cercariae to attach onto a suitable substrate; this is reinforced by the finding that GF102903X blocked cercariae attachment to LA. In *S. mansoni* cercariae, the sensory papillae are thought to have chemo, photo and/or thermo-sensory properties (Dorsey, 2002) and the dorsal and ventral nerve cords are possibly involved in processing information from environmental stimuli (Dorsey, 2002; Collins *et al.*, 2011) that might contribute to neuromuscular function including that needed for gland release. PKC activity was also found in areas close to the acetabular glands where muscle, nerve and parenchyma cells closely surround the glands and are considered to regulate the secretory process (Dorsey and Stirewalt, 1971). Hence, PKC activity localized in regions of *S. mansoni* cercaria, which are crucial for host detection, attachment and skin degradation, suggests an involvement for PKC signalling in cercariae infective processes.

The effects of GF109203X or PMA on cercariae behaviour further support a role for PKC in regulation of neuromuscular events in this life-stage. Without LA, PKC inhibited cercariae, displayed longer resting phases and gradually stopped swimming (after 1 h) suggesting a decrease in muscular activity. On the contrary PMA induced cercariae exploratory behaviour and proteolytic enzymes release suggesting an increase in muscular activity. It is known that cercarial body contractions aid in squeezing out secretions from acetabular glands (Stirewalt, 1973; Samuelson *et al.*, 1984) and PKC could be a major player in this contractile process. The results are in harmony with what is known about PKC in neuromuscular function in other systems; for example PKC regulates neuromuscular junction activity in invertebrates and vertebrates (Worden, 1998; Fox and Lloyd, 1999).

Matsumura *et al.* (1990) reported that PZQ stimulates release of *S. mansoni* cercarial acetabular gland contents causing the sudden and violent contraction of muscle in the presence of Ca^{2+} and that this release is partially inhibited by the Ca^{2+} chelator EGTA. LA is also known to stimulate calcium uptake in cercariae (Fusco *et al.*, 1991). Thus, calcium seems important to the process of acetabular gland content release and interestingly, in cercariae exposed to LA, changes in distribution of the ~116 kDa PKC (likely a classical calcium-sensitive PKC type, see Chapters 1 and 3) were observed. However, the cercarial PKC protein significantly activated by LA was the ~81 kDa PKC which we believe to be a calcium insensitive isotype, as it lacks a calcium binding

domain (see Chapter 1 and 3). If these putative PKC assignments are correct the mechanisms of cercarial acetabular gland content release are more complex than previously assumed, possibly involving several different molecular pathways.

6.4.4 LA-induced ERK activation is associated with homeostatic and sensory processes

In general, activated ERK was found in the sensory papillae and flame cells of *S. mansoni* cercariae, when exposed or not to LA. The presence of activated ERK in the excretory system of *S. mansoni* adult worms (Chapter 4) and cercariae, suggests a conserved function for ERK signalling in schistosome excretory processes.

In the presence of LA increased ~43 kDa ERK activity was observed at 10, 15 and 30 min and was localized within structures not observed in the controls such as the surface of the head organ, sensory papillae in the tail, all flame cells and tail excretory tubules. This LA-induced ERK activation in regions of the excretory system, suggests that LA exposure up-regulates ERK activity associated with excretory processes. LA and released acetabular gland contents are known to initiate the cercaria to schistosomule transformation process that includes changes in water tolerance (Salafsky and Fusco, 1987). As water balance is controlled by permeability through the outer surface (glycocalyx) and by excretion of the excess fluid by the excretory tubules (Dorsey, 2002), ERK activity associated with the body surface and protonephridial system of cercariae is likely important to cercariae homeostasis, particularly during transition between water and host blood. That ERK activity has also been associated with the malpighian tubules of *Drosophila* (Gabay *et al.*, 1997) and the excretory system of planaria (Rink *et al.*, 2011) demonstrates that ERK function in invertebrate excretion is likely conserved irrespective of existence (free-living or parasitic).

The LA-induced ERK activity associated with the surface of the cercariae head might be important to the shedding of the glycocalyx as LA is known to initiate transformation. The glycocalyx is a complex carbohydrate coat, which protects the cercaria against osmotic shock from water and is shed early as the cercaria transforms to a schistosomula (Samuelson and Caulfield, 1982). The shedding of the glycocalyx is also necessary for infection because it is a potent inducer of complement activation (Samuelson and Caulfield, 1982; Samuelson *et al.*, 1984; McKerrow and Salter, 2002).

Without LA activated ERK was not only associated with excretory organs but also with the acetabulum region and acetabular nerves, head/tail junction and sensory papillae at the tip of the head. This basal ERK distribution shows a rooted presence for ERK activity in normal cercarial sensory and perhaps muscular functions. However, activation of ERK in the sensory papillae with or without LA suggests that the ERK function in these papillae is not switched on by chemoattraction. In contrast, activated ERK was found associated with structures at the tail surface suspected to be sensory organs (Dorsey, 2002) only in the presence of LA; it appears that ERK in sensory structures can be activated by LA.

A role for ERK in release of acetabular gland contents is supported by the strong inhibition observed with U0126. Interestingly, ERK activation associated with the acetabular nerves (where PKC activity was also detected) suggests that ERK and PKC signalling is inter-connected in *S. mansoni* cercariae, like in adult worms (Chapter 4). Overall, the findings support a strikingly multifunctional role for ERK in cercariae.

6.4.5 Cercarial p38 MAPK activity is associated with sensory and neuronal structures

Although p38 MAPK activation did not change significantly in the presence of LA, changes in visual distribution of activated p38 MAPK activity were observed.

In the presence of LA, activated p38 MAPK was mostly associated with putative sensory neurons in the tail and the cephalic ganglia (central nervous system). This distribution profile suggests a possible involvement of p38 MAPK in regulation of *S. mansoni* cercarial neurological and chemosensory processes perhaps related to LA-induced acetabular gland content release. Moreover, p38 MAPK inhibition attenuated the release of acetabular gland contents supporting a role for p38 MAPK in this process. These results suggest that inhibition of sensory/neural function with SB203580 affects the response to LA. Interestingly, p38 MAPK has been linked to sensory responses in other organisms; in rats, p38 MAPK is involved in glial cell induced tactile pain hypersensitivity (Piao *et al.*, 2006). No p38 MAPK activity was seen in the sensory papillae at the tip of the head; thus this pathway might only be involved in chemo-perception at the tail.

In general, cercariae treated with SB203580 behaved similarly to control cercariae however appeared slightly more active with increased changes in head first- and tail first- swimming with less resting phases. With LA, less cercariae appeared to be

attracted to the bottom of the well. This supports the suggestion that p38 MAPK is involved in the sensory perception of cercariae.

6.4.6 PKC and ERK inhibition reduces LA-induced release of acetabular gland contents but stimulates release in control cercariae

Strikingly, the PKC and ERK inhibitors GF109203X and U0126, respectively, induced acetabular gland content release of cercariae without LA, however the vehicle control (DMSO) and the p38 MAPK inhibitor (SB203580) did not. Although cercarial acetabular gland release is known to be stimulated by specific signals of the host skin, other compounds have also been reported to cause enzyme release e.g. PZQ, (Matsumura *et al.*, 1990), lectins (Coles *et al.*, 1988), silver ions (King and Higashi, 1992), calcium modulators and phorbol esters (Matsumura *et al.*, 1991; Fusco *et al.*, 1991). Indeed, Haas and Schmitt (1982a), investigated the effects of hundreds of compounds on the behaviour of *S. mansoni* cercariae and found that some toxic compounds stimulated cercariae to penetrate into agar showing a relationship between toxic effects and acetabular gland contents release. This response to chemicals suggests that *S. mansoni* cercariae might possess an emergency program that initiates penetration attempts into any substrate when under stress. The complex movement patterns that multicellular cercariae show during penetration and acetabular gland secretion (Stirewalt, 1966) are finely tuned by neuromuscular signalling events which PKC and ERK seem to be associated. Hence alteration of these events by ERK/PKC inhibition could have caused involuntary release of contents. Therefore, while the effect of GF109203X or U0126 were likely due to changes in the normal signalling equilibrium or neuromuscular function of cercariae, toxicity might have played a role.

6.4.7 Conclusions

The combined LA and CFDA-SE assay was shown to be valuable tool for monitoring gland release by cercariae. Staining for activated PKC, ERK, and p38 MAPK in cercariae yielded interesting data concerning the location of these kinases in response to LA; activated kinases were found associated with neuromuscular and neurosensory structures near the acetabulum, acetabular glands, and parasite surface respectively. This knowledge when coupled with inhibition assays has identified complex roles for these kinases in acetabular gland release in response to LA. It would be valuable to determine the effects of PKC, ERK or p38 MAPK inhibition in cercariae

on the success of mouse infection. Because some avian schistosomes are accidental parasites of humans but are arrested by immune responses at the cercaria/schistosomule stage, a more complete understanding of cercarial molecular biology of invasion could provide new targets for a protective vaccine.

Chapter 7

Involvement of PKC and MAPK signalling in *S. mansoni* cercariae thermokinesis and photokinesis

7.1 Introduction

Governed by circadian rhythm, light is the main trigger that stimulates emergence of *S. mansoni* cercariae from *B. glabrata*. Moreover, the cercariae swim intermittently in light, and swim towards increases in temperature (positive thermotaxis) to facilitate host finding (reviewed by Smyth and Halton, 1983; Saladin, 1982; Haas, 1992, 1994; Haas and Harberl, 1997). Swimming cercariae are oriented towards light by interplay of two swimming modes; active swimming or backward (tail-first) swimming strictly stimulated and orientated towards light (positive photokinesis), or the passive or forward (body-first) swimming which shows a pronounced response to shadow moving away from light (negative photokinesis) (Saladin, 1982; Grabe and Haas, 2004). When cercariae approach the skin of a susceptible host they switch to the strictly photo-negative forward-swimming mode (Saladin, 1982), and once host penetration is initiated survival is dependent on negative phototaxis as the parasite moves into the epidermis (Stirewalt, 1974; Grabe and Haas, 2004). The effects of light and temperature on the swimming and penetration behaviour of cercariae have been well studied but little is known on the mechanosensory structures that exist in *S. mansoni* cercariae. Ultrastructural studies have revealed the existence of various putative sensory structures (terminals of nerve processes) in the tail and head region possibly involved in photo-, mechano-, or/and chemo-reception (Dorsey *et al.*, 2002). Very little is also known of the signalling mechanisms involved in translating these stimuli to a behavioural response, however, PKC and MAPK are important regulators of photo- and thermo-perception in vertebrates and invertebrates (Yarfitz and Hurley, 1994; Okochi *et al.*, 2005; Hyde *et al.*, 2011).

Gene expression profiling using expressed sequence tags (ESTs) has revealed that two different photoreceptors exist in *S. mansoni* cercariae and it is likely that positive and negative phototaxis are mediated by two different photoreceptor systems. Two ESTs were found with significant homology towards genes encoding proteins involved in mammalian light reception mechanisms, Gq-coupled rhodopsin photoreceptor (EST AA5596680) and rod phosphodiesterase δ subunit (EST AA559625) (Santos *et al.*, 1999). The *S. mansoni* EST AA5596680, which shows 67% homology to a molluscan Gq-coupled rhodopsin, is a serpentine receptor associated with responses to light, classically known to undergo conformational changes after it has absorbed a photon becoming "photoexcited" leading to the activation of a GTP

binding protein (Yarfitz and Hurley, 1994). This type of photoreceptor is commonly found in vertebrates and invertebrates and could be associated with the positive photokinesis system of *S. mansoni* cercariae (Yarfitz and Hurley, 1994; Santos *et al.*, 1999). EST AA559625 shows a 78% homology to the δ inhibitory subunit of bovine rod cGMP phosphodiesterase, a photoreceptor also found in vertebrates and invertebrates; in *C. elegans* its function might be to translocate membrane-anchored proteins into the cytosol (Hanzal-Bayer, 2002; Zhang *et al.*, 2004).

At the molecular level, invertebrate light perception mechanisms are similar to those of vertebrates, based on 11-cis-retinal chromophore and rhodopsin (Yarfitz and Hurley, 1994). The excitation of rhodopsin by a photon is known to affect GPCRs, however downstream transduction pathways diverge between vertebrates and invertebrates (del Pilar Gomez and Nasi, 1995). In some invertebrates, photo-transduction by microvilar photoreceptors uses the G-protein coupled phosphoinositide signalling pathway, where hydrolysis of phosphatidyl inositol 4,5-biphosphate (PIP_2) by phospholipase C generates inositol 1,4,5-triphosphate ($InsP_3$) leading to activation of Ca^{2+}-permeable light-sensitive channels and the release of Ca^{2+} from intracellular stores. However, in other invertebrates such as *Drosophila* a lipid messenger such as DAG may mediate excitation (reviewed by Hardie, 2001). This typically triggers PKC activation amongst other signalling proteins leading to a neurophysiologic effect on the organism (Hardle *et al.*, 1993). In fact, studies have revealed PKC to be required for light adaptation of *Drosophila* photoreceptors (Hardle *et al.*, 1993).

Thermotaxis is directed locomotion up or down a temperature gradient. In 1974, Stirewalt demonstrated the ability of *S. mansoni* cercariae to sense and respond to changes in temperature swimming towards an increase in temperature which was later confirmed by Mckerrow (2003). Thermotaxis is especially important in small organisms with small mass and thus small heat capacities (Garrity *et al.*, 2010). Thermosensory neurons have not yet been identified in schistosome cercariae and nothing is known about the receptors that could be involved in thermotaxis. However, several sensory papillae have been found (Dorsey *et al.*, 2002) and unidentified heat-induced proteins have been associated with the transformation of *S. mansoni* cercariae to schistosomules (Blanton *et al.*, 1987). Thermo receptors have been better researched in parasitic nematodes, including skin penetrating species, which are fascinatingly similar to those in non-parasitic nematode *C. elegans* (Ashton and Schad, 1999).

For *Drosophila* and *C. elegans* thermosensory mechanisms are well described, at the molecular level (Garrity *et al.*, 2010). Both of these organisms can quickly switch

from positive thermotaxis when navigating at temperatures below 20°C to negative thermotaxis when above 30°C (Garrity *et al.*, 2010) governed by two distinct sets of thermosensory neurons located in the anterior of the larva (Garrity *et al.*, 2010; Luo *et al.*, 2010). Several molecules have been found to be involved in thermo sensitivity; in *C. elegans*, calcineurin A and calcium/DAG activated PKCs (PKCε) are directly associated with the organism sensory neurons, interneurons and motor neurons (Okochi *et al.*, 2005). In *Drosophila* genetic studies in both larvae and adults have highlighted genes that contribute to thermal information processing which include TRP (Transient Receptor Potential) channel genes, receptors for histamine, phospholipase C signalling pathway components and cAMP signalling pathway genes (Hong *et al.*, 2006, 2008; Kwon *et al.*, 2008; Garrity *et al.*, 2010).

In Chapter 6 a putative involvement of PKC and MAPK signalling in chemoperception by *S. mansoni* cercariae was demonstrated. This chapter describes an investigation into these kinases in photo- and thermo- perception. Furthermore, as detached cercariae tails are responsive to light the signalling involved in this phenomenon was also investigated.

7.2 Materials and Methods

7.2.1 Exposure of S. mansoni *cercariae to different light and temperature regimes*

Cercariae were obtained and handled as detailed in Sections 2.3 and 2.4.2 and were enumerated by counting those present in 20 µl aliquots after adding Lugol's solution. They were then left to equilibrate for 1 h at ambient conditions (room temperature (~24°C) and normal laboratory light intensity). Then, cercariae were equally divided into clear 1.5 ml microfuge tubes (~ 800/tube in FTW) and incubated at 24°C (room temperature) or 37°C (host body temperature) for 15, 30 and 60 min under the following light regimes: dark, normal laboratory light, or direct non-heating light (Table 7.1). After the respective durations cercariae were immediately placed on ice for 30 s, quickly spun down by pulse centrifugation, the supernatant removed but the least 30 µl and the cercariae processed for western blotting, or fixed in ice cold 80% acetone for subsequent immunohistochemistry (Section 2.6); actin was stained with anti-actin Cy3 conjugated antibodies instead of rhodamine phalloidin. For western blotting, 30 µl of cercarial suspension was homogenised with a plastic motorized pastle with 6 µl 5x RIPA buffer and 1 µl HALT phosphatase/protease inhibitor cocktail and then processed as previously described (Section 2.5). Anti-phospho-PKC (βII Ser660) polyclonal, anti-phospho-PKC (ζ Thr410), anti-phospho-p44/42 MAPK (ERK1/2) (Thr202/Tyr204), and anti-phospho-p38 MAPK (Thr180/Tyr182) monoclonal antibodies were employed.

7.2.2 Exposure of detached cercariae tails to bright light and dark conditions

The following experiment was performed due to the unexpected finding that after mechanical transformation of cercariae to schistosomules the detached tails carried on moving and seemed to be responsive to increased light intensity (positive photokinesis), slowing down movement when intensity was reduced. Detached tails were separated into clear 1.5 ml microfuge tubes and then exposed to bright light (direct non-heating light from a lamp) for 1 min (as tail responses towards light were almost immediate and sustained) or placed in the dark (foiled microfuge tubes); both at ambient temperature (24°C). They were then, immediately placed on ice for 1 min, pulse centrifuged, the supernatant removed and either processed for western blotting as for cercariae (above) or fixed in 80% acetone for immunohistochemistry and confocal microscopy (Section 2.6).

Table 7.1 - The various temperature and light regimes applied to recently-emerged *S. mansoni* cercariae. [1] Normal = normal ambient light provided by standard laboratory room lighting; [2] Intense light = direct non-heating light from a lamp; [3] Dark = foiled microfuge tubes (24°C) or interior of dark incubator (37°C). Normal and intense light treatments shown in D and E were performed in a water bath to maintain 37°C.

Room temperature	Normal[1]/~24°C **(A)**	Intense Light[2]/~24°C **(B)**	Dark[3]/~24°C **(C)**
Human body temperature	Normal[1]/37°C **(D)**	Intense Light[2]/37°C **(E)**	Dark[3]/37°C **(F)**

7.3 Results

7.3.1 Phosphorylation of S. mansoni *cercaria PKC, ERK and p38 MAPK is affected by different light and temperature conditions*

Schistosoma mansoni cercariae were exposed to six different combinations (Table 7.1) of light intensity and temperature for 15, 30 and 60 min and processed for western blotting (Figure 7.1). Additionally, cercariae were processed for immunohistochemistry for localization of kinase activation at the durations when significant differences in phosphorylation were observed.

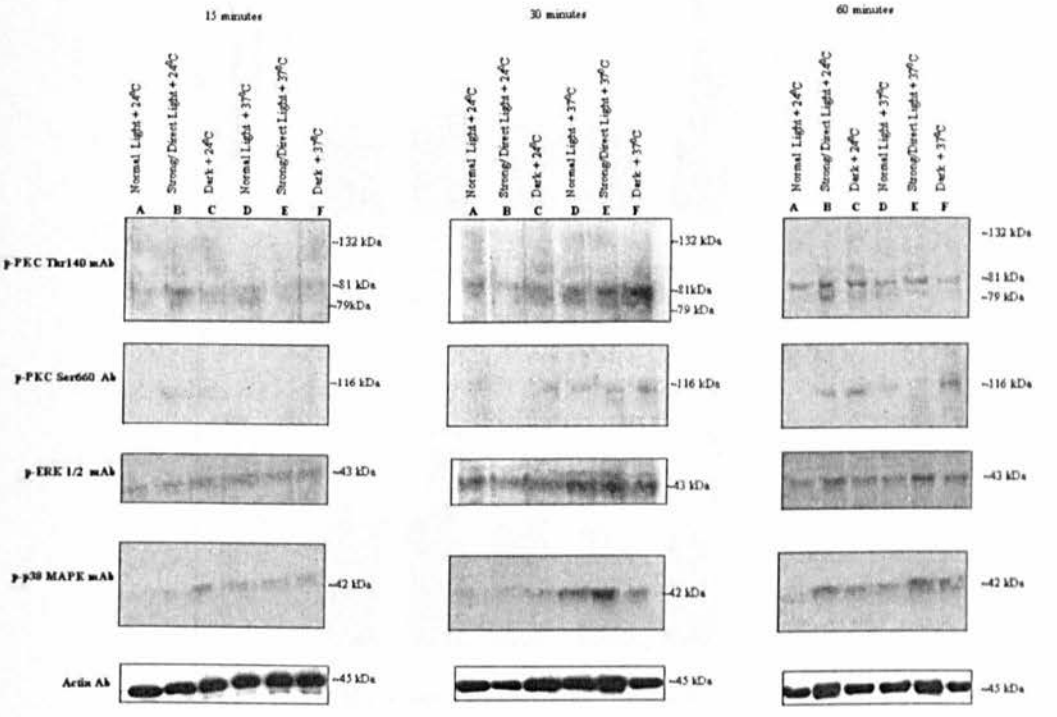

Figure 7.1 - Effect of different temperature and light intensity regimes on PKC, ERK and p38 MAPK phosphorylation in *S. mansoni* cercariae. Western blot showing phosphorylated PKC, ERK and p38 MAPK in *S. mansoni* cercariae maintained for 15, 30 and 60 min at different temperatures and light intensity: (A) natural light, 24°C; (B) intense light, 24°C; (C) dark, 24°C; (D) natural light, 37°C; (E) intense light, 37°C; and (F) dark, 37°C. Cercariae (~1000 per treatment) were homogenized and proteins processed for western blotting with anti-phospho PKC (Thr410), anti-phospho PKC (Ser660), anti-phospho p44/42 MAPK (ERK 1/2), and anti-phospho p38 MAPK antibodies. Blots were also probed with anti-actin antibodies to ascertain protein loading levels. The blots are representative of those from three independent experiments.

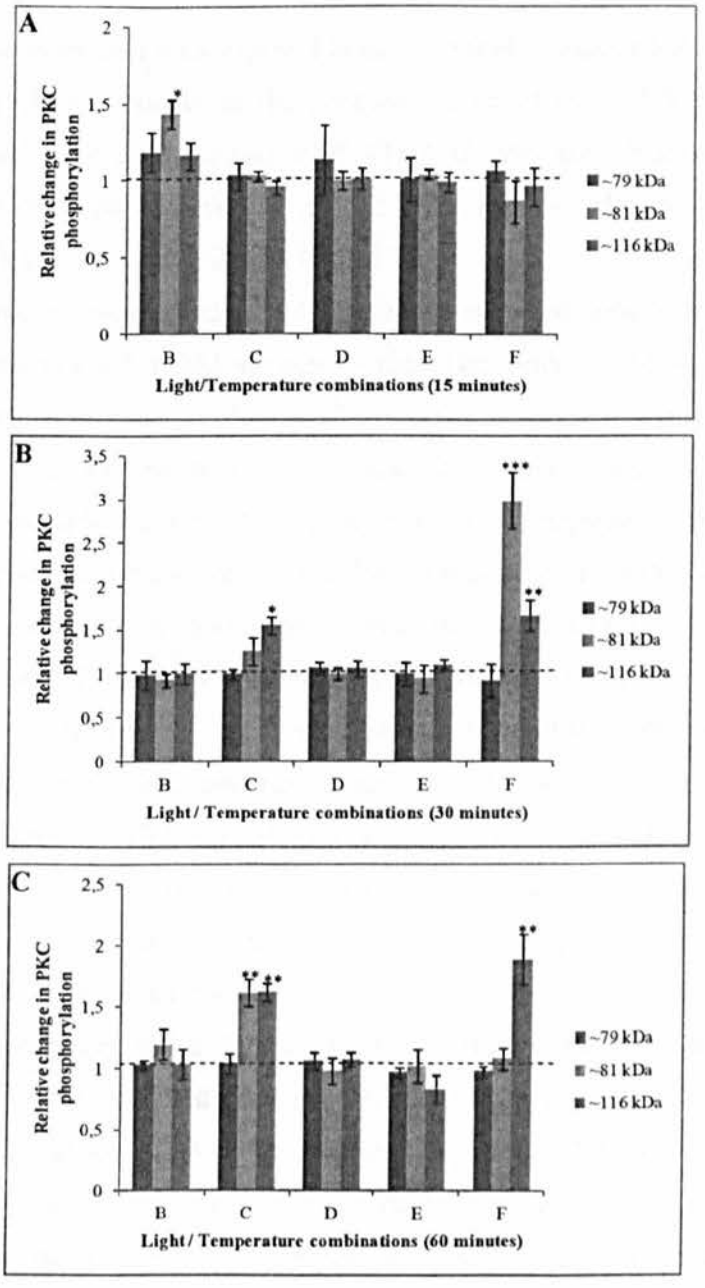

Figure 7.2 - Relative change in PKC phosphorylation in *S. mansoni* cercariae maintained at different temperature and light intensity regimes. Immunoreactive bands on blots obtained from experiments shown in Figure 7.1 were analysed using GeneTools. Panels A, B and C show the relative change in PKC phosphorylation in cercariae maintained for 15, 30 and 60 min, respectively, at different temperatures and light intensities: (B) intense light, 24°C; (C) dark, 24°C; (D) natural light, 37°C; (E) intense light, 37°C; and (F) dark, 37°C. Mean relative change (n=3 blots each; +/- SEM) was determined relative to control values for Treatment A (natural light, 24°C), which was assigned a value of 1 (shown on each graph as a dotted line). Three immunoreactive PKCs were analysed, ~79 kDa, ~81 kDa and ~116 kDa detected with anti-phospho PKC (Thr410) (~79 kDa and ~81 kDa) and anti-phospho PKC (Ser660) (~116 kDa). Values quantified for each band were normalised relative to actin as a loading control. *= $p \leq 0.05$, **= $p \leq 0.01$ and ***= $p \leq 0.001$.

7.3.1.1 PKC activation

Schistosome cercariae exposed to dark, normal or intense light at 24°C or 37°C displayed significant changes in the phosphorylation of the ~81 kDa and ~116 kDa PKCs detected with anti-phospho PKC (Thr410) and anti-phospho PKC (Ser660) antibodies, respectively (Figures 7.1 and 7.2). The phosphorylation of the other PKCs did not significantly change (Figures 7.1 and 7.2).

Relative to control conditions (room temperature and normal light), after 15 min, strong light induced a 1.4-fold increase in phosphorylation of the ~81 kDa PKC only when cercariae were maintained at 24°C (treatment B; $p \leq 0.05$) (Figures 7.1 and 7.2 A); this was transient returning to baseline at 30 min (Figures 7.1 and 7.2 B). Interestingly, phosphorylation of this protein was also triggered by the dark; after 30 min at 37°C phosphorylation increased 3-fold (treatment F; $p \leq 0.001$) (Figures 7.1 and 7.2 B) whereas after 60 min phosphorylation increased 1.6-fold at 24°C (treatment C; $p \leq 0.01$) (Figures 7.1 and 7.2 C). Immunolocalization with anti-phospho PKC (Thr410) antibodies show that these treatments also affected the level and distribution of activated PKCs. When cercariae were maintained under control conditions (normal light intensity and room temperature) PKC activation was mainly associated with dorsal nerve cords, acetabular nerves and the oral sucker (Figure 7.3 A). However, when cercariae were kept under a strong light at room temperature for 15 min activated PKC, likely the ~81 kDa isotype, was associated not only with the acetabular nerves but also the acetabular gland region, tegument and diffusedly distributed throughout the posterior end of the anterior organ where parts of the nervous system are found (Figure 7.3 B). On the other hand, cercariae kept for 30 min in the dark at 37°C displayed phosphorylated PKC also associated with the acetabular nerves and with the sub-tegument (Figure 7.3 C). When cercariae were maintained for 60 min in the dark at 24°C, fluorescence was found associated with the sensory papillae, acetabular gland region, diffusedly distributed throughout the posterior end of the anterior organ, and sometimes the head/tail junction (Figure 7.3 D). These results show that the ~81 kDa PKC, believed to be Smp_096310 aPKC iota type, is stimulated by increased light intensities and by dark, with activation associated with regions of the sub-tegument and structures that are sensory and neurological in nature.

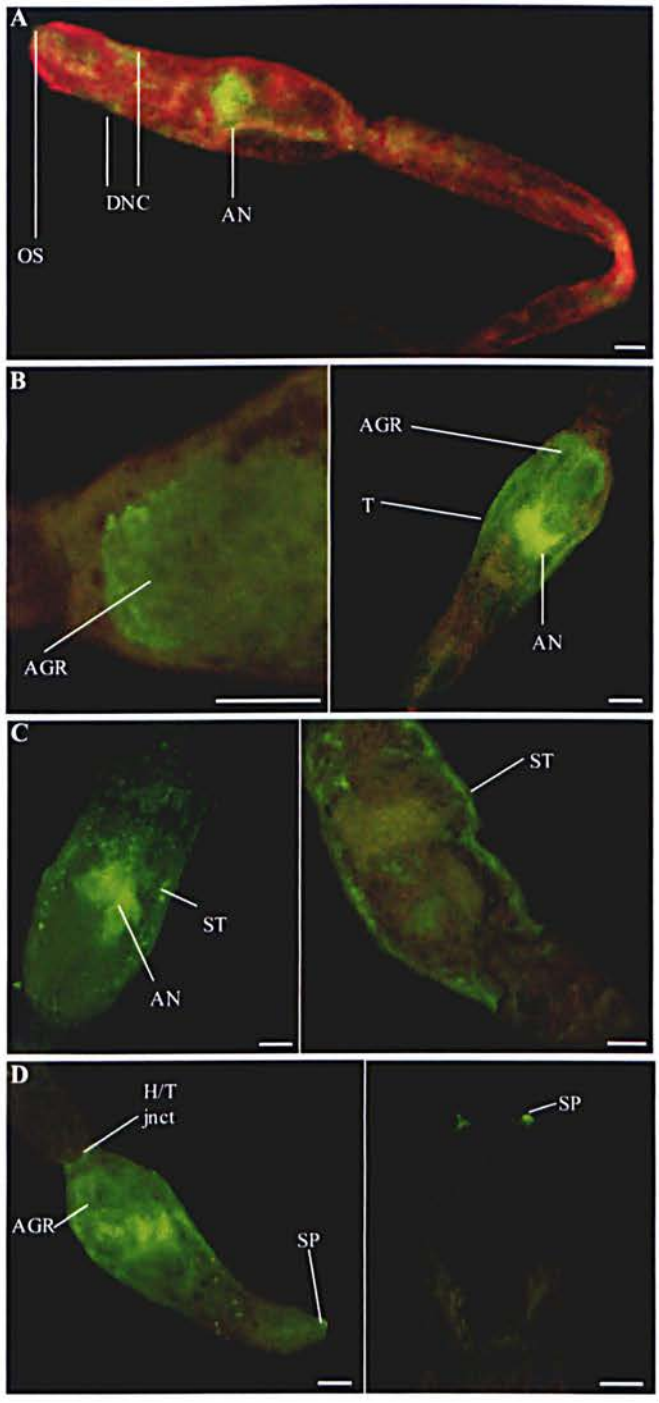

Figure 7.3 - *In situ* localization of activated PKC (Thr410) in *S. mansoni* cercariae maintained in different temperature and illumination conditions. After treatment, cercariae were fixed in acetone and incubated with anti-phospho PKC (Thr410) primary antibodies and Alexa Fluor 488 secondary antibodies (green); actin was stained with anti-actin Cy3 conjugated antibodies (red). Confocal laser scanning microscope fluorescence images of *S. mansoni* cercariae exposed to: (**A**) control conditions (normal light intensity, 24ºC) showing activated PKC mainly associated with the acetabular nerves (AN), oral sucker (OS), and dorsal nerve cords (DNC); (**B**) intense light, 24ºC for 15 min showing activity associated not only with the acetabular nerve (AN) and acetabular gland regions (AGR), but also with the tegumental surface (T); (**C**) dark for 30 min at 37ºC with activated PKC mainly localized with sub-tegument (ST) and acetabular nerve (AN); (**D**) dark for 60 min at 24ºC with PKC activation associated with sensory papillae (SP), acetabular gland regions (AGR) and sometimes the head/tail junction (H/T jnct). Cercariae were photographed with a 40x oil immersion objective; images are maximum projections of ~100 z-sections. Scale bar = 10µm. Results are representative of those observed in cercarial populations from two independent experiments.

Contrary to the ~81 kDa PKC, phosphorylation of the ~116 kDa PKC detected with anti-phospho PKC (Ser660) antibodies does not seem to be affected by strong light. However, dark induced a significant 1.5- to 1.9-fold increase in phosphorylation, at 30 and 60 min at either 24°C or 37°C ($p \leq 0.05$; treatments C and F), with the 1.9-fold increase seen after 60 min at 37°C ($p \leq 0.01$) (Figures 7.1 and 7.2 B and C). *In situ* localization studies with anti-phospho PKC (Ser660) antibodies and control cercariae revealed activated PKC associated with the acetabular gland region, head gland and acetabular nerves (Figure 7.4 A). In the dark for both 30 min and 60 min at either 24°C or 37°C fluorescence was strongly associated with the acetabular gland region and with the sensory papillae located at the tip of the head (Figure 7.4 B).

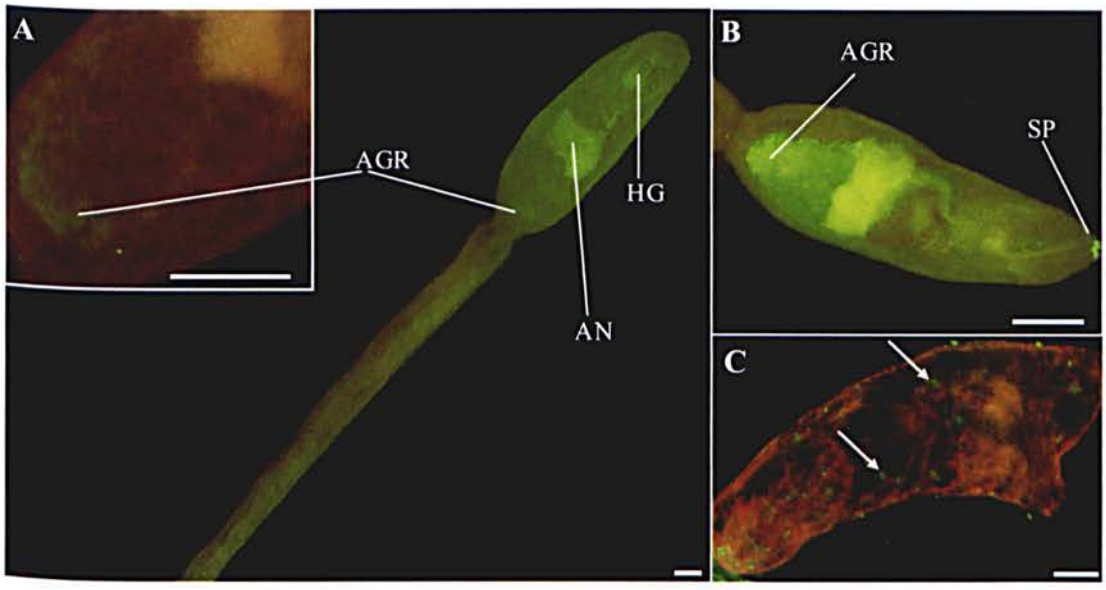

7.4 - *In situ* localization of activated PKC (Ser660) in *S. mansoni* cercariae maintained in different temperature and illumination conditions. After treatment, cercariae were fixed in acetone and incubated with anti-phospho PKC (Ser660) primary antibodies and Alexa Fluor 488 secondary antibodies (green); actin was stained with anti-actin Cy3 conjugated antibodies (red). Confocal laser scanning microscope fluorescence images of *S. mansoni* cercariae exposed to: (**A**) control conditions (normal light intensity, 24°C) with fluorescence associated with the acetabular gland region (AGR), acetabular nerves (AN) and region of the head gland (HG); (**B**) dark for 30 min at 37°C showing areas of PKC activation associated with the acetabular gland region (AGR) and sensory papillae (SP) (although with a different localization pattern compared with control); (**C**) dark for 60 min at 37°C showing areas of PKC activation associated with well defined regions at the surface (arrows). Cercariae were photographed with a 40x oil immersion objective; images are maximum projections of ~100 z-sections. Scale bar =10 µm. Results are representative of those observed in cercarial populations from two independent experiments.

Activated PKC from cercariae in the dark for 60 min at 37°C was sometimes also found in unknown structures at the surface of the head/body (Figure 7.4 C). These structures appeared round and have never been detected by us before, although surface

localization suggests these to possibly be sensory receptors; reports state *S. mansoni* cercariae to have sensory receptors at the surface of the anterior organ and acetylcholinesterase staining in *S. mansoni* cercariae revealed similar structures which were termed sensory papillae (Bruckner and Voge, 1974; Saladin *et al.*, 1982). Because the anti-phospho PKC (Ser660) antibodies largely detect the ~116 kDa PKC (suspected to be cPKC beta type Smp_176360) in cercariae, we assume that the new regions seen due to incubation in the dark are due to ~116 kDa PKC activity.

7.3.1.2 ERK activation

The phosphorylation of the ~43 kDa ERK was only significantly stimulated at 30 min and only when cercariae were kept at 37°C; this was independent of light intensity (Figures 7.1 and 7.5 B, treatments D-F). Immunoblots showed that activation increased 2-fold under normal illumination ($p \leq 0.001$), 1.8-fold under intense illumination ($p \leq 0.01$) and 1.6-fold in dark ($p \leq 0.01$) compared to the normal illumination treatments at room temperature, or to the same illumination conditions at 24°C (Figures 7.1 and 7.5 B). *In situ* localisation revealed that when compared to control (24°C and normal light; Figure 7.6 A) samples, cercariae maintained for 30 min at 37°C under normal light conditions showed an apparent increase in fluorescence associated with the acetabular gland region, sensory papillae, acetabular tubules, and flame cells (Figure 7.6 B). Whereas cercariae kept at 37°C for 30 min under intense light showed an increase in activation associated with the tegumental surface, acetabular gland region, the peripheral nervous system of the head/body region, sensory receptor–like structures other undefined structures localized in the tail, and sensory papillae localized at the oral sucker (Figure 7.6 C). Cercariae maintained in the dark at 37°C for 30 min showed fluorescence associated with the nerve cord in the tail extending up to the head/tail junction, flame cells, acetabular glands, sensory papillae and the surface of acetabular tubules where nervous structures are known to exist and the ventral sucker or acetabulum (Figure 7.6 D).

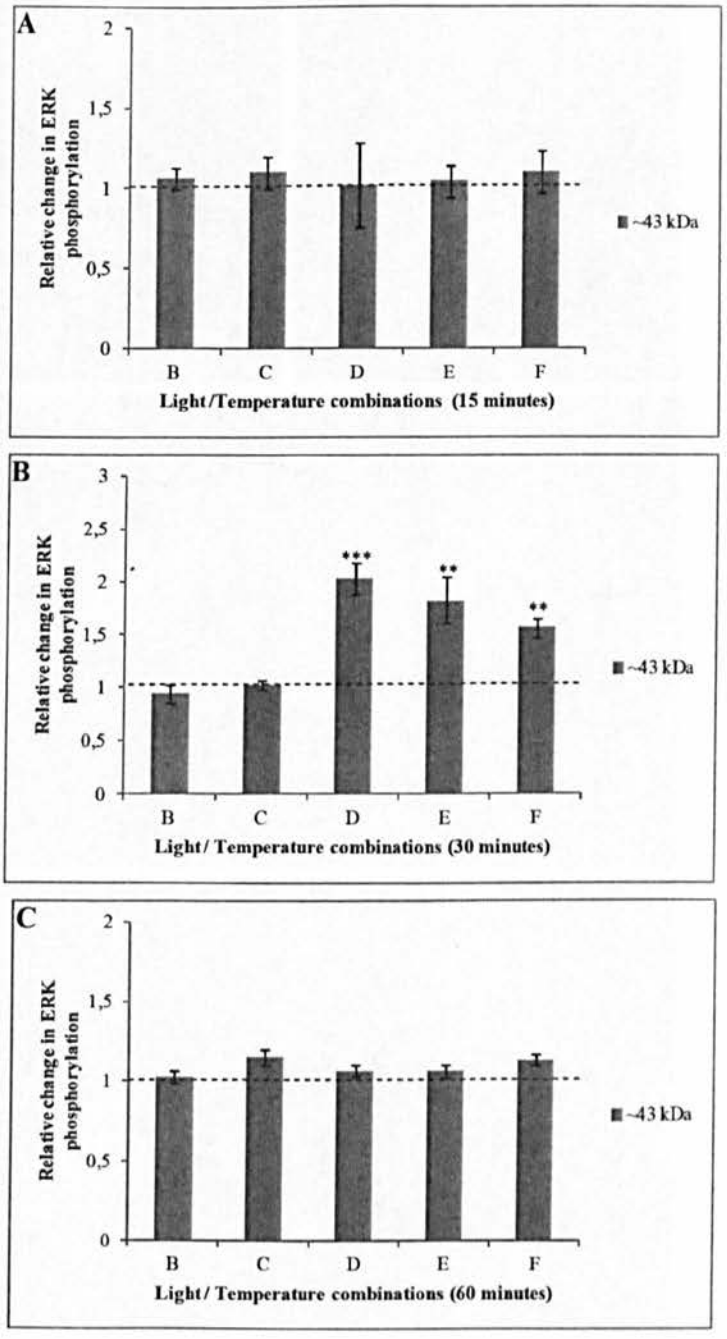

7.5 - Relative change in ERK phosphorylation of *S. mansoni* cercariae maintained at different temperature and light intensity regimes. Immunoreactive bands on blots obtained from experiments shown in Figure 7.1 were analysed using GeneTools. Panels (**A**), (**B**) and (**C**) show the relative change in ERK phosphorylation in cercariae maintained for 15, 30 and 60 min, respectively, at different temperature and light intensities: B - intense light, 24°C; C - dark, 24°C; D - natural light, 37°C; E - intense light, 37°C; and F - dark, 37°C. Mean relative change (n=3 blots each; +/- SEM) was determined relative to control values for Treatment A (natural light, 24°C), which was assigned a value of 1 (shown on each graph as a dotted line). Values quantified for each band were normalised relative to actin as a loading control. **= $p \leq 0.01$ and ***= $p \leq 0.001$.

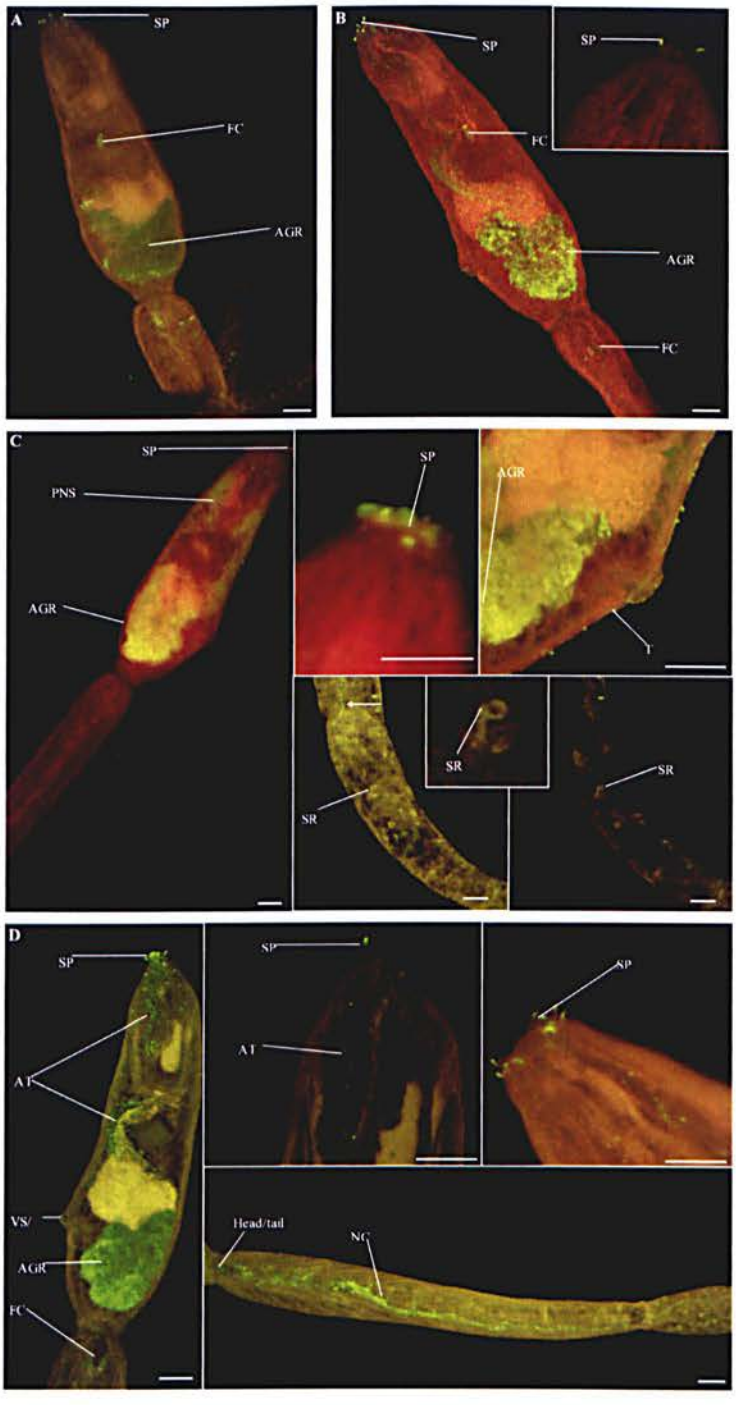

Figure 7.6 - *In situ* localization of activated ERK in *S. mansoni* cercariae maintained in different temperature and illumination conditions. After treatment, cercariae were fixed in acetone and incubated with anti-phospho p44/42 MAPK primary antibodies and Alexa Fluor 488 secondary antibodies (green); actin was stained with anti-actin Cy3 conjugated antibodies (red). Confocal laser scanning microscope fluorescence images of *S. mansoni* cercariae exposed to: (**A**) control conditions (normal light intensity, 24°C) with activated ERK in sensory papillae (SP), flame cells (FC) and acetabular gland region (AGR); (**B**) normal light at 37°C for 30 min, with activity similarly distributed to that of controls; (**C**) 37°C under intense illumination for 30 min with activity associated with sensory papillae (SP), sensory receptor (SR) at the tail, tegumental surface (T), in specific regions on the tail (arrow), peripheral nervous system (PNS) and acetabular gland region (AGR); (**D**) dark at 37°C for 30 min, with ERK activation associated with the sensory papillae (SP), acetabular tubules (AT), ventral sucker (VS), acetabular gland region (AGR), and tail structure that is likely the nerve cord (NC). Cercariae were photographed with a 40x oil objective; images are maximum projections of ~100 z-sections. Scale bar = 10 μm. Results are representative of those observed in cercarial populations from two independent experiments.

7.3.1.3 P38 MAPK activation

The phosphorylation of p38 MAPK also changed when cercariae were maintained under different light/temperature conditions. After 15 min, p38 MAPK activity significantly increased only when cercariae were exposed to the dark at 24°C (1.5-fold, $p \leq 0.05$) (Figures 7.1 and 7.7 A). However at 30 min, activation increased with incubation at 37°C irrespective of light regime, displaying ~1.5-fold ($p \leq 0.05$), ~1.8-fold ($p \leq 0.05$), and ~1.5-fold ($p \leq 0.05$) increases in normal light, intense light or dark, respectively (Figures 7.1 and 7.7 B). At 60 min, p38 MAPK remained stimulated at 37°C but only when cercariae were kept in the dark ($p \leq 0.05$) (Figures 7.1 and 7.7 C). Immunolocalization revealed activated p38 MAPK in control cercariae associated weakly associated with the acetabular gland region, sometimes with the sensory papillae, head gland and flame cells (Figure 7.8 A). At 15 min in the dark at 24°C pronounced fluorescence was associated with the acetabular gland region and sensory papillae (Figure 7.8 B). Cercariae maintained at 37°C in either normal light or dark showed activated p38 MAPK mainly associated with sub-tegumental regions and acetabular gland region but not with the sensory papillae at the tip of the oral sucker (Figure 7.8 C). When cercariae were maintained at 37°C under intense light active p38 MAPK was associated with the head and tail tegument, sensory papillae, flame cells, acetabular tubules and structures at the surface which have not yet been identified but are suspected to have a sensory or excretory function (Figure 7.8 D). Results therefore show that the most prominent changes in p38 MAPK activation were observed under a thermokinetic environment of 37°C and negative photokinetic environment (dark) for 30 min, with activity mainly associated with the tegument and sensory papillae.

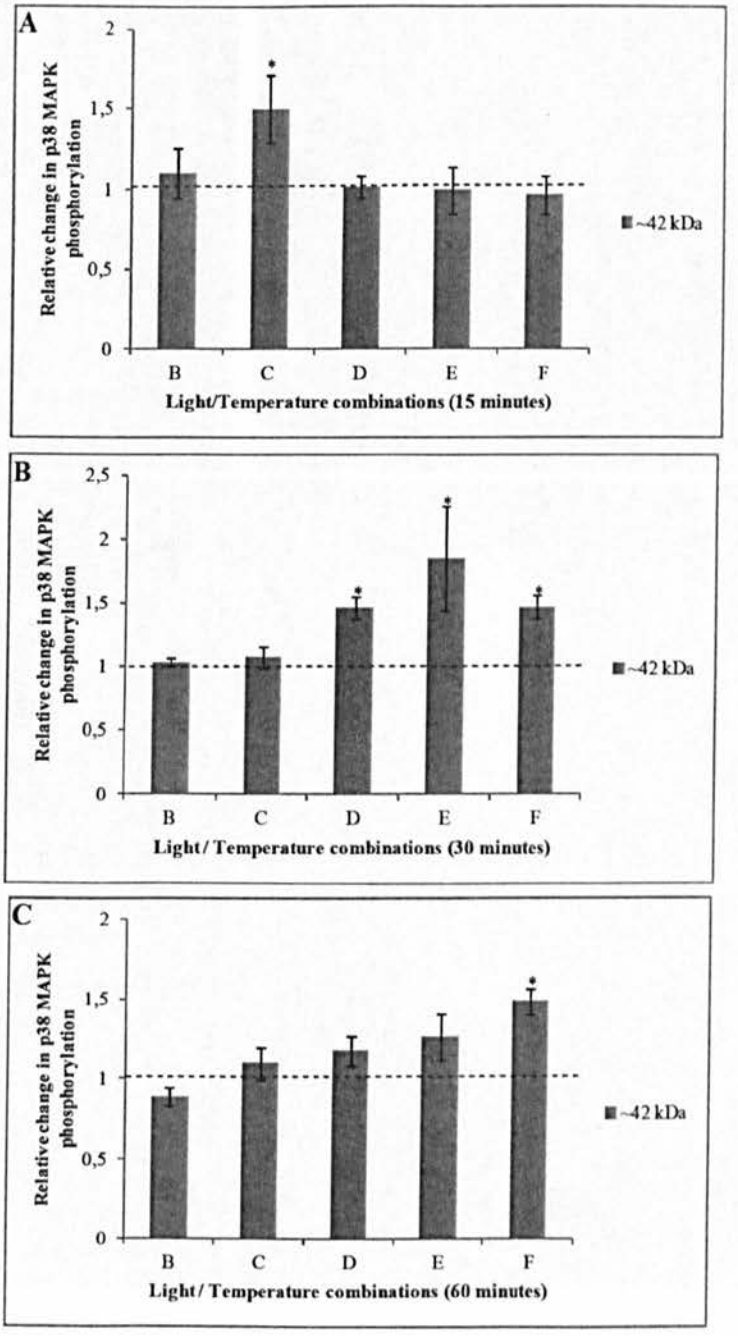

Figure 7.7 - Relative change in p38 MAPK phosphorylation of *S. mansoni* cercariae maintained at different temperature and light intensity regimes. Immunoreactive bands on blots obtained from experiments shown in Figure 7.1 were analysed using GeneTools. Panels (**A**), (**B**) and (**C**) show the relative change in ERK phosphorylation in cercariae maintained for 15, 30 and 60 min, respectively, at different temperature and light intensities: B - intense light, 24°C; C - dark, 24°C; D - natural light, 37°C; E - intense light, 37°C; and F - dark, 37°C. Mean relative change (n=3 blots each, +/- SEM) was determined relative to control values for treatment A (natural light, 24°C), which was assigned a value of 1 (shown on each graph as a dotted line). Values quantified for each band were normalised relative to actin as a loading control. Immunoreactivity values were quantified for each band and normalised with the respective actin detection. *= $p \leq 0.05$.

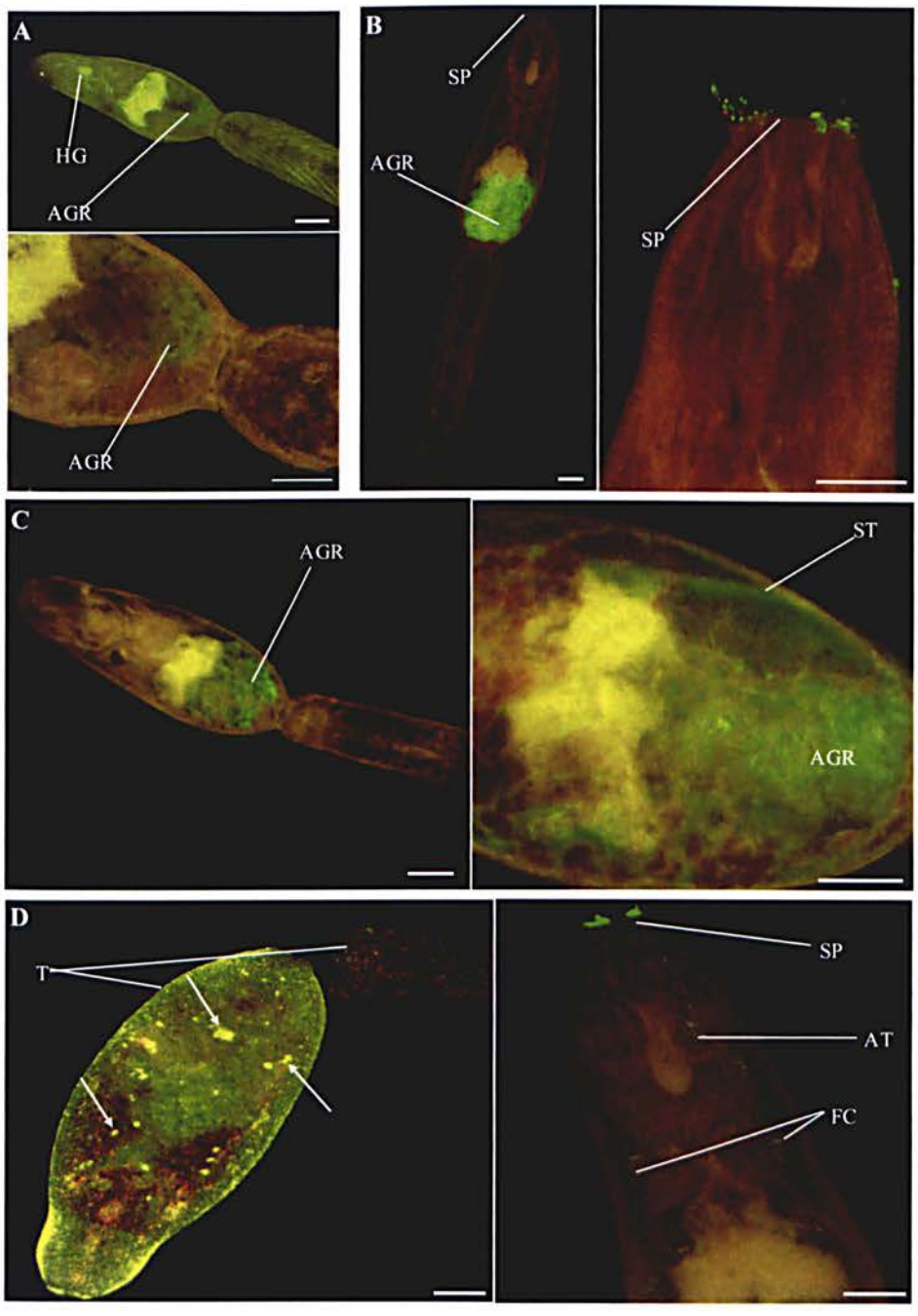

Figure 7.8 - *In situ* localization of activated p38 MAPK in *S. mansoni* cercariae maintained in different temperature and illumination conditions. After treatment, cercariae were fixed in acetone and incubated with anti-phospho p38 MAPK primary antibodies and Alexa Fluor 488 secondary antibodies (green); actin was stained with anti-actin Cy3 conjugated antibodies (red). Confocal laser scanning microscope fluorescence images of *S. mansoni* cercariae exposed to: (**A**) control conditions (normal light intensity, 24°C) with activated p38 MAPK mainly associated with the head gland (HG) and acetabular gland region (AGR); (**B**) dark for 15 min at 24°C with pronounced fluorescence in the acetabular gland region (AGR) and sensory papillae (SP); (**C**) 37°C in normal light or dark conditions showing p38 MAPK activity mainly associated with the sub-tegument (ST) and acetabular gland region (AGR); (**D**) 37°C in intense light with activation associated with the tegument surface (T), sensory papillae (SP), flame cells (FC), acetabular tubules (AT) and surface structures which have not yet been identified (arrows). Cercariae were photographed with a 40x oil immersion objective; images are maximum projections of ~100z-sections. Scale bar = 10 μm. Results are representative of those observed in cercarial populations from two independent experiments.

7.3.2 Effects of light intensity on the phosphorylation of PKC, ERK and p38 MAPK from the detached tails of cercariae

When *S. mansoni* cercariae are mechanically transformed into schistosomules (Chapter 2) tail detachment from the head occurs. It was observed that the detached tails continued contractile movements independent of the head/body and were responsive to increases in light intensity (increasing rate of tail movement). In light of this phenomenon, which to our knowledge has never been reported in the literature, a simple experiment was designed. Detached tails were exposed to intense illumination for 1 min or placed in the dark and the phosphorylation status and localization of PKC, ERK and p38 MAPK investigated. The phosphorylation status of ERK and PKC was found to be altered by increased light. The ~81 kDa PKC displayed a 1.9-fold increase in phosphorylation ($p \leq 0.001$) (Figures 7.9 A and B) and under intense light activated PKC mostly localized within the tegument, sub-tegumental region associated with the musculature of the tail, structures which resemble myocytes, and other structures with unknown identity but suspected neurosensory function (Figure 7.10). Phosphorylation of the ~43 kDa ERK increased 2.2-fold ($p \leq 0.001$) when tails were exposed to intense light (Figures 7.9 A and B). Activated ERK was found associated with regions at the surface of the tail and within structures which resemble sensory receptors and myocytes (Figure 7.11). No significant changes in the activity of p38 MAPK and the ~79 kDa, ~116 kDa or ~132 kDa PKC proteins were observed (data not shown).

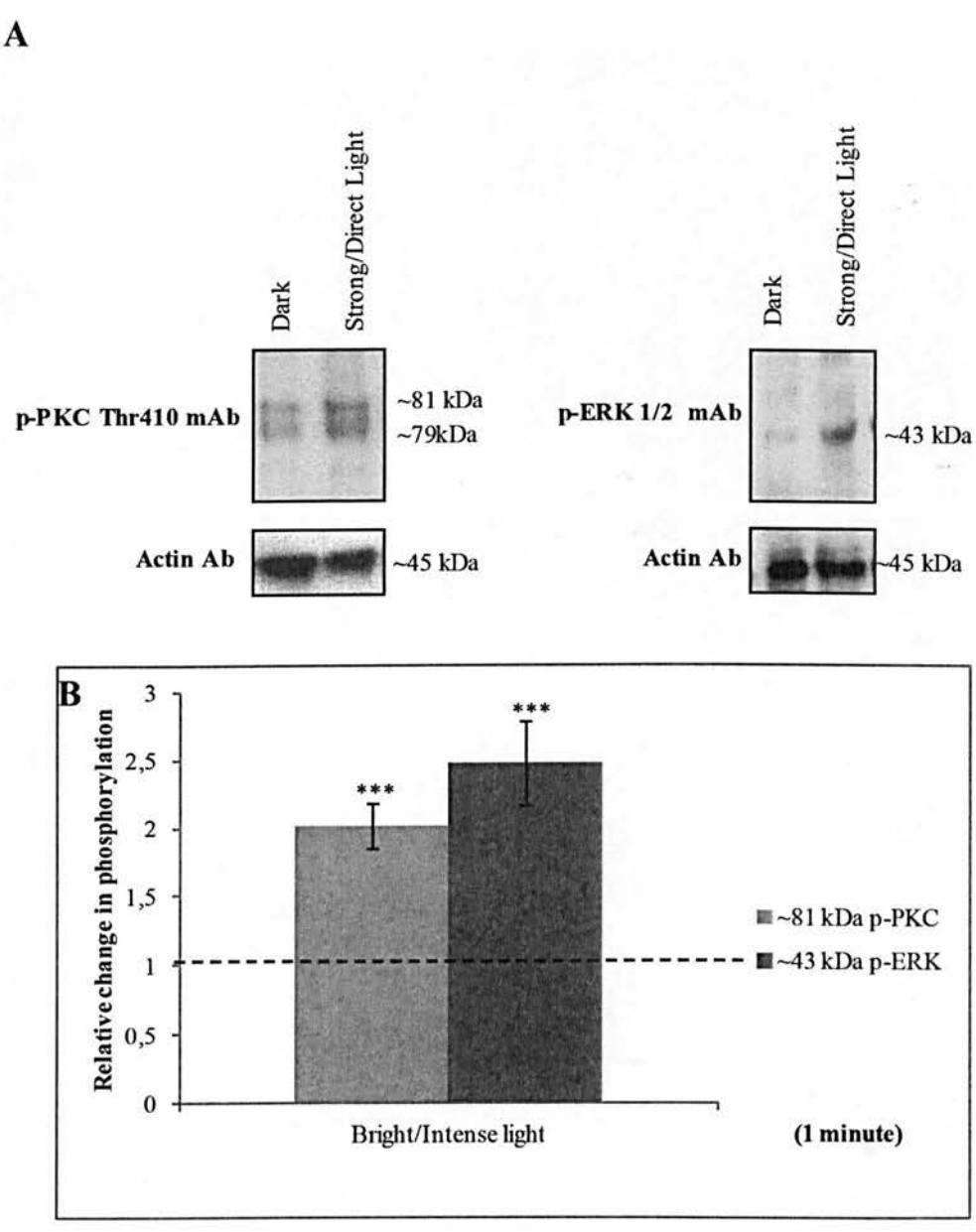

Figure 7.9 - Immunodetection of PKC and ERK phosphorylation in cercariae tails maintained in the dark or under intense illumination for 1 min. (**A**) Western blot of phosphorylated PKCs and ERKs detected with anti-phospho PKC (Thr410)/anti-phospho PKC (Ser660), and anti-phospho p44/42 MAPK antibodies, respectively, obtained from detached cercariae tails maintained in the dark or under intense/strong illumination for 1 min. Immunoreactive bands were quantified using GeneTools and the mean increase in phosphorylation (n=6; +/- SEM) for (**B**) PKC, and (**C**) ERK, quantified with respect to levels seen in tails maintained in the dark that were assigned a value of 1 (shown as the dotted line). Blots are representative of two independent experiments each with three replicates. ***= $p \leq 0.001$.

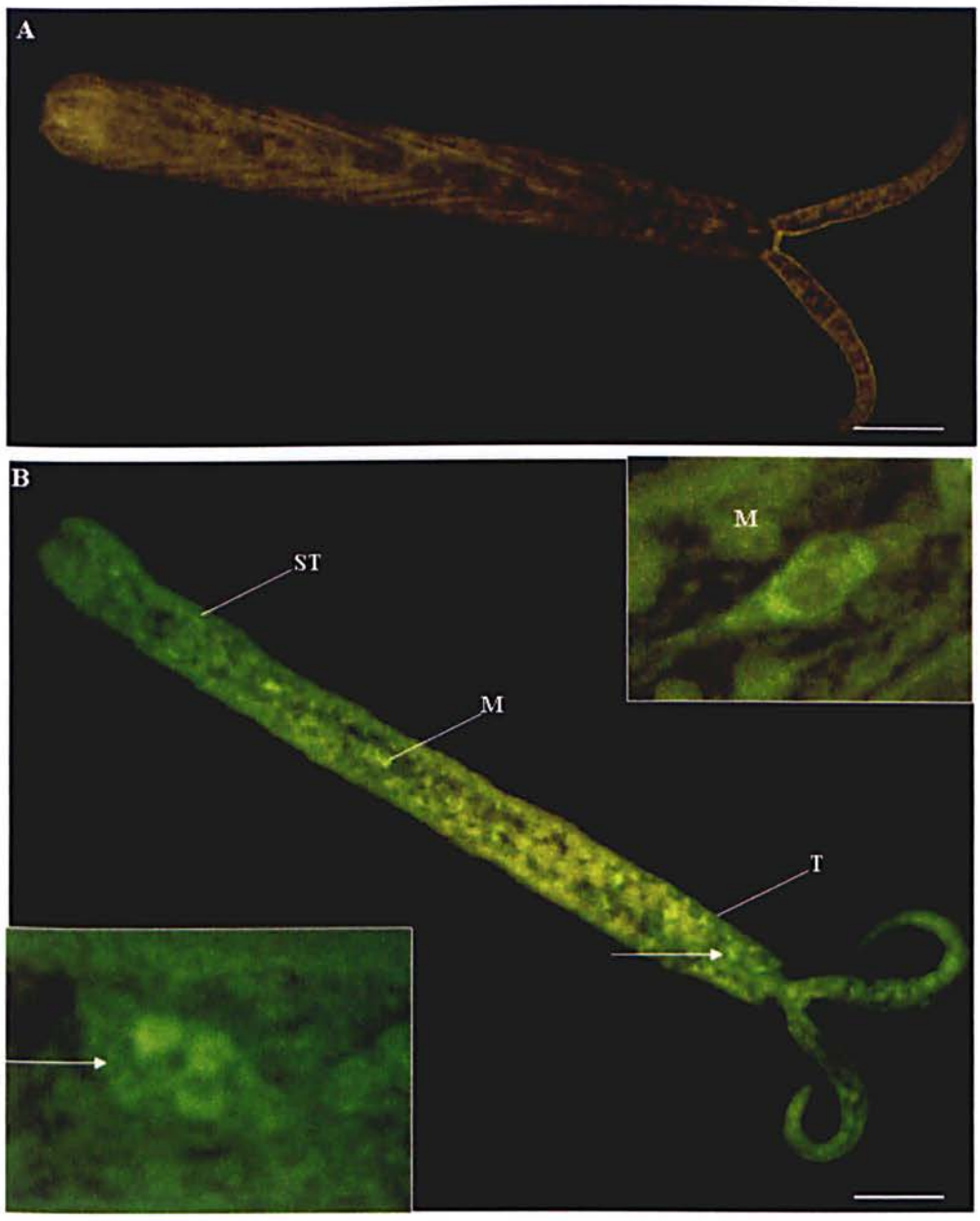

Figure 7.10 - *In situ* localization of phosphorylated PKC in detached *S. mansoni* cercariae tails maintained in the dark or under intense illumination for 1 min. After treatment, tails were fixed in acetone and incubated with anti-phospho PKC (Thr410) primary antibodies and Alexa Fluor 488 secondary antibodies (green); actin was stained with anti-actin Cy3 conjugated antibodies (red). Panel (**A**) detached tail kept in the dark for 1 min. Panel (B) detached tail kept in intense light for 1 min; showing green fluorescence associated with the tail surface (TS), sub-tegument (ST), myocytes (M) and structure with unknown identity but suspected neurosensory function (arrows). Tails were photographed with a 40x oil immersion objective; images are maximum projections of ~40 z-sections. Scale bars =10 μm. Results are representative of those observed from two independent experiments.

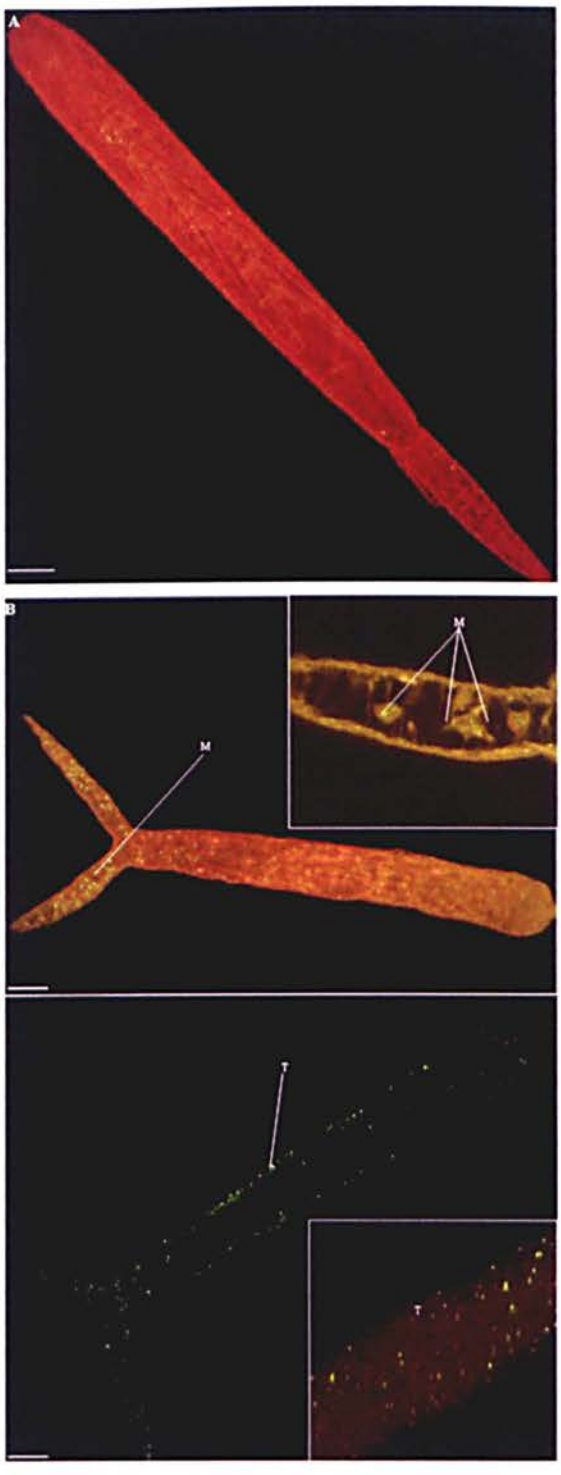

Figure 7.11 - *In situ* localization of phosphorylated ERK in detached *S. mansoni* cercariae tails maintained in the dark or under intense illumination for 1 min. After treatment, tails were fixed in acetone and incubated with anti-phospho PKC (Thr410) primary antibodies and Alexa Fluor 488 secondary antibodies (green); actin was stained with anti-actin Cy3 conjugated antibodies (red). Panel (**A**) detached tail kept in the dark for 1 min. Panel (**B**) detached tails exposed to intense light for 1 min showing fluorescence associated with the tegumental surface (T) and myocytes (M). Tails were photographed with a 40x oil immersion objective; images are maximum projections of ~40 z-sections. Scale bar = 10 μm. Results are representative of those observed from two independent experiments.

7.4 Discussion

The behaviour of *S. mansoni* cercariae and schistosomules is tuned by environmental cues such as changes in temperature and light intensity but the molecular mechanisms involved in synchronizing/transducing the stimulus-responses remain unknown. Given the numerous sensory structures present in *S. mansoni* cercariae, the possible involvement of PKC, ERK or/and p38 MAPK in photo- and thermo-sensation of *S. mansoni* cercariae was investigated.

7.4.1 Activated PKC ERK and p38 MAPK are associated with sensory papillae

In control conditions (24°C and normal light), activated PKC, ERK and p38 MAPK were associated with the sensory papillae present in the anterior organ at the tip of the oral sucker of *S. mansoni* cercariae. Moreover, activation of these kinases at these papillae appeared to be differentially induced by different temperature and light intensity combinations suggesting a complex effect of photo and thermal stimuli. Sensory papillae are terminals or nerve processes located at the surface of the cercariae that contact the environment, either by cilia or through openings in the tegument (Short and Cartrett, 1973; Short and Gagne 1975; Dorsey and Cousin, 1986; Dorsey *et al.*, 2002). According to Short and Cartrett (1973), many of these papillae are localized on the oral tip, mid body section, and tail of *S. mansoni* cercariae however they tend to be less numerous on the tail. Unfortunately, the function of these papillae is unknown but they are thought to have a photo-, mechano-, thermo- and/or chemo-receptive nature (Dorsey *et al.*, 2002). It is difficult to define if these papillae are involved in detecting a specific stimulus or a wider array, especially as kinase activation at these structures occurred at different temperature/light intensity combinations. Also, given that the oral tip is one of the first organs to contact the host and that activated PKC also associates with these structures in response to LA (Chapter 6), it seems likely that these papillae respond to more than one stimulus and that various signalling molecules are involved in sensory transduction.

Additionally, it is important to note that activation of such signalling pathways can lead to changes in gene expression which might be important to the transformation of cercariae to parasitic schistosomules; these kinases are crucial for eukaryotic cell function with known roles in control of proliferation, growth, and differentiation

(Chong *et al.*, 2003). It is known that increased p38 MAPK activity induces transformation of *S. mansoni* miracidia to mother sporocysts, *in vitro* (Ressurreição *et al.*, 2010b) and an ERK-like protein has been implicated in the growth rate of *T. brucei* (Ellis *et al.*, 2004). Also, PKC controls metamorphosis of the sea urchin *S. purpuratus* (Amador-Cano *et al.*, 2006). Activated PKC, ERK and/or p38 MAPK observed in the current study could therefore be associated with triggering development to schistosomules.

7.4.2 Activity of ~81 kDa PKC is stimulated by photokinetic and thermokinetic changes

At 24°C, the PKC detected with anti-phospho PKC (Thr410) antibodies, believed to be Smp_096310 aPKC ι-type (Chapter 3), is transiently stimulated by intense light at 15 minutes (positive photokinesis) and dark (negative photokinesis) at 60 minutes. At 37°C, this response to dark is seen earlier, appearing at 30 minutes. This PKC activity was associated with organs of cercariae with suspected sensory and neurological function. For instance, activated PKC was not only evident in the sensory papillae at the oral tip but was also found associated with the surface and subtegumental regions of the anterior body in areas similar to the central nervous system of *S. mansoni* cercariae previously detected with anti-synapsin antibodies (Collins *et al.*, 2011). In *C. elegans*, PKC associates with the nervous system and is considered a major regulator of the activity of various sensory neurons (Okochi *et al.*, 2005). Interestingly, in *Drosophila*, PKC activity is required for light adaptation, which allows photoreceptors to adjust their sensitivity over a wide range of ambient light intensities (Shapley and Enroth-Cugell, 1984; Hardle *et al.*, 1993). The *Drosophila inaC* gene which encodes a photoreceptor-specific PKC is required for light adaptation and normal desensitization to background illumination (reviewed by Yarfitz and Hurley, 1994) and PKC-deficient *Drosophila* are able to learn without performance which is often assumed to be a prerequisite for task learning (Kane *et al.*, 1997). Therefore, the ~81 kDa PKC could perhaps be involved in light adaptation by *S. mansoni* cercariae as it was activated at 15 minutes under bright illumination at 24°C, acting to desensitise the cercariae to the constant bright light. Results also suggest association of PKC with negative photokinesis, as PKC activity increased with maintenance in the dark for 30 and 60 minutes). Under these conditions activated PKC was mostly localized in the nervous system and sensory papillae. Ciliary lamellate bodies respond only to decreased

illumination, representing the "off" response, or shadow response. Such ciliary bodies have been found in the anterior body region of *S. mansoni* cercariae and are morphologically similar to ciliary structures in the gastropod *Onchidium* and the bivalve *Cardium*, which are both concerned with shadow responses (Short and Gagné, 1975).

Interestingly, in mice PKC is implicated in bio-clock regulation indicating that light and darkness exert a strong regulatory influence on PKC synthesis, activation, and transport in retinal neurons (Schak and Harrington, 1999; Gabriel *et al.*, 2001). In mammals, light is received by rhodopsin, which in turn activates Gα and phosphodiesterase, leading to closure of a cGMP-gated cation channel, which in turn could activate the PKC/MAPK signalling (Ebrey and Koutalos, 2001). Photoreceptors similar to rhodopsin, and phosphodiesterase, exist in *S. mansoni* cercariae (Santos *et al.*, 1999), supporting the hypothesis that PKC is involved in photo-sensation by cercariae. PKC could be involved in the cercarial circadian rhythm, important for emergence of cercariae from the tissues of the snail host, which only happens when snails, and possibly cercariae (as the snail tissues are partially transparent) are exposed to light.

The increased PKC activity associated with subtegumental regions when cercariae were maintained for 30 minutes in the dark at 37°C might be important to initiating transformation whereby the surface undergoes remodelling; membrane transport activity and endocytosis is increased at 37°C (Ribeiro *et al.*, 1998; Thornhill *et al.*, 2010). Activated PKC was also found at the head/tail junction, a site of separation during host penetration. The mechanism by which the tail is detached from cercariae is not understood, however the popular theory is that the physical process of the cercariae passing through the skin causes tail release. This is corroborated with the fact that vortexing or syringe passaging causes tail detachment. At Kingston we have found that incubating cercariae at 37°C before vortexing leads to faster and more effective tail detachment (data not shown), and a mixture of unsaturated fatty acids is known to trigger cercarial tail release by possibly enhancing calcium influx (Hara *et al.*, 1993). Hara *et al.* (1993), used the PKC inhibitor H-7 in an attempt to prevent tail loss however little effect was observed, suggesting that PKC was not involved in tail detachment. Importantly, however, Hara *et al.* (1993) did not pre-incubate cercariae with H-7 and only added it at the same time as fatty acids were added to stimulate release. Therefore, further experiments need to be performed to elucidate whether or not PKC plays a role in cercarial tail detachment.

7.4.3 Activity of ~116 kDa classical PKC is mainly stimulated by dark conditions (negative photokinesis)

Activity of the ~116kDa PKC, suspected to be cPKC β-type Smp_176360 (Chapter 3), was stimulated when cercariae were maintained for 30 or 60 minutes in the dark regardless of temperature. Under these conditions, activated PKC was often associated with sensory papillae localized at the oral tip and a new set of suspected sensory papillae at the surface of the anterior body region, a unique localization pattern which was not found with any of the other kinases studied here. This reveals the likely involvement of this PKC in photo-perception. The staining pattern observed with the anti-phospho PKC (Ser660) antibodies in structures at the surface of the cercarial anterior organ when cercariae were in darkness is similar to that obtained with acetylcholinesterase staining of cercariae, which stained sensory papillae at the anterior surface of the head/body (Bruckner and Voge, 1974). Interestingly, Short and Gagné (1975) identified, using electron microscopy, two ciliary photoreceptor-like structures near the head of *S. mansoni* cercariae that the authors suggested were involved in the cercarial inverse photokinesis. Subsequently, it was demonstrated that in invertebrates, cilliary photoreceptors are commonly associated with negative photokinesis (Saladin *et al.*, 1992; Santos *et al.*, 1999). Therefore, activated PKC might be associated with such ciliary receptors. In the photoreceptor of the horseshoe crab *Limulus polyphemus*, PKC inhibits the phototransduction cascade (Dabdoub and Payne, 1999). Perhaps PKC is active at later stages in the dark to prevent positive photokinesis. Light adaptation (ability of rapid transition from peak to plateau following a onset of bright light) of *Drosophila* is severely reduced by null PKC mutants where PKC is thought to be required to terminate the light-induced negative feedback process mediated by rise in cytosolic Ca^{2+} (Hardle *et al.*, 1993).

Furthermore, increased ~116 kDa PKC activation was also associated with the acetabular gland region. PKC activity in this region could be related to acetabular gland function as detailed in Chapter 6. For cercariae penetrating the host, temperature rise from ambient to 37°C coupled with darkness would, in natural conditions, be paired with a host-derived chemical stimulus (skin unsaturated fatty acids) (Chapter 6; Haas, 1994); thus interactions will be complex.

7.4.4 P38 MAPK and ERK are involved with positive thermokinesis by cercariae

At 24°C p38 MAPK activation was only enhanced when cercariae were in the dark for 15 minutes, returning to basal thereafter. However, at 37°C normal, high light intensity, and dark stimulated activity at 30 minutes; whereas at 60 minutes only dark stimulated p38 MAPK activity. Thus at 15 minutes, temperature rise does not impact p38 MAPK activity and this is only observed after 30 minutes. Darkness always affects p38 MAPK activity in cercariae with different temporal kinetics; therefore seems to respond in a way which is negatively photokinetic (stimulated by dark) and positively thermokinetic (temperature rise to 37°C). Activated p38 MAPK was mainly associated with sensory papillae at the oral sucker and acetabular gland region.

When cercariae were maintained at 37°C, ERK activity was also stimulated regardless of light condition, supporting the involvement of ERK in cercarial thermo-sensory behaviour and positive thermokinesis. Under these conditions ERK activation was mainly associated with the walls of the acetabular tubule/collecting ducts, sensory papillae at the tip of the anterior organ, acetabular gland region and longitudinal nerve cord. This supports a role for ERK in neurotransmission processes linked to thermosensation. Interestingly, in most parasitic nematodes the thermosensory organs are found in the tip of the organisms' head immediately adjacent to the mouth (Ashton and Schad, 1999).

The circuit components required to transform thermal information into defined behavioural responses remain unclear in invertebrates, but recently PKC and ERK have been implicated in *C. elegans* mechanosensory response (Hyde *et al.* 2011). Here it is shown that the *S. mansoni* MAPK family members, ERK and p38 MAPK, seem to be involved in thermosensation mainly at 30 minutes. Of the six different sensory receptors present in cercariae, some of which are only in the head/body (Dorsey *et al.*, 2002), it is likely that a number sense and transport thermal information to these kinase pathways.

7.4.5 PKC and ERK are involved in cercarial tail photokinesis

PKC and ERK phosphorylation increased in detached cercariae tails when briefly exposed to intense light (1 minute) when compared to tails kept in the dark. Activated PKC/ERK were associated with structures of neuromuscular nature (myocytes), and structures that span the tegument and sub-tegument likely to be sensory receptors. These findings reveal that PKC and ERK are involved in photo transduction by the *S. mansoni* cercarial tail. The tail is a highly specialized organ that provides

motility to the cercaria during its free-living existence in water. The tail is packed with myocytes, neurons, osmoregulatory cells and supporting cells. Myocytes are organized in an inner longitudinal, sub-tegumental and three outer circular muscle layers that form the tail musculature (Dorsey *et al.*, 2002). The tail is packed with large mitochondria, large numbers of ribosomes and glycogen (Dorsey *et al.*, 2002). PKC signalling was found to be interconnected with ERK signalling in adult worms (Chapter 4)

The distribution pattern of phosphorylated ERK observed in tails exposed to intense light is similar to that seen in tails stained for acetylcholinesterase, which stained the sensory papillae on the cercarial tail (Bruckner and Voge, 1974). The increased movement of detached tails when exposed to intense light (positive photokinesis) and coincident increased ERK and PKC activity, likely result from light absorption by nerves, tail muscle and other tissues (Saladin, 1982). Dorsey *et al.* (2002) found "uniciliated sheathed papillae" and "uniciliated unsheathed papillae" in *S. mansoni* cercariae tails by electron microscopy. Although the function of these receptors is unknown in cercariae, these types are expected to be involved in mechano-reception (Bogéa and Caira, 2001; Bogéa, 2004). Localization of activated PKC and ERK to the myocytes of *S. mansoni* cercarial tails supports a role in tail contractile movement. This could also be pivotal to the emergence of cercariae from the tissues of *B. glabrata* perhaps by light activating PKC and ERK which in turn activating muscle contraction through a neuro-sensory-motor system.

7.4.6 Conclusions

PKC, ERK and p38 MAPK activation was significantly affected by different light conditions and temperatures and was localized within tissues with neuronal and sensory function demonstrating the complexity of cercarial sensory signal transduction mechanisms. Further comprehensive studies on the regulation of *S. mansoni* cercariae thermotaxis and phototaxis would be beneficial for understanding the molecular mechanisms of cercariae behaviour and the stimulus response. It would be of interest to further investigate PKC, ERK and p38 MAPK signalling during different light and temperature conditions over broader durations, in combination with skin components, and with other signalling molecules.

Chapter 8

Investigation of PKC and MAPK signalling during *in vitro* development of *S. mansoni* schistosomules

8.1 Introduction

The first major morphological change that occurs during schistosome infection of the definitive host is the loss of the glycocalyx attached to the cercarial membrane and replacement of the trilaminate surface to a heptalaminate tegument; this transformation is usually complete three hours post infection (Hockley and McLaren, 1973; Payares *et al.*, 1985a; Blanton *et al.*, 1987). At this point, the new double lipid bilayered tegument represents the point of interaction between the parasite and host. Membrane components are incorporated into the surface by fusion of cytoplasmic multilaminate vesicles (Hockley and McLaren, 1973) and this surface remodelling alters the membrane permeability accompanied by many biochemical changes (Blanton *et al.*, 1987; Thornhill *et al.*, 2010). Furthermore, uptake of host macromolecules occurs through apertures including the nephridiopore, pre-acetabular gland ducts, the excretory subtegumental region in older schistosomules, or apertures such as those leading to the oesophagus and head gland (Thornhill *et al.*, 2009, 2010).

These initial transformations are important for parasite survival enabling protection from host immune response and, possibly, incorporation of host factors for signalling pathway complementation (Jenkins *et al.*, 2005). During the first three days schistosomules migrate through the host dermal layers until the lumen of a capillary is reached and at days five to six they are found in the lung vasculature (Moser *et al.*, 1980; Gobert *et al.*, 2010). These lung-stage schistosomules are resistant to antibody-mediated damage, acquiring erythrocytes (Goldring *et al.*, 1976) and cellular proteins (Clegg *et al.*, 1971) onto their teguments to cloak themselves in host blood group antigens aiding immune evasion (Simpson *et al.*, 1984; Payares *et al.*, 1985b; Clegg *et al.*, 1971). Thirteen to fifteen days after infection schistosomules arrive at the portal system and start sexual maturation (Walker, 2011).

Like the schistosome tegument is crucial for parasite survival (reviewed by Dzik, 2006), the intestine or gastrodermis of schistosomes secretes proteins and is thus another point of interaction with host tissue (blood). Schistosomes ingest red blood cells as a primary nutrient (hematophagy) and this is initiated in the oesophageal region (reviewed by Ernst, 1975; Truscott *et al.*, 2013). Despite the availability of the *S. mansoni* genome (Berriman *et al.*, 2009) and the secreted proteome (secretome) (van Balkom *et al.*, 2005; Braschi *et al.*, 2006; Braschi and Wilson, 2006) the schistosome gastrodermal proteome has not yet been defined and the transcriptional changes in *S.*

mansoni caused by the presence of erythrocytes has only been recently studied by using *in vitro* cultured schistosomules (Gobert *et al.*, 2010).

Host–derived molecules such as growth factors and hormones are exploited by schistosomes and other endoparasites to help evade the host immune response and compensate their own signalling pathways to regulate cellular functions including those involved in development and reproduction (Morales-Montor *et al.*, 2001; Remoué *et al.*, 2002; Ghansah *et al.*, 2002; Shibayama *et al.*, 2003). For instance, in *S. mansoni*, hypothalamic-pituitary-adrenal axix (HPA) hormones negatively affect reproduction, viability and oviposition by binding to classical nuclear receptors inhibiting glucose metabolism (Morales-Montor *et al.*, 2001). Furthermore, *S. mansoni* receptors that bind 17-β-estradiol and nuclear receptors for steroids, thyroid hormones and ecdysteroids show high homology to those of humans (Barrabes et *al.*, 1986; de Mendonça *et al.*, 2000). Epidermal growth factor (EGF) stimulates development of the filarial parasite *Brugia malayi* (Dissanayake, 2000) *in vitro* and increases *T. brucei* DNA synthesis, growth and metabolic activity (Ghansah *et al.*, 2002). Insulin increases gametocyte number in *P. falciparum* (Lingnau *et al.*, 1993) and increases expression of genes involved in growth and development in *S. japonicum* adult worms (You *et al.*, 2009), while granulocyte-macrophage-colony-stimulating factor (GM-CSF) increases growth of *Leishmania mexicana amazonensis* (Charlab *et al.*, 1990). Sex and pregnancy associated hormones also have an effect; testosterone reduces fertility in *S. haematobium* (Remoué *et al.*, 2002), whereas estradiol increases (by 200%) reproductive capacity, viability and growth of *T. crassiceps* cystecerci (Larralde *et al.*, 1995) and androgen, progesterone and 16-α-bromoepiandrosterone increase gametocyte number in *P. falciparum* (Lingnau *et al.*, 1993). In addition to lipid soluble hormones, water soluble factors might bind receptors at the plasma membrane and activate downstream pathways such as those involving PKC and MAPK regulating processes such as growth, infectivity differentiation and reproduction (Escobedo *et al.*, 2005).

More needs to be understood about the molecular processes underpinning *S. mansoni* development within the mammalian host. Unfortunately, *in vivo* experiments are impractical because obtaining sufficient numbers of schistosomules directly from tissue is time consuming, and uniformity in parasite maturation cannot be achieved due to the variation in time taken for individual parasites to penetrate host skin and enter the vasculature (Gobert *et al.*, 2010). Fortunately, *in vitro* cercarial transformation and

schistosomule culture techniques have been developed and used for many years (Basch, 1981; Mann *et al.*, 2010; Gobert *et al.*, 2010). Transforming and cultivating schistosomes *in vitro* avoids the use of a mammalian host, simplifies visualization of schistosomes, allows high yields of transformed parasites and grants uniformity in parasite maturation; facilitating the collection of the parasites for large-scale experimental analysis including genetic and molecular manipulation. Previous studies have compared the morphological and biochemical properties of *in vivo* and *in vitro* transformed cercariae (Salafsky et al., 1988). In general, the ultrastructure of those transformed and cultured *in vitro* is similar compared to those *in vivo* (Salafsky et al., 1988) and the growth rate is identical for the first twelve days (Clegg and Smithers, 1972). A recent study showed only 38 out of ~11,000 genes were differentially expressed between mechanically transformed and skin transformed cercariae demonstrating that mechanical transformation is a suitable alternative (Protasio *et al.*, 2013).

Direct assessments of gene function in schistosomes have been hampered by the lack of effective tools to alter gene expression but now schistosomes have entered the post-genomic era more tools have been developed. Recently, using biolistics, square-wave electroporation, or soaking schistosomes have been transiently transformed with mRNA, plasmid DNA, reporter-gene constructs or virions enabling gene expression analysis and promoter studies (Heyers *et al.*, 2003; Correnti and Pearce, 2004; Correnti *et al.*, 2007; Mann *et al.*, 2010; Dvořák *et al.*, 2010; Kines *et al.*, 2010). The RNA interference (RNAi) principle of gene silencing originally developed for *C. elegans* (Fire *et al.*, 1998), has been adapted for schistosomes providing new perspectives for reverse genetic approaches (Correnti *et al.*, 2005; Krautz-Peterson *et al.*, 2007; Ndegwa *et al.*, 2007; Moraes Mourão *et al.*, 2009; Beckmann *et al.*, 2010). Several *S. mansoni* life-stages have been proven to be susceptible to RNAi-induced gene suppression including sporocysts, adult worms and schistosomules (Skelly *et al.*, 2003; Boyle *et al.*, 2003; Osman *et al.*, 2006; Sayed *et al.*, 2006). Also, in *in vitro* cultured schistosomules, several studies on gene suppression by RNAi have been performed. For instance, incubating schistosomules with double-stranded (ds)RNA encoding the peroxyredoxinn1 gene resulted in reduced peroxiredosin activity and lowered survival of cultured parasites (Sayed *et al.*, 2006). Furthermore, either by electroporation or soaking in dsRNA suppression of a major gut associated cathepsin B cysteine protease resulted in retarded parasite growth when treated schistosomules were introduced into

mice (Skelly *et al.*, 2003; Correnti *et al.*, 2005). Optimizing RNAi in *S. mansoni* schistosomules has revealed that the efficiency of dsRNA or 21bp short interfering (si)RNA is equally efficient (Krautz-Peterson *et al.*, 2007). Recently, analysis of the efficacy of RNAi methods for large-scale screening of *S. mansoni* schistosomules has been performed showing that either soaking or electroporation are suitable delivery methods with over 75% knockdown achieved (Stefanic *et al.*, 2010).

To discover functional roles for PKC and MAPKs in *S. mansoni* schistosomules, the life-stage resistant to current chemotherapeutics, the distribution of PKC, ERK and p38 MAPK activity and the effects of pharmacological modulation on *in vitro* transformed *S. mansoni* schistosomules were investigated. Additionally, the effects of host-derived hormones, growth factors and mouse erythrocytes on the phosphorylation of these kinases were studied to give insights into how the host environment might affect such signalling. Finally, transfection of specific siRNAs was attempted to discover aberrant phenotypes.

8.2 Materials and Methods

For all experiments, cercariae and schistosomules were obtained and handled as detailed in Chapter 2. After cercariae transformation to schistosomules organisms were maintained overnight in serum free-BME (Basal Medium Eagle) and on the following day media was changed to Basch's medium at 600 – 1200 schistosomules/ml; and changed every three days thereafter.

8.2.1 PKC, ERK and p38 MAPK activation during early development of S. mansoni *schistosomules*

During culture (first 16 h in serum-free BME and Basch's medium thereafter), the phosphorylation of PKC, ERK and p38 MAPK was assessed at 3 h, 16 h, 24 h, 48 h, 72 h and 96 h by western blotting or immunohistochemistry. For western blotting, at each time point, schistosomules were transferred to 1.5 ml microfuge tubes, placed on ice for 30 s and pulse centrifuged and processed for western blotting as detailed in Section 2.5. From each sample, 2 µl were removed for protein quantification. Immunohistochemistry was performed as detailed in Section 2.6. Anti-phospho-PKC (pan) (βII Ser660), anti-phospho-PKC (pan) (ζ Thr410) (190D10), anti-phospho-p44/42 MAPK (ERK1/2) (Thr202/Tyr204), and anti-phospho-p38 MAPK (Thr180/Tyr182) antibodies were employed.

8.2.2 EGF, IGF and insulin transactivation in S. mansoni *schistosomules*

To understand if PKC, ERK or p38 MAPK signalling could be activated by host growth factors and hormones EGF (Calbiochem), insulin-like growth factor-I (IGF-I) (Sigma) or insulin (INS) (Sigma) were added to 3 day-old cultured schistosomules. The time points and concentrations used were adapted from studies conducted in *S. japonicum* by You *et al.* (2009), and also from published work on transactivation studies with EGF in *T. brucei* (Ghansah *et al.*, 2002). Schistosomules (1000/ml) were maintained overnight in serum-free BME medium (no FBS) and the following day the medium was replaced with Bash's medium until parasites were 48 h-old. Then, larvae were washed twice in serum-free BME medium and starved for 18 h in serum-free

BME. Starved schistosomules were treated with 15 ng/ml EGF. At each time point (5, 15, 30 and 60 min) schistosomules were transferred into 1.5 ml microfuge tubes, placed on ice for 60 s, pulse centrifuged and processed for western blotting as detailed in Section 2.5, or fixed for immunohistochemistry (Section 2.6). Two controls were employed, one with no EGF (i.e. 0 min) and one in which organisms neither starved nor treated with EGF. The same procedure was done for both IGF-I (15 ng/ml) and INS (1 μM) treatments, however INS was only tested at 30 and 60 min. All experiments were repeated independently three times with two replicates each with the exception of IGF-I studies.

8.2.3 Effects of red blood cells on PKC, ERK and p38 MAPK activation in S. mansoni *schistosomules*

It is suggested that consumption of host erythrocytes by *S. mansoni* regulates their development and immune evasion (Bogitsh and Carter, 1977; Gobert *et al.*, 2010; Gobert *et al.*, 2010) and that in *in vitro* cultured schistosomules, signs of red blood cell digestion are evident at 5 days of culture (Bogitsh and Carter, 1977; Moser *et al.*, 1980). Hence, to investigate if PKC, ERK or p38 MAPK phosphorylation is affected by ingestion of red blood cells, 5 day cultured schistosomules were supplemented with packed mouse erythrocytes (Matrix biological Ltd, Hull, UK). Red blood cells (1 ml) were washed once with BME (10 ml) containing 1% HEPES buffer and 2x antiboiotic/antimycotic in a 15 ml conical tube followed by centrifugation at 1000 *g* for 5 min. Schistosomules (1000) were transferred into 1.5 ml microfuge tubes, placed on ice for 60 s, pulse centrifuged and processed for western blotting as detailed in Section 2.5 either 1 h before, 1 h after, or 24 h after the addition of 50 μl red blood cells to the culture well. Schistosomules from all treatments were also fixed in acetone and processed for immunohistochemistry as detailed in Section 2.6.

8.2.4 Role of PKC in transferrin uptake by S. mansoni *schistosomules*

To ascertain whether PKC inhibition affects transferrin uptake by schistosomules, Alexa Fluor 635 conjugated transferrin (Invitrogen) was used. For this 24 h schistosomules (cultured in BME) were exposed to 20 μM GF10203X for 120 min and were washed in PBS twice to remove media. After 250 μg/ml transferrin-Alexa

Fluor 635 conjugate was added; this concentration has been previously used by Clemens and Basch (1989). Schistosomules/ transferrin-Alexa Fluor 635 conjugate (20 µl) were immediately pipetted onto a concave glass slide and a coverslip applied; the preparation was then maintained on ice for transfer to the confocal microscope. Live imaging of transferrin uptake by schistosomules was performed over 40 min on the Leica SP2 AOBS confocal laser scanning microscope and using 635 nm excitation and 650 nm emission.

8.2.5 Pharmacological assays

Freshly transformed schistosomules (~300 per well) were maintained overnight in individual wells of a 48-well tissue culture plate in 300 µl of serum-free BME containing various concentrations (1, 2, 5, 10, 20, 30, 50 and 100 µM) of GF109203X, U0126, SB203580 or PMA. The next day the BME was replaced with 300 µl Basch's medium containing the various concentrations of the different pharmacological agents. Two controls were also used, one containing only Basch's medium and the other containing Basch's medium with three different concentrations of vehicle DMSO (for U0126 and PMA; lowest (0.1%), medium (1%) and highest (5%)). Movies (each 1 min long, ~13 frames/s) were the taken of the schistosomules with a digital Motic camera attached to a Motic inverted microscope 1, 24 and 48 h after adding the components in Basch's medium, and the behavioural and morphological effects observed and quantified as detailed in Section 8.2.6, below. The behavioural/morphological effects determined were: 1) contractile movements, calculated as the standard deviation of organism's perimeter in pixels 2) average length, and 3) average area. Other phenotypic changes such as darkened, granulated, small and round or segmented bodies and dark gut were also enumerated. At 48 h 100 parasites per treatment were removed and used for FDA/PI viability assays (Section 8.2.7). For each experiment and each dose at least 60 schistosomules were enumerated, with each experiment independently repeated 3 times.

8.2.6 Video analysis of schistosomules

Quantification of schistosomule contractile movement as standard deviation of perimeter in pixels was performed using ImageJ (rsbweb.nih.gov/ij/) and the wrMTrck

plugin available at (www.phage.dk/plugins/download/wrMTrck.pdf); this plug-in has been designed for *C. elegans* motility analysis, however it gives several sets of data which for the first time are shown here to give reliable and quantitative analysis of schistosomule movement. The following protocol is a combination of the protocol for *C. elegans* motility analysis with optimizations for the analysis of schistosomules with a x20 objective lens. Firstly, movies were transformed into uncompressed "old format" AVIs with the VirtualDub software version 1.8.8 (www.virtualdub.com); this was done because ImageJ is unable to read compressed AVIs. After, uncompressed movies were opened with ImageJ and a total of 200 frames were selected and converted into grey scale followed by background subtraction at generally rolling ball radius of 10 to 30 pixels. The threshold was then adjusted and applied using the automatic threshold logarithm "Otsu" so that the schistosomules appeared red. No scaling/conversion of pixels to mm was used, as the analysis was best performed in pixel values due to the fact that all videos were taken with the same camera at the same magnification. Following background subtraction and threshold adjustment of videos, the wrMTrck plug-in was used with the optimized calibration for the analysis of schistosomules (Appendix B). From the results three values were used; average total area, average total length and Standard Deviation of the Perimeter which shows the total variability of the organisms perimeter in all the frames (such as contraction as distensions). Analysed organisms were labelled with a "track number" and therefore for each analysis results were compared to the respective organism in the movie to confirm that the results obtained are from the schistosomules and not from debris in the image, and that the activity of each individual in the movie was in accordance with the values obtained. When two schistosomules were too close together (touching) the results of those individuals were discarded as the software acknowledges the two organisms as one.

8.2.7 Viability assay

Schistosomules (100) were transferred from culture wells into 1.5 ml microfuge tubes, washed twice in 300 µl pre-warmed (37°C) PBS by centrifuging for 9 s at 200*g* and carefully removing all supernatant. After washing, 200 µl PBS containing 2 µg/ml of propidium iodine (PI) and 0.5 µg/ml of fluorescein diacetate (FDA) was added to each tube. Immediately after this, parasites were pipetted into black walled, clear flat bottomed 96-well plates (Fisher Scientific), and samples measured from below in dual

chromatic mode with 544 nm excitation/620 nm emission (to detect PI/dead) and 485 nm excitation/520 nm emission (to detect FDA/live) with a FluorStar Optima plate reader (BMG Labtech). All fluorescence values were obtained at 5 and 10 min with the plate reader incubator set at 37°C to keep temperature constant and to ensure sufficient esterase conversion of fluorescein diacetate to fluorescein within live organisms (Peak *et al.*, 2010). Two controls were always employed, a positive control comprising untreated schistosomes (live) and a negative control of heat-killed schistosomes (65°C for 10 min); a blank of PBS PI and FDA (media only) was used to compensate for any inter-plate variation. In order to ascertain percentage of live and dead schistosomules in each treatment group the following formula was used: viability = Live (FDA fluorescence)/[Dead (PI fluorescence) * Live (FDA fluorescence)] x 100. Where Live (FDA fluorescence) = (sample – neg. control) / (pos. control – neg. control) and Dead (PI Fluorescence) = (sample – media control) / (neg. control – media control) (Peak *et al.*, 2010). The 10 min time point was chosen as optimal due to the fact that FDA was known to be most effective between 3 and 12 min and PI was most effective between 4 and 120 min (Peak *et al.*, 2010).

8.2.8 PKC and ERK gene silencing through small interference RNA (siRNA)

8.2.8.1 Design of siRNA

Established guidelines to optimize siRNA efficacy were taken into account for the design of siRNA duplexes (Gong *et al.*, 2006). A total of 7 small inhibitory RNAs (siRNAs) were designed using the on-line IDT RNAi Design Tool (http://www.idtdna.com/Scitools/Applications/RNAi/RNAi.aspx) and synthesized by Thermo Scientific. Briefly, designed siRNA duplexes were composed of 21-nt sense and 21-antisense strands, paired to have a 2-nt 3' overhang. The sequence of the 2-nt overhang makes a small contribution to the specificity of target recognition restricted to the unpaired nucleotide adjacent to the first pair; and nucleotide sequences with TT in the overhang are known to work best (Gong *et al.*, 2006). Furthermore, the sequence was targeted at around 50 to 100 nucleotides downstream of the start codon. Therefore, to design an siRNA duplex a 23-nt sequence motif AA(N19)TT (where N is any nucleotide) was searched for and hits with approximately 50% G/C content were selected. When no suitable sequences were found, the search was extended using the motif NA(N21). The sequence of the sense siRNA corresponds to (N19)TT or N21

(position 3 to 23 of the 23-nt motif), respectively. An siRNA design with symmetric 3'TT overhangs, was preferred as the symmetric 3' overhangs help ensure that the siRNPs are formed with approximately equal ratios of sense and antisense target RNA cleaving siRNPs (Elbashir *et al.*, 2001a, b). The *S. mansoni* gene sequences were compared to their predicted protein sequences on the NCBI database to identify non-coding areas to be avoided for design. A non-target "off the shelf" negative control siRNA was adopted from a previous study (Krautz-Peterson *et al.*, 2007). This sequence was checked to ensure it did not match any gene from the recently updated *S. mansoni* genome assembly by using the Basic Local Alignment Tool (BLAST) at http://www.sanger.ac.uk/Projects/S_mansoni/ (Altschul *et al.*, 1990). Table 8.1 in Appendix B lists the double stranded siRNA sequences used for *S. mansoni* schistosomules including the 'off-target' scrambled negative control. The RNA sequences targeted to knockdown predicted *PKC* and *ERK* genes were those corresponding to the *S. mansoni* genome database protein annotations (Smps); Smp_176360 (PKC) (area targeted excluding the extended part), Smp_128480 (PKC), Smp_096310 (PKC), Smp_131700 (PKC), Smp_17630 (PKC) (targeting the extended part of the sequence), Smp_142050 (ERK) and Smp047900 (ERK). All sequences were synthesized as annealed siRNA duplexes.

8.2.8.2 siRNA delivery by soaking and schistosomule phenotype analysis

All double-stranded siRNAs were prepared as 64 μM stock solutions (each nucleotide base being 0.33 μg/nmol. For experiments, 2 μM of each siRNA was used without transfection agents as such agents have been reported to be harmful to *S. mansoni* schistosomules (Krautz-Peterson *et al.*, 2007). Schistosomules (~1000) were cultured for 24 h in 250 μl serum-free BME in individual wells of a 24 well culture plate. After 24 h, schistosomules were washed with serum-free BME and Basch's medium containing the siRNA was added to the culture plates and then left rocking for 1 h and incubated at 37°C and 5% CO_2. The following day, phenotypic changes were monitored and documented by videoing schistosomules using a Motic 2.0 megapixel camera attached to an inverted Motic microscope; such observations were repeated daily. On day 5 of siRNA treatment, schistosomules were collected and processed for western blotting analysis as previously described (above, and Section 2.5), or were quickly washed twice in PBS, snap frozen in liquid nitrogen and stored at -80°C until

mRNA extraction and RT-qPCR assay (Section 8.2.9). Material was harvested from a minimum of two biological replicates each from three independent experiments. Besides using the siRNA designed targets two controls were used; the "off the shelf" scrambled negative control siRNA that does not match any *S. mansoni* gene to confirm that the siRNA duplexes do not cause unspecific effects, and a control were no siRNA was added and schistosomules were simply maintained in Basch's medium.

8.2.9 Reverse-Transcription and Quantitative Polymerase Chain Reaction (RT-qPCR)

8.2.9.1 Primer design

Primers to detect predicted *PKC* and *ERK* genes were designed using the Primer 3 engine (version 0.4.0; http://frodo.wi.mit.edu/) and resulting sequences (Table 8.2 Appendix B) checked for probability of formation of secondary structures using the sigma calculator (http://sigma-genosys.com/calc/DNACalc.asp). Sequences were blasted (http://blast.ncbi.nlm.nih.gov/) to check that no similarity existed with other human or *S. mansoni* proteins.

8.2.9.2 mRNA isolation and genomic DNA "wipeout"

The reverse transcription and genomic DNA "wipeout" components were prepared before starting mRNA extractions due to the high vulnerability of RNA to degradation compared to cDNA. The mRNA extraction was done according to the manufacturer's instructions. Firstly, Dynabeads were washed by transferring the bead suspension to a 1.5 ml PCR tube and placing on the magnet, after 10 s the supernatant was removed and beads washed with 350 µl lysis buffer, and resuspended again with 350 µl lysis buffer (for 1000 schistosomules lysate 20 µl Dynabeads were necessary). After bead preparation, frozen samples were homogenized on ice in 100 µl lysis buffer (supplied with the mRNA extraction kit) with a plastic microfuge tube pestle. The resulting lysate was transferred into a PCR tube containing the washed Dynabeads, and the suspension mixed before turning for 5 min at room temperature on a microfuge tube rotator; during this time base pairing occurs between the polyA residues at the 3' end of most mRNA, and the oligo $(dT)_{25}$ residues covalently coupled to the surface of the Dynabeads. After, samples were placed on the magnet and when the lysate cleared, the supernatant was discarded and 100 µl washing buffer A was added and beads

resuspended by careful pipetting. This process was repeated once more. Samples were then placed in the magnet, the supernatant discarded, and 100 µl wash buffer B added; this was repeated twice and beads transferred to a new tube, placed on the magnet and the supernatant removed. Finally, beads were eluted by adding 10 µl ice-cold elution buffer and incubating for 2 min at 70°C, immediately tubes were placed on the magnet and the supernatant transferred to a new PCR tube and placed on ice.

At this point any remaining genomic DNA was removed from samples by adding 1/7 of the final reaction volume with a prepared master mix of gDNA "wipeout" according to the manufacturer's instructions (Qiagen). Samples were then incubated for 2 min at 42°C and placed immediately on ice. To perform mRNA and cDNA quantity/quality assessment 1 µl sample was collected after DNA wipeout and also after reverse transcription cDNA and concentration and purity determined with a spectrophotometer (ND-1000, NanoDrop Technologies) and the necessary volume to be used in the PCR assay calculated.

8.2.9.3 Reverse transcription

The reverse transcription master mix was prepared according to the manufacturer's instructions (QuantiTect, Qiagen), which advises addition of 5% reverse transcriptase, 20% of 5x reverse transcription buffer, 5% of primer mix and 70% template. Templates (schistosomule mRNA) were added to each tube containing the master mix and incubated for 15 min at 42°C and then 3 min at 95°C to stop the reaction. Samples (cDNA) were then stored at -20°C.

8.2.9.4 qPCR optimization and analysis

Primers were reconstituted in DNase/RNase free H_2O and used at 500 nM final concentration. First, components of the QuantiTect PCR kit and primers were tested with samples with different concentrations of mRNA from schistosomules and adult worms to optimize assay conditions. Each final reaction (15 µl) comprised 7.5 µl 2x SYBR Green master mix, 1.2 µl template, 1 µl forward primer, 1 µl reverse primer and 4.3 µl DNase/RNase free water. Reactions were prepared in a white 96CFX pcr plates (Biorad). The final cDNA concentration per assay was 0.5 µg. Stock solutions (100 mM) of primers were made in RNase/DNase-free water and were diluted in water to make working solutions of 5 µM (to set up reactions). Standard curves were run once

for all targets to assess reaction efficiency, which was calculated as 92.5% using the on-line calculator (http://www.thermoscientificbio.com/webtools/qpcrefficiency/).

For all assays, two housekeeping genes, α tubulin and GAPDH, were also tested; these have been previously used as RT qPCR reference genes in *S. mansoni* schistosomules (Patoka and Ribeiro, 2007). Two further controls were performed in duplicate, containing all assay components except template or primer which was replaced by water. After optimization settings were as follows: 15 min at 95°C (hot start), then 45 cycles of 15 s at 94°C, 30 s at 55°C and 30 s at 72°C, with a final extension step at 72°C. Data acquisition was performed during extension with a Biorad C1000/CFX96. At the end of each assay a melt curve was constructed to confirm that products had the expected melting temperature and that only one product was obtained for each sample.

8.2.9.5 Analysis of qPCR data

All data is represented as the mean (± S.E.M) of 3 replicates and 3 independent assays. Minitab 16 was used to analyse all qPCR related data using the Fisher's least significant difference post-hoc multiple comparison test. For graphical representation of qPCR data, mean raw cycle threshold (Cq) values were used. However, for siRNA treatments Cq values for each sample were converted to fraction of control transcript levels using the delta-delta Cq (ΔΔCq) method (Livak and Schmittgen, 2001) with α-tubulin gene levels as an internal standard. In order to make statistical comparisons of the different treatment groups, data was not analysed as ΔΔCq as the process requires conversion to fraction of the reference gene. Instead, the Cq value of the reference gene was subtracted from the Cq value of the gene of interest for each sample/primer combination, and these raw values (ΔCq) analysed using ANOVA.

8.3 Results

8.3.1 Phosphorylation of PKC, ERK and p38 MAPK in S. mansoni *schistosomules*

The phosphorylation (activation) levels and *in situ* localization of active PKC, ERK and p38 MAPK detected with anti-phospho PKC (Thr410), anti-phospho PKC (Ser660), anti-phospho ERK 1/2 and anti-phospho p38 MAPK antibodies were assessed at various times in *S. mansoni* schistosomules maintained *in vitro* for 4 days. In immunohistochemistry, control schistosomules probed without primary antibodies showed negligible fluorescence (Figure 8.2).

Presence of phosphorylated PKCs in *S. mansoni* schistosomules was somewhat similar in cercariae and adult worms (Chapter 3) with four proteins of ~78 kDa, ~81 kDa, ~116 kDa and ~132 kDa detected (Figure 8.1). The largest protein (~132 kDa) was weakly detected and was often unseen (Figure 8.1 A). Activation of the ~132 kDa, ~116 kDa and ~78 kDa PKCs did not significantly change over 4 days (Figure 8.1 A), but phosphorylation of the ~81 kDa protein consistently increased at 72 h (2.4-fold; $p \leq 0.001$), when compared with 3 h schistosomules (Figures 8.1 A and B). This increased phosphorylation was sustained at 96 h (Figure 8.1 A). Localization using anti-phospho PKC (Ser660) antibodies revealed that activated PKC was differentially distributed over time, especially between day one and thereafter (Figure 8.3). During the first 16 h activated PKC associated with the tegument (Figure 8.3, 3 h and 16 h) but after 24 h and 48 h fluorescence reduced from here and appeared at internal structures (Figure 8.3). At 72 h and 96 h activated PKC remained in the internal structures and was weakly seen at the tegument (Figure 8.3). Using anti-phospho PKC (Thr410) antibodies (Figure 8.4) after 3 h and 16 h of culture, activated PKC was also associated with the tegument and various internal structures; such structures are possibly the developing gut/cecum, oesophagus, acetabular nerves and nephridiopore (Figure 8.4). After 24 h and 48 h PKC activation was maintained at the tegumental surface but was also present at other specific regions (Figure 8.4). Interestingly at 72 h and 96 h phosphorylated PKC was generally found throughout the whole organism including the subtegumental region, cecum, nephridiopore, pharyngeal muscles, germinal cell mass and oesophagus (Figure 8.4)

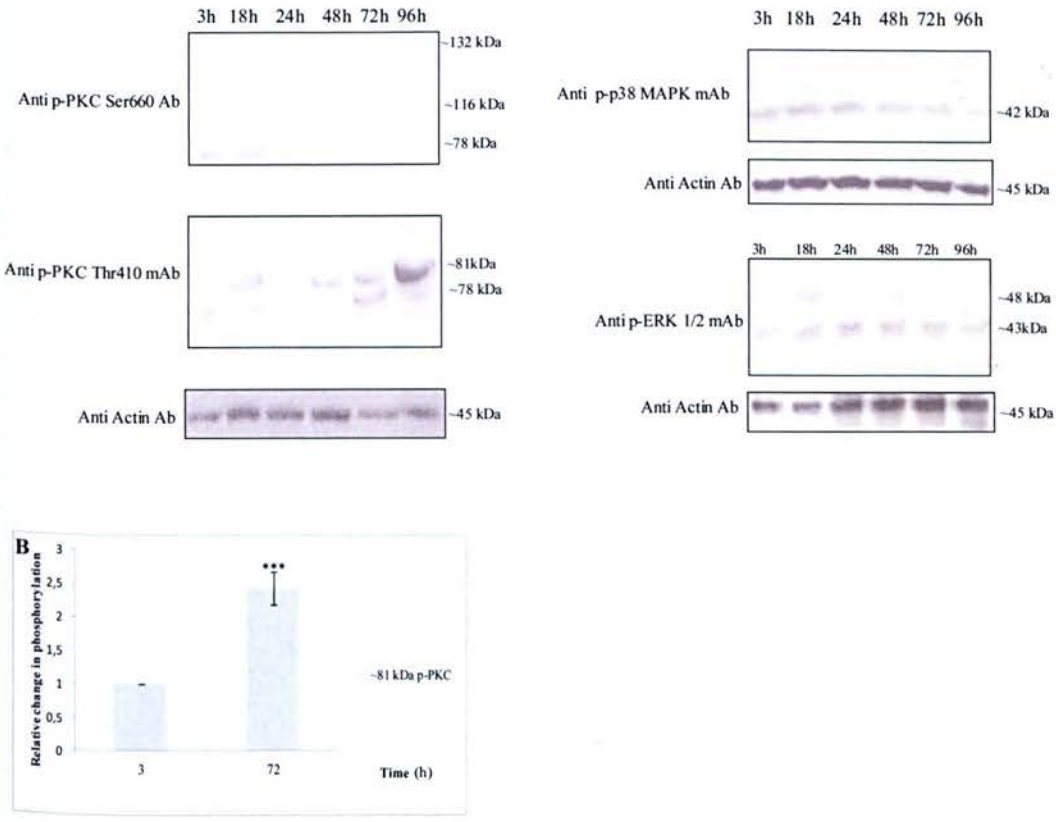

Figure 8.1 – Phosphorylation of *S. mansoni* schistosomule PKCs, ERKs and p38 MAPK over time in culture. Panel (**A**) detection of phosphorylated PKCs, ERKs and p38 MAPK using anti-phospho PKC (Thr410), anti-phospho PKC (Ser660), anti-phospho ERK1/2 and anti-phospho p38 MAPK antibodies following different times in *in vitro* culture (3 -96 h) (~600 schistosomules per lane). Polyclonal anti-actin antibodies were used to confirm equal loading of protein. Panel (**B**) quantification of ~81 kDa PKC immunoreactive band after 72 h culture expressed as mean (± SEM) relative change in phosphorylation against 3 h schistosomules that were assigned a value of 1. Immunoreactive bands were detected and quantified with a GeneGnome and Gene tools. ***$p \leq 0.001$; results are representative of two independent experiments each performed in duplicate n = 4.

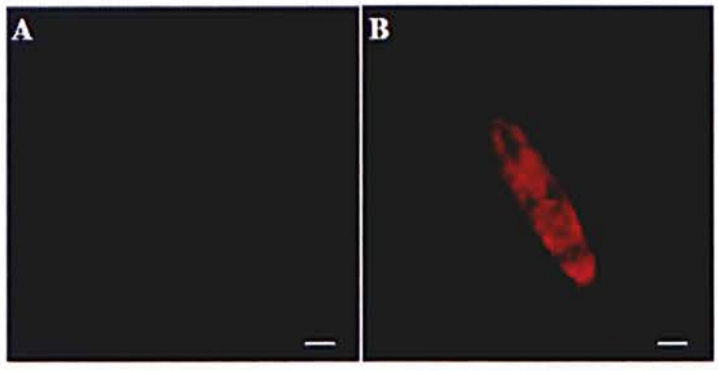

Figure 8.2 - Representative confocal micrograph of negative control *S. mansoni* schistosomules probed without primary antibodies but with Alexa Fluor 488 secondary antibodies. Panel (**B**) maximum projection of a schistosomule with rhodamine phalloidin showing actin. Panel (**A**) the background green signal from Alexa Fluor 488/autofluorescence which is almost undetectable. Bar = 10 µm.

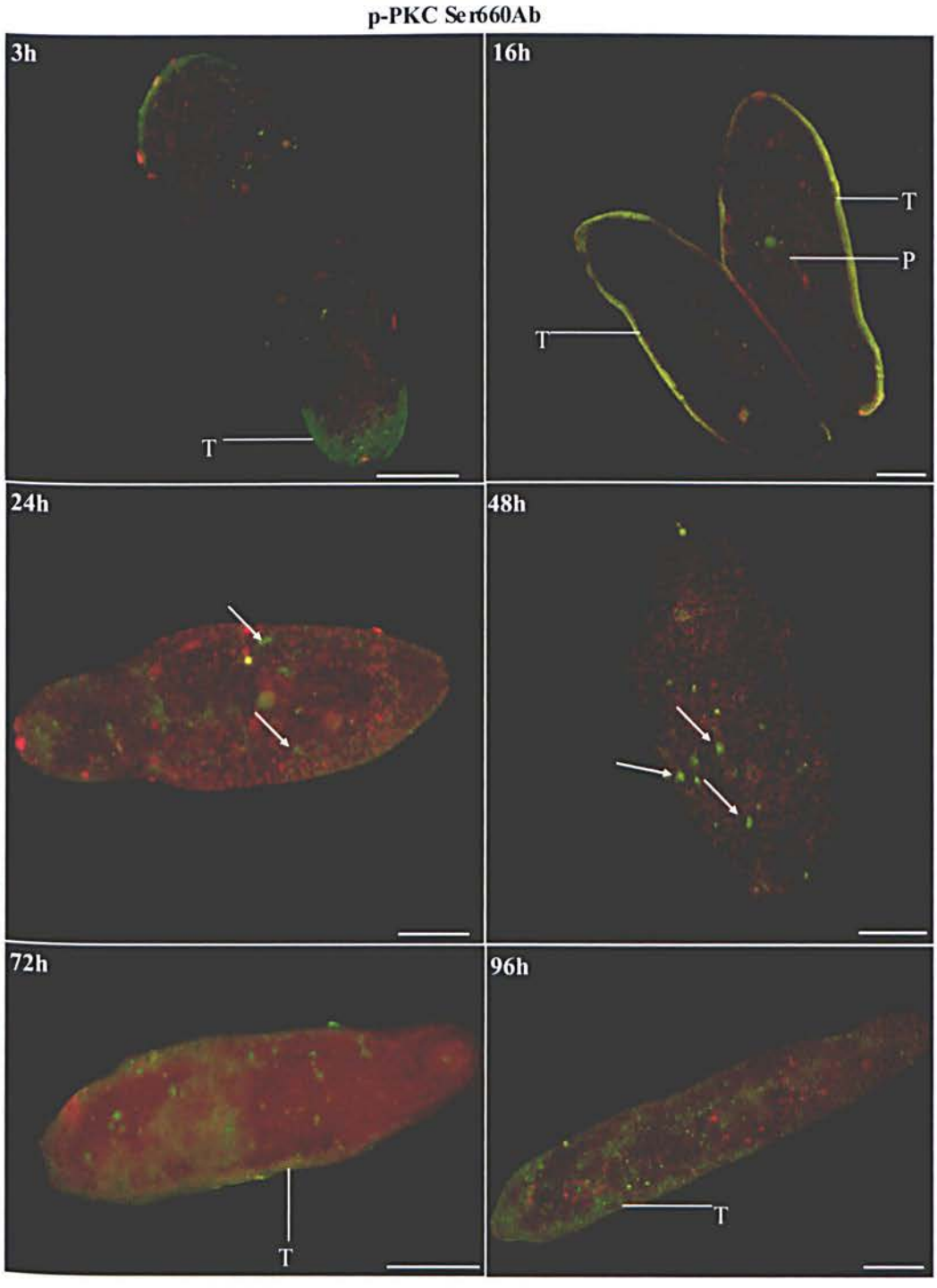

Figure 8.3 – *In situ* localization of phosphorylated PKC in intact *S. mansoni* schistosomules during culture detected with anti-phospho PKC (Ser660) antibodies. Schistosomules were cultured for 3 h, 16 h, 24 h, 48 h, 72 h and 96 h and were acetone fixed for immunolocalization of PKC activity (green) using anti-phospho PKC (Ser660) and AlexaFluor 488 secondary antibodies; they were also stained with rhodamine phalloidin to stain filamentous actin (red). Representative micrographs of schistosomules are shown as z-axis projections viewed in maximum pixel brightness mode. The tegument (T) is indicated and arrows represent regions of PKC activity of unknown identity. Bars = 10 μm.

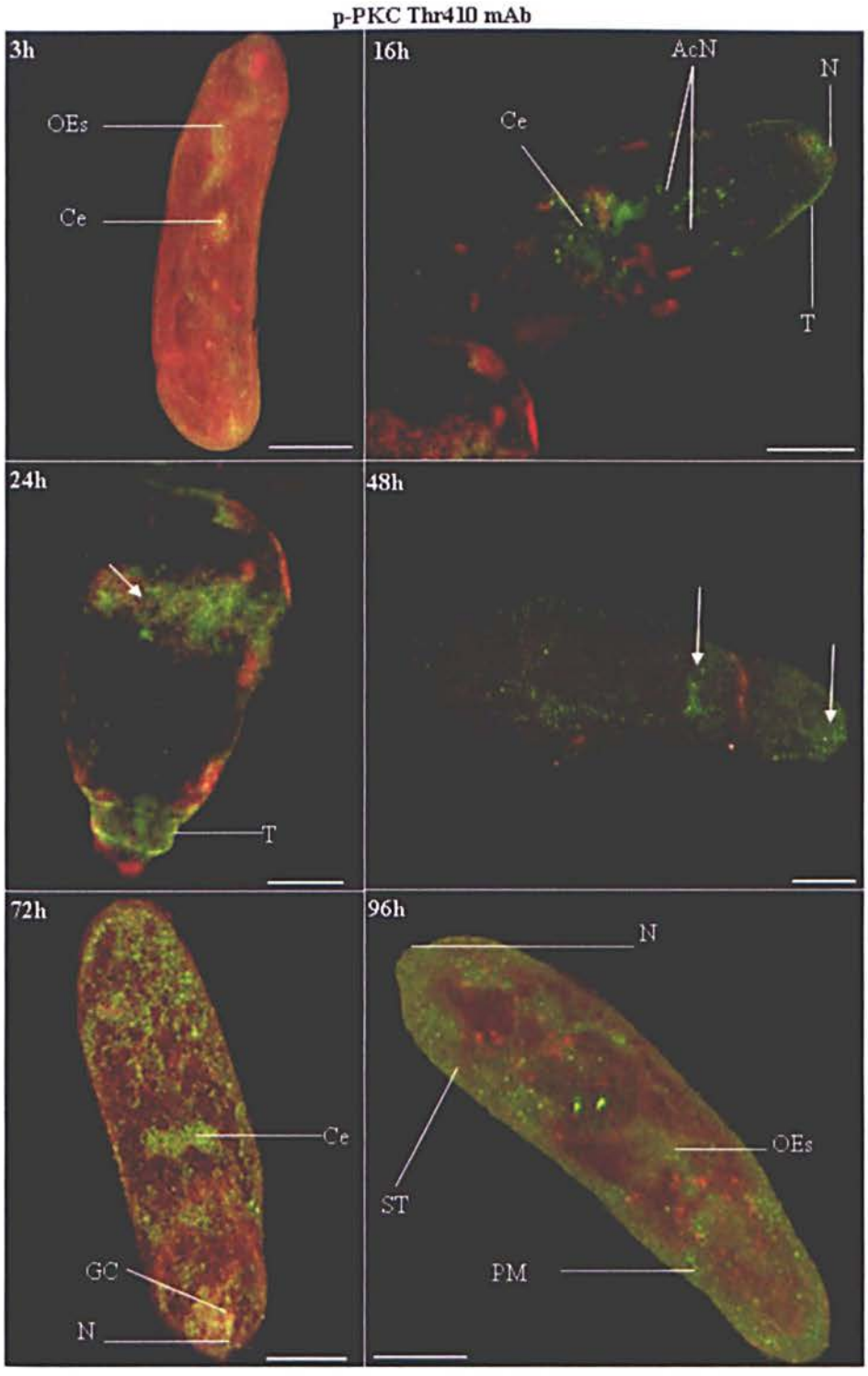

Figure 8.4 – *In situ* localization of phosphorylated PKC in intact *S. mansoni* schistosomules during culture detected with anti-phospho PKC (Thr410) antibodies. Schistosomules were cultured for 3 h, 16 h, 24 h, 48 h, 72 h and 96 h and were acetone fixed for immunolocalization of PKC activity (green) using anti-phospho PKC (Thr410) and AlexaFluor 488 secondary antibodies; they were also stained with rhodamine phalloidin to stain filamentous actin (red). Representative micrographs of schistosomules are shown as z-axis projections viewed in maximum pixel brightness mode. Activity was associated with: (Oes) – oesophagus, (Ce) – cecum, (GC) – germinal cell mass, (AcN) – acetabular nerves, (T) – tegument, (GC) – germinal cells, (N) – nephridiopore, (ST) – subtegument, (PM) – pharyngeal mass; arrows represent regions of unknown identity. Bars = 10 μm.

Two proteins were detected with anti-phospho ERK 1/2 antibodies in schistosomules with similar molecular weights to those detected in adult worms pairs (Figure 8.1 A); the ~48 kDa band was weakly detected and the ~43 kDa was the most immunoreactive (Figure 8.1 A). The activation status of both immunodetected proteins did not significantly change over time in culture. *In situ* localization showed phosphorylated ERK mainly associated with the tegument and muscle/nerve fibres throughout the different times in culture (Figure 8.5). Sometimes the acetabulum, oesophagus, and pharyngeal muscle, were also detected (Figure 8.5).

Activated p38 MAPK in cultured schistosomules detected with anti-phospho p38 MAPK antibodies was weak, and this low phosphorylation level was similar throughout 96 h (Figure 8.1 A). Confocal microscopy revealed phosphorylated p38 MAPK associated with the tegument and region of the cecum after 3 h and 16 h (Figure 8.6). Thereafter activated p38 MAPK was also associated with the pharyngeal muscle, parenchyma, acetabular glands, regions of the cecum, oesophagus and other unidentified internal regions (Figure 8.6).

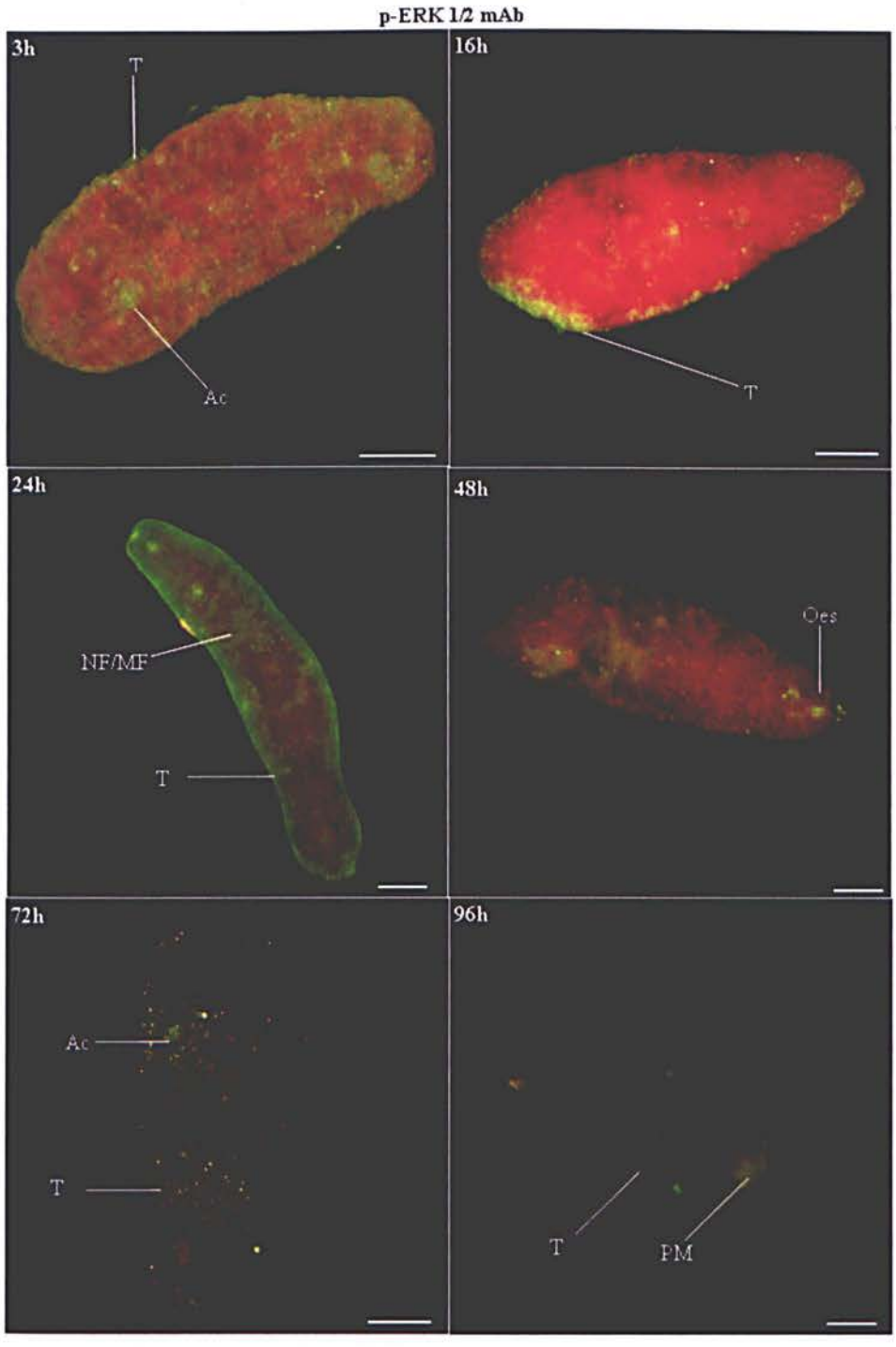

Figure 8.5– *In situ* localization of phosphorylated ERK in intact *S. mansoni* schistosomules during culture detected with anti-phospho ERK 1/2 antibodies. Schistosomules were cultured for 3 h, 16 h, 24 h, 48 h, 72 h and 96 h and were acetone fixed for immunolocalization of ERK activity (green) using anti-phospho ERK1/2 and AlexaFluor 488 secondary antibodies; they were also stained with rhodamine phalloidin to stain filamentous actin (red). Representative micrographs of schistosomules are shown as z-axis projections viewed in maximum pixel brightness mode. Activity found was mostly associated with the (Ac) – acetabulum , (Oes) – oesophagus, (T) – tegument, (Ac) – acetabulum, (PM) – pharyngeal muscle and (NF/MF) – nerve or muscle fibres. Bars = 10 μm.

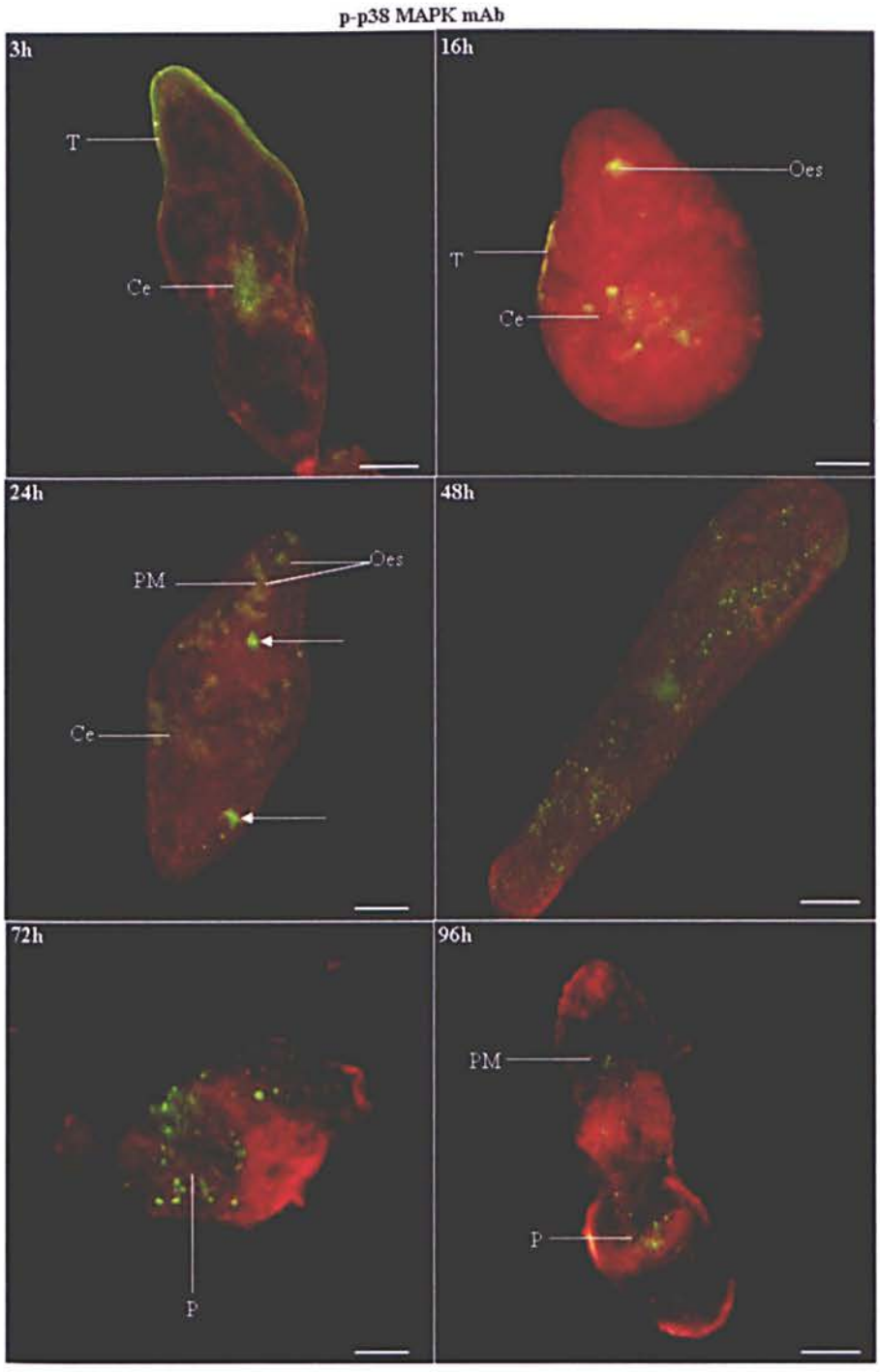

Figure 8.6 – *In situ* localization of phosphorylated p38 MAPK in *S. mansoni* schistosomules during culture detected with anti-phospho p38 MAPK antibodies. Schistosomules were cultured for 3 h, 16 h, 24 h, 48 h, 72 h and 96 h and were acetone fixed for immunolocalization of p38 MAPK activity (green) using anti-phosphop38 MAPK and AlexaFluor 488 secondary antibodies; they were also stained with rhodamine phalloidin to stain filamentous actin (red). Representative micrographs of schistosomules are shown as z-axis projections viewed in maximum pixel brightness mode. P38 MAPK activity mainly associated with the tegumental surface (T), cecum (Ce), oesophagus (Oes), pharyngeal muscles (PM), parenchyma (P); arrows represent activation at unknown structures. Bars = 10 μm.

8.3.2 Effect of human EGF on schistosomule PKC and ERK phosphorylation

Two-day-old *S. mansoni* schistosomules starved overnight and treated with human EGF (15 ng/ml) for 5, 15, 30 and 60 min displayed significantly increased ERK (~43 kDa) and PKC (~81 kDa) phosphorylation (Figure 8.7). At 15 min activity of ~81 kDa PKC increased ~2-fold ($p \leq 0.001$), declining to ~1.6-fold ($p \leq 0.01$) at 30 min and 60 min (Figure 8.7 B). The ~43 kDa ERK activation was only significantly increased after 30 min (2-fold, $p \leq 0.001$) (Figure 8.7 B). Phosphorylation levels of other PKC, ERK and p38 MAPK proteins were not significantly affected (Figure 8.7 A). *In situ* localization with anti-phospho PKC (Thr410) antibodies revealed that EGF increased PKC phosphorylation in the tegument, oesophagus, and unidentified structures when compared to controls (Figure 8.8 A). In the presence of EGF for 15 min no striking changes in activated ERK were detected (Figure 8.8 B). However, after 30 min, strong fluorescence appeared at the tegument and sometimes also in subtegumental regions.

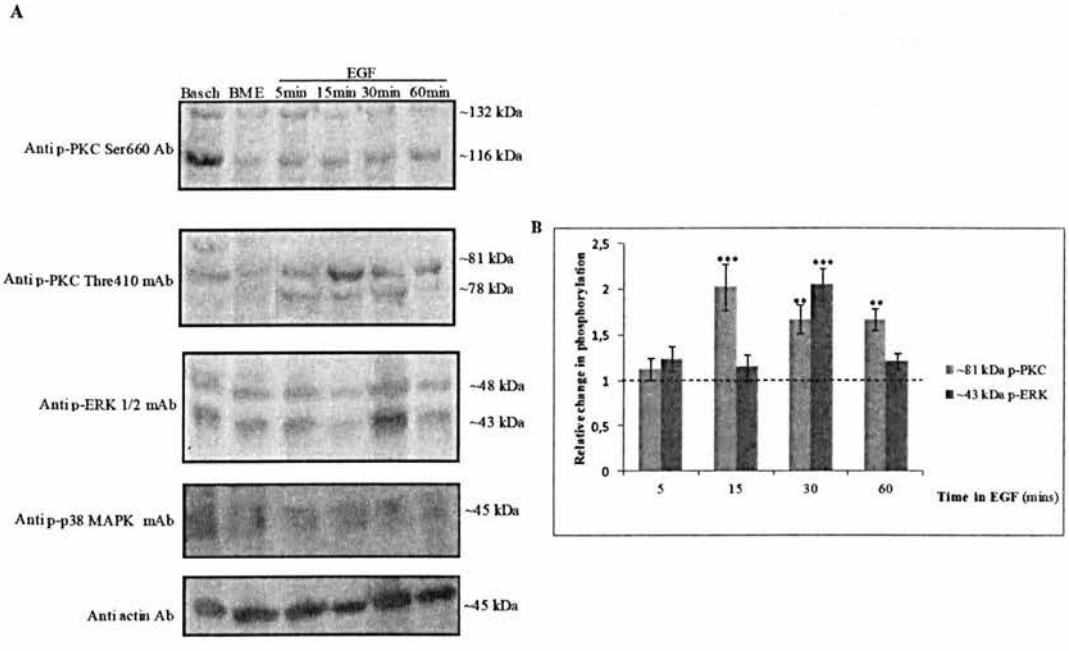

Figure 8.7 – Phosphorylation of PKCs, ERKs and p38 MAPK in 72 h *S. mansoni* schistosomules in the presence of human EGF (15ng/ml). **(A)** Detection of phosphorylated PKCs, ERKs and p38 MAPK with anti-phospho PKC (Thr410), anti-phospho PKC (Ser660), anti-phospho ERK1/2 and anti-phospho p38 MAPK antibodies after exposure schistosomules to 15ng/ml EGF for 5, 15, 30 and 60 min;, controls represent schistosomules starved in Basch or BME media. Anti-actin antibodies were used to confirm equal loading of protein. **(B)** Quantification of ~81 kDa PKC and ~43 kDa ERK immunoreactivity after different times in EGF represented as mean (± SEM) relative change in phosphorylation of schistosomules without EGF that were assigned a value of 1. Immunoreactive bands were detected and quantified with a GeneGnome and Gene tools. $^{**}p \leq 0.01$, $^{***}p \leq 0.001$. Results are representative of a minimum of two independent experiments n = 5.

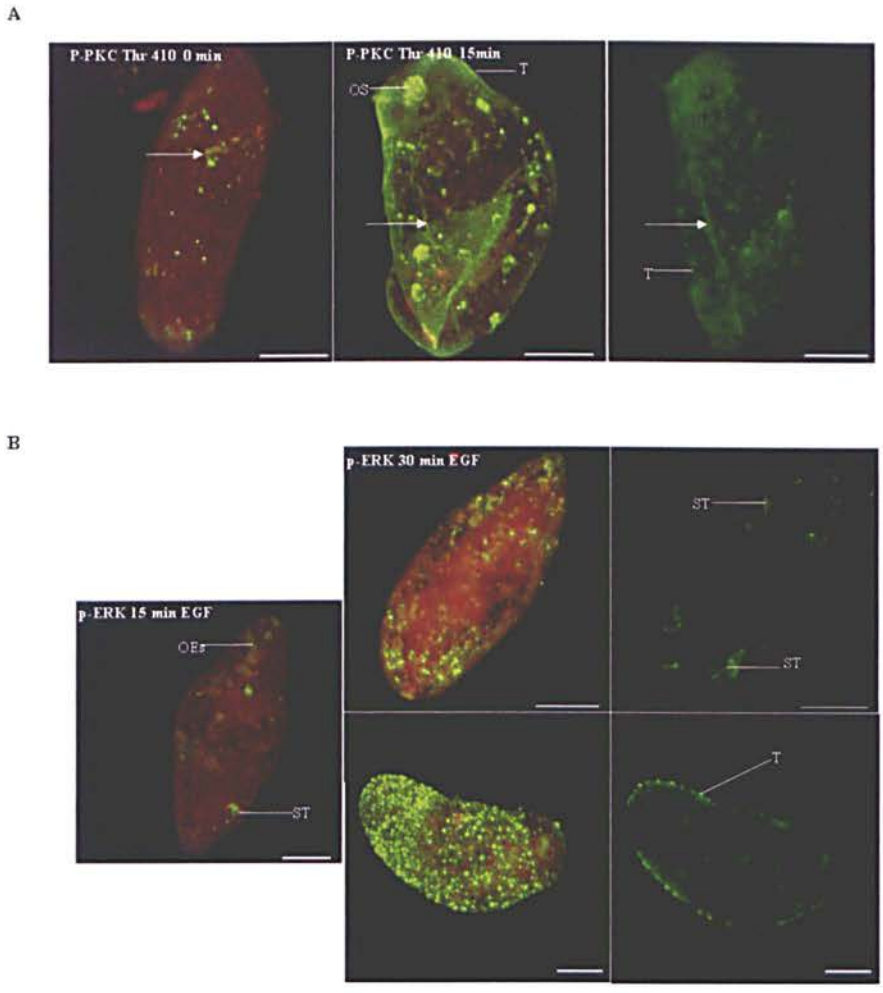

Figure 8.8 – *In situ* localization of phosphorylated PKC and ERK in 72 h *S. mansoni* schistosomules in the presence of human EGF (15 ng/ml). PKC and ERK activation (green signal) detected using (**A**) anti-phospho PKC (Thr410) or (**B**) anti-phospho ERK 1/2 antibodies, and Alexa Fluor 488 secondary antibodies. Representative micrographs of schistosomules at different times in the presence of EGF showing activity mostly associated with the tegument (T), oral sucker (OS), subtegument (ST) and oesophagus (Oes); arrows indicate activation at unidentified structures. Red signal represents actin filaments stained with rhodamine/phalloidin and z-axis projections are shown in maximum pixel brightness mode. Bars = 10 μm.

8.3.3 Effect of INS on schistosomules PKC and ERK phosphorylation

Addition of human insulin (ISN) (1 μM) to starved schistosomules significantly affected the activation of both ~116 kDa PKC and ~43 kDa ERK. The activity of the ~116 kDa PKC increased ~2-fold after 30 min ($p \leq 0.01$) (Figure 8.9 A and B), whereas the ~43 kDa ERK phosphorylation increased 3.2-fold ($p \leq 0.001$) at 30 min decreasing to basal levels after 60 min (Figure 8.9 A and B). The activation status of other PKC, ERK and p38 MAPK proteins was not significantly affected. INS also induced changes in the distribution pattern of PKC and ERK activation compared to controls. With anti-phospho PKC (Ser660) antibodies (that detect ~116 kDa PKC) fluorescence in

schistosomules treated with INS for 30 min was strongly associated with the tegument, cecum, ventral sucker and regions within the parasite of suspected neural function (Figure 8.10). However, at 60 min activated PKC was only found in the tegument and oesophagus (Figure 8.10). Activated ERK was found strongly associated with the tegument, cecum, oral sucker and subtegumental regions (Figure 8.11).

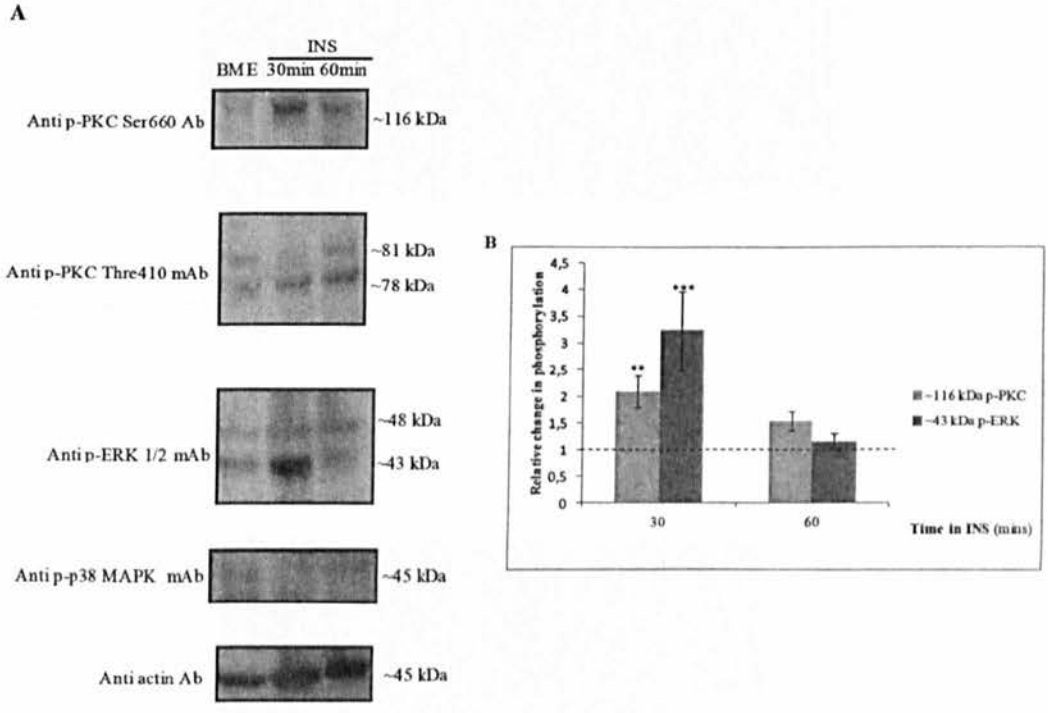

Figure 8.9 – Phosphorylation of PKCs, ERKs and p38 MAPK in 72 h *S. mansoni* schistosomules in the presence of human INS (1 µM). **(A)** Detection of phosphorylated PKCs, ERKs and p38 MAPK with anti-phospho PKC (Thr410), anti-phospho PKC (Ser660), anti-phospho ERK1/2 and anti-phospho p38 MAPK antibodies after exposure schistosomules to 1 µM INS for 30 or 60 min. The first lane represents serum starved (overnight in BME) schistosomules before adding INS. An anti-actin antibody was used to confirm equal loading of protein. **(B)** When strong changes in activity were observed these were quantified and expressed as relative change in phosphorylation against serum starved schistosomules that were assigned a value of 1. Values shown are means (± SEM), for each time point and each treatment from three independent experiments n=6. Immunoreactive bands were detected and quantified with a GeneGnome and Gene tools. $^{**}p \leq 0.01$, and $^{***}p \leq 0.001$.

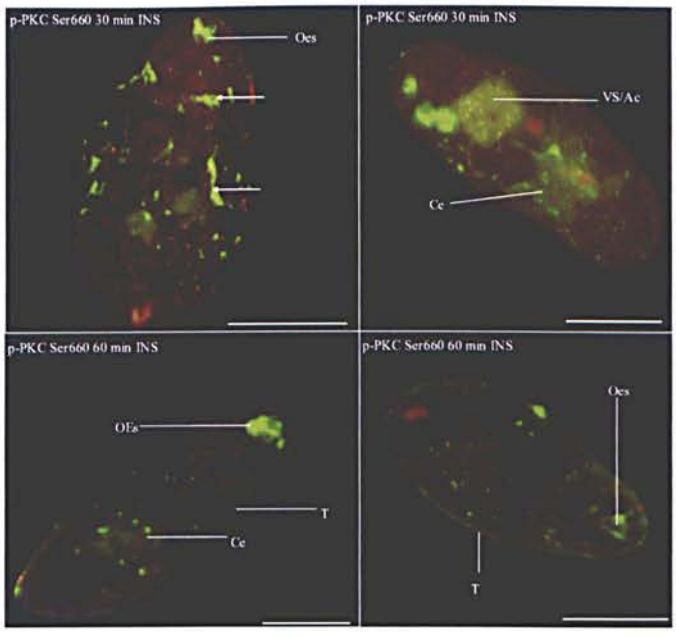

Figure 8.10 – *In situ* localization of phosphorylated PKC in 72 h *S. mansoni* schistosomules in the presence of human INS (1 μM). Schistosomules were exposed to INS, acetone fixed and stained with anti-phospho PKC (Ser660) and AlexaFluor 488 antibodies (green). Representative micrographs of z-axis projections in maximum pixel brightness mode show activation after 30 and 60 min mostly associated with the tegument surface (T), oesophagus (Oes), cecum (Ce), ventral sucker or acetabulum (VS/Ac); arrows represent regions of putative neurological function such as nerve fibres. Red signal represents actin filaments stained with rhodamine phalloidin. Bars = 10 μm.

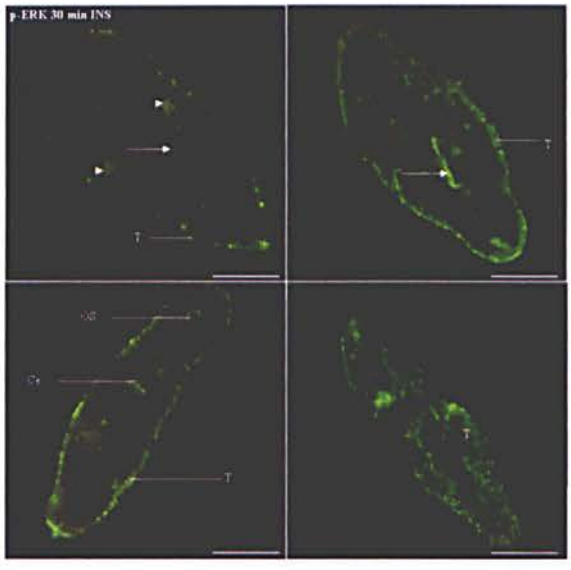

Figure 8.11 – *In situ* localization of phosphorylated ERK in 72 h *S. mansoni* schistosomules in the presence of human INS (1 μM). Schistosomules were exposed to INS, acetone fixed and stained with anti-phospho ERK 1/2 and AlexaFluor 488 antibodies (green). Representative micrographs of z-axis projections in maximum pixel brightness mode show activation after 30 min mostly associated with the tegument surface (T), cecum (Ce), oral sucker (OS); arrows represent putative nerve fibres and arrow heads unidentified subtegumental structures. Red signal represents actin filaments stained with rhodamine phalloidin. Bars = 10 μm.

8.3.4 Human IGF-I increases activation of ~116 kDa PKC

After 30 and 60 min in the presence of 15 ng/ml of human insulin-like growth factor 1 (IGF-I) the activity of ~116 kDa PKC in schistosomules increased (Figure 8.12 A). Confocal microscopy revealed that under these conditions PKC phosphorylation detected with anti-phospho PKC (Ser660) antibodies was mainly associated with the caecum, oesophagus, nephridiopore and other unknown regions (8.12 B). Phosphorylation of other PKC, ERK and p38 MAPK proteins was unchanged (data not shown).

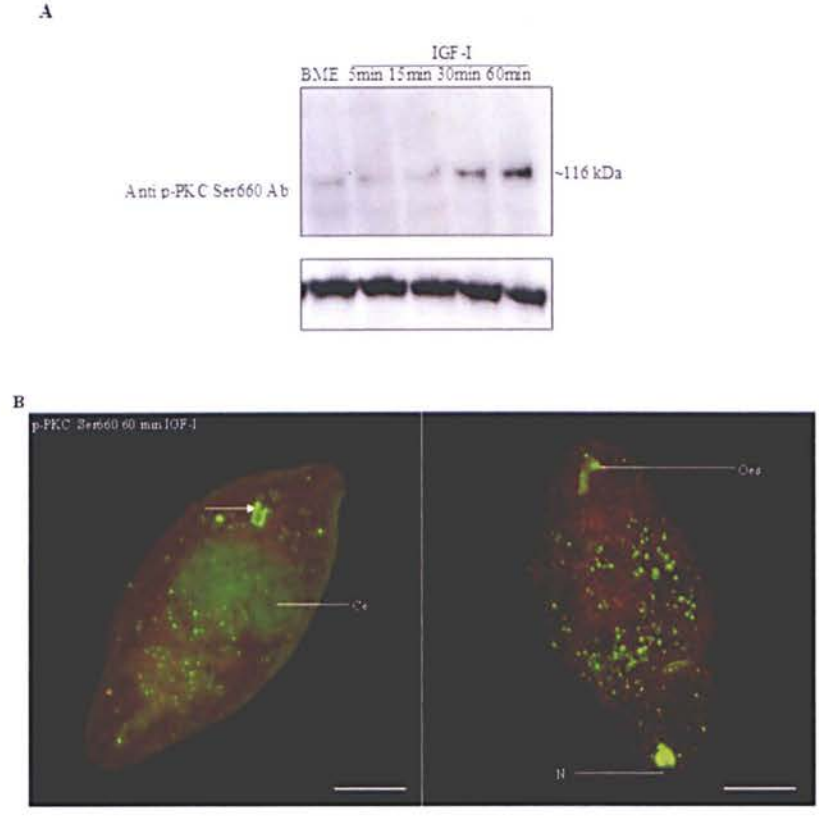

Figure 8.12 – Effect of human IGF-I (15ng/ml) on ~116 kDa PKC phosphorylation in 72 h *S. mansoni* schistosomules. (A) Representative immunoblot of schistosomules exposed to IGF-I for 5, 15, 30 and 60 min; blots were probed with anti-phospho PKC (Ser660) antibodies. The first lane represents serum starved schistosomules (overnight in BME) before adding IGF-I. Anti-actin antibodies were used to confirm equal loading of protein. **(B)** Immunolocalization of PKC activity (green) following acetone fixing of parasites and staining with anti-phospho PKC (Ser660) and AlexaFluor 488 antibodies. Representative micrographs of schistosomules are shown after 60 min exposure to IGF-I showing activity mostly associated with the cecum (Ce), oesophagus (OEs), nephridiopore (N); the arrow indicates an identified structure. Red signal represents actin stained with rhodamine phalloidin. Z-azis projections are shown in maximum pixel brightness mode. Bars = 10 μm.

8.3.5 Addition of erythrocytes to cultured schistosomules increases PKC and p38 MAPK phosphorylation

Murine red blood cells were added to five day-old cultured schistosomules, the time at which *S. mansoni* schistosomules started ingesting red blood cells (Bogitsh and Carter, 1977; Moser *et al.*, 1980). After 1 h of adding red blood cells p38 MAPK phosphorylation increased to 1.9-fold that of the control ($p \leq 0.001$) (Figure 8.13 B), returning to basal levels after 24 h. Meanwhile, activation of the ~78 kDa PKC was also affected; 1 h after addition erythrocytes phosphorylation increased 2.5-fold ($p \leq 0.001$), and this was sustained at 24 h compared to levels prior adding the erythrocytes (Figure 8.13 B). Activated PKC in schistosomules fed red blood cells for 1 h or 24 h was strongly associated with the pre-acetabular glands, tegument and oesophagus compared to a more sub-tegumental localization observed in prior to addition of red blood cells (Figure 8.14).

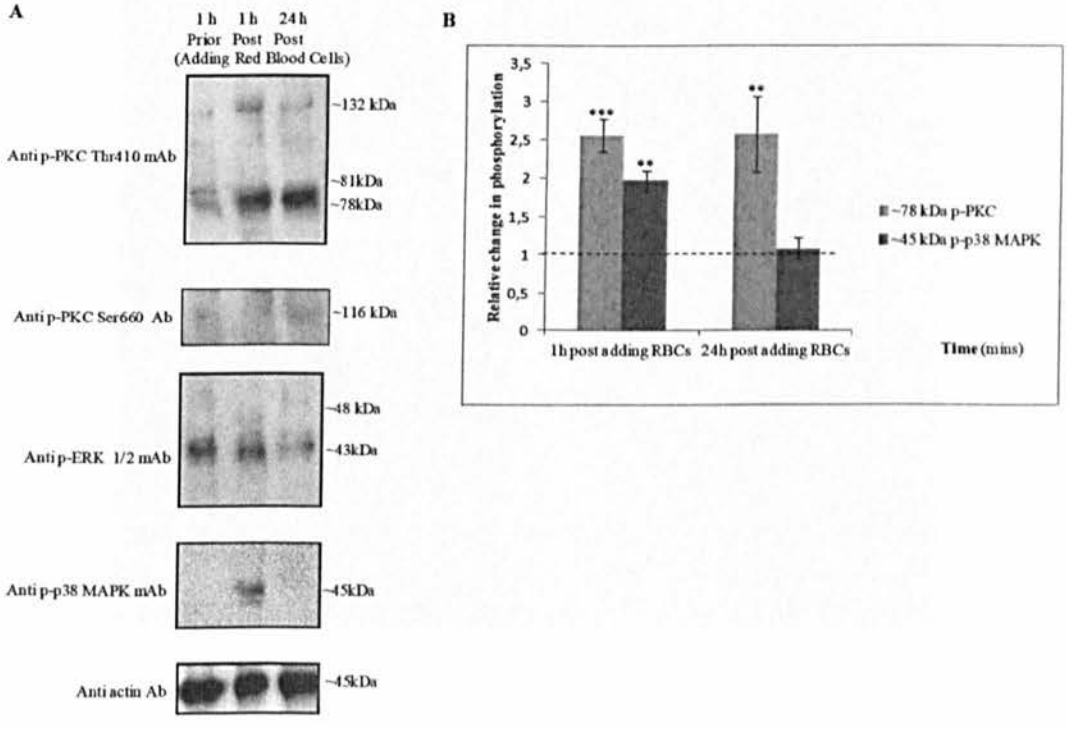

Figure 8.13- Phosphorylation of PKC, ERK and p38 MAPK in cultured *S. mansoni* schistosomules before and after adding red blood cells. (A) Representative immunoblot of schistosomules (~800) before and 1 h or 24 h after adding red blood cells; antibodies used were anti-phospho PKC (Thr410), anti-phospho PKC (Ser660), anti-phospho ERK1/2 and anti-phospho p38 MAPK. **(B)** Relative change in phosphorylation of the immunoreactive proteins detected in schistosomules which showed increases in activity. Mean values shown (± SEM) represent relative change in phosphorylation from three independent experiments (n=3) when compared to control (1 h before) levels that were assigned a value of 1. Immunoreactive bands were detected and quantified with a GeneGnome and Gene tools. $^{**}p \leq 0.01$ and $^{***}p \leq 0.001$.

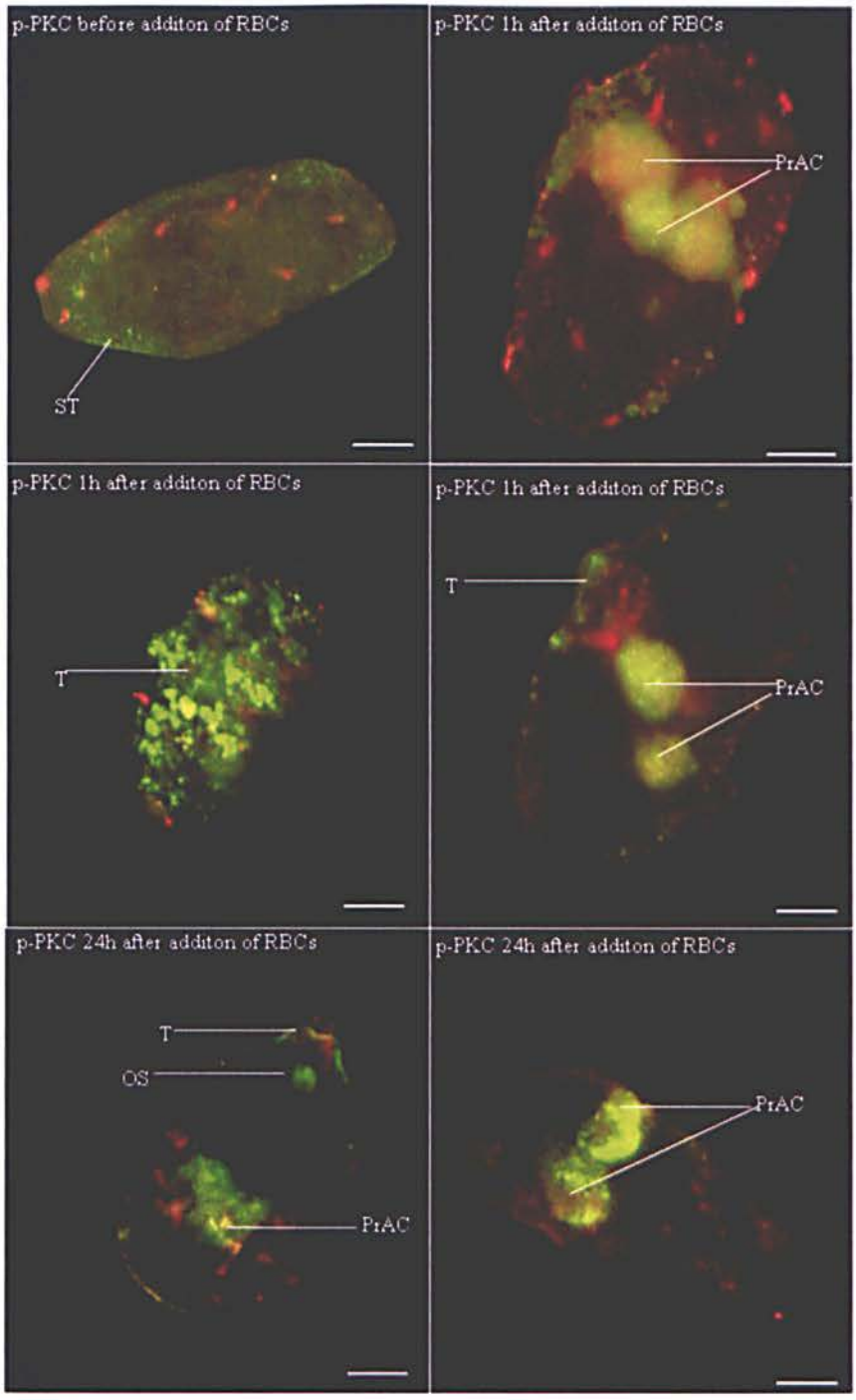

Figure 8.14 – *In situ* localization of PKC activation in 5 day *S. mansoni* schistosomules in the presence of murine red blood cells. Schistosomules were fed red blood cells for 1 h or 24 h and parasites fixed in acetone and stained with anti-phospho PKC (Thr410) and Alexa Fluor 488 antibodies (green); schistosomules fixed 1 h before adding blood cells served as a control. Representative micrographs of schistosomules, shown in maximum pixel brightness mode, show activity mostly associated with the tegument (T), pre-acetabular glands (PrAC), oral sucker (OS) region and sub-tegument (ST). Red signal represents actin filaments stained with rhodamine phalloidin. Bars = 10 μm.

8.3.6 *PKC appears to be involved in regulation of transferrin uptake in schistosomules*

It is known that transferrin (Tf), an iron transporter molecule, positively affects the growth and survival of *in vitro* cultured schistosomules (Clemens and Basch, 1989) and that PKC activation accelerates transferrin receptor internalization in human cells (Eichholtz *et al.*, 1992). Using fluorescently labelled Tf it is shown that Tf is absorbed through the tegument and after 30 min is localized in the schistosomule gut (Figure 8.15 A). Furthermore, PKC inhibition with 20 μM GF109023X for 120 min prior to adding transferrin appears to delay Tf internalization/absorption by ~40 min with Tf distributed throughout the tissues while in controls it is mainly localized centrally (Figure 8.15 B).

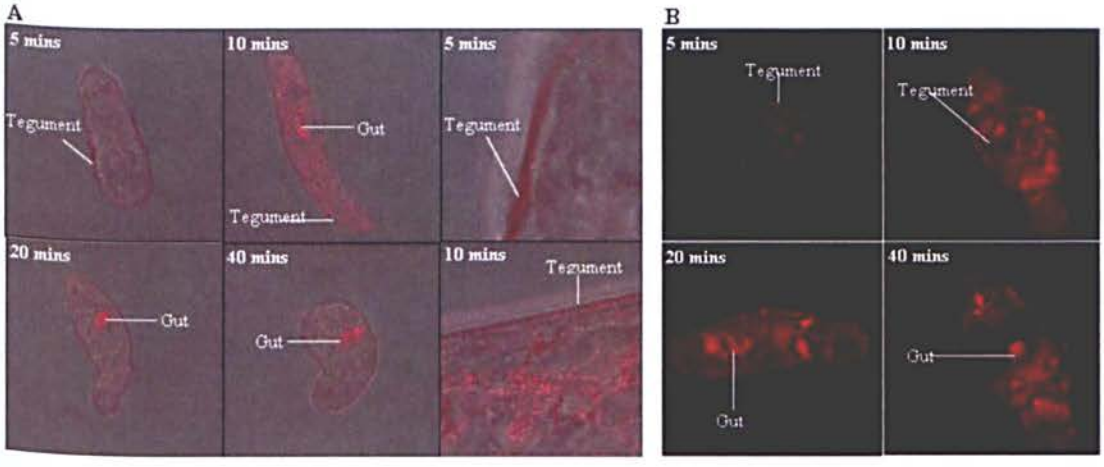

Figure 8.15 – Effect of GF109203X on transferrin uptake by *S. mansoni* schistosomules. (**A**) transferrin (red signal) uptake over time at room temperature. (**B**) Transferrin uptake over time after schistosomules were treated with 10 μM GF1093203X. Results are representative of the population from two independent experiments and show z-axis projections displayed in maximum pixel brightness mode.

8.3.7 *Modulation of PKC, ERK and p38 MAPK activity significantly affects viability, morphology and movement of schistosomules*

The effects of PMA, GF109203X, U0126 and SB203580 on schistosomule phenotype were tested in one-day-old cultured schistosomules. These compounds significantly affect PKC, ERK and p38 MAPK activity in other *S. mansoni* life-stages (Ressurreição *et al.*, 2011a, Chapters 4 and 6). Schistosomules were maintained for two days in different concentrations of each compound; untreated controls/DMSO vehicle

controls were also employed. Physiological effects were observed at 2 h, 24 h and 48 h and on the last day viability was assessed. Effects on morphology, standard deviation of perimeter, area and length of the parasites were quantified. Phenotypes were also categorized into those showing darkened body, darkened middle, granulated body, swollen body, elongated body, small and round body, or segmented body (Figure 8.16).

No significant changes in any parameter were observed between untreated control groups and 0.1% or 1% DMSO treatments. However 5% DMSO significantly increased the percentages of parasites with dark body, granulated and swollen morphologies ($p \leq 0.001$; Figure 8.17). These effects are somewhat similar to those observed by Stefanic *et al.* (2010) when culturing schistosomules in RPMI and Schneider's media. Therefore extra care needs to be taken in results interpretation when high DMSO concentrations ($\geq 5\%$) were used as a co-solvent.

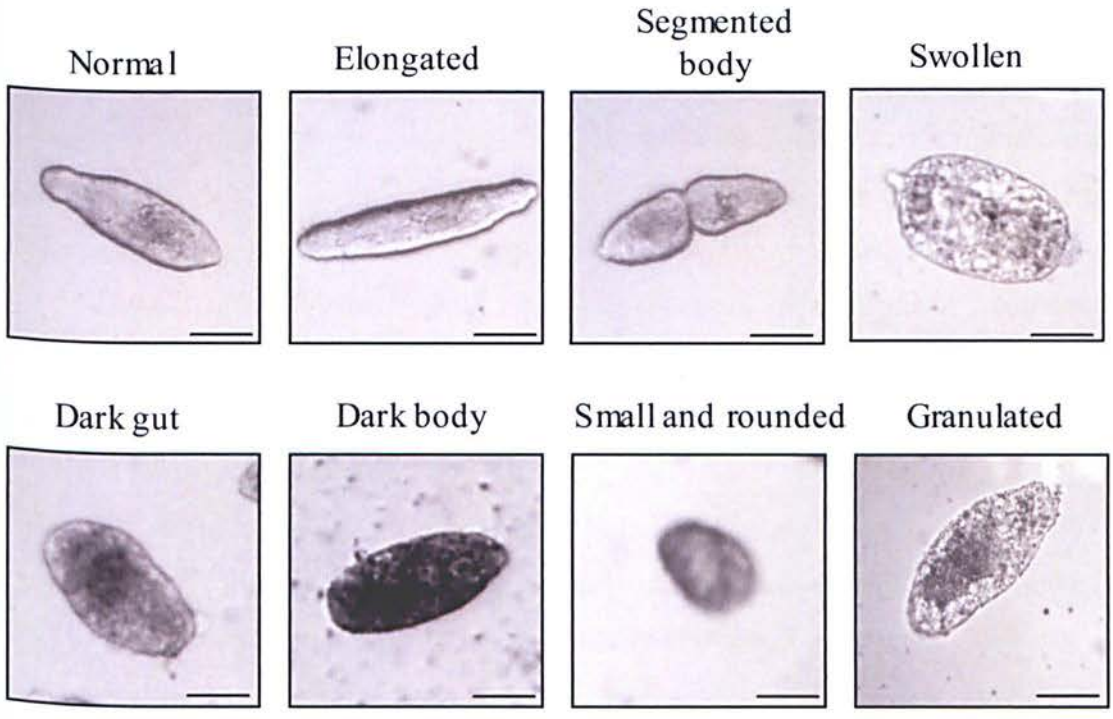

Figure 8.16 – Brightfield micrographs of phenotypes observed in cultured *S. mansoni* schistosomules during pharmacological assays. The normal and elongated phenotypewere those mostly observed throughout the assay in the untreated controls. The other phenotypes: schistosomules with segmented body, swollen, dark gut, fully dark body, small and rounded shape or granulated were considered abnormal. Results are representative of those seen in schistosomule populations obtained from three independent experiments Bars = 20 µm.

8.3.7.1 Effects of PKC inhibition and activation

PKC inhibition with GF109203X significantly altered the morphology, normal movement and viability of schistosomules. For instance after 24 h, 10 μM GF109203X or greater increased the proportion of schistosomules displaying darkened middles (guts) with increases of 27% ($p \leq 0.05$), 57% ($p \leq 0.001$), and 81% ($p \leq 0001$) observed for 10 μM, 30 μM and 50 μM, respectively compared to controls (Figure 8.17). At 100 μM, GF109203X also increased the number of schistosomules with dark bodies by 25% ($p \leq 0.05$) (Figure 8.17). Appearance of schistosomules with granulated bodies was also significantly increased at 30 μM or above ($p \leq 0.01$) with ~100% of schistosomules appearing this way at 50 μM. Finally, at 50 μM GF109203X the number of schistosomules seen with segmented bodies increased to 20% ($p \leq 0.05$) (Figure 8.17).

GF109203X did not affect area or length of schistosomules at any inhibitor concentration, at any time (Figure 8.18 D-I). However, for most GF109230X concentrations a significant reduction in standard deviation of perimeter was observed after 24 h and 48 h, and after 48 h almost all schistosomules were immobile ($p \leq 0.001$) (Figure 8.18 B and C). Schistosomule viability after 48 h GF109203X treatment was significantly reduced at 50 μM and 100 μM (44% and 48%, respectively; $p \leq 0.05$), compared to mean 89% viability of untreated controls (Figure 8.22A).

PMA also induced significant differences in schistosomule morphology compared to DMSO controls, especially darkened and granulated phenotypes. With 5 μM PMA or higher a significant increase in darkened body phenotype was observed ($p \leq 0.05$) (Figure 8.17) approaching 80% at 50 μM. High PMA concentrations (50 μM and 100 μM) also increased the presence of granulated phenotypes to 77% ($p \leq 0.01$) and ~50% ($p \leq 0.001$), respectively compared to the respective DMSO controls (Figure 8.17). At 100 μM PMA all organisms showed granulated bodies, a ~60% increase compared to the associated vehicle control ($p \leq 0.001$; Figure 8.17). PMA did not significantly affect the length or area of the organisms, however the standard deviation of perimeter significantly increased after 2 h with 2 μM, 5 μM, 10 μM and 20 μM peaking at 10 μM (Figure 8.19 B and C). The standard deviation of perimeter was then significantly reduced, after 24 and 48 hours, at concentrations of 20 μM or greater (Figure 8.19 B and C). The viability of 48 h PMA treated schistosomules was reduced at concentrations of 10 μM or higher with reductions ranging from 55% at 10 μM ($p \leq 0.05$) to 32% at 50 μM ($p \leq 0.01$), and 12% at 100 μM ($p \leq 0.05$) (Figure 8.22 C).

8.3.7.2 Effects of ERK pharmacological inhibition of activity

The MEK/ERK inhibitor U0126 significantly increased the number of parasites with dark, granulated and segmented bodies compared to respective DMSO controls (Figure 8.17). After 24 h, at all the different concentrations of U0126 tested significant increases in the number of dark bodied schistosomules to a maximum of 91% for 100 μM ($p \leq 0{,}001$) were observed. At 30 μM, 50 μM and 100 μM the number of schistosomules with a granulated appearance increased to 23% ($p \leq 0.05$), 33% ($p \leq 0.05$) and 60% ($p \leq 0.01$), respectively. Furthermore, at 50 μM U0126, 30% of the schistosomules possessed segmented bodies ($p \leq 0{,}001$) (Figure 8.17). Schistosomule behaviour was also affected; after 24 h and 48 h in 50 μM or 100 μM U0126 schistosomule motility was almost completely blocked (represented as standard deviation of perimeter) ($p \leq 0.001$) (Figure 8.20 B and C). U0126 did not significantly alter the average area and length of the cultured schistosomes (Figure 8.20). The viability of schistosomules treated with 50 μM and 100 μM U0126, determined after 48h, was also significantly reduced with decreases of ~30% ($p \leq 0.05$) and ~80% ($p \leq 0.001$), respectively (Figure 8.22 B).

8.3.7.3 Effects of pharmacological inhibition of p38 MAPK activity

At 100 μM the p38 MAPK inhibitor SB203580 increased to 21% the frequency of schistosomules with swollen phenotype ($p \leq 0.001$). Furthermore, at 2 μM, 5 μM and 10 μM the number of parasites with a small and rounded morphology increased 23%, 33%, 26%, respectively ($p \leq 0.01$), peaking at 5 μM (Figure 8.17). No other significant changes in morphology were detected however, behavioural changes were observed. The standard deviation of perimeter significantly increased after 2 h at 50 μM ($p \leq 0.05$) and 100 μM ($p \leq 0.01$) returning to control levels at 24 h and 48 h (Figure 8.21 A, B and C). Interestingly, the length of organisms was not significantly reduced but the total area was significantly lower in schistosomules maintained for 24h and 48h in 50 μM and 100 μM SB203580 ($p \leq 0{,}05$) (Figure 8.21 E and F). Viability of SB203580 treated schistosomules was not significantly affected by treatments (Figure 8.22 D).

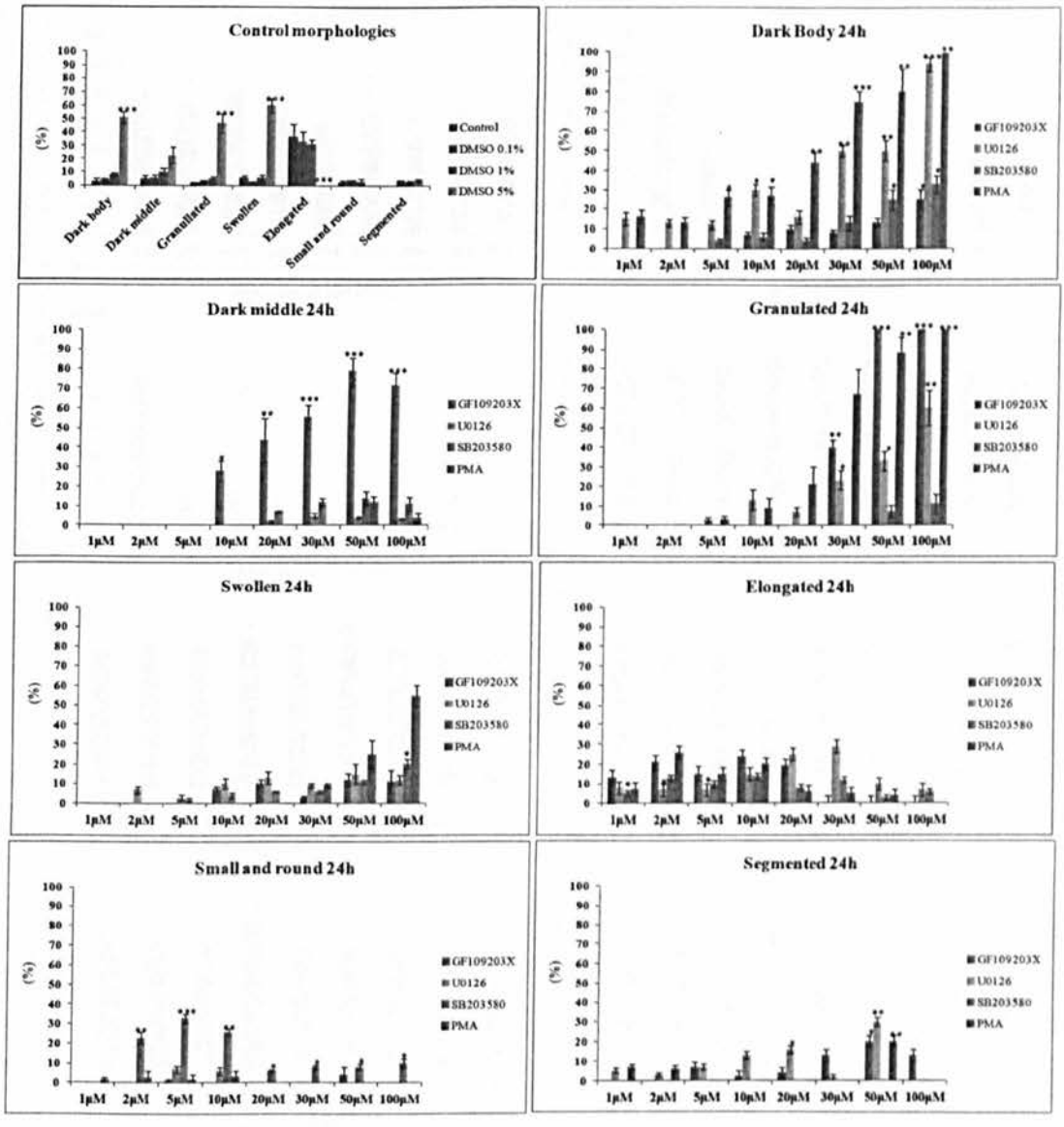

Figure 8.17 – Various phenotypes observed in cultured *S. mansoni* schistosomules under the different pharmacological treatments for 24 h. Schistosomules were treated with various concentrations of PKC inhibitor (GF109203X), PKC activator (PMA), ERK inhibitor (U0126), p38 MAPK inhibitor (SB203580), vehicle (DMSO), or were left untreated and were filmed. Presence of dark body, dark middle, granulated, swollen, elongated, small and round, and segmented phenotypes were quantified. Data are presented as mean (± SEM) percentage seen of the total population under each condition. n=90; *** = $p \leq 0.001$. ** = $p \leq 0.01$, and * = $p \leq 0.05$. Results are from three independent experiments with two replicates each.

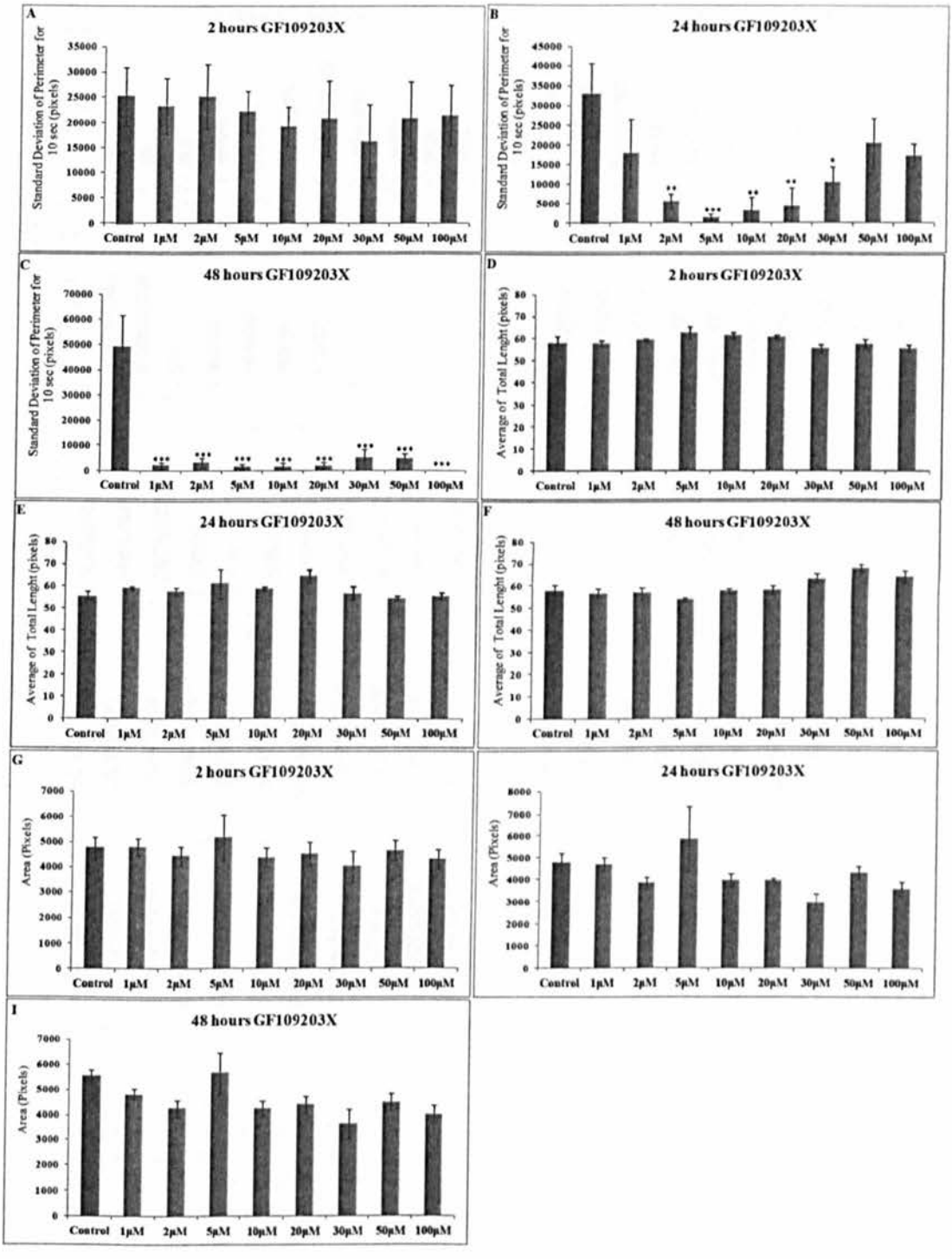

Figure 8.18 – Effects of various concentrations of GF109203X on schistosomule standard deviation of perimeter, area and length at 2, 24 and 48 h. (**A-C**) Mean standard deviation of the schistosomule perimeter over 10 s. (**D-F**) Mean length of schistosomules (**G-I**) Area of schistosomules. Each parameter was measured in pixels and means (± SEM) are shown, n=60. *** = $p \leq 0.001$, ** = $p \leq 0.01$ and * = $p \leq 0.05$) when compared to media only controls. These results are from three independent experiments with two replicates each.

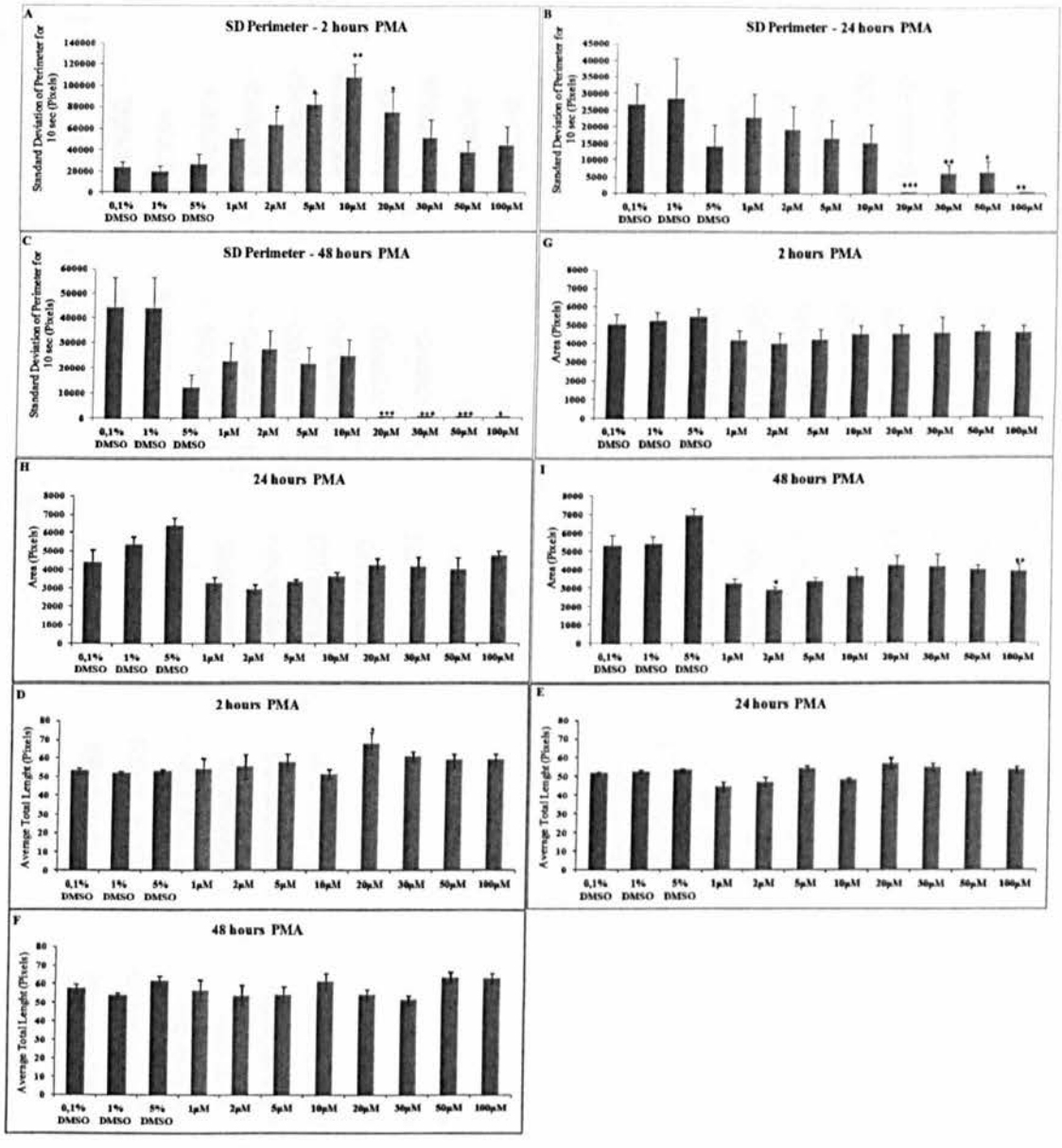

Figure 8.19 – Effects of various concentrations of PMA on schistosomule standard deviation of perimeter, area and length at 2, 24 and 48 h. (A-C) Mean standard deviation of the schistosomule perimeter over 10 s. **(D-F)** Mean length of schistosomules **(G-I)** Area of schistosomules. Each parameter was measured in pixels and means (± SEM) are shown, n=60, *** = $p \leq 0.001$, ** = $p \leq 0.01$, and * = $p \leq 0.05$, when compared to the respective DMSO control. The results are from three independent experiments with two replicates each.

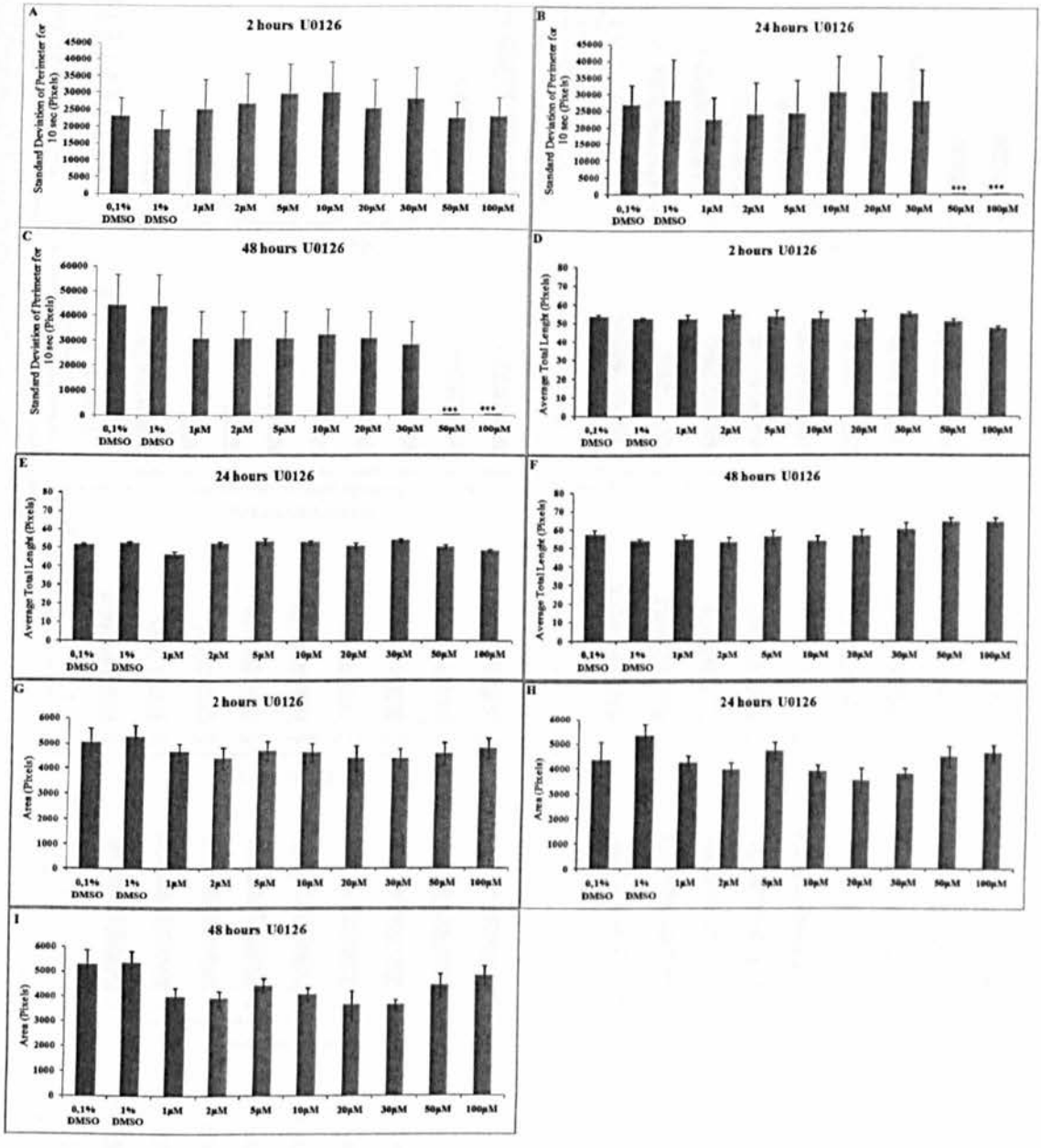

Figure 8.20 – Effects of various concentrations of U0126 on schistosomule standard deviation of perimeter, area and length at 2, 24 and 48 h. **(A-C)** Mean standard deviation of schistosomule perimeter over10 s. **(D-F)** Mean length of schistosomules **(G-I)** Mean area of schistosomules. Each parameter was measured in pixels and means (± SEM) are shown, n=60. *** = $p \leq 0.001$) ** = $p \leq 0.01$, and * = $p \leq 0.05$, when compared to the respective DMSO control. The results are from three independent experiments with two replicates each.

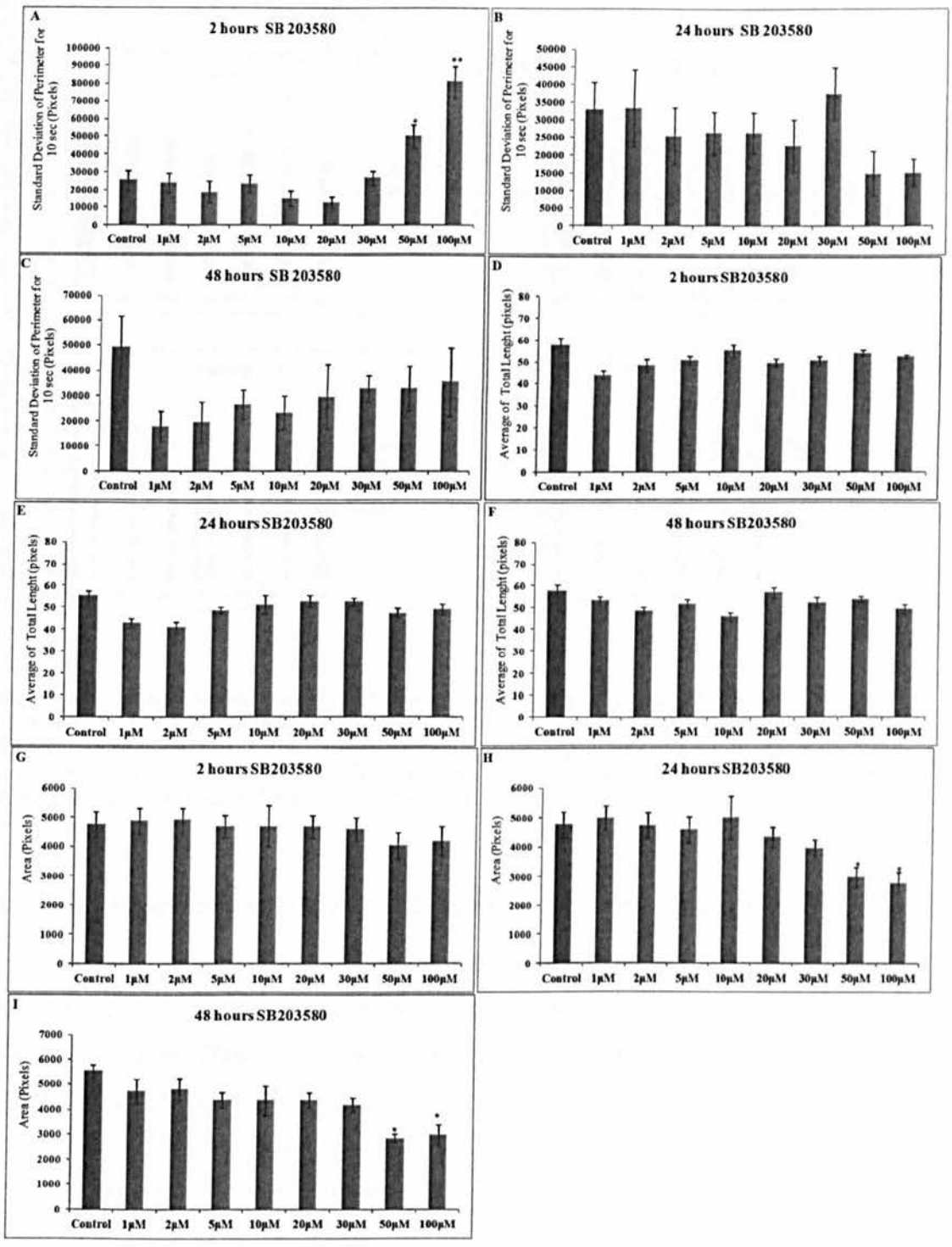

Figure 8.21 – Effects of various concentrations of SB203580 on schistosomule standard deviation of perimeter, area and length at 2, 24, and 48 h. (A-C) Mean standard deviation of the schistosomule perimeter over 10 s. **(D-F)** Mean length of schistosomules. **(G-I)** Mean area of schistosomules. Each parameter was measured in pixels and means (± SEM) are shown, n=60. *** =$p \leq 0.001$, ** = $p \leq 0.01$ and * = $p \leq 0.05$, when compared to media only controls. The results are from three independent experiments with two replicates each.

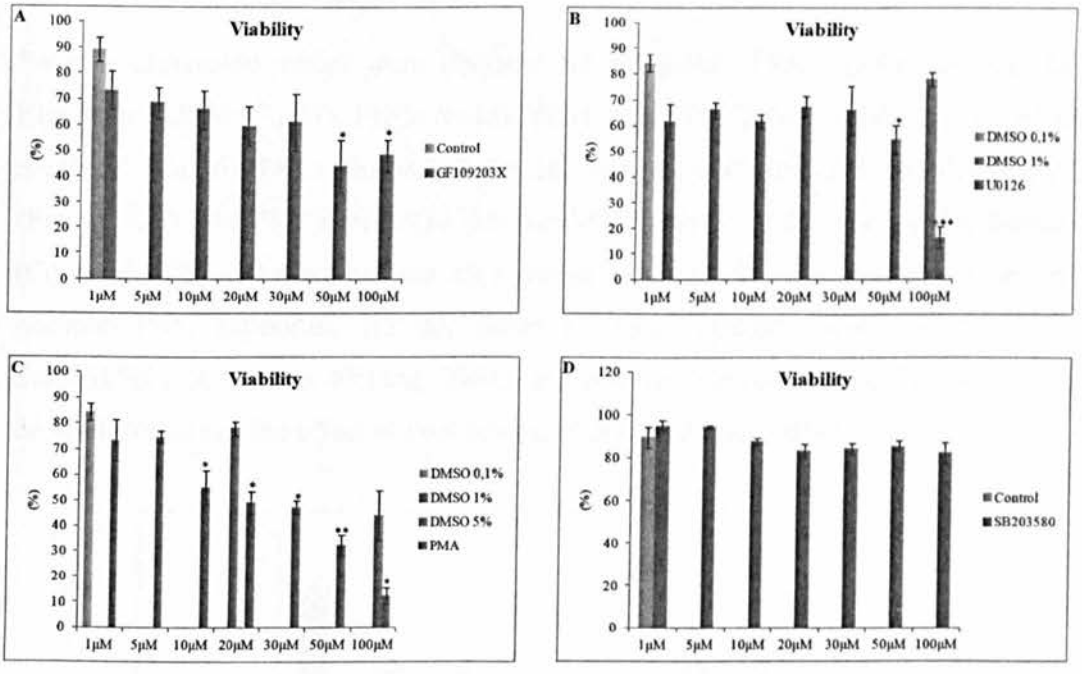

Figure 8.22 – Schistosomule viability at 48 h in various treatments from fluorescent measurements after dual FDA and PI staining. Mean viability (%, ± SEM) of schistosomules in response to various concentrations of GF109203X, U0126, SB203580, PMA and DMSO (vehicle) after 48 h culture. *** = $p \leq 0.001$), ** = $p \leq 0.01$, and * = $p \leq 0.05$, when compared to the appropriate control. Results are from three independent experiments with two replicates each.

8.3.8 RNA interference of PKC and ERK expression in cultured schistosomules

Specific primers were developed to amplify DNA sequence of four *S. mansoni* PKC (*Sm128480*, *Sm096310*, *Sm17630* and *Sm131700* and two ERK (*Sm142050* and *Sm047900*) genes (Table 8.1) and gene expression assessed by qRT-PCR. Two housekeeping genes (*α-tubulin* and *GAPDH*) previously used as controls (Moraes Mourão *et al.*,2009) and other primers for the *Sm176030* gene previously used with *S. mansoni* sporocysts (Moraes Mourão *et al.*, 2009) were also employed (Table 8.2 in Appendix B). After detection of PKC and ERK gene expression, siRNAs were designed to knockdown gene expression (Table 8.2) and physiological effects of knockdown on schistosomules assessed over 6 days.

8.3.8.1 Detection of gene expression

Positive expression values were obtained for all genes: ERK2 *Sm047900* (Cq 28), ERK1 *Sm142050* (Cq 31), PKCε *Sm131700* (Cq 26), PKCβ *Sm128480* (Cq 28), PKCβ *Sm17630* (Cq 26), PKCι *Sm096310* (Cq 28), *α-tubulin* (Cq 23) and *GAPDH* (Cq 22) (Figure 8.23). The PKC Sm176030 (Moraes Mourão *et al.*, 2009) was weakly detected (Cq value >35) and therefore not used further (Figure 8.23). Interestingly, both anti-phospho PKC antibodies did not detect a phosphorylated ~96kDa PKC (PKCε; Smp131700) in western blotting. However, as gene expression was detected it was decided to also test the effect of knockdown of this gene with siRNA.

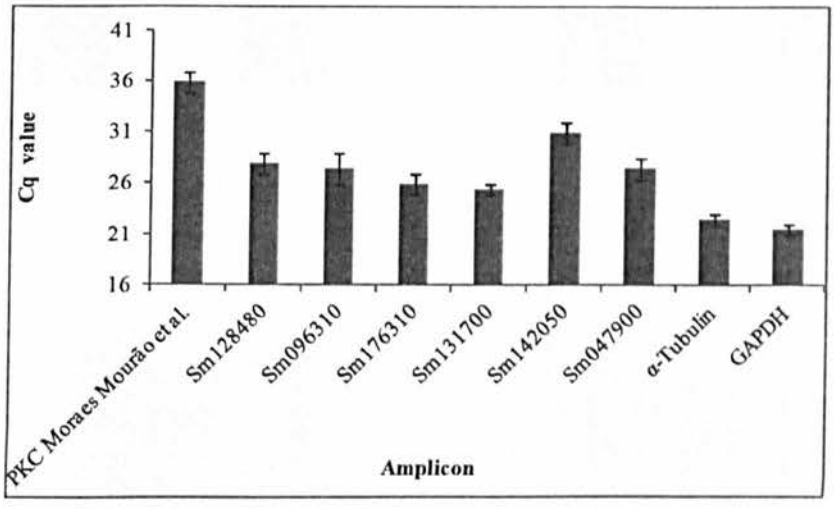

Figure 8.23 – PKC and ERK gene expression in schistosomules. Schistosomules maintained 72h after mechanical transformation of cercariae were isolated and mRNA extracted. 0.1 µg of schistosomule cDNA and 0.5 µM of each primer was used for amplification of the respective genes and the mean (± SEM) expression of PKC from Moraes Mourão *et al.* (2009), Sm176310 (PKCβ ~116kDa), Sm128480 (PKCβ ~77kDa), Sm096310 (PKCι ~81kDa), Sm17630 (PKCβ ~116kDa), Sm131700 (PKCε ~96kDa), Sm142050 (ERK1 ~48 kDa) and Sm047900 (ERK2 ~43 kDa) determined by quantitative RT-PCR. The expression of the two housekeeping genes α-tubulin and GAPDH were determined as internal controls using sequences previously published. Results are from two independent experiments with three replicates each.

8.3.8.2 Knockdown and selection of most effective siRNAs

Schistosomules were soaked for five days with 2 µM siRNA sequences designed to knockdown PKC and ERK gene expression; a non-target siRNA was used as a control (Table 8.1 in Appendix B). Although expression of all genes was detected (Figure 8.23) significant knockdown was only achieved with siRNAs targeting PKC Sm176360 and ERK Sm047900 with a reductions of 25% and 30% ($p < 0.05$), respectively compared to non-siRNA treated and housekeeping gene expression levels

(Figure 8.24 A and B). This gene suppression did not affect mRNA levels of α-tubulin and GAPDH. Furthermore, western blotting showed a reduction in activation of ~116 kDa PKC to less than 60% of control levels with siRNA targeting Sm176360 but not of the ~43kDa ERK with the siRNA target for Sm1047900 (Figure 8.24 C and D). Interestingly, schistosomules treated with siRNA Sm176360 displayed increased activity of the ~81kDa PKC (Figure 8.24 C and D), possibly as a result of compensation.

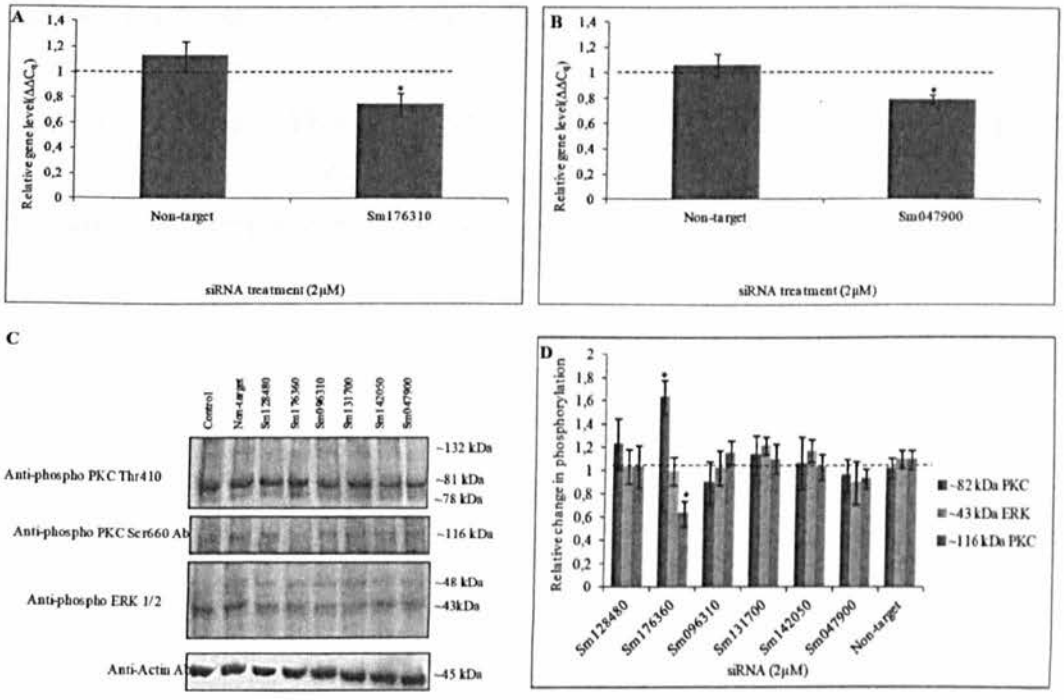

Figure 8.24 – Effects of PKC and ERK expression knockdown in schistosomules with siRNA. (A) Expression of ERK and PKC mRNA in schistosomules after RNAi experiments (at 6 days) with siRNAs designed against Sm128480 (PKCβ ~77kDa), Sm096310 (PKCι ~81kDa), Sm176360 (PKCβ ~116kDa), Sm131700 (PKCε ~96kDa), Sm142050 (ERK1 ~48 kDa), Sm047900 (ERK2 ~43 kDa), non-target scrambled control, or no siRNA (untreated control). **(A)** and **(B)** Mean ΔΔ Cq values for PKC Sm176360 (~116kDa) and ERK Sm047900 (~43 kDa) determined by quantitative RT-PCR. **(C)** Immunoblot with anti-phospho PKC (Ser660), anti-phospho PKC (Thr410) and anti-phospho ERK antibodies revealing phosphorylation status of PKC and ERK in schistosomule protein extracts after siRNA treatments. **(D)** Graphic representation of mean relative change (± SEM) in phosphorylation of kinases, which correspond to the gene sequences significantly affected by RNAi, dashed line represent untreated control. The C_q values from technical replicates were averaged. The ΔC_q of each replicate was exponentially transformed to the ΔC_q expression before averaging and determining the standard deviation. The mean was then normalized to the expression of each PKC or ERK gene from a separate well treated with control untreated (no siRNA) to find the $\Delta\Delta C_q$ expression. Results are expressed as the ratio of the targeted ΔC_q expression to the non-targeted ΔC_q expression. Results are from two independent experiments each performed in duplicate n=4. *** = $p \leq 0{,}001$, ** = $p \leq 0{,}01$, and * = $p \leq 0.05$.

8.3.8.3 Effects of PKC Sm176360 and ERK Sm1047900 knockdown on viability, morphology and movement of schistosomules

Schistosomules treated with siRNAs against PKC Sm176360 and ERK Sm047900 and those treated with non-target siRNA (siRNA control) or without siRNA (control) were videoed and photographed daily for 5 days and the viability, standard deviation of perimeter, total area, length and morphological changes assessed. No significant differences were observed in these parameters between schistosomules from all treatments relative to controls but large variability was observed within each treatment. Although, ERK Sm047900 knockdown increased the mean length of schistosomules by 33% the effect was not statistically significant due to the high individual variability observed (data not shown).

8.4 Discussion

Schistosomules are resistant to currently available anti-schistosome chemotherapy and are adapted to use host signals to complement their own signalling pathways (Walker, 2011). To ensure survival within the host this larval stage undergoes several morphological, physiological and metabolic changes during and after transformation from *S. mansoni* cercariae (Clegg and Smithers, 1972; Brink *et al.*, 1977). As sensing and responding to host factors is essential for schistosomes, studying signal transduction mechanisms is important for elucidating schistosome host-parasite interactions and parasite biology (Bahia *et al.*, 2006; Dissous *et al.*, 2006; Dissous *et al.*, 2007b; You *et al.*, 2010).

8.4.1 Roles for PKC, ERK and p38 MAPK signalling during the development of early-stage S. mansoni *schistosomules*

The activation of PKC, ERK and p38 MAPK was assessed in *S. mansoni* schistosomules maintained in culture for four days. This period corresponds *in vivo* to the skin stage (Gobert *et al.*, 2010) when many tegumental and metabolic transformations occur together with orientated movement towards deeper layers of the dermis (Stirewalt, 1974; Hockley and McLaren, 1973; Samuelson *et al.*, 1982). At this stage all the PKC, ERK and p38 MAPK signalling proteins detected in other *S. mansoni* life-stages (see Chapters 3, 5 and 6) were active, however the ~135 kDa PKC, ~48 kDa ERK and p38 MAPK were weakly phosphorylated. The most activated proteins were the ~81 kDa, ~79 kDa and ~116 kDa PKCs and the ~43 kDa ERK.

8.4.1.1 Putative roles for ~81 kDa PKC during the skin- to lung-stage transition

During the four days culture, phosphorylation of the ~81 kDa PKC significantly changed, increasing at day three. Concomitantly activated PKC [detected with anti-phospho PKC (Thr410) antibodies that detect this PKC] was associated with the surface and several internal structures including the subtegument, caecum, oesophagus, nephridiopore, germinal cell mass and pharyngeal muscles. Interestingly, the increased PKC activity occurred at a time similar to that when schistosomules develop to the

lung-stage in the circulation (Osman *et al.*, 2003) where morphological changes and muscular activity occurs (Hockley and McLaren, 1973; Moser *et al.*, 1980; Crabtree and Wilson, 1980). *In* vivo, at day three, schistosomules start to elongate (Crabtree and Wilson, 1980) and increase muscular activity with more cycles of elongations and contractions (Moser *et al.*, 1980). Also, around the fourth day the mid-body spines and the head capsule musculature disappear (Crabtree and Wilson, 1980). This suggests an involvement of the ~81 kDa PKC in developmental differentiation and neuromuscular activity especially as the PKC inhibitor GF109203X reduced schistosomule movement (expressed as standard deviation of perimeter) at concentrations as low as 2 μM and PMA increased muscular activity. Moreover, ≥10 μM GF109203X increased the frequency of the segmented body phenotype (an aberrant phenotype not previously reported in the literature) that could be result from abnormal neuromuscular function.

Interestingly, inhibition of PKC with ≥50μM GF109203X or activation with ≥10μM PMA reduced schistosomule viability, which correlated with more aberrant phenotype indicators of toxicity (dark bodied and granulated bodied larvae) (Stefanic *et al.*, 2010). GF109203X (≥10 μM) also increased the numbers of schistosomules with dark guts suggesting necrosis since absorptive processes are unlikely as the gut is not functional until day five (El-Shehabi *et al.*, 2009).

Changes in the pattern of PKC activation in schistosomules were also observed with the anti-phospho PKC (Ser660) antibody (that does not detect ~81 kDa PKC). Fluorescence was transiently associated with the tegument 16 h post transformation, suggesting an involvement of other PKCs in the remodelling of the parasite surface that is known to happen at this time (Hockley and McLaren, 1973). In older schistosomules activated PKC was observed in internal structures of unknown function. PKC therefore appears to play various isotype-specific roles in the schistosomule life-stage.

8.4.1.2 Schistosomule ERK activity is associated with neuromuscular structures

Throughout the four days culture, ERK activation and the *in situ* distribution of activated ERK did not change significantly. ERK was mainly associated with the tegument, muscle or nerve fibres, and sometimes acetabulum and oesophagus suggesting roles for ERK in tegumental and muscular functions. Prominent activation was associated with the network of fibres that run along the length of the body suspected to be crucial for muscular contraction (Patocka and Ribeiro, 2012). This is

relevant as after cercarial transformation, the newly transformed schistosomule migrates by burrowing through the skin to find the vasculature, an act that requires extensive muscular contraction (Hockley and McLaren, 1973). Therefore ERK could be directly involved in this migratory process, *via* regulation of muscular processes.

Surprisingly, low concentrations of the ERK inhibitor U0126 did not affect schistosomule movement. Movement was, however, completely attenuated with higher concentrations of the inhibitor at 24 h (≥ 50 μM). Although this might be associated with toxicity since the viability of schistosomules decreased at 48 h and dark/granulated bodied schistosomules increased, not all schistosomules were killed by 50 μM U0126. The appearance of schistosomules with segmented bodies may suggest alterations of neuromuscular function. To further understand roles of ERK in schistosomules, longer exposure times at later stages of development would be necessary, and perhaps migration assays might identify if migratory behaviour is affected by ERK inhibition.

8.4.1.3 Putative roles for p38 MAPK

Although p38 MAPK activation did not change significantly, changes in the distribution of activated p38 MAPK were observed during the four days culture. Active p38 MAPK was initially associated with the tegument and cecum but after the first day it disappeared from the tegument and was seen at the pharyngeal muscle, parenchyma, acetabular glands, caecum, oesophagus and other unidentified regions. This change in phosphorylated p38 MAPK distribution coincided with transference from serum-free BME medium to complete Basch's medium, suggesting a role for p38 MAPK in schistosomule nutrition. In this context, p38 MAPK inhibition with low concentrations of SB203580 (≥ 2 μM) increased the number of small rounded schistosomules but did not affect viability. P38 MAPK is an evolutionary conserved regulator of apoptotic processes (Wada and Penninger, 2004) and the lack of death at 100 μM SB203580 shows that inhibition likely sustains survival as has been observed in free-living planarians in our laboratory (Anthony Walker, personal communication).

8.4.1.4 PKC, ERK and p38 MAPK in the tegument

The tegument represents the host-parasite interface (Moraes *et al.*, 2012) and is extensively remodelled during cercarial transformation and the initial stages of

schistosomule development (Hockley and McLaren 1972). During this process new surface membranes are formed and membrane maturation occurs (Wiest et al., 1988). Activated PKC, ERK and p38 MAPK were found associated with the tegument at various time points evidencing the importance of these kinases in tegumental processes which occur during such development. In addition to tegument transformation, parasite-host communication and/or immune system modulation are thought to occur (Hockley and McLaren, 1973; Moser *et al.*, 1980; Skelly and Alan Wilson, 2006). PKC has previously been implicated in maintaining tegument integrity of schistosomes (Espinoza *et al.*, 1991; Wiest *et al.*, 1994) and PKC (and possibly ERK and p38 MAPK) could thus have critical roles in parasitic immune evasion. Stirewalt (1961, 1963) described rapid changes in the antigenic nature and permeability of cercariae after host penetration that may be connected with the changes in the membrane. Smithers *et al.* (1969) suggested that antigens at the parasite surface enable host immune evasion and it is known that most schistosomules are protected within 24 h against damage by antibodies (Clegg and Smithers 1972). As proteins at the surface of schistosomules and adult worms are logical targets for vaccine and drug development (Loukas et al., 2007), PKC, ERK and p38 MAPK appear to represent potential therapeutic targets.

8.4.2 Lack of significant phenotypic effects from siRNA knockdown

Increasing evidence indicates that loss-of-function genetic manipulation through RNAi may be generally applicable for investigation of schistosome genes (Krautz-Peterson *et al.*, 2007; Correnti *et al.*, 2005). Indeed, an orthologue of dicer, one of the central enzymes of the RNAi cascade, has been characterized in *S. mansoni* and its expression appears to be highest in schistosomules (Krautz-Peterson and Skelly, 2008). The short interfering RNAs join with the effector nuclease complex (Tavernarakis *et al.*, 2000) which recognizes and attacks the homologous target mRNAs, leading to long-term knockdown and silencing of the target gene in schistosomes (Correnti *et al.*, 2005). In terms of delivery of dsRNA, electroporation and soaking of schistosomules has proved to be an effective delivery method for gene silencing within this developmental stage (Krautz-Peterson *et al.*, 2007; Correnti *et al.*, 2005).

Here, although all gene targets (PKC Sm128480, PKC Sm096310, PKC Sm17630, PKC Sm131700, ERK Sm142050 and ERK Sm047900) were expressed, only PKC Sm176360 and ERK Sm047900 dsRNAs were effective in knocking down

their respective genes. Unfortunately, no significant behavioural and morphological changes were observed due to the large variability seen. Two factors/mechanisms might be responsible for this failure; compensation for the enzyme loss *via* over expression of other isoform(s) and/or uneven uptake of the dsRNA by the schistosomules. Western blot analysis showed reduced activation of the ~116kDa PKC after siRNA knockdown, that might have been compensated by the increased ~ 81 kDa PKC activity observed. This phenomenon, widely described in the literature (review by Prelich, 2012), could constitute a major obstacle for the analysis of functions of signalling proteins *in vivo*.

The variability of altered phenotypes is consistent with results reported in several model eukaryotes including cultured *S. mansoni* schistosomules (Correnti *et al.*, 2005), *C. elegans* (Grant and Hirsh, 1999; Hashmi *et al.*, 2002; Simmer *et al.*, 2003) and *T. brucei* (Ullu *et al.*, 2004) in which such variation is considered to be due to unequal take up of dsRNA. Since the mouth of schistosomules remains closed until 7 days after transformation, entry of dsRNA through this orifice is not possible for younger parasites (Krautz-Peterson *et al.*, 2007). Instead, the dsRNA likely enters young schistosomules through the remnant acetabular glands (Krautz-Peterson *et al.*, 2007).

8.4.3 Involvement of PKC, ERK but not p38 MAPK activity in parasite-host communication

Diverse molecular pathways dependent on kinase signalling have been described in schistosomes and are thought to be involved in host-parasite relationships (Dissous et al., 2006). Receptors for human EGF, IGF-I and INS have been identified in schistosomes (Shoemaker *et al.*, 1992; Vicogne *et al.*, 2003; Khayath *et al.*, 2007; Ahier *et al.*, 2008; You *et al.*, 2010), although how these factors affect schistosome signalling has not previously been investigated (You *et al.*, 2009)

8.4.3.1 Human factors stimulate S. mansoni *PKC and/or ERK activity*

This study shows for the first time that host molecules directly affect PKC and ERK signalling in schistosomules. Human EGF is known to induce cellular processes such as proliferation and differentiation by acting *via* MAPK, PI3K/Akt and STAT 5 pathways (Citri and Yarden, 2006), and in parasites such as *T. brucei* has been involved

with growth rate regulation (Sterneberg and McGuigan, 1994). In three day-old schistosomules human EGF increased the phosphorylation of ~81 kDa PKC at 15 min and ~43 kDa ERK at 30 min. PKC was found to act upstream of ERK in adult worms (Chapter 4) and ERK activation by human EGF has been reported in the helminth parasite *E. multilocularis* (Spiliotis *et al.*, 2006). Moreover, the *S. mansoni* EGFR (SER), the first of its kind to be described in schistosomes, contains an extracellular domain for binding EGF (Shoemaker *et al.*, 1992; Dissous *et al.*, 2006). It has been proposed that parasitic helminths bind hormones to their external surfaces activating downstream signalling essential for growth, infectivity and differentiation (Escobedo *et al.*, 2005; Walker 2011). That PKC and ERK were activated at the surface of the parasite suggests that this could occur in schistosomules. Unfortunately, certain regions showing considerable activity were seen within the parasite but were hard to identify due to the lack of literature on schistosomula morphology and the fact that this life-stage is characterised by constant growth, reorganization and differentiation.

Insulin exerts wide effects on mammalian systems modulating a variety of biological processes and metabolic pathways such as glucose and lipid metabolism, protein synthesis and degradation, cell growth and differentiation (Pollak, 2007). It has been demonstrated that INS stimulates the growth and metabolism of schistosome larvae (Vicogne et al., 2004), increases glucose uptake by schistosomes (Ahier *et al.*, 2008; You *et al.*, 2009), and INS injection of mice infected with S. *mansoni* increases worm burden and parasite size (Saule *et al.*, 2005). Two types of INS receptors have been reported in *S. mansoni*, which were shown to interact with human INS (Vicogne *et al.*, 2003). In the present study INS (1μM) increased ~116 kDa PKC and ~43 kDa ERK activity after 30 min. These results agree with other systems in which INS activates PKC and ERK through GPCRs (Sugano *et al.*, 2006; Kang *et al.*, 2008). *In situ* localization revealed increased PKC activity associated with the tegument, fibre like structures, ventral sucker and oesophagus in response to INS treatment. Furthermore, ERK activity was associated with the tegument surface. These results suggest that INS might not only regulate tegumental signalling and function, but also oesophageal and neuromuscular functions.

IGF-I is a protein with high sequence similarity to INS associated with several functions including neurotrophic, muscular, and insulin complementation (Boucher *et al.*, 2007). Interestingly, IGF-I increased activation of the ~116 kDa PKC (β type), the same PKC affected by human INS. This supports that this PKC isoform is associated

with schistosome transregulation by both INS and IGF-I. *In situ* localization showed PKC activity associated with the cecum, unidentified internal structures, oesophagus and the nephridiopore suggesting roles in differentiation and absorptive processes. However, in contrast to INS but mainly EGF treatment, no association with the tegument was observed.

8.4.3.2 PKC involvement in schistosomule transferrin internalization via *the tegument*

Use of fluorescently labelled transferrin enabled internalization of this iron transporter molecule to be tracked in schistosomules, revealing that its incorporation occurs *via* the tegument. Moreover, PKC inhibition with 20μM GF109023X delayed transferrin incorporation showing that active PKC is involved in the regulation of this mechanism. The fact that PKC affects the rate of transferrin intake in human cells (Eichholtz et al., 1992) suggests a conserved function for this signalling protein in iron uptake. To confidently associate PKC activity with transferrin internalization, RNAi studies should be further explored. Nevertheless, here a way of studying transferrin internalization in schistosomules has been developed that could benefit future studies. Given that transferrin has been reported to equal the effect that serum has in the growth and development of early stage *S. mansoni* schistosomules further work into transferrin uptake is warranted (Clemens and Basch, 1989).

8.4.3.3 Host erythrocytes stimulate PKC activity in schistosomules

Adding packed mouse red blood cells to five day-old schistosomules increased ~78 kDa PKC activation at 1 and 24 h with the activated kinase strongly associated with the acetabular glands and developing gut. This suggests that erythrocyte-mediated up-regulation of PKC activity could be associated with digestive and perhaps absorptive processes, such as proteolysis of haemoglobin (McCarthy *et al.*, 2004; Delcroix *et al.*, 2006). Moreover, PKC inhibition markedly increased the frequency of schistosomules with dark guts (likely due to gut necrosis) supporting a role for PKC in digestive functions. In the presence of red blood cells the stimulation of p38 MAPK phosphorylation was transient, peaking 1 h after erythrocyte addition and returning to basal levels at 24 h. This increment in activation might be due to environmental stress as this kinase is activated by a variety of cellular stresses (Coulthard *et al.*, 2009). It is known that heme released from haemoglobin digestion is toxic to schistosomes but a

mechanism of aggregation of transforming heme into an isoluble form (hemozoin) followed by its regurgitation averts this toxic effect (Oliveira et al., 2004).

8.4.3 Conclusions

Investigation of the levels and localization of activated PKC, ERK and p38 MAPK in skin-stage schistosomules coupled with functional assays has revealed valuable insights into the biology of schistosomules in the context of early development and survival. Furthermore, the involvement of ERK and PKC signalling in the molecular crosstalk mediating the *S. mansoni* response to the host's microenvironment was demonstrated for the first time. And a new method using labelled transferrin to track host macromolecule uptake in schistosomules was developed disclosing the involvement of the tegument and of PKC in the internalization process. This new method could be employed in research involving other host molecules. It would be valuable to determine the roles of PKC, ERK and p38 MAPK in older schistosomules and to further optimize RNAi studies to understand the isotype-specific roles of PKC and ERK. Nevertheless, the presented data provides the first steps for further detailed investigation of the molecular biology and transactivation mechanisms between conserved signalling systems of *S. mansoni* and its mammalian host. Such knowledge will contribute significantly to the understanding of schistosome biology and may reveal novel anthelmintic targets particularly as the skin-stage is regarded as a vulnerable stage for parasite killing (Wilson and Coulson, 2009).

Chapter 9

Final Conclusions

Human schistosomiasis imposes enormous social, economic and public health impact in tropical and subtropical regions of the world causing extensive morbidity in infected individuals (Steinmann *et al.*, 2006). Affecting the world's "bottom billion", this neglected tropical disease has direct consequences on the economic development of a country and is far from being eradicated. The drug of choice (PZQ) for the treatment of schistosomiasis is inexpensive and has been incorporated into many successful control programmes. However, it acts *via* unknown mechanisms, is only effective against the egg laying adult stage, does not prevent reinfection, and threatening genetic resistance is emerging (Cioli and Pica-Mattoccia, 2003; Caffrey, 2007; Geary *et al.*, 2010). Hence, a better understanding of schistosome molecular biology is essential to identify molecular targets for new therapeutics and to increase the chance of successful disease control and perhaps eradication. This study set out to explore the molecular biology of human infective and dependent life-stages of *S. mansoni* (cercariae, schistosomules and adult worms), particularly focusing on the involvement of PKC, ERK and p38 MAPK signalling in schistosome function.

Three commercially available anti-phospho antibodies (anti-phospho-PKC (Thr410), anti-phospho PKC α/βII (Thr638/641) and anti-phospho p44/p42 MAPK (ERK)) were found to be suitable for studying *S. mansoni* PKC and ERK signalling, detecting three previously unstudied phosphorylated (activated) PKC (~81 kDa, ~116 kDa and ~132 kDa) and two phosphorylated ERK (~43 kDa and ~48 kDa) isotypes. The detected proteins possessed PKC/ERK activities and responded to pharmacological modulation with inhibitors and activator. Although high levels of conservation in key domains exist between schistosome and mammalian forms of these kinases some regions show low sequence homology, possibly making them suitable for selective drug targeting. The activation of PKCs and ERKs varied in different life-stages suggesting isotype specific roles during development, with a higher number of active PKC and ERK isotypes in complex life-stages such the adult worm showing a relationship between parasite complexity and signalling complexity. Detection of an unusually large ~132 kDa PKC-like protein, not predicted in the genome annotation, but detected with three different anti-phospho PKC antibodies, suggests conservation of the ancestral character of the PKC family in schistosomes.

The second goal was to investigate the functional roles of these kinases in schistosomes. In-depth analysis of PKC, ERK and p38 MAPK signalling *via* localization of enzymatically active forms, pharmacological modulation, transient gene

silencing by RNAi and the use of novel methods to induce behavioural responses, unveiled not only life-stage specific functions for these kinases, but also conservation of roles. New insight into the possible mode of action of PZQ towards adult schistosomes was gained as activity of PKC and ERK increased in the presence of this drug. This increase in activity was localized in structures with suspected nervous/excretory functions showing how the parasite might react and attempt to cope with PZQ intake. In addition to targets published (Lima *et al.*, 1994; Ribeiro *et al.*, 1998; Tallima and Ridi, 2007; Angelucci *et al.*, 2007; Pica-Mattoccia *et al, 2008*), it is thus likely that PZQ affects multiple proteins directly or indirectly. Therefore it is proposed that the effects of PZQ on kinase activities are studied to further unravel its mechanisms of action.

PKC signalling, known to play important roles in eukaryotes (Nishizuka, 1986), was also important in schistosomes. Wide distribution in localization of the four active PKC isotypes was seen in adult worms (oesophagus, oesophageal gland, musculature, tegument, nerve structures and reproductive organs), cercariae (sensory papillae, acetabular glands, and neuromuscular structures) and skin-stage schistosomules (tegument, subtegument, oesophagus, germ cells and nephridiopore). Association of PKC activity with neuromuscular structures in all three life-stages and the effects of pharmacological modulation on neuromuscular processes suggest a conserved function irrespective of life-stage. For example, PKC inhibition or activation affected schistosome motility (adult worms, schistosomules and cercariae), ventral sucker attachment in adult worms, and cercarial acetabular gland release induced by linoleic acid, a process that involves detection of chemical gradients and sensory/neuromuscular mechanisms. A sensory function for PKC is evident in adults and cercariae; in adults it seems to be involved in thigmoattraction (as different sex ratios affect activity status and pharmacological inhibition decouples pairs), while in cercariae it is involved in thermo and photo perception (as PKC activation was influenced by light/temperature change).

The broad regional distribution of the two active ERK isotypes in adult worms (tegument, flame cells, excretory tubules, ventral sucker, gynaecophoric canal and male and female reproductive organs), cercariae (flame cells, excretory tubules, sensory papillae, glycocalyx and acetabular nerves) and skin-stage schistosomules (muscular fibres, tegument and subtegument) supports a variety of roles for ERK signalling in schistosomes. Interestingly, ERK is also involved in neuromuscular processes in all life-stages perhaps in association with the PKC cascade as cross-talk was found to exist

between these pathways in adult worms. ERK inhibition affected adult ventral sucker attachment, cercarial acetabular gland release induced by linoleic acid, and motility in adults, cercariae and schistosomules. Furthermore, in unpaired adults, different sex ratios affected ERK signalling while in cercariae ERK activity was affected by temperature change and was associated with the sensory papillae suggesting a role for ERK in cercarial sensory perception. ERK appears to also have a function in maintenance of pairing as it is present in the gynaecophoric canal of unpaired adult males and pharmacological inhibition reduces pairing. Moreover, activated ERK was evident in the tegument of all the three-life-stages and in the reproductive organs of adults.

Studies on cercariae tails revealed that detached tails are positively photokinetic acting independently of the head, and that PKC and ERK activation in tails is stimulated by increased light localizing in a number of cells and putative sensory structures. This gives new insights into the how increased light intensity is perceived by cercariae. Further studies of PKC and MAPK signalling in detached tails could contribute to efforts to achieve successful schistosome cell culture as it has been reported that detached tails in culture show high mitotic activity (Coultas and Zhang, 2012). Generation of such a schistosome cell line would be enormously beneficial to schistosome research.

Schistosome p38 MAPK activation was less studied and unfortunately no pharmacological modulation of this kinase was performed in adult worms. Nevertheless, activated p38 MAPK was widely distributed in adults (tegument, gynaecophoric canal and reproductive organs), cercariae (sensory papillae, surface, acetabular nerves and cephalic ganglia) and skin-stage schistosomules (tegument and the parenchyma). A sensory and neuronal role for p38 MAPK is evident by the presence of active p38 MAPK in the tegument of all life-stages and in the sensory papillae and neural structures of cercariae. This sensory and neuronal function is likely important for survival and successful infection as schistosomes are fine tuned to respond to changes in their environment. Interestingly, p38 MAPK inhibition did not induce toxicity or affect viability in schistosomules even the highest concentration tested, indicating a possible association of p38 MAPK activity with apoptosis in schistosomes, as in higher organisms (Chang and Karin, 2001).

Activated PKC, ERK and p38 MAPK were found associated with the tegument surface in endoparasitic stages (adults and schistosomules) and thus could be accessible

to developed drugs. Furthermore, the presence of PKC and ERK activity in the male tubercles is noteworthy, as several neurotransmitters and proteins considered attractive targets for chemotherapeutic intervention have also been identified in these structures. That activated PKA is also present in tubercles (de Saram *et al.*, 2013) highlights that complex signalling pathways exist here and might be involved in processes such as host-parasite communication, secretion, and neuroperception.

Although pharmacological modulation was valuable in ascertaining functional roles for PKC, ERK and p38 MAPK in schistosomes, unfortunately, siRNA knockdown of all PKC/ERK genes was inefficient with only ~33% success achieved. Following successful PKC gene knockdown, increased activation of another PKC isotype was observed, showing a possible compensation mechanism, which could explain why significant phenotypes were not observed. It is known that siRNA can be difficult in schistosomes (e.g. Krautz-Peterson *et al.*, 2010) but it is worth further exploring knockdown of PKCs and ERKs in future studies including with different life-stages.

A further goal of the study was investigate whether host-derived molecules modulate (transactivate) PKC and MAPK signalling pathways. Phosphorylation of the ~81 kDa and ~116 kDa PKC and the ~43 kDa ERK was stimulated by human EGF and INS, while the ~116 kDa PKC was also stimulated by IGF-I; this suggests isotype specific roles for PKC and ERK signalling in transactivation mechanisms. The association of increased PKC and ERK activity with the tegument strongly supports a host-parasite interactive role. Furthermore, schistosomule PKC activity was stimulated by the presence of erythrocytes, the primary food source of schistosomes with activity found mainly associated with the developing gut and acetabular glands. It is also shown that the iron transport molecule transferrin, known to induce growth of schistosomules, is internalized through the tegument and that PKC inhibition delays the internalization process, evidencing a putative role in transferrin uptake. These findings establish a framework for further studies investigating the effects of human host factors on schistosome signalling and downstream function, particularly in the context of parasite growth and survival.

In addition to developing new methodologies and approaches for studying cell signalling schistosomes and delivering novel findings of importance to schistosome biology and the schistosome research community, this study provides evidence that *S. mansoni* PKC, ERK and p38 MAPK proteins are excellent candidates for further research as therapeutic targets together with PKA (Swierczewski and Davies, 2009; de

Saram *et al.*, 2013). In future work it would be beneficial to sequence the detected PKCs and ERKs and to assess PKC, ERK and p38 MAPK activities during long term schistosomule culture in the presence of human factors. The identification of upstream regulators and downstream effectors of these kinases and investigating their possible involvement in host immune system modulation, could enable further novel research in host parasite communication; it might also provide valuable knowledge for improving current culture methods to enable full maturation of worms *in vitro* reducing the need for animals in schistosome research. In the context of drug development it is hoped that on-going research in our laboratory together with that of other laboratories will result in the development of new drugs that interfere with schistosome growth, development and survival in the human host. These could be deployed together with existing control strategies to help in the effort to eliminate schistosomiasis from endemic regions bettering the quality of life for millions of humans worldwide.

References

Reference

Abeliovich, A., Chen, C., Goda, Y., Silva, A. J., Stevens, C. F., and Tonegawa, S. (1993) Modified hippocampal long-term potentiation in PKCγ-mutant mice. *Cell*, **75**(7), 1253-1262.

Aberdam, E., and Dekel, N. (1985) Activators of protein C stimulate meiotic maturation of rat oocytes. *Biochemical and Biophysical Research Communications*, **132**, 520-574.

Adamson, P. B. (1976) Schistosomiasis in antiquity. *Medical History*, **2**, 176-188.

Agboh, K. C., Webb, T. E., Evans, R. J., and Ennion S. J. (2004) Functional characterization of a p2X receptor from *Schistosoma mansoni*. *Journal of Biological Chemistry*, **279**, 41650-41657.

Ahier, A., Khayath, N., Vicogne, J., and Dissours, C. (2008) Insulin receptors and glucose uptake in the human parasite *Schistosoma mansoni*. *Parasite*, **15**, 357-366.

Aley, K. O., Messing, R. O., Mochly-Rosen, D., and Levine, J. D. (2000) Chronic hypersensitivity for inflammatory nociceptor sensitization mediated by the ε isozyme of protein kinase C. *The Journal of Neuroscience*, **20**(12), 4680-4685.

Altschul, S. F., Gish, W., Miller, W., Myers, E. W., and Lipman, D. J. (1990) Basic local alignment search tool. *Journal of Molecular Biology*, **215**(3), 403-410.

Amador-Cano, G., Carpizo-Ituarte, E., and Cristino-Jorge, D. (2006) Role of protein kinase C, G-protein coupled receptors, and calcium influx during metamorphosis of the seas urchin *Strongylocentrotus purpuratus*. *The Biological Bulletin*, **210**(2), 121-131.

Amiri, P., Locksley, R.M., Parslow, T.G., Sadick, M., Rector, E., Ritter, D. and McKerrow, J.H. (1992) Tumor necrosis factor a restores granulomas and induces parasite egg laying in schistosome-infected *scid* mice. *Nature*, **356**, 604-607.

Andrade, L.F., Nahum, L.A., Avelar, L.G.A., Silva, L.L. and Zerlotini, A. (2011) Eukaryotic protein kinases (ePKs) of the helminth parasite *Schistosoma mansoni*. *BMC Genomics*, **12**, 215.

Angelucci, F., Basso, A., Bellelli, A., Brunori, M., Mattoccia, L., and Valle, C. (2007) The anti-schistosomal drug praziquantel is an adenosine antagonist. *Parasitology*, **134**, 1215-1221.

Aragon, A. D., Imani, R. A., Blackburn, V. R., and Cunningham, C. (2008) Microarray based analysis of temperature and oxidative stress induced messenger RNA in *Schistosoma mansoni*. *Molecular and Biochemical Parasitology*, **162**(2), 134-141.

Arkhammar, P., Juntti-Berggren, L., Larsson, O., Welsh, M., Nånberg, E., Sjöholm, A., and Berggren, P. O. (1994) Protein kinase C modulates the insulin secretory process by maintaining a proper function of the beta-cell voltage-activated Ca^{2+} channels. *Journal of Biological Chemistry*, **269**(4), 2743-2749.

Ashton, F. T., Li, J., & Schad, G. A. (1999) Chemo-and thermosensory neurons: structure and function in animal parasitic nematodes. *Veterinary Parasitology*, **84**(3), 297-316.

Babu, G. J., Lalli, M. J., Sussman, M. A., Sadoshima, J., and Periasamy, M. (2000) Phosphorylation of elk-1 by MEK/ERK pathway is necessary for *c-fos* gene activation during cardiac myocyte hypertrophy *Journal of Molecular and Cellular Cardiology*, **32**, 1447–1457.

Bahia, D., Avelar, L., Mortara, R.A., Khayath, N., Yan, Y., Noël, C., Capron' M., Dissous, C., Pierce, R.J. and Oliveira, G. (2006) SmPKC1, a new protein kinase C identified in the platyhelminth parasite *Schistosoma mansoni*. *Biochemical and Biophysical Research Communications*, **345**, (3) 1138-1148.

Bahia, D., Mortara, R.A., Kusel, J.R., Andrade, L.F., Ludolf, F., Kuser, P.R., Avelar, L., Trolet, J., Dissous, C., Pierce, R.J. and Oliveira, G. (2007) *Schistosoma mansoni*: expression of Fes-like tyrosine kinase SmFes in the tegument and terebratorium suggests its involvement in host penetration. *Experimental Parasitology*, **116**, 225–232.

Ballif, B. A. and J. Blenis. (2001) Molecular mechanisms mediating mammalian mitogen-activated protein kinase (MAPK) kinase (MEK)-MAPK cell survival signals. *Cell Growth and Differentiation*, **12**, 397-408.

Bardwell, L. and Shah, K. (2006) Analysis of mitogen-activated protein kinase activation and interactions with regulators and substrates. *Methods*, **40**, 213–223.

Barrabes, A., Goma-Mouanda, J., Reynouard, F., and Combescot C., (1986) 17 beta-estradiol receptors in *Schistosoma mansoni*. Contribution to the explanation of the protective power of this hormone in *Schistosoma mansoni* bilharziasis in the mouse. Preliminary study. *Annales de Parasitologie Humaine et Compare*, **61**, 637-641.

Basch, P. F. and DiConza, J. J. (1974) The miracidium-sporocyst transition in *Schistosoma mansoni*: surface changes in vitro with ultrastructural correlation, *Journal of Parasitology*, **60**, 935–941.

Basch, P. F., and Gupta, B. C. (1988) Immunocytochemical localization of regulatory peptides in six species of trematode parasites. *Comparative Biochemistry and Physiology Part C: Comparative Pharmacology*, **91**(2), 565-570.

Basch, P.F. (1981) Cultivation of *Schistosoma mansoni in vitro*. I. Establishment of cultures from cercariae and development until pairing. *Journal of Parasitology*, **67**: 179–185.

Bates, W. R. (2007) HSP90 and MAPK activation are required for ampulla development in the direct-developing ascidian *Molgula pacifica*. *Invertebrate Biology*, **126**(1), 90-98.

Beall, M.J., McGonigle, S. and Pearce, E.J. (2000) Functional conservation of *Schistosoma mansoni* Smads in TGF-β signaling. *Molecular and Biochemical Parasitology*, **111**, 131–142.

Beaumier, C. M., Gillespie, P. M., Hotes, P. J., and Bottazzi, M. E, (2013) New vaccines for neglected parasitic diseases and dengue. *Translational Research*, **162**(3), 144–155.

Becker, W. (1980) Metabolic interrelationships of parasitic trematodes and mollusks, especially *Schistosoma mansoni* in *Biomphalaria glabrata*. *Parasitology Research*, **63**, 101-111.

Beckmann, S., Buro, C., Dissous, C., Hirzmann, J., and Grevelding, C. G. (2010) The Syk kinase SmTK4 of *Schistosoma mansoni* is involved in the regulation of spermatogenesis and oogenesis. *PLoS Pathogens,* **6**(2), e1000769.

Beckmann, S., Hahnel, S., Cailliau, K., Venderstraete, M., Browaeys, E., Dissous, C., and Grevending, C. G. (2011) Characterization of the Src/Abl Hybrid Kinase SmTK6 of *Schistosoma mansoni*. *International Journal of Biological Chemistry.* **286,** 42325-42336.

Ben-Levy, R., Hooper, S., Wilson, R., Paterson, H.F., and Marshall, C. J. (1998) Nuclear export of the stress-activated protein kinase p38 mediated by its substrate MAPKAP kinase-2. *Current Opinions in Biology*, **8,** 1049-1057.

Bennett, J. L., Day, T., Feng-Tao, L., Ismail, M., and Farghaly, A. (1997) The development of resistance to anthelmintics: a perspective with an emphasis on schistosomal drug PZQ. *Experimental Parasitology,* **87**, 260-267.

Berriman, M., Haas, B., LoVerde, P., Wilson, R., Dillon, P., Cerqueira, G., Mashiyama, S., Al-Lazikani, B., Andrade, L., Ashton, P., Aslett, M., Bartholomeu, D., Blandin, G., Caffrey, C., Coghlan, A., Coulson, R., Day, T., Delcher, A., DeMarco, R., Djikeng, A., Eyre, T., Gamble, J., Ghedin, E. and Gu, Y. (2009) The genome of the blood fluke *Schistosoma mansoni*. *Nature*, **460**, 352-358.

Bershadsky, A. D., Ivanova, O. Y., Lyass, L. A., Pletyushkina, O. Y., Vasiliev, J. M., and Gelfand, I. M. (1990) Cytoskeletal reorganizations responsible for the phorbol ester-induced formation of cytoplasmic processes: possible involvement of intermediate filaments. *Proceedings of the National Academy of Sciences*, **87**(5), 1884-1888.

Bishop, W. R., Kirschmeier, P., George, S. J., Cramer, S. P., and Hendrickson, W. A. (1991) Identification and characterization of zinc binding sites in protein kinase C. *Science*, **254**(5039), 1776-1779.

Blair, K.L., Bennett, J.L. and Pax, R.A. (1988) *Schistosoma mansoni*: evidence for protein kinase C-like modulation of muscle activity. *Experimental Parasitology*, **66**, 243-52.

Blank, R.B., Lamb, E.W., Tocheva, A.S., Crow, E.T., Lim, K.C., McKerrow and J.H., Davies, S.J. (2006) The common gamma chain cytokines IL-2 and IL-7 indirectly modulate blood fluke development via effects on CD4+ T cells. *Journal of Infectious Diseases*, **194**, 1609–1616.

Blanton, R., Loula, E. C., and Parker, J. (1987) Two heat-induced proteins are associated with transformation of *Schistosoma mansoni* cercariae to schistosomula. *Proceedings of the National Academy of Sciences*, **84**(24), 9011-9014.

Bluthgen N, Legewie S. (2008) Systems analysis of MAPK signal transduction. *Essays Biochemistry*, **45**, 95–107.

Bogéa, T. (2004) Functional and phylogenetic components in cercarial nervous systems. *Folia Parasitologica*, **51**(4), 311-319.

Bogéa, T., & Caira, J. N. (2001) Ultrastructure and chaetotaxy of sensory eeceptors in the cercaria of a species of Allopodocotyle Pritchard, 1966 (Digenea: Opecoelidae). *Memórias do Instituto Oswaldo Cruz*, **96**(2), 205-214.

Bogitsh, B. J., and Carter, O. S. (1977) *Schistosoma mansoni*: ultrastructural studies on the esophageal secretory granules. *The Journal of Parasitology*, 681-686.

Borisov, N., Aksamitiene, E., Kiyatkin, A., Legewie, S., Berkhout, J., Maiwald, T., Kaimachnikov, N. P., Timmer, J., Hoek, J. B., and Kholodenko, B. N. (2009) Systems-level interactions between insulin-EGF networks amplify mitogenic signaling. *Molecular Systems Biology,* **5**, 256.

Bostic, J. R., and Strand, M. (1996) Molecular cloning of a *Schistosoma mansoni* protein expressed in the gynecophoral canal of male worms. *Molecular and biochemical parasitology*, **79**(1), 79-89.

Boucher, J., Tseng, Y. H., and Kahn, C. R. (2010) Insulin and insulin-like growth factor-1 receptors act as ligand-specific amplitude modulators of a common pathway regulating gene transcription. *Journal of Biological Chemistry*, **285**(22), 17235-17245.

Boyle, J. P., Wu, X. J., Shoemaker, C. B., and Yoshino, T. P. (2003) Using RNA interference to manipulate endogenous gene expression in *Schistosoma mansoni* sporocysts. *Molecular and Biochemical Parasitology*, **128**(2), 205-215.

Brachs, S., and Haas, W. (2008) Swimming behavior of *Schistosoma mansoni* cercariae: responses to irradiance changes and skin attractants. *Parasitology Research*, **102**,685–690

Bradshaw, R. A. and Dennis, E. A. (2004) Handbook of Cell Signalling. Volume 2. *Academic Press*, London.

Braschi, S. and Wilson, R.A. (2006) Proteins exposed at the adult schistosome surface revealed by biotinylation. *Molecular & Cellular Proteomics, 5, 347-356.*

Braschi, S., Borges, W.C. and Wilson, R.A. (2006) Proteomic analysis of the schistosomes tegument and its surface membranes. *Memórias do Instituto Oswaldo Cruz*, **101**(1), 205–212.

Breitbart, H. (2003) Signaling pathways in sperm capacitation and acrosome reaction. *Cellular and Molecular Biology*, **49**(3), 321-327.

Breitbart, H., Lax, Y., Rotem, R., and Naor, Z. (1993) Role of protein kinase C in the acrosome reaction of mammalian spermatozoa. *Biochemical Journal,* **281**, 473–476.

Brindley, P. J., Kalinna, B. H., Dalton, J. P., Day, S. R., Wong, J. Y., Smythe, M. L., and McManus, D. P. (1997) Proteolytic degradation of host hemoglobin by schistosomes. *Molecular and Biochemical Parasitology*, **89**(1), 1-9.

Brink, L. H., McLaren, D. J., and Smithers, S. R. (1977) *Schistosoma mansoni*: a comparative study of artificially transformed schistosomula and schistosomula recovered after cercarial penetration of isolated skin. *Parasitology*, **74**, 73

Brito, C. F. A., Oliveira, G. C., Oliveira, S. C., Street, M., Riengrojpitak, S., Wilson, R. A., Simpson, A. J. G., and Correa-Oliveira, R. (2002) Sm14 gene expression in different stages of the *Schistosoma mansoni* life cycle and immunolocalization of the Sm14 protein within the adult worm. *Brazilian Journal of Medical and Biological Research,* **35**(3), 377-381.

Brownlee, D. J. A., Holden-Dye, L., Fairweather, I., and Walker, R. J. (1995) The action of serotonin and the nematode neuropeptide KSAYMRFamide on the pharyngeal muscle of the parasitic nematode, *Ascaris suum*. *Parasitology*, **111**(03), 379-384.

Bruckner, D. A, and Voge, M. (1974) The nervous system of larval *Schistosoma mansoni* as revealed by acetylcholinesterase staining, *The Journal of Parasitology*, *60*(3), 437-446

Burke, M.L., Jones, M.K., Goberty, G.N., Li, Y.S. and Ellis, M.K. (2009) Immunopathogenesis of human schistosomiasis. *Parasite Immunology*, **31**, 163-176.

Caffrey, C. R. (2007) Chemotherapy of schistosomiasis: present and future. *Current Opinion in Chemical Biology*, **11**(4), 433-439.

Campbell, S. L., Khosravi-Far, R., Rossman, K.L., Clark, G.J. and Der, C.J. (1998) Increasing complexity of Ras signaling. *Oncogene*, **17**, 1395-1413.

Campbell, W. C., and Todd, A.C. (1995) Behaviuor of the miracidum of *Fascioloides magna* (Bassi 1875) Ward 1971 in presence of a snail host. *Transactions of the American Microscopical Society*, **74** (4), 342-347.

Capron, A., Riveau, G., Capron, M. and Trottein, T. (2005) Schistosomes: the road from host–parasite interactions to vaccines in clinical trials. *Trends in Parasitology*, **21,** (3), 143-149.

Cardenas, M., Fabila, Y. V., Yum, S., Cerbon, J., Böhmer, F. D., Wetzker, R., Fujisawa, T., Bosch, T. C. G., and Salgado, L. M. (2000) Selective protein kinase inhibitors block head-specific differentiation in hydra. *Cellular Signalling*, **12**(9), 649-658.

Castagna, M., Takai, Y., Kaibuchi, K., Sano, K., Kikkawa, U., & Nishizuka, Y. (1982) Direct activation of calcium-activated, phospholipid-dependent protein kinase by tumor-promoting phorbol esters. *Journal of Biological Chemistry*, **257**(13), 7847-7851.

Cesare, P., Dekker, L. V., Sardini, A., Parker, P. J., and McNaughton, P. A. (1999) Specific involvement of PKC-ε in sensitization of the neuronal response to painful heat. *Neuron*, **23**(3), 617-624.

Chang, L., & Karin, M. (2001) Mammalian MAP kinase signalling cascades. *Nature*, **410**, 37-40.

Charlab, R., Blaineau, C., Schechtman, D., and Barcinski, M. A. (1990) Granulocyte-Macrophage Colony-Stimulating Factor is a Growth-Factor for Promastigotes *of Leishmania mexicana amazonensis*. *Journal of Eukaryotic Microbiology*, **37**(5), 352-357.

Chen, Y. G., Liu, F., & Massague, J. (1997) Mechanism of TGFβ receptor inhibition by FKBP12. *The EMBO Journal*, **16**(13), 3866-3876.

Chen, Z., Gibson, T.B., Robinson, F., Silvestro, L., Pearson, G., Xu, B., Wright, A., Vanderbilt, C. and Cobb, M.H. (2001) MAP kinases. *Chemical. Reviews*, **101,** 2449-2476.

Cheng, G., Fu, Z., Lin, J., Shi, Y., Zhou, Y., Jin, Y., and Cai, Y. (2009) *In vitro* and *in vivo* evaluation of small interference RNA-mediated gynaecophoral canal protein silencing in *Schistosoma japonicum*. *The Journal of Gene Medicine*, **11**(5), 412-421.

Chitsulo, L., Engels. D., Montresor, A. and Savioli, L. (2000) The global status of schistosomiasis and its control, *Acta Tropica,* **77**, 41–51.

Chong, H., Vikis, H. G., and Guan, K. L. (2003) Mechanisms of regulating the Raf kinase family. *Cellular Signalling*, **15**(5), 463-469.

Chu, Z. L., Jones, R. M., He, H., Carroll, C., Gutierrez, V., Lucman, A., and Leonard, J. (2007) A role for β-cell-expressed G protein-coupled receptor 119 in glycemic control by enhancing glucose-dependent insulin release. *Endocrinology*, **148**(6), 2601-2609.

Cioli, D. and Pica-Mattoccia L. (2003) Praziquantel. *Parasitology Research*, **90** (1), 3-9.

Citri, A., and Yarden, Y. (2006) EGF–ERBB signalling: towards the systems level. *Nature Reviews Molecular Cell Biology*, **7**(7), 505-516.

Clegg, J. A., & Smithers, S. R. (1972) The effects of immune rhesus monkey serum on schistosomula of *Schistosoma mansoni* during cultivation in vitro. *International Journal for Parasitology*, **2**(1), 79-98.

Clegg, J.A., Smithers, S.R. and Terry, R.J. (1971) Acquisition of human antigens by *Schistosoma mansoni* during cultivation *in vitro*. *Nature*, **232**: 653–654.

Clemens, L. E., and Basch, P. F. (1989) *Schistosoma mansoni*: effect of transferrin and growth factors on development of schistosomula in vitro. *The Journal of Parasitology*, 417-421.

Cohen, P. (2002) The origins of protein phosphorylation. *Nature Cell Biology*, **4**, 127 -130.

Coles, G. C., Jansson, H. B., and Zuckerman, B. M. (1988) Lectin studies of surface carbohydrates and induction of gland secretion in the free-living stages of *Schistosoma mansoni*. *Journal of Chemical Ecology*, **14**(2), 691-700.

Colley, D.G. and Wikel, S.K. (1974) *Schistosoma mansoni*: simplified method for the production of schistosomules. *Experimental Parasitology,* **35**, 44-51.

Collins III, J. J., King, R. S., Cogswell, A., Williams, D. L., and Newmark, P. A. (2011) An atlas for Schistosoma mansoni organs and life-cycle stages using cell type-specific markers and confocal microscopy. *PLoS Neglected Tropical Diseases*, **5**(3), e1009.

Correnti, J. M., and Pearce, E. J. (2004) Transgene expression in *Schistosoma mansoni*: introduction of RNA into schistosomula by electroporation. *Molecular and Biochemical Parasitology*, **137**(1), 75-79.

Correnti, J. M., Brindley, P. J., and Pearce, E. J. (2005) Long-term suppression of cathepsin B levels by RNA interference retards schistosome growth. *Molecular and Biochemical Parasitology*, **143**(2), 209-215.

Correnti, J. M., Jung, E., Freitas, T. C., and Pearce, E. J. (2007) Transfection of *Schistosoma mansoni* by electroporation and the description of a new promoter sequence for transgene expression. *International Journal of Parasitology*, **37**(10), 1107-1115.

Coulombe, P., and Meloche, S. (2007) Atypical mitogen-activated protein kinases: structure, regulation and functions. *Biochimica et Biophysica Acta (BBA)-Molecular Cell Research*, **1773**(8), 1376-1387.

Coulson, P.S. and Wilson, R.A. (1997) Recruitment of lymphocytes to the lung through vaccination enhances the immunity of mice exposed to irradiated schistosomes. *Infection and Immunity,* **65** (1): 42-48.

Coulthard, L. R., White, D. E., Jones, D. L., McDermott, M. F., and Burchill, S. A. (2009) p38MAPK: stress responses from molecular mechanisms to therapeutics. *Trends in Molecular Medicine*, **15**(8), 369-379.

Cousin, C. E., Stirewalt, M. A., and Dorsey, C. H. (1981) *Schistosoma mansoni*: Ultrastructure of early transformation of skin-and shear-pressure-derived schistosomules. *Experimental Parasitology*, **51**(3), 341-365.

Coussens, L., Rhee, L., Parker, P. J.,and Ullrich, A. (1987) Alternative splicing increases the diversity of the human protein kinase C family. *DNA*, **6**, 389-394.

Coutlas, K. A., and Zhang, S., (2012) In vitro cercariae transformation: comparison of mechanical and nonmechanical methods and observation of morphological changes of detached cercariae tails. *Biochemical Journal of Parasitology*, **98**(2), 1257-1261.

Crabtree, J. E., and Wilson, R. A. (1980) *Schistosoma mansoni*: a scanning electron microscope study of the developing schistosomulum. *Parasitology*, **81**(3), 553-564.

Dabdoub, A., and Payne, R. (1999) Protein Kinase C Activators Inhibit the Visual Cascade in *Limulus* Ventral Photoreceptors at an Early Stage. *The Journal of Neuroscience*, **19**(23), 10262-10269.

Da'dara, A., Tsai M.H., Tao, L.F., Marx, K.A., Shoemaker, C.B., Harn, D.A. and Skelly P.J. (2001) *Schistosoma mansoni*: molecular characterization of a tegumental Ca-ATPase (SMA3). *Experimental Parasitology*, **98** (4), 215-222.

Dan, I., Watanabe, N. M., and Kusumi, A. (2001) The Ste20 froup kinases as regulators of MAP Kinase cascades. *Trends in Cell Biology*, **11**, 220-230.

Davies, S., Reddy, H., Caivanno, M., and Cohen, P. (2000) Specificity and mechanism of action of some commonly used protein kinase inhibitors. *Biochemistry Journal*, **351**, 95-105.

Davies, S.J., Shoemaker, C.B. and Pearce, E.J. (1998) A divergent member of the transforming growth factor b receptor family from *Schistosoma mansoni* is expressed on the parasite surface membrane. *The Journal of Biological Chemistry*, **273** (18), 11234–11240.

Davies,J., Grogan, J. L., Blank, R. B., Lim, K. C., Locksley, R. M., and McKerrow J. H. (2001) Modulation of blood fluke development in the liver by hepatic $CD4^+$ lymphocytes. Science, **294**, 1358–1361.

Davis, R. J. (1994) MAPKs: new JNK expands the group. *Trends in Biochemical Sciences*, **19**(11), 470-473.

Day, T. A., Bennett, J. L., and Pax, R. A. (1992) Praziquantel: the enigmatic antiparasitic. *Parasitology Today*, **8**(10), 342-344.

De Luca, C., and Valacchi, G. (2010) Surface lipids as multifunctional mediators of skin responses to environmental stimuli. *Mediators of Inflammation*, 321494.

de Mendonça, R. L., Escrivá, H., Bouton, D., Laudet, V., and Pierce, R. J. (2000) Hormones and nuclear receptors in schistosome development. *Parasitology Today*, **16**(6), 233-240.

de Mendonça, R.L, Bouton, D., Bertin, B., Escriva, H., Noel, C., Vanacker, J.M., Cornette, J., Laudet, V. and Pierce, R.J. (2002) A functionally conserved member of the FTZ-F1 nuclear receptor family from *Schistosoma mansoni*. *European Journal of Biochemistry*, **269,** 5700-5711.

de Moraes Maciel, R., Silva Dutra, D.L., Rumjaneka, F.D.,Juliano, L., Juliano, M.A. and Fantappié, M.R. (2004) *Schistosoma mansoni* histone acetyltransferase GCN5: linking histone acetylation to gene activation. *Molecular and Biochemical Parasitology*, **133**, 131–135.

de Saram, P.S.R., Ressurreição, M., Davies, A.J., Rollinson, D., Emery, A.M. and Walker, A.J. (2013) Functional mapping of protein kinase A reveals its importance in adult *Schistosoma mansoni* motor activity. *PLoS Neglected Tropical Diseases*, **7**(1), e1988.

del Pilar Gomez, M., and Nasi, E. (1995) Activation of light-dependent K^+ channels in ciliary invertebrate photoreceptors involves cGMP but not the IP3/Ca^{2+} cascade. *Neuron*, **15**(3), 607-618.

Delcroix, M., Sajid, M., Caffrey, C. R., Lim, K. C., Dvořák, J., Hsieh, I, and McKerrow, J. H. (2006) A multienzyme network functions in intestinal protein digestion by a platyhelminth parasite. *Journal of Biological Chemistry*, **281**(51), 39316-39329.

Dempsey, E. C., Newton, A. C., Mochly-Rosen, D., Fields, A. P., Reyland, M. E., Insel, P. A., & Messing, R. O. (2000) Protein kinase C isozymes and the regulation of diverse cell responses. *American Journal of Physiology-Lung Cellular and Molecular Physiology*, **279**(3), L429-L438.

Derijard, B., Hibi, M., Wu, I. H., Barret, T., Su, B., Deng, T., Karin, M. and Davis, R. J. (1994) JNK1: protein kinase stimulated by UV light and Has-Ras that binds and phosphorylates the c-jun activation domain. *Cell*, **76**, 1025-1037.

Dickens, M., Rogers, J., Cavanagh, J., Raitano, A., Xia, Z., Halpern, J. R., Greenberg, M. E., Sawyers, C., and Davis, R. J. (1997) A cytoplasmic inhibitor of the JNK signal transduction pathway. *Science*, **277**, 693–696

Dissanayake, S. (2000) Upregulation of a raf kinase and a DP-1 family transcription factor in epidermal growth factor (EGF) stimulated filarial parasites. *International Journal for Parasitology*, **30**(10), 1089-1097.

Dissous, C. and Grevelding, C.G. (2010) Piggy-backing the concept of cancer drugs for schistosomiasis treatment: a tangible perspective? *Trends in Parasitol*oly, **27**, 59-66.

Dissous, C., Ahier, A., and Khayath, N. (2007a) Protein tyrosine kinases as new potential targets against human schistosomiasis. *Bioessays*, **29**(12), 1281-1288.

Dissous, C., Khayath, N., Vicogne. J. and Capron, M., (2006) Growth factor receptors in helminth parasites: signalling and host-parasite relationships. *FEBS Letters, **580***, 2968-2975.

Dissous, C., Khayath, N., Vicogne. J. and Capron, M., (2007b) Growth factor receptors in helminth parasites: signalling and host-parasite relationships. *FEBS Letters, **580***, 2968-2975.

Doenhoff, M. J., Cioli, D. and Utzinger, J. (2008) Praziquantel: mechanisms of action, resistance and new derivatives for schistosomiasis. *Current Opinion in Infectious Diseases*, **21**, 659–667.

Dominguez, I., Diaz-Meco, M. T., Municio, M. M., Berra, E., De Herreros, A. G., Cornet, M. E., Sanz, L., and Moscat, J. (1992) Evidence for a role of protein kinase C zeta subspecies in maturation of *Xenopus laevis* oocytes. *Molecular and Cellular Biology*, **12**(9), 3776-3783.

Dorsey, C. H. (1975) *Schistosoma mansoni*: Development of acetabular glands of cercaria at ultrastructural level. *Experimental Parasitology*, **37**(1), 37-59.

Dorsey, C. H., & Cousin, C. E. (1986) *Schistosoma mansoni*: A new parenchymal cell in cercariae. *Experimental Parasitology*, **61**(1), 33-41.

Dorsey, C. H., & Stirewalt, M. A. (1971) *Schistosoma mansoni*: Fine structure of cercarial acetabular glands. *Experimental Parasitology*, **30**(2), 199-214.

Dorsey, C.H., Cousin, C.E., Lewis, F.A. and Stirewalt, M.A. (2002) Ultrastructure of the *Schistosoma mansoni* cercaria. *Micron*, **33**(3), 279-323.

Dvořák, J., Beckmann, S., Lim, K. C., Engel, J. C., Grevelding, C. G., McKerrow, J. H., and Caffrey, C. R. (2010) Biolistic transformation of *Schistosoma mansoni*: Studies with modified reporter-gene constructs containing regulatory regions of protease genes. *Molecular and Biochemical Parasitology*, **170**(1), 37-40.

Dzik J. (2005) Molecules released by helminth parasites involved in host colonization. *Acta Biochimica*, **53**:33–64.

Ebrey, T., and Koutalos, Y. (2001) Vertebrate photoreceptors. *Progress in Retinal and Eye Research*, **20**(1), 49-94.

Eichholtz, T., Vossebeld, P., van Overveld, M., and Ploegh, H. (1992) Activation of protein kinase C accelerates internalization of transferrin receptor but not of major histocompatibility complex class I, independent of their phosphorylation status. *Journal of Biological Chemistry*, **267**(31), 22490-22495.

Elbashir, S. M., Harborth, J., Lendeckel, W., Yalcin, A., Weber, K., and Tuschl, T. (2001a) Duplexes of 21-nucleotide RNAs mediate RNA interference in cultured mammalian cells. *Nature*, **411**, 494-498.

Elbashir, S. M., Martinez, J., Patkaniowska, A., Lendeckel, W., and Tuschl, T. (2001b) Functional anatomy of siRNAs for mediating efficient RNAi in Drosophila melanogaster embryo lysate. *The EMBO Journal*, **20**(23), 6877-6888.

Ellinger-Ziegelbauer, H., Brown, K., Kelly, K., and Siebenlist, U. (1997) Direct activation of the stress-activated protein kinase (SAPK) and extracellular signal-regulated protein kinase (ERK) pathways by an inducible mitogen-activated protein kinase/ERK kinase kinase 3 (MEKK) derivative. *Journal of Biological Chemistry*, **272**(5), 2668-2674.

Ellis, J. G., Davila, M., and Chakrabarti, R. (2003) Potential Involvement of Extracellular Signal-regulated Kinase 1 and 2 in Encystation of a Primitive Eukaryote, Giardia lamblia stage specific activation and intracellular localization. *Journal of Biological Chemistry*, 278(3), 1936-1945.

Ellis, J., Sarkar, M., Hendriks, E., and Matthews, K. (2004) A novel ERK-like, CRK-like protein kinase that modulates growth in Trypanosoma brucei via an autoregulatory C-terminal extension. *Molecular Microbiology*, **53**(5), 1487-1499.

El-Shehabi, F., and Ribeiro, P. (2010) Histamine signalling in *Schistosoma mansoni* : Immunolocalisation and characterisation of a new histamine-responsive receptor (SmGPR-2). *International Journal for Parasitology*, **40**(12), 1395-1406.

El-Shehabi, F., Taman, A., Moali, L. S., El-Sakkary, N., and Ribeiro, P. (2012) A novel G Protein-Coupled receptor of *Schistosoma mansoni* (SmGPR-3) is activated by dopamine and is widely expressed in the nervous system. *PLoS Neglected Tropical Diseases*, **6**(2), e1523.

El-Shehabi, F., Vermeire, J. J., Yoshino, T. P., and Ribeiro, P. (2009) Developmental expression analysis and immunolocalization of a biogenic amine receptor in *Schistosoma mansoni*. *Experimental Parasitology*, **122**(1), 17-27.

Engels D., Chitsulo L., Montresor A. and Savioli L. (2002) The global epidemiological situation of schsitosomiasis and new approaches to control and research. *Acta Tropica*, **82**, (2), 139-46.

Erasmus, D. A. (1973) A comparative study of the reproductive system of mature, immature and "unisexual" female *Schistosoma mansoni*. *Parasitology*, **67**(2), 165-183.

Erasmus, D. A. (1975) *Schistosoma mansoni*: Development of the vitelline cell, its role in drug sequestration, and changes induced by Astiban. *Experimental Parasitology*, **38**(2), 240-256.

Ernst, S. C. (1975) Biochemical and cytochemical studies of digestive-absorptive functions of esophagus, cecum, and tegument in *Schistosoma mansoni*: acid phosphatase and tracer studies. *The Journal of parasitology*, 633-647.

Escobedo, G., Camacho-Arroyo, I., Hernández-Hernández, O. T., Ostoa-Saloma, P., García-Varela, M., and Morales-Montor, J. (2009) Progesterone induces scolex evagination of the human parasite *Taenia solium*: evolutionary implications to the host-parasite relationship. *BioMed Research International*, **2010**, 591079- 591089.

Escobedo, G., Roberts, C. W., Carrero, J. C., and Morales-Montor, J. (2005) Parasite regulation by host hormones: an old mechanism of host exploitation? *Trends in Parasitology*, **21**(12), 588-593.

Escobedo, G., Soldevila, G., Ortega-Pierres, G., Chavez-Rios, J.R., Nava, K., Fonseca-Linan, R., Lopez-Griego, L., Hallal-Calleros, C., Ostoa-Saloma, P. and Morales-Montor, J. (2010) A new MAP kinase protein involved in estradiol-stimulated reproduction of the helminth parasite *Taenia crassiceps*. *Journal of Biomedicine and Biotechnology*, 1110-7251.

Espinoza, B., Silman, I., Arnon, R., and Tarrabahd-Hazdai, R. (1991) Phosphatidylinositol-specific phospholipase C induces biosynthesis of acetylcholinesterase via diacylglycerol in *Schistosoma mansoni*. *European Journal of Biochemistry*, **195**(3), 863-870.

Estabile, J. (2003): http://rgmg.cpqrr.fiocruz.br/content/schistosoma-mansoni-transcriptome-project

Eveland, L. K., and Haseeb, M. A. (1989) *Schistosoma mansoni:* onset of chemoattraction in developing worms. *Experientia*, **45**(3), 309-310.

Faghiri, Z., Camargo, S. M., Huggel, K., Forster, I. C., Ndegwa, D., Verrey, F., and Skelly, P. J. (2010) The tegument of the human parasitic worm *Schistosoma mansoni* as an excretory organ: the surface aquaporin SmAQP is a lactate transporter. *Plos One*, **5**(5), e10451.

Fallon, P. G., and Doenhoff, M. J. (1994) Drug-resistant schistosomiasis: resistance to praziquantel and oxamniquine induced in Schistosoma mansoni in mice is drug specific. *The American Journal of Tropical Medicine and Hygiene*, **51**(1), 83-88.

Fantappié, M. R., Freebern, W. J., Osman, A., LaDuca, J., Niles, E. G., & LoVerde, P. T. (2001) Evaluation of *Schistosoma mansoni* retinoid X receptor *Sm* RXR1 and *Sm* RXR2 activity and tissue distribution. *Molecular and Biochemical Parasitology*, **115**(1), 87-99.

Farhan, H., Wendeler, M. W., Mitrovic, S., Fava, E., Silberberg, Y., Sharan, R., and Hauri, H. P. (2010) MAPK signaling to the early secretory pathway revealed by kinase/phosphatase functional screening. *The Journal of Cell Biology*, **189**(6), 997-1011.

Favata, M. F., Horiuchi, K. Y., Manos, E. J., Daulerio, A. J., Stradley, D. A., Feeser, W. S., and Trzaskos, J. M. (1998) Identification of a novel inhibitor of mitogen-activated protein kinase kinase. *Journal of Biological Chemistry*, **273**(29), 18623-18632.

Fenwick, A., Savioli, L., Engels, D., Bergquist, R. and Todd, M. (2003) Drugs for the control of parasitic diseases: current status and development in schistosomiasis. *Trends in Parasitology*, **19**, 509–515.

Fire, A., Xu, S., Montgomery, M. K., Kostas, S. A., Driver, S. E., and Mello, C. C. (1998) Potent and specific genetic interference by double-stranded RNA in *Caenorhabditis elegans*. *Nature*, **391**(6669), 806-811.

Fishelson, Z., Amiri, P., Friend, D. S., Marikovsky, M., Petitt, M., Newport, G., and Mckerrow, J. H. (1992) *Schistosoma mansoni*: Cell-specific expression and secretion of a serine protease during development of cercariae. *Experimental Parasitology*, **75**(1), 87-98.

Fitzpatrick, J. M., & Hoffmann, K. F. (2006) Dioecious *Schistosoma mansoni* express divergent gene repertoires regulated by pairing. *International Journal for Parasitology*, **36**(10), 1081-1089.

Fitzpatrick, J.M., Hirai, Y., Hirai, H. and Hoffmann, K.F. (2007) Schistosome egg production is dependent upon the activities of two developmentally regulated tyrosinases. *FASEB Journal*, **21**, 823-835.

Fox, L. E., and Lloyd, P. E. (1999) Glutamate is a fast excitatory transmitter at some buccal neuromuscular synapses in Aplysia. *Journal of Neurophysiology*, **82**(3), 1477-1488.

Freebern, W.J., Niles, E.G., and LoVerde, P.T. (1999a) RXR-2, a member of the retinoid x receptor family in *Schistosoma mansoni*. *Gene*, **233**, 33–38.

Freebern, W.J., Osman, A., Niles, E.G., Christen, L. and LoVerde, P.T. (1999b) Identification of a cDNA encoding a retinoid X receptor homologue in *Schistosoma mansoni*. Evidence for a role in female-specific gene expression. *Journal of Biological Chemistry*, **274**, 4577–4585.

Freitas, T. C., and Pearce, E. J. (2010) Growth factors and chemotactic factors from parasitic helminths: Molecular evidence for roles in host–parasite interactions versus parasite development. *International Journal for Parasitology*, **40**(7), 761-773.

Freitas, T.C., Jung, E. and Pearce, E.J. (2007) TGF-beta signaling controls embryo development in the parasitic flatworm *Schistosoma mansoni*. *PLoS Pathogens*, **3**, 52.

Freitas, T.C., Jung, E. and Pearce, E.J. (2009) A bone morphogenetic protein homologue in the parasitic flatworm, *Schistosoma mansoni*. *International Journal for Parasitology*, Volume **39** (3), 281-287.

Freshney, N. W., Rawlinson, L., Guesdon, F., Jones, E., Cowley, S., Hsuan, J., and Saklatvala, J. (1994) Interleukin-1 activates a novel protein kinase cascade that results in the phosphorylation of Hsp27. *Cell*, **78**(6), 1039-1049.

Fried, B., & Graczyk, T. K. (2004) Recent Advances in the Biology of *Echinostoma* species in the "revolutum" Group. *Advances in Parasitology*, **58**, 139-195.

Fusco, A. C., Salafsky, B., Vanderkooi, G., and Shibuya, T. (1991) *Schistosoma mansoni*: the role of calcium in the stimulation of cercarial proteinase release. *Journal of Parasitology*, **77**, 649– 657

Gabay, L., Seger, R. and Shilo, B.Z. (1997) MAP kinase in situ activation atlas during *Drosophila* embryogenesis. *Development*, **124**, 3535-3541.

Gabriel, R., Lesauter, J., Silver, R., Garcia-España, A., and Witkovsky, P. (2001) Diurnal and circadian variation of protein kinase C immunoreactivity in the rat retina. *Journal of Comparative Neurology*, **439**(2), 140-150.

Galcheva-Gargova, Z., Derijard, B., Wu, I. H., and Davis, R. J. (1994) An osmosensing signal transduction pathway in mammalian cells. *Science*, **265**(5173), 806-808.

Garrity, P. A., Goodman, M. B., Samuel, A. D., and Sengupta, P. (2010) Running hot and cold: behavioral strategies, neural circuits, and the molecular machinery for thermotaxis in C. elegans and Drosophila. *Genes & development*, **24**(21), 2365-2382.

Geary, T. G., Woo, K., McCarthy, J. S., Mackenzie, C. D., Horton, J., Prichard, R. K., and Bundy, D. A. (2010) Unresolved issues in anthelmintic pharmacology for helminthiases of humans. *International Journal for Parasitology*, **40**(1), 1-13.

Geerts, S. and Gryseels, B. (2000) Drug resistance in human helminths: current situation and lessons from livestock. *Clinical Microbiology Reviews*, **13**, (2), 207-222.

Ghansah, T.J., Ager, E.C., Freeman-Junior, P., Villalta, F. and Lima, M.F. (2002) Epidermal growth factor binds to a receptor on *Trypanosoma cruzi* amastigotes inducing signal transduction events and cell proliferation. *Journal Eukaryot Microbiology*, **49**, 383–390.

Gil, P., Dewey, E., Friml, J., Zhao, Y., Snowden, K.C., Putterill, J., Palme, K., Estelle, M., and Chory, J. (2001) A calossin-like protein required for polar auxin transport in Arabidopsis. *Genes Development*. **15**, 1985–1997.

Global Network for Neglected Tropical Diseases Control (GNNTDC) (2006). http://gnntdc.sabin. org/

Gloer, J. B., Meinwald, J., Shirazian, D., Childs, J. E., and Schiller, E. L. (1986) Extraction of intersexual chemoattractants from *Schistosoma mansoni*. *Journal of Chemical Ecology*, **12**(8), 1725-1728.

Gobert, G. N., Tran, M. H., Moertel, L., Mulvenna, J., Jones, M. K., McManus, D. P., and Loukas, A. (2010) Transcriptional changes in *Schistosoma mansoni* during early schistosomula development and in the presence of erythrocytes.*PLoS Neglected Tropical Diseases*, **4**(2), e600.

Goldberg, M., Zhang, H. L., & Steinberg, S. F. (1997) Hypoxia alters the subcellular distribution of protein kinase C isoforms in neonatal rat ventricular myocytes. *Journal of Clinical Investigation*, **99**(1), 55.

Goldring, O.L., Clegg, J.A., Smithers, S.R. and Terry, R.J. (1976) Acquisition of human blood group antigens by *Schistosoma mansoni*. *Clinical & Experimental Immunology*, **26**, 181–187.

Gong, W., Ren, Y., Xu, Q., Wang, Y., Lin, D., Zhou, H., and Li, T. (2006) Integrated siRNA design based on surveying of features associated with high RNAi effectiveness. *BMC Bioinformatics*, **7**(1), 516.

Gonzalez, F.A., Seth, A., Raden, D.L. Bowman, D. S., Fay, F. S. and Davis, R. J. (1993) Serum-nduced translocation of mitogen-activated protein kinase to the cell surface rufling membrane and the nucleus. *Journal of Cell Biology*, **122**, 1089–1101.

Gould, C. M., and Newton, A. C. (2008) The life and death of protein kinase C. *Current Drug Targets*, **9**(8), 614-625.

Grabe K. and Haas W. (2004) Navigation within host tissues: cercariae orientate towards dark after penetration. Parasitology Research. 93: 111-113

Grant, B., and Hirsh, D. (1999) Receptor-mediated endocytosis in the *Caenorhabditis elegans* oocyte. *Molecular Biology of the Cell*, **10**(12), 4311-4326.

Granzer, M., and Haas, W. (1986) The chemical stimuli of human skin surface for the attachment response of *Schistosoma mansoni* cercariae. *International Journal for Parasitology*, **16**(6), 575-579.

Greenberg, G.M. (2005) Are Ca^{2+} channels targets of praziquantel action? *International Journal for Parasitology*, **35**, 1–9.

Grvelding C. G., Sommer G. and Kunz W. (1997) Female-specific gene expression of *Schistosoma mansoni* is regulated by pairing. *Parasitology*. **115** (6), 635-640.

Gryseels, B., Polman, K., Clerinx, J. and Kestens, L. (2006) Human schistosomiasis. *Lancet*, **368**, 1106-1118.

Gschwendt, M., Kittstein, W., & Marks, F. (1991) Protein kinase C activation by phorbol esters: do cysteine-rich regions and pseudosubstrate motifs play a role? *Trends in Biochemical Sciences*, **16**, 167-169.

Gupta, B. C., and Basch, P. F. (1987) The role of Schistosoma mansoni males in feeding and development of female worms. *The Journal of Parasitology*, 481-486.

Gwendolen F. Rees. (1977) The development of the tail and the excretory system in the cercaria of Cryptocotyle lingua (Creplin) (Digenea: Heterophyidae from Littorina littorea (L.)). *Proceedings of the Royal Society*, **195**, 425-452.

Haas, W. (1992) Physiological analysis of cercarial behavior. *The Journal of Parasitology*, 243-255.

Haas, W. (1994) Physiological analyses of host-finding behaviour in trematode cercariae: adaptations for transmission success. *Parasitology* **109**, 15–29.

Haas, W., and Schmitt, R. (1982) Characterization of chemical stimuli for the penetration of *Schistosoma mansoni* cercariae. *Zeitschrift für Parasitenkunde*, **66**(3), 293-307.

Haas, W., Diekhoff, D., Koch, K., Schmalfuss, G., and Loy, C. (1997) *Schistosoma mansoni* cercariae: stimulation of acetabular gland secretion is adapted to the chemical composition of mammalian skin. *The Journal of Parasitology*, **83**(6), 1079-1085.

Haas, W., Grabe, K., Geis, C., Päch, T., Stoll, K., Fuchs, M., Haberl B. and Loy C. (2002) Recognition and invasion of human skin by *Schistosoma mansoni* cercariae: the keyrole of L-arginine. *Parasitology*, **124**, 153–167.

Haas, W., Haberl, B., Schmalfuss, G. and Khayyal M. T. (1994) *Schistosoma haematobium* cercarial host-finding and host-recognition differs from that of *S. mansoni*. *Journal of Parasitology*, **80**, 345–353.

Haas, W., Haeberlein, S., Behring, S., and Zoppelli, E. (2008) *Schistosoma mansoni*: Human skin ceramides are a chemical cue for host recognition of cercariae. *Experimental Parasitology*, **120**(1), 94-97.

Haeberlein, *S.* and Haas, W. (2008) Chemical attractants of human skin for swimming *Schistosoma mansoni* cercariae. *Parasitology Research*, **102**, 657–662.

Hagan, P., Appleton, C., Coles, G. and Kusel, J. R.(2004) Schistosomiasis control: keep taking the tablets. *Trends in Parasitology*, **20**, (2), 92-97.

Hall, S. L., Braschi, S., Truscott, M., Mathieson, W., Cesari, I. M., and Wilson, R. A. (2011) Insights into blood feeding by schistosomes from a proteomic analysis of worm vomitus. *Molecular and Biochemical Parasitology*, **179**(1), 18-29.

Hallberg, S. I., Rayter, J., and Downward, J. (1994) Interaction of Ras and Raf in intact mammalian cells upon extracellular stimulation *Journal of Biological Chemistry*, **269**, 3913–3916

Halton D. W. and Maule. A. G. (2004) Flatworm nerve-muscle: structural and functional analysis. *Canadian Journal of Zoology*. **82**, 316-333.

Halton, D. W., and Gustafsson, M. K. S. (1996) Functional morphology of the platyhelminth nervous system. *Parasitology*, **113**, S47-S72.

Hamdan, F.F., Abramovitz, M., Mousa, A., Xie, J., Durocher, Y. and Ribeiro, P. (2002) A novel *Schistosoma mansoni* G protein-coupled receptor is responsive to histamine. *Molecular and Biochemical Parasitology*, **119** (1), 75-86

Hanks, S. K. (2003) Genomic analysis of the eukaryotic protein kinase superfamily: a perspective. *Genome Biology*, **4**(5), 111.

Hanks, S. K., Quinn, A. M. and Hunter, T. (1988) The protein kinase family: conserved features and deduced phylogeny of the catalytic domains. *Science, 241*, 42-52.

Hanzal-Bayer, M., Renault, L., Roversi, P., Wittinghofer, A., and Hillig, R. C. (2002) The complex of Arl2-GTP and PDEδ: from structure to function. *The EMBO Journal*, **21**(9), 2095-2106.

Hara, I., Hara, S., Fusco, A. C., Salafsky, B., and Shibuya, T. (1993) Role of calcium ion in *Schistosoma mansoni* cercarial tail loss induced by unsaturated fatty acids. *The Journal of Parasitology*, **79**(4), 504-509.

Harayama, H., and Miyake, M. (2006) A cyclic adenosine 3', 5'-monophosphate-dependent protein kinase C activation is involved in the hyperactivation of boar spermatozoa. *Molecular Reproduction and Development*, **73**(9), 1169-1178.

Harder, A., Goossens, J. and Andrews P. (1988) Influence of praziquantel and Ca^{2+} on the bilayer-isotropic-hexagonal transition of model membranes. *Molecular and Biochemical Parasitology*, **29**:55–9.

Hardie, R. C., & Raghu, P. (2001) Visual transduction in Drosophila. *Nature*, **413**(6852), 186-193.

Hardle R.C., Peretz A., Suss-Toby E., Rom-Glast A., Bishop S. S., Selinger Z. and Minke B. (1993) Protein Kinase C is required for light adaptation in Drosophila photoreceptors. Letter to Nature. **363**, 634-637.

Harrop, R., and Wilson, R. A. (1993) Protein synthesis and release by cultured schistosomula of Schistosoma mansoni. *Parasitology*, **107**, 265-274.

Haseeb, M. A., and Eveland, L. K. (1991) *Schistosoma mansoni*: a chemoattractive factor released by males and its receptor in females. *Experientia*, **47**(9), 970-974.

Haseeb, M. A., Thors, C., Linder, E., and Eveland, L. K. (2008) *Schistosoma mansoni*: Chemoperception through n-acetyl-D-galactosamine-containing receptors in females offers insight into increased severity of schistosomiasis in individuals with blood group A. *Experimental Parasitology*, **119**, 63-73.

Hashmi, S., Britton, C., Liu, J., Guiliano, D. B., Oksov, Y., and Lustigman, S. (2002) Cathepsin L is essential for embryogenesis and development ofCaenorhabditis elegans. *Journal of Biological Chemistry*, **277**(5), 3477-3486.

Hayashida T., Decaestecker M., and Schnaper H. W. (2003) Cross-talk between ERK MAP kinase and Smad signaling pathways enhances TGF-beta-dependent responses in human mesangial cells. *FASEB Journal*. **17**, 1576–1578

Henklova, P., Vrzal, R., Papouskova, B., Bednar, P., Jancova, P., Anzenbacherova, E., and Dvorak, Z. (2008) SB203580, a pharmacological inhibitor of p38 MAP kinase transduction pathway activates ERK and JNK MAP kinases in primary cultures of human hepatocytes. *European journal of pharmacology*, 593(1), 16-23.

Hernandez, D.C., Lim, K.C., McKerrow, J.H. and Davies, S.J. (2004) *Schistosoma mansoni*: sex-specific modulation of parasite growth by host immune signals. *Experimental Parasitology*, **106**, (2), 59 – 61.

Herskowitz, I. (1995) MAP kinase pathways in yeast: For mating and more. *Cell*, **80**, 187-197.

Heyers, O., Walduck, A. K., Brindley, P. J., Bleiß, W., Lucius, R., Dorbic, T., and Kalinna, B. H. (2003) *Schistosoma mansoni* miracidia transformed by particle bombardment infect *Biomphalaria glabrata* snails and develop into transgenic sporocysts. *Experimental parasitology*,**105**(2), 174-178.

Hibi, M., Lin, A., Smeal, T., Minden, A., and Karin, M. (1993) Identification of an oncoprotein-and UV-responsive protein kinase that binds and potentiates the c-Jun activation domain. *Genes & Development*, **7**(11), 2135-2148.

Hilger, R. A., Schelulen, M. E., and Strumberg, D. (2002) The Ras-Raf-MEK-ERK pathway in the treatment of cancer. *Onkologie*, **25**, 511-518.

Hiramatsu, Y., Sekiguchi, N., Hayashi, M., Isshiki, K., Yokota, T., King, G. L., and Loeken, M. R. (2002) Diacylglycerol production and protein kinase C activity are increased in a mouse model of diabetic embryopathy. *Diabetes*, **51**(9), 2804-2810.

Hockley, D. J. and McLaren, D. J. (1973) *Schistosoma mansoni*: changes in the outer membrane of the tegument during development from cercaria to adult worm. *International Journal for Parasitology*, **3**, 13–25

Hoffmann, K. F., Johnston, D. A., and Dunne, D. W. (2002) Identification of Schistosoma mansoni gender-associated gene transcripts by cDNA microarray profiling. *Genome Biology*, **3**(8), 41.

Homma, A., Tanuri, A., Duarte, A. J., Marques, E., de Almeida, A., Martins, R., and Possas, C. (2013) Vaccine research, development, and innovation in Brazil: A translational science perspective. *Vaccine*, **31**, B54-B60.

Hong, S. T., Bang, S., Hyun, S., Kang, J., Jeong, K., Paik, D., and Kim, J. (2008) cAMP signalling in mushroom bodies modulates temperature preference behaviour in Drosophila. *Nature*, **454**(7205), 771-775.

Hong, S. T., Bang, S., Paik, D., Kang, J., Hwang, S., Jeon, K., and Kim, J. (2006) Histamine and its receptors modulate temperature-preference behaviors in Drosophila. *The Journal of Neuroscience*, **26**(27), 7245-7256.

Hoste, H., and Torres-Acosta, J. F. J. (2011) Non chemical control of helminths in ruminants: adapting solutions for changing worms in a changing world. *Veterinary Parasitology*, **180**(1), 144-154.

Hotez, P. J., Bethony, J. M., Diemert, D. J., Pearson, M., & Loukas, A. (2010) Developing vaccines to combat hookworm infection and intestinal schistosomiasis. *Nature Reviews Microbiology*, **8**(11), 814-826.

Hotez, P., Ottesen, E., Fenwick, A. and Molyneux, D. (2006) The neglected tropical diseases: the ancient afflictions of stigma and poverty and the prospects for their control and elimination. *Advances in Experimental Medicine and Biology*, **582**, 23–33.

House, C., and Kemp, B. E. (1987) Protein kinase C contains a pseudosubstrate prototope in its regulatory domain. *Science*, **238**(4834), 1726-1728.

Huang, F.L., Yoshida, Y., Cunha-Melo, J.R., Beaven, M.A. and Huang, K.P. (1989) Differential down-regulation of protein kinase C isozymes. *Journal of Biology and Chemistry*, **264**, 4238–4243.

Hyde, R., Corkins, M. E., Somers, G. A., and Hart, A. C. (2011) PKC-1 acts with the ERK MAPK signaling pathway to regulate Caenorhabditis elegans mechanosensory response. *Genes, Brain and Behavior*, **10**(3), 286-298.

Inoue, M., Kimashimoto, A., Takay, Y., and Nishizuka, Y. (1977) Studies on a cyclic nucleotide-independent protein kinase and its proenzyme in mammalian tissues. II. Proenzyme and its activation by calcium-dependent protease from rat brain. *Journal Biological Chemistry*, **252**, 7610-7616.

Ismail, M., Botros, S., Metwally, A., William, S., Farghally, A., Tao, I. F., Day, T. and Bennett, J. I. (1999) Resistance to praziquantel: direct evidence from *Schistosoma mansoni* isolated from Egyptian villagers. *American Journal of Tropical Medicine and Hygiene*, **60**, 932-935.

Ivanchenko, M. G., Lerner, J. P., McCormick, R. S., Toumadje, A., Allen, B., Fischer, K., Hedstrom, O., Helmrich, A., Barnes, D. W., Bayne C. J. (1999) Continuous in vitro propagation and differentiation of cultures of the intramolluscan stages of the human parasite *Schistosoma mansoni*. *Proceedings of the National Academy of Sciences*, **96**, 4965–4970.

Jenkins, S. J., and Mountford, A. P. (2005) Dendritic cells activated with products released by schistosome larvae drive Th2-type immune responses, which can be inhibited by manipulation of CD40 costimulation. *Infection and Immunity*, **73**(1), 395-402.

Jenkins, S. J., Hewitson, J. P., Jenkins, G. R., and Mountford, A. P. (2005) Modulation of the host's immune response by schistosome larvae. *Parasite immunology*, **27**(10-11), 385-393.

Jeong, H. J., Kim, J. B., Hong, S. H., An, N. H., Kim, M. S., Park, B. R., and Kim, H. M. (2005) Vascular endothelial growth factor is regulated by hypoxic stress via MAPK and HIF-1α in the inner ear. *Journal of Neuroimmunology*, **163**(1), 84-91.

Jeziorski, M.C. and Greenberg, R.M. (2006) Voltage-gated calcium channel subunits from platyhelminths: potential role in praziquantel action. *International Journal for Parasitology*, **36**, 625–632.

Johannes, F.J., Prestle, J., Eis, S., Oberhagemann, P., and K. Pfizenmaier. (1994) PKCu is a novel, atypical member of the protein kinase C family. *Journal of Biological Chemistry*, **269**,6140–6148.

Jones Jr, S. and, Bennett, R. (2011) Fungal mating pheromones: Choreographing the dating game. *Fungal Genetics and Biology*, **48**, 668–676.

Jones, M. K., Bong, S. H., Green, K. M., Holmes, P., Duke, M., Loukas, A., and McManus, D. P. (2008) Correlative and dynamic imaging of the hatching biology of *Schistosoma japonicum* from eggs prepared by high pressure freezing. *PLoS Neglected Tropical Diseases*, **2**(11), e334.

Jones, M. K., Gobert, G. N., Zhang, L., Sunderland, P., and McManus, D. P. (2004) The cytoskeleton and motor proteins of human schistosomes and their roles in surface maintenance and host–parasite interactions. *Bioessays*, **26**(7), 752-765.

Kabatereine, N., Vennervald, B., Ouma, J., Kemijumbi, J., Butterworth, A., Dunne, D. and Fulford, A. (1999) Adult resistance to schistosomiasis mansoni: age-dependence of reinfection remains constant in communities with diverse exposure patterns, *Parasitology*, **118**, 101–105.

Kaibuchi, K., Fukumoto, Y., Oku, N., Hori, Y., Yamamoto, T., Toyoshima, K., and Takai, Y. (1989) Activation of the serum response element and 12-O-tetradecanoylphorbol-13-acetate response element by the activated c-raf-1 protein in a manner independent of protein kinase C. *Journal of Biological Chemistry*, **264**(35), 20855-20858.

Kallunki, T., Deng, T., Hibi, M., and Karin, M. (1996) c-Jun can recruit JNK to phosphorylate dimerization partners via specific docking interactions. *Cell*, **87**(5), 929-939.

Kallunki, T., Su, B., Tsigelny, I., Sluss, H. K., Dérijard, B., Moore, G., and Karin, M. (1994) JNK2 contains a specificity-determining region responsible for efficient c-Jun binding and phosphorylation. *Genes & Development*, **8**(24), 2996-3007.

Kamada, Y., Jung, U. S., Piotrowski, J., and Levin, D. E. (1995) The protein kinase C-activated MAP kinase pathway of Saccharomyces cerevisiae mediates a novel aspect of the heat shock response. *Genes & Development*, **9**(13), 1559-1571.

Kane, N. S., Robichon, A., Dickinson, J. A., and Greenspan, R. J. (1997) Learning without performance in PKC-deficient Drosophila. *Neuron*, **18**(2), 307-314.

Kang, M. A., Mott, T. M., Tapley, E. C., Lewis, E. E., and Luckhart, S. (2008) Insulin regulates aging and oxidative stress in Anopheles stephensi. *Journal of Experimental Biology*, **211**(5), 741-748.

Kaplan, R. M. (2004) Drug resistance in nematodes of veterinary importance: a status report. *Trends in Parasitology*, **20**, 477–481

Kapp, K., Knobloch,J., Schüßler, P., Sroka, S., Lammers, R., Kunz, W. and Grevelding, C.G. (2004) The *Schistosoma mansoni* Src kinase TK3 is expressed in the gonads and likely involved in cytoskeletal organization. *Molecular and Biochemical Parasitology*, **138** (2), 171-182.

Kapp, K., Schuessler, P., Kunz, W. and Grevelding, C.G. (2001) Identifcation, isolation and characterization of a Fyn-like tyrosine kinase from *Schistosoma mansoni*. *Parasitology*, **122**, 317-327.

Karin, M. (1995) The regulation of AP-1 activity by mitogen-activated protein kinases. *Journal of Biological Chemistry*, **270**, 16483–16486

Keiser, J. (2010) *In vitro* and *in vivo* trematode models for chemotherapeutic studies. *Parasitology*, **137**(3), 589.

Kemp, W. M., Brown, P. R., Merritt, S. C., and Miller, R. E. (1980) Tegument-associated antigen modulation by adult male Schistosoma mansoni. *The Journal of Immunology*, **124**(2), 806-811.

Keranen, L.M., Dutil, E.M. and Newton, A.C. (1995) Protein kinase C is regulated *in vivo* by three functionally distinct phosphorylations. *Current Biology*, **5**, 1394–1403.

Khalil, M. (1922) The morphology of the cercaria of *Schistosomum mansoni* from Planorbis boissyi of Egypt. *Proceedings of the Royal Society of Medicine*, **15**, 27.

Khasar, S. G., Lin, Y. H., Martin, A., Dadgar, J., McMahon, T., Wang, D., and Messing, R. O. (1999) A novel nociceptor signaling pathway revealed in protein kinase C ε mutant mice. *Neuron*, **24**(1), 253-260.

Khayath, N. Vicogne, J. Ahier, A. Benyounes, A. Konrad, C. Trolet, J. Viscogliosi E., Brehm K. and C. Dissous. (2007) Diversification of the insulin receptor family in the helminth parasite *Schistosoma mansoni*, *The FEBS Journal* **274**, 659–676.

Kiley, S. C., and Parker, P. J. (1995) Differential localization of protein kinase C isozymes in U937 cells: evidence for distinct isozyme functions during monocyte differentiation. *Journal of Cell Science*, **108**(3), 1003-1016.

Kines, K. J., Rinaldi, G., Okatcha, T. I., Morales, M. E., Mann, V. H., Tort, J. F., and Brindley, P. J. (2010) Electroporation facilitates introduction of reporter transgenes and virions into schistosome eggs. *PLoS Neglected Ttropical Diseases*, **4**(2), e593.

King, A.J., H. Sun, B. Diaz, D. Barnard, W. Miao, S. Bagrodia, and M.S. Marshall. (1998) The protein kinase Pak3 positively regulates Raf-1 activity through phosphorylation of serine 338. *Nature*, **396**,180–183.

King, C. L., and Higashi, G. I. (1992) *Schistosoma mansoni*: Silver ion (Ag^+) stimulates and reversibly inhibits lipid-induced cercarial penetration. *Experimental Parasitology*, **75**(1), 31-39.

King, C.H., Sturrock, R.F., Kariuki, H.C. and Hamburger, J. (2006) Transmission control for schistosomiasis – why it matters now. *Trends in Parasitology*, **22** (12), 575-582.

Knobloch J., Winnen, R., Quack, M., Kunz, W. and Grevelding, C.G. (2002) A novel Syk-family tyrosine kinase from *Schistosoma mansoni* which is preferentially transcribed in reproductive organs. *Gene*, **294**, (1), 87-97.

Knobloch, J., Beckmann, S., Burmeister, C., Quack, T., and Grevelding, C. G. (2007) Tyrosine kinase and cooperative TGFβ signaling in the reproductive organs of *Schistosoma mansoni*. *Experimental Parasitology*, **117**(3), 318-336.

Knobloch, J., Kunz, W., and Grevelding, C. G. (2006) Herbimycin A suppresses mitotic activity and egg production of female *Schistosoma mansoni*. *International Journal for Parasitology*, **36**(12), 1261-1272.

Knobloch, J., Rossi, A., Osman, A., LoVerde, P.T., Klinkert, M.Q. and Grevelding, C.G. (2004) Cytological and biochemical evidence for a gonad-preferential interplay of SmFKBP12 and SmTbetaR-I in *Schistosoma mansoni*. *Molecular and Biochemical Parasitology*, **138** (2), 227-36.

Knudsen, G. M., Medzihradszky, K. F., Lim, K. C., Hansell, E., and McKerrow, J. H. (2005) Proteomic analysis of Schistosoma mansoni cercarial secretions. *Molecular & Cellular Proteomics*, **4**(12), 1862-1875.

Kohno, M., and Pouyssegur, J. (2003) Pharmacological inhibitors of the ERK signaling pathway: application as anticancer drugs. *Progress in Cell Cycle Research*, **5**, 219.

Kolch W. (2005) Coordinating ERK/MAPK signalling through scaffolds and inhibitors. *Nature Reviews Molecular Cell Biology*, **6**(11), 827-837

Kolch, W. (2000) Meaningful relationships: the regulation of the Ras/Raf/MEK/ERK pathway by protein interactions. *Biochemistry Journal*, **351**, 289-305.

Koster, B., Hall, M. R., and Strand, M. (1993) *Schistosoma mansoni*: Immunoreactivity of Human Sera with the Surface Antigen Sm23. *Experimental Parasitology*, **77**(3), 282-294.

Krautz-Peterson, G., and Skelly, P. J. (2008) *Schistosoma mansoni*: The dicer gene and its expression. *Experimental Parasitology*, **118**(1), 122-128.

Krautz-Peterson, G., Radwanska, M., Ndegwa, D., Shoemaker, C. B., and Skelly, P. J. (2007) Optimizing gene suppression in schistosomes using RNA interference. *Molecular and Biochemical Parasitology*, **153**(2), 194-202.

Krens, S. F., He, S., Spaink, H. P., and Snaar-Jagalska, B. E. (2006) Characterization and expression patterns of the MAPK family in zebrafish.*Gene Expression Patterns*, **6**(8), 1019-1026.

Kruger, K. E., Sossin, W. S., Sacktor, T. C., Bergold, P. J., Beushausen, S., and Schwartz, J. H. (1991) Cloning and characterization of Ca (2+)-dependent and Ca (2+)-independent PKCs expressed in Aplysia sensory cells. *The Journal of Neuroscience*, **11**(8), 2303-2313.

Kültz, D., and Burg, M., (1998) Evolution of osmotic stress signaling via MAP kinase cascades. *Journal of Experimental Biology*, **201**(22), 3015–3021.

Kuntz, A.N., Davioud-Charvet, E., Sayed, A.A., Califf, L.L., Dessolin, J., Arnér, E.S.J. and Williams, D.L. (2007) Thioredoxin glutathione reductase from *Schistosoma mansoni:* An essential parasite enzyme and a key drug target. *PLOS Medicine*, **4** (6), 1071-1086.

Kunz, W. (2001) *Schistosome* male-female interaction: induction of germ-cell differentiation. *Trends in Parasitology*, **17**, 227-231.

Kusel, J. R. (1970) Studies on the structure and hatching of the eggs of *Schistosoma mansoni*. *Parasitology*, **60**(1), 79-88.

Kusel, J. R., McVeigh, P., and Thornhill, J. A. (2009) The schistosome excretory system: a key to regulation of metabolism, drug excretion and host interaction. *Trends in Parasitology*, **25**(8), 353-358.

Kwon, Y., Shim, H. S., Wang, X., and Montell, C. (2008) Control of thermotactic behavior via coupling of a TRP channel to a phospholipase C signaling cascade. *Nature Neuroscience*, **11**(8), 871-873.

Kyriakis, J. M., and Avruch, J. (1990) pp54 microtubule-associated protein 2 kinase. A novel serine/threonine protein kinase regulated by phosphorylation and stimulated by poly-L-lysine. *Journal of Biological Chemistry*, **265**(28), 17355-17363.

Kyriakis, J. M., and Avruch, J. (2001) Mammalian mitogen-activated protein kinase signal transduction pathways activated by stress and inflammation. *Physiological Reviews*, **81**(2), 807-869.

Kyriakis, J. M., App, H., Zhang, X. F., Banerjee, P., Brautigan, D. L., Rapp, U. R., and Avruch, J. (1991) Raf-1 activates MAP kinase-kinase, *Nature*, 417-421.

Kyriakis, J. M., Banerjee, P., Nikolakaki, E., Dai, T., Rubie, E. A., Ahmad, M. F., and Woodgett, J. R. (1994) The stress-activated protein kinase subfamily of c-Jun kinases. *Nature*, 156-160.

Land, M., Islas-Trejo, A., Freedman, J.H. and Rubin, C.S. (1993) Structure and expression of a novel, neuronal protein kinase C (PKC1B) from *Caenorhabditis elegans*. *Journal of Biology and Chemistry*, **269**, 9234-9244.

Larralde, C., Morales, J., Terrazas, I., Govezensky, T., and Romano, M. C. (1995) Sex hormone changes induced by the parasite lead to feminization of the male host in murine *Taenia crassiceps* cysticercosis. *The Journal of Steroid Biochemistry and Molecular Biology*, **52**(6), 575-580.

Lazdins, J. K., Stein, M. J., David, J. R., and Sher, A. (1982) *Schistosoma mansoni*: Rapid isolation and purification of schistosomula of different developmental stages by centrifugation on discontinuous density gradients of Percoll. *Experimental Parasitology*, **53**(1), 39-44.

Lee, J. C., Kassis, S., Kumar, S., Badger, A., and Adams, J. L. (1999) p38 mitogen-activated protein kinase inhibitors - mechanisms and therapeutic potentials. *Pharmacology & Therapeutics*, **82**(2), 389-397.

Lee, J. C., Kumar, S., Griswold, D. E., Underwood, D. C., Votta, B. J., and Adams, J. L. (2000) Inhibition of p38 MAP kinase as a therapeutic strategy. *Immunopharmacology*, **47**(2), 185-201.

Lee, J., Hong, F., Kwon, S., Kim, S., Kim, D., Kang, H., Lee, S., Ha, J. and Kim, S. (2002) Activation of p38 MAPK induces cell cycle arrest via inhibition of Raf/ERK pathway during muscle differentiation. *Biochemical and Biophysical Research Communications*, **298** (5), 765-771.

Leiper, R. T. (1915) Report on the Results of the Bilharzia Mission in Egypt, 1915. *Journal of the Royal Army Medical Corps*, **25**(1; 2).

Lenormand, P., Sardet, C., Pages, G., L'Allemain, G., Brunet, A., and Pouysségur, J. (1993) Growth factors induce nuclear translocation of MAP kinases (p42mapk and p44mapk) but not of their activator MAP kinase kinase (p45mapkk) in fibroblasts. *The Journal of Cell Biology*, **122**(5), 1079-1088.

Levin, D. E., and Bartlett-Heubusch, E. (1992) Mutants in the *S. cerevisiae* PKC1 gene display a cell cycle-specific osmotic stability defect. *The Journal of Cell Biology*, **116**(5), 1221-1229.

Levin, D. E., and Errede, B. (1995) The proliferation of MAP kinase signaling pathways in yeast. *Current Opinion in Cell Biology*, **7**(2), 197-202.

Levin, D. E., Fields, F. O., Kunisawa, R., Bishop, J. M., and Thorner, J. (1990) A candidate protein kinase C gene, *PKC1*, is required for the S. cerevisiae cell cycle. *Cell*, **62**(2), 213-224.

Lewis, F. A. (1999) Schistosomiasis. *Current Protocols in Immunology*, **3**, 19.1.1 – 19.1.28.

Lewis, F., Liang, Y., Raghavan, N. and Knight, M. (2008) The NIH-NIAID Schistosomiasis Resource Center. *PLoS Neglected Tropical Diseases*, **2**(7), e267

Lewis, T. S., Shapiro, P. S., Ahn N. G. (1998) Signal transduction through MAP kinase cascades. *Advances in Cancer Research*, **74**, 49–139.

Lima, S. F., Vieira, L. Q., Harder, A., and Kusel, J. R. (1994) Effects of culture and praziquantel on membrane fluidity parameters of adult *Schistosoma mansoni*. *Parasitology*, **109**, 57-57.

Lingnau, A., Margos, G., Maier, W. A., and Seitz, H. M. (1993) The effects of hormones on the gametocytogenesis of *Plasmodium falciparum in vitro*. *Applied Parasitology*, **34**(3), 153.

Liu, S.W. and Heckman, C.A. (1998) The sevenfold way of PKC regulation. *Cellular Signalling Topical Review*, **10**(8), 529-542.

Liu. F., Zhou, Y., Wang, Z. Q., Lu. G., Zheng, H., Brindley, P. J., McManus, D. P., Blair, D., Zhang, Q. H., Zhong, Y., Wang, S., Han, Z. G. and Chen, Z. (2009) The *Schistosoma japonicum* genome reveals features of host-parasite interplay. *Nature*, **46** (7253), 345-51.

Livak, K. J., and Schmittgen, T. D. (2001) Analysis of Relative Gene Expression Data Using Real-Time Quantitative PCR and the 2ΔΔCT Method. *Methods*, **25**(4), 402-408.

Loukas, M.T. and Pearson, M.S. (2007) *Schistosome* membrane proteins as vaccines. *International Journal for Parasitology*, **37**, 257-263.

LoVerde, P. T., Andrade, L. F., and Oliveira, G. (2009) Signal transduction regulates schistosome reproductive biology. *Current Opinion in Microbiology*, **12**(4), 422-428.

LoVerde, P. T., Niles, E. G., Osman, A., and Wu, W. (2004) *Schistosoma mansoni* male-female interactions. *Canadian Journal of Zoology*, **82**(2), 357-374.

LoVerde, P. T., Osman, A. and Hinck, A. (2007) *Schistosoma mansoni*: TGF-beta signalling pathways. *Experimental Parasitology, 117*, 304-317.

Ludtmann, M. (2008) Protein Kinase C Signalling in *Schistosoma mansoni* and its role in larval development. Thesis of Master of Science by Research. Kingston University.

Ludtmann, M., Rollinson, D., Emery, A. and Walker, A. (2009) Protein kinase C signalling during miracidium to mother sporocyst development in the helminth parasite, *Schistosoma mansoni*. *International Journal of Parasitology*, **39** (11), 1223-1233.

Luo, L., Gershow, M., Rosenzweig, M., Kang, K., Fang-Yen, C., Garrity, P. A., and Samuel, A. D. (2010) Navigational decision making in Drosophila thermotaxis. *The Journal of Neuroscience*, **30**(12), 4261-4272.

Luo, Y., Sunderland, T., Roth, G., and Wolozin, B. (1996) Physiological levels of β-amyloid peptide promote PC12 cell proliferation. *Neuroscience Letters*, **217**, 125-128.

Machado-Silva, J. R., Galvão, C., Oliveira, R. M. F., Presgrave, O. A. F., Gomes, D. C. (1995) *Schistosoma mansoni* Sambon, 1907: comparative morphological studies of some Brazilian strains. *Revista do Instituto Medico Tropical de São Paulo* **37**, 441-447.

Machado-Silva, J. R., Lanfredi, R. M., and Gomes, D. C. (1997) Morphological study of adult male worms of *Schistosoma mansoni* Sambon, 1907 by scanning electron microscopy. *Memórias do Instituto Oswaldo Cruz*, **92**, 647-653.

Machado-Silva, J. R., Pelajo-Machado, M., Lenzi, H. L., and Gomes, D. C. (1998) Morphological study of adult male worms of *Schistosoma mansoni* Sambon, 1907 by confocal laser scanning microscopy. *Memórias do Instituto Oswaldo Cruz*, *93*, 303-307.

Macinnis, A. J. (1969) Identification of Chemicals triggering Cercarial Penetration Responses of *Schistosoma mansoni*. *Nature*, **224**, 1221-1222.

Maioli, M., & Ventura, C. (2001) Protein kinase C control of gene expression. *Critical Reviews in Eukaryotic Gene Expression*, **11**(1-3).

Malmberg, A. B., Chen, C., Tonegawa, S., and Basbaum, A. I. (1997) Preserved acute pain and reduced neuropathic pain in mice lacking PKCγ. *Science*, **278**(5336), 279-283.

Mann, V. H., Morales, M. E., Rinaldi, G., and Brindley, P. J. (2010) Culture for genetic manipulation of developmental stages of *Schistosoma mansoni*. *Parasitology*, **137**(3), 451.

Marshall, C. J. (1995) Specificity of receptor tyrosine kinase signaling: transient versus sustained extracellular signal-regulated kinase activation. *Cell*, 80(2), 179-185.

Martín-Blanco, E. (2000) p38 MAPK signalling cascades: ancient roles and new functions. *BioEssays*, **22**(7), 637-645.

Matsumura, K., Mitsui, Y., Sato, K., Sakamoto, M., and Aoki, Y. (1991) *Schistosoma mansoni*: Possible involvement of protein kinase C in linoleic acid-induced proteolytic enzyme release from cercariae. *Experimental parasitology*, **72**(3), 311-320.

Matsumura, K., Shimada, M., Sato, K., and Aoki, Y. (1990) Praziquantel-induced secretion of proteolytic enzyme from *Schistosoma mansoni* cercariae. *Journal of Parasitology*, **76**(3), 436-438.

McCarthy, E., Stack, C., Donnelly, S. M., Doyle, S., Mann, V. H., Brindley, P. J., and Dalton, J. P. (2004) Leucine aminopeptidase of the human blood flukes, *Schistosoma mansoni* and *Schistosoma japonicum*. *International Journal for Parasitology*, **34**(6), 703-714.

McCormick, F. (1994) Activators and effectors of *ras* p21 proteins. *Current Opinion in Genetics & Development*, **4**(1), 71-76.

McGonigle, S., Beall, M.J. and Pearce, and E.J. (2002) Eukaryotic initiation factor 2α subunit associates with TGFβ receptors and 14-3-3ε and acts as a modulator of the TGFβ response. *Biochemistry*, **41** (2), 579 -587.

McGonigle, S., Beall, M.J., Feeney, E.L. and Pearce, E.J. (2001a) Conserved role for 14-3-3e downstream of type I TGFL receptors. *FEBS Letters*, **490**, 65-69.

McGonigle, S., Feeney, E.L., Beall, M.J. and Pearce, E.J. (2001b) SIP, a novel SH3 domain-containing protein, interacts with *Schistosoma mansoni* receptor kinase 1. *Molecular and Biochemical Parasitology*, **114,** 119-123.

McKerrow, J. H. (2003) Invasion of skin by schistosome cercariae: some neglected facts: Response from James J. McKerrow. *Trends in Parasitology*, **18**, 66–68.

McKerrow, J. H., and Salter, J. (2002) Invasion of skin by *Schistosoma cercariae*. *Trends in Parasitology*, **18**, 193–195.

McKerrow, J. H., Jones, P., Sage, H., and Pino-Heiss, S. (1985) Proteinases from invasive larvae of the trematode parasite *Schistosoma mansoni* degrade connective-tissue and basement-membrane macromolecules. *Biochemical Journal*, **231**, 47-51.

McLaren, D. J. (1980) *Schistosoma mansoni*: the parasite surface in relation to host immunity. Research Studies Press. John Wiley & Sons Ltd, Baffins Lane, Chichester, West Sussex PO19 1UD.

McManus, D.P. and Loukas, A. (2008) Current status of vaccines for schistosomiasis. *Clinical Microbiology Reviews*, **21**(1), 225-242.

McVeigh, P., Atkinson, L., Marks, N. J., Mousley, A., Dalzell, J. J., Sluder, A., and Maule, A. G. (2012) Parasite neuropeptide biology: Seeding rational drug target selection? *International Journal for Parasitology: Drugs and Drug Resistance*, **2**, 76-91.

McVeigh, P., Mair, G. R., Atkinson, L., Ladurner, P., Zamanian, M., Novozhilova, E., and Maule, A. G. (2009) Discovery of multiple neuropeptide families in the phylum Platyhelminthes. *International Journal for Parasitology*, **39**(11), 1243-1252.

Mehlhorn, H., Becker, B., Andrews, P., Thomas, H. and Frenkel, J.K. (1981) *In vivo* and *in vitro* experiments on the effects of praziquantel on *Schistosoma mansoni*. A light and electron microscopic study. *Arzneimittelforschung*, **31**, 544–554.

Mellor, H. and Parker, P.J. (1998) The extended protein kinase C superfamily. *Biochemical Journal*, **332**, 281-292.

Mendoza, M. C., Er, E. E., and Blenis, J. (2011) The Ras-ERK and PI3K-mTOR pathways: cross-talk and compensation. *Trends in Biochemical Sciences*, **36**(6), 320-328.

Mercer, K. E., & Pritchard, C. A. (2003) Raf proteins and cancer: B-Raf is identified as a mutational target. *Biochimica et Biophysica Acta (BBA)-Reviews on Cancer*, **1653**(1), 25-40.

Meuleman, E. A., Holzmann, P. J., and Peet, R. C. (1980) The development of daughter sporocysts inside the mother sporocyst of *Schistosoma mansoni* with special reference to the ultrastructure of the body wall. *Zeitschrift für Parasitenkunde*, **61**(3), 201-212.

Meyer, T., Sekljic, H., Fuchs, S., Bothe, H., Schollmeyer, D., and Miculka, C. (2009) Taste, a new incentive to switch to (R)-Praziquantel in schistosomiasis treatment. *PLoS Neglected Tropical Diseases*, **3**(1), e357.

Michaels, R. M. (1969) Mating of *Schistosoma mansoni in vitro*. *Experimental Parasitology*, **25**, 58-71.

Milhon, J.L., Albert, T.A., Vande Waa, E.A., O'Leary, K.A., Jackson, R.N., Kessler, M.A., Schuler, L.A. and Tracy, J.W. (2000) *Sm*MAK16, the *Schistosoma mansoni* homologue of MAK16 from yeast, targets protein transport to the nucleolus. *Molecular and Biochemical Parasitology*, **108**, 225–236.

Miranda-Saavedra, D., Stark, M. J., Packer, J. C., Vivares, C. P., Doerig, C., and Barton, G. J. (2007) The complement of protein kinases of the microsporidium Encephalitozoon cuniculi in relation to those of Saccharomyces cerevisiae and *Schizosaccharomyces pombe*. *BMC Genomics*, **8**(1), 309.

Mizukami, Y., Yoshioka, K., Morimoto, S., and Yoshida, K. I. (1997) A novel mechanism of JNK1 activation Nuclear translocation and activation of JNK1 during ischemia and reperfusion. *Journal of Biological Chemistry*, **272**(26), 16657-16662.

Molkentin, J. D., and Dorn II, G. W. (2001) Cytoplasmic signaling pathways that regulate cardiac hypertrophy. *Annual Review of Physiology*, **63**(1), 391-426.

Mondadori, R. G., Neves, J. P., and Gonçalves, P. B. D. (2008) Protein kinase C (PKC) role in bovine oocyte maturation and early embryo development. *Animal Reproduction Science*, **107**(1), 20-29.

Montresor, A., Crompton, D. W. T., Gyorkos, T. W. and Savioli, L. (2002) *Helminth Control in School-age Children: A Guide for Managers of Control Programmes*, WHO, Geneva.

Moore, D. V. and Sandground, J. H. (1956) The relative egg producting capacity of *Schistosoma mansoni* and *Schistosoma japonicum*. *American Journal of Tropical Medicine and Higiene*, **5**, 831-840.

Moraes Mourão, M., Dinguirard, N., Franco, G. R., and Yoshino, T. P. (2009) Phenotypic screen of early-developing larvae of the blood fluke, Schistosoma mansoni, using RNA interference. *PLoS neglected tropical diseases*, 3(8), e502.

Morales-Montor, J., Newhouse, E., Mohamed, F., Baghdadi, A., and Damian, R. T. (2001) Altered levels of hypothalamic-pituitary-adrenocortical axis hormones in baboons and mice during the course of infection with Schistosoma mansoni.*Journal of Infectious Diseases*, **183**(2), 313-320.

Morris, G. P., and Threadgold, L. T. (1967) A presumed sensory structure associated with the tegument of *Schistosoma mansoni*. *The Journal of Parasitology*, 537-539.

Moser, G., Wassom, D. L., and Sher, A. (1980) Studies of the antibody-dependent killing of schistosomula of *Schistosoma mansoni* employing haptenic target antigens. Evidence that the loss in susceptibility to immune

damage undergone by developing schistosomula involves a change unrelated to the masking of parasite antigens by host molecules. *Journal of Experimental Medicine*, **152**, 41–53.

Mukai, H., Kitagawa, M., Shibata, H., Takanaga, H., Mori, K., Shimakawa, M., and Ono, Y. (1994) Activation of PKN, a novel 120-kDa protein kinase with leucine zipper-like sequences, by unsaturated fatty acids and by limited proteolysis. *Biochemical and Biophysical Research Communications*, **204**(1), 348-356.

Mulder, K. M. (2000) Role of Ras and Mapks in TGFβ signaling. *Cytokine & Growth Factor Reviews*, **11**(1), 23-35.

Murakami, K., and Routtenberg, A. (1985) Direct activation of purified protein kinase C by unsaturated fatty acids (oleate and arachidonate) in the absence of phospholipids and Ca^{2+}. *FEBS Letters*, **192**(2), 189-193.

Naor, Z., Shearman, M. S., Kishimoto, A., and Nishizuka, Y. (1988) Calcium-independent activation of hypothalamic type I protein kinase C by unsaturated fatty acids. *Molecular Endocrinology*, **2**(11), 1043-1048.

Ndegwa, D., Krautz-Peterson, G., and Skelly, P. J. (2007) Protocols for gene silencing in schistosomes. *Experimental Parasitology*, **117**(3), 284-291.

Neel, B. G., and Tonks, N. K. (1997) Protein tyrosine phosphatases in signal transduction. *Current Opinion in Cell Biology*, **9**(2), 193-204.

Nelson, T.J. and Alkon, D.L. (2009) Neuroprotective *versus* tumorigenic protein kinase C activators. *Trends in Biochemistry Science*, **34**, 136–145.

Newton, A. (2003) Regulation of the ABC kinases by phosphorylation: protein kinase C as a paradigm. *Biochemistry Journal*, **370**, 361-371.

Newton, A. C. (2001) Protein kinase C: structural and spatial regulation by phosphorylation, cofactors, and macromolecular interactions. *Chemical Reviews*, **101**(8), 2353-2364.

Newton, A.C. (2010) Protein kinase C: poised to signal. *American Journal of Physiology-Endocrinology and Metabolism*, **298**, 395-402.

Nishizuka, Y. (1986) Studies and perspectives of protein kinase C. *Science*, **233**(4761), 305-312.

Nishizuka, Y. (1989). The family of protein kinase C for signal transduction.*JAMA: the journal of the American Medical Association*, **262**(13), 1826-1833.

Norton, A. J., Rollinson, D. Richerds, L., and Webster, J. P. (2008) Simultaneous infection of *Schistosoma mansoni* and *S. rhodan* in *Biomphalaria glabrata*: impact on chronobiology and cercarial behaviour. *Parasites & Vectors*, **1**(43), 1-9.

Okochi, Y., Kimura, K. D., Ohta, A., and Mori, I. (2005) Diverse regulation of sensory signaling by C. elegans nPKC-epsilon/eta TTX-4. *The EMBO Journal*, **24**(12), 2127-2137.

Olds, R. G., and Dasarathy, S. (2001) Recent advances in schistosomiasis. *Current Infectious Disease Reports*, **3**(1), 59-67.

Oliveira, M. F., d'Avila, J. C., Tempone, A. J., Soares, J. B. C., Rumjanek, F. D., Ferreira-Pereira, A., and Oliveira, P. L. (2004) Inhibition of heme aggregation by chloroquine reduces Schistosoma mansoni infection. *Journal of Infectious Diseases*, **190**(4), 843-852.

Ono, Y., Fu, J., Ogita, T., Kikkawa, K., Igarashi, U., and Nishizuka, Y. (1989) Protein kinase C zeta subspecies from rat brain: its structure, expression, and properties. *Proceedings of the National Academy of Sciences*, **86**(9), 3099-3103.

Osman, A., Niles, E.G. and LoVerde, P.T. (1999) Characterization of the Ras homologue of *Schistosoma mansoni*. *Molecular Biochemmistry Parasitology*, **100**: 27-41.

Osman, A., Niles, E.G. and LoVerde, P.T. (2001) Identification and characterization of a Smad2: homologue from *Schistosoma mansoni*, a transforming growth factor-β signal transducer. *Journal of Biological Chemistry*, **276**, 10072–10082.

Osman, A., Niles, E.G. and LoVerde, P.T. (2004) Expression of functional *Schistosoma mansoni* Smad4: Role in Erk-mediated transforming growth factor beta (TGF-beta) down-regulation. *Journal of Biological Chemistry*, **279** (8), 6474–6486.

Osman, A., Niles, E.G., Verjovski-Almeida, S. and LoVerde, P.T. (2006) *Schistosoma mansoni* TGF-b receptor II: role in host ligand-induced regulation of a schistosome target gene. *PLOS Pathogens*, **2** (6), e54.

Palmer, R. H., and Parker, P. J. (1995) Expression, purification and characterization of the ubiquitous protein kinase C-related kinase 1. *Biochemical Journal*, **309**, 315-320.

Pan, C. T. (1996) *Schistosoma mansoni*: the ultrastructure of larval morphogenesis in *Biomphalaria glabrata* and of associated host-parasite interactions, *Japanese Journal of Medical Science and Biology*, **49**, 129–149.

Pan, C. T., (1995) Studies of the host-parasite relationship between *Schistosoma mansoni* and the snail *Australorbis glabratus*. *American Journal of Tropical Medicine and Hygiene*, **14**, 931-976

Pan, C.T. (1980) The fine structure of the miracidium of *Schistosoma mansoni*. *Journal of Invertebrate Pathology*, **36**, 307-372.

Parekh, D. B., Ziegler, W., and Parker, P. J. (2000) Multiple pathways control protein kinase C phosphorylation. *The EMBO Journal*, **19**(4), 496.

Parker, P.J. and Murray-Rust, J. (2004) PKC at a glance. *Journal of Cell Science*, **117**, 131-132.

Patocka, N., and Ribeiro, P. (2007) Characterization of a serotonin transporter in the parasitic flatworm *Schistosoma mansoni*: Cloning, expression and functional analysis. *Molecular and Biochemical Parasitology*, **154**(2), 125-133.

Patocka, N., and Ribeiro, P. (2012) The functional role of a serotonin transporter in *Schistosoma mansoni* elucidated through immunolocalization and RNA interference (RNAi). *Molecular and Biochemical Parasitology*, **187**(1), 34-42

Paveley, R. A., Aynsley, S. A., Cook, P. C., Turner, J. D., and Mountford, A. P. (2009) Fluorescent imaging of antigen released by a skin-invading helminth reveals differential uptake and activation profiles by antigen presenting cells. *PLoS Neglected Tropical Diseases*, **3**(10), e528.

Payares, G., McLaren, D.J., Evans, W.H. and Smithers, S.R. (1985a) Changes in the surface antigen profile of *Schistosoma mansoni* during maturation from cercaria to adult worm. *Parasitology*, **91**(1), 83–99.

Payares, G., McLaren, D.J., Evans, W.H. and Smithers, S.R. (1985b) Antigenicity and immunogenicity of the tegumental outer membrane of adult *Schistosoma mansoni*. *Parasite Immunology*, **7**: 45–61.

Peak, E., Chalmers, I. W., and Hoffmann, K. F. (2010) Development and validation of a quantitative, high-throughput, fluorescent-based bioassay to detect schistosoma viability. *PLoS Neglected Tropical Diseases*, **4**(7), e759.

Pearce, E. J. and MacDonald, A. S. (2002) The immunobiology of schistosomiasis, *Nature Review Immunology*, **2**, 499–511.

Pearce, E. J., James, S. L., Hieny, S., Lanar, D. E., and Sher, A. (1988) Induction of protective immunity against *Schistosoma mansoni* by vaccination with schistosome paramyosin (Sm97), a nonsurface parasite antigen. *Proceedings of the National Academy of Sciences*, **85**(15), 5678-5682.

Pearson, G., Robinson, F., Gibson, T. B., Xu, B. E., Karandikar, M., Berman, K., & Cobb, M. H. (2001) Mitogen-activated protein (MAP) kinase pathways: regulation and physiological functions. *Endocrine Reviews*, **22**(2), 153-183.

Pelley, R. P., Karp., R., Mahmoud, A. and Warren, K. S. (1976) Antigen dose response and specificity of production of the lymphokine eosinophil stimulation promoter. *Journal of Infectious Disease*, **134**, 230-237.

Peyssonnaux, C., and Eychène, A. (2001) The Raf/MEK/ERK pathway: new concepts of activation. *Biology of the Cell*, **93**(1-2), 53-62.

Piao, Z. G., Cho, I. H., Park, C. K., Hong, J. P., Choi, S. Y., Lee, S. J., and Oh, S. B. (2006) Activation of glia and microglial p38 MAPK in medullary dorsal horn contributes to tactile hypersensitivity following trigeminal sensory nerve injury. *Pain*, **121**(3), 219-231.

Pica-Mattoccia, L. and Cioli, D. (2004) Sex- and stage-related sensitivity of *Schistosoma mansoni* to *in vivo* and *in vitro* praziquantel treatment. *International Journal of Parasitology*, **34**, 527–533.

Pica-Mattoccia, L., Moroni, R., Tchuem Tchuente, L. A., Southgate, V. R., and Cioli, D. (2000). Changes of mate occur in Schistosoma mansoni. *Parasitology*, **120**(05), 495-500.

Pica-Mattoccia, L., Orsini, T., Basso, A., Troiani, A., Festucci, A. F., Liberti, P., Guidi, A., Maggi, A., Santana, S., Troiani, A., Cioli D. and Vale, C. (2008) *Schistosoma mansoni*: Lack of correlation between paraziquantel-induced intra-worm calcium influx and parasite death, *Experimental Parasitology*, **119**, (3), 332–335.

Pica-Mattoccia, L., Valle, C., Basso, A., Troiani, A. R., Vigorosi, F., Liberti, P., Festucci, A. and Cioli, D. (2007) Cytochalasin D abolishes the schistosomicidal activity of praziquantel, *Experimental Parasitology*, **115**, 344–351.

Plows, L.D., Cook, R. T., Davies, A. J. and Walker, A. J. (2004) Activation of extracellular-signal regulated kinase is required for phagocytosis by *Lymnaea stagnalis* Haemocytes.*BBA - Molecular Cell Research*, **1692**(1), 25-33.

Pollak, M. N. (2007) Insulin, insulin-like growth factors, insulin resistance, and neoplasia. *The American Journal of Clinical Nutrition*, **86**(3), 820S-821S.

Popiel, I., & Erasmus, D. A. (1981) *Schistosoma mansoni:* Niridazole-induced damage to the vitelline gland. *Experimental Parasitology*, **52**(1), 35-48.

Popiel, I., and Basch, P. F. (1984) Reproductive development of female Schistosoma mansoni (Digenea: Schistosomatidae) following bisexual pairing of worms and worm segments. *Journal of Experimental Zoology*, **232**(1), 141-150.

Prelich, P. (2012) Gene Overexpression: Uses, Mechanisms, and Interpretation. *Genetics*, **190**, 841–854.

Protasio, A. V., Dunne, D. W., and Berriman, M. (2013) Comparative Study of Transcriptome Profiles of Mechanical-and Skin-Transformed *Schistosoma mansoni* Schistosomula. *PLoS Neglected Tropical Piseases*, **7**(3), e2091.

Pulverer, B. J., Kyriakis, J. M., Avruch, J., Nikolakaki, E., and Woodgett, J. R. (1991) Phosphorylation of c-jun mediated by MAP kinases. *Nature*, **353**(6345), 670-674.

Quest, A.F.G., Bioomenthal, J.B., Bardes, E.S.G. and Bell, R.M. (1992) The regulatory domain of protein kinase C coordinates four atoms of zinc. *Journal of Biological Chemistry*. **267**,10193–10197.

Raingeaud J., Gupta, S., Rogers, J. S., Dickens, M., Han, J., Ulevitch, R. J. and Davis, R. J. (1995) Pro-inflammatory cytokines and environmental stress cause p38 mitogen-activated protein kinase activation by dual phosphorylation on tyrosine and threonine. Journal of Biological Chemistry, **270**, 7420–7426.

Ramachandran, H., Skelly, P. J. and Shoemaker, C. B. (1996 The *Schistosoma mansoni* epidermal growth factor receptor homologue, SER, has tyrosine kinase activity and is localized in adult muscle. *Molecular Biochemical Parasitology, **83***, 1-10.

Rangarajan, R., Bei, A. K., Jethwaney, D., Maldonado, P., Dorin, D., Sultan, A. A., and Doerig, C. (2005) A mitogen-activated protein kinase regulates male gametogenesis and transmission of the malaria parasite *Plasmodium berghei*. *EMBO Reports*, **6**(5), 464-469.

Redman, C.A, Robertson, A., Fatlon, P.G., Modha, J., Kusel, J.R., Doenhoff, M. J. and Mattin, R.J (1996) Praziquantel: Urgent and exciting challenge. *Parasitology Today*, **12**, (1) 14-20.

Remoué, F., Mani, J. C., Pugnière, M., Schacht, A. M., Capron, A., and Riveau, G. (2002) Functional specific binding of testosterone to *Schistosoma haematobium* 28-kilodalton glutathione S-transferase. *Infection and Immunity*,**70**(2), 601-605.

Ressurreição, M., Rollinson, D., Emer, A.M. and Walker, A.J. (2011a) A role for p38 MAPK in the regulation of ciliary motion in a eukaryote. *BMC Cell Biology*, **12**(6).

Ressurreição, M., Rollinson, D., Emery, A.M. and Walker, A.J. (2011b) A role for p38 mitogen-activated protein kinase in early post-embryonic development of *Schistosoma mansoni*. *Molecular and Biochemical Parasitology*, **180**(1), 51-55.

Ribeiro P and Geary, T. G. (2010) Neuronal signalling in schistosomes: current status and prospects for postgenomics. Canadian Journal of Zoology, **88**(1), 1–22.

Ribeiro, F., Coelho, P. M. Z., Vieira, L.Q., Watson, D.G. and Kusel, J.R. (1998) The effect of praziquantel treatment on glutathione concentration in *Schistosoma mansoni*, *Parasitology*, **116**, 229–236.

Ribeiro, P., El-Shehabi, F., Patocka, N. (2005) Classical transmitters and their receptors in flatworms. *Parasitology*. **131**, S19-40.

Rink, J. C., Vu, H. T. K., and Alvarado, A. S. (2011) The maintenance and regeneration of the planarian excretory system are regulated by EGFR signaling. *Development*, **138**(17), 3769-3780.

Roberts, P. J., and Der, C. J. (2007) Targeting the Raf-MEK-ERK mitogen-activated protein kinase cascade for the treatment of cancer. *Oncogene*, **26**(22), 3291-3310.

Roberts, S. and Javony, L. (2000) Foundations of Parasitology: Sixth Edition. New York: McGraw Hill.

Rodriguez, M. M., Ron, D., Touhara, K., Chen, C. H., & Mochly-Rosen, D. (1999) RACK1, a protein kinase C anchoring protein, coordinates the binding of activated protein kinase C and select pleckstrin homology domains in vitro. *Biochemistry*, **38**(42), 13787-13794.

Rose-Hellekant, T. A., and Bavister, B. D. (1996) Roles of protein kinase A and C in spontaneous maturation and in forskolin or 3-isobutyl-1-methylxanthine maintained meiotic arrest of bovine oocytes. *Molecular Reproduction and Development*, **44**(2), 241-249.

Ross, A. G., Bartley, P. B., Sleigh, A. C., Olds, G. R., Li, Y., Williams, G. M. and McManus, D. P. (2002) Schistosomiasis. *New England Journal of Medicine*, **346**, (16), 1212-20.

Rouse, J., Cohen, P., Trigon, S., Morange, M., Alonso-Llamazares, A., Zamanillo, D., Hunt, T., Nebreda, A. R. (1994) A novel kinase cascade triggered by stress and heat shock that stimulates MAPKAP kinase-2 and phosphorylation of the small heat shock proteins. *Cell*, **78**(6), 1027-1037.

Roux, P. P., and Blenis, J. (2004) ERK and p38 MAPK-activated protein kinases: a family of protein kinases with diverse biological functions. *Microbiology and Molecular Biology Reviews*, **68**(2), 320-344.

Saladin, K. S. (1982) *Schistosoma mansoni*: cercarial responses to irradiance changes. *The Journal of parasitology*, 120-124.

Salafsky, B., and Fusco, A. C. (1987) *Schistosoma mansoni*: A comparison of secreted vs nonsecreted eicosanoids in developing schistosomulae and adults. *Experimental Parasitology*, **64**(3), 361-367.

Salafsky, B., Fusco, A. C., Whitley, K., Nowicki, D., and Ellenberger, B. (1988) *Schistosoma mansoni*: Analysis of cercarial transformation methods. *Experimental Parasitology*, **67**(1), 116-127.

Salafsky, B., Wang, Y. S., Fusco, A. C., and Antonacci, J. (1984) The role of essential fatty acids and prostaglandins in cercarial penetration (*Schistosoma mansoni*). *The Journal of Parasitology*, **70**(4), 656-660.

Samueleson, J. C. and Stein, L. D. (1989).*Schistosoma mansoni*: increasing saline concentration signals cercariae to transform to schistosomula. *Experimental Parasitology*, **69**, (1), 23-9.

Samuelson, J. C., and Caulfield, J. P. (1982) Loss of covalently labeled glycoproteins and glycolipids from the surface of newly transformed schistosomula of *Schistosoma mansoni*. *The Journal of Cell Biology*, **94**(2), 363-369.

Samuelson, J. C., Quinn, J. J., and Caulfield, J. P. (1984) Hatching, chemokinesis, and transformation of miracidia of *Schistosoma mansoni*. *The Journal of Parasitology*, 321-331.

Santos, T. M., Johnston, D. A., Azevedo, V., Ridgers, I. L., Martinez, M. F., Marotta, G. B., and Pena, S. D. (1999) Analysis of the gene expression profile of *Schistosoma mansoni* cercariae using the expressed sequence tag approach. *Molecular and Biochemical Parasitology*, **103**(1), 79-97.

Saule, P., Vicogne, J., Delacre, M., Macia, L., Tailleux, A., Dissous, C., and Wolowczuk, I. (2005) Host glucose metabolism mediates T4 and IL-7 action on Schistosoma mansoni development. *Journal of Parasitology*, **91**(4), 737-744.

Saunders, N., Wilson, R. A., and Coulson, P. S. (1987) The outer bilayer of the adult schistosome tegument surface has a low turnover rate in vitro and in vivo. *Molecular and Biochemical Parasitology*, **25**(2), 123-131.

Sayed, A. A., Cook, S. K., Williams, D. L. (2006) Redox balance mechanisms in *Schistosoma mansoni* rely on peroxiredoxins and albumin and implicate peroxiredoxins as novel drug targets. *Journal of Biological Chemistry*, **281**, 17001–17010.

Schak, K. M., and Harrington, M. E. (1999) Protein kinase C inhibition and activation phase advances the hamster circadian clock. *Brain Research*, **840**(1), 158-161.

Schistosoma japonicum Genome Sequencing and Functional Analysis Consortium. (2009). *Nature*, **460**, 345-351.

Schüßler, P., Greveldin, C. G. and Kunz, W. (1997) Identification of Ras, MAP kinases and GAP protein in *Schistosoma mansoni* by immunobloting and their putative involvement in male-female interaction. *Journal of Parasitology*, **115**, 629–634.

Schussler, P., Grevelding, C. G., Kunz, W. (1997) Identification of Ras, MAP kinases, and a GAP protein in *Schistosoma mansoni* by immunoblotting and their putative involvement in male-female interaction. *Parasitology* **115**, 629-634.

Sealey, K.L., Kirk, R.S., Walker, A.J., Rollinson, D. and Lawton, S.P. (2013) Adaptive radiation within the vaccine target tetraspanin-23 across nine *Schistosoma* species from Africa. *International Journal for Parasitology*, **43**(1), 95-103.

Seger, R., and Krebs, E. G. (1995) The MAPK signaling cascade. *The FASEB Journal*, **9**(9), 726-735.

Senft, A. W. and Maddison, S. E. (1975) Hypersensitivity to parasite proteolytic enzyme in schistosomiasis. *American Journal of Tropical Medicine and Hygiene*, **24**, (1), 83–89.

Serova, M., Ghoul, A., Benhadji, K.A., Cvitkovic, E., Faivre, S., Calvo, F., Lokiec, F. and Raymond, E. (2006) Preclinical and clinical development of novel agents that target the protein kinase C family. *Seminars in Oncology*, **33**, 466–478.

Shao, X., Davletov, B. A., Sutton, R. B., Südhof, T. C., and Rizo, J. (1996) Bipartite Ca2+-binding motif in C2 domains of synaptotagmin and protein kinase C. *Science*, **273**(5272), 248-251.

Shapley, R. J., and Enroth-Cugell, C. (1984) Visual adaptation and retinal gain controls. *Progress in Retinal and Eye Research*, **3**, 263-346

Sharkey, N. A., and Blumberg, P. M. (1985) Kinetic evidence that 1, 2-diolein inhibits phorbol ester binding to protein kinase C via a competitive mechanism. *Biochemical and Biophysical Research Communications*, **133**(3), 1051-1056.

Shaw, J. R. (1977) *Schistosoma mansoni*: Pairing *in vitro* and development of females from single sex infections. *Experimental Parasitology*, **41**(1), 54-65.

Shaw, J. R., & Erasmus, D. A. (1981) *Schistosoma mansoni*: an examination of the reproductive status of females from single sex infections. *Parasitology*, **82**(1), 121-124.

Shaw, M. K. (1987) *Schistosoma mansoni*: vitelline gland development in females from single sex infections. *Journal of Helminthology*, **61**(3), 253-259.

Shaw, M. K., and Erasmus, D. A. (1983) *Schistosoma mansoni:* dose-related tegumental surface changes after in vivo treatment with praziquantel. *Zeitschrift für Parasitenkunde*, **69**(5), 643-653.

Sher, A., Hall, B. F. and Vadas, M. A. (1978) Acquisition of murine major histocompatibility complex gene products by schistosomula of *Schistosoma mansoni*. *Journal of Experimental Medicine*, **148**, 46-57.

Shibayama, M., Serrano-Luna, J. D. J., Rojas-Hernández, S., Campos-Rodríguez, R., and Tsutsumi, V. (2003) Interaction of secretory immunoglobulin A antibodies with *Naegleria fowleri* trophozoites and collagen type I. *Canadian Journal of Microbiology*, **49**(3), 164-170.

Shiff, C. J., and Graczyk, T. K. (1994) A chemokinetic response in *Schistosoma mansoni* cercariae. *Journal of Parasitology*, **80**, 879-883

Shiff, C. J., Cmelik, S. H. W., Ley, H. E., and Kriel, R. L. (1972) The influence of human skin lipids on the cercarial penetration responses of *Schistosoma haematobium* and *Schistosoma mansoni*. *The Journal of Parasitology*, 476-480.

Shoemaker, C., Gross, A., Gebremichael, A., and Harn, D. (1992) cDNA cloning and functional expression of the *Schistosoma mansoni* protective antigen triose-phosphate isomerase. *Proceedings of the National Academy of Sciences*, **89**(5), 1842-1846.

Short, R. B., & Cartrett, M. L. (1973) Argentophilic" papillae" of *Schistosoma mansoni* cercariae. *The Journal of Parasitology*, **59**(6), 1041-1059.

Short, R. B., and Gagné, H. T. (1975) Fine structure of a possible photoreceptor in cercariae of Schistosoma *mansoni*. *The Journal of Parasitology*, **61**(1), 69-74.

Siddiqui, A.A., Podesta, R.B. and Clarke, M.W. (1991) *Schistosoma mansoni:* characterization and identification of calcium-binding proteins associated with the apical plasma membrane and envelope. *Experimental Parasitology*, **72**, (1), 63-68.

Sieburth, D., Madison, J. M., and Kaplan, J. M. (2006) PKC-1 regulates secretion of neuropeptides. *Nature Neuroscience*, **10**(1), 49-57.

Simmer, F., Moorman, C., van der Linden, A. M., Kuijk, E., van den Berghe, P. V., Kamath, R. S., and Plasterk, R. H. (2003) Genome-wide RNAi of *C. elegans* using the hypersensitive rrf-3 strain reveals novel gene functions. *PLoS Biology*, **1**(1), e12.

Simpson, A.J., Payares, G., Walker, T., Knight, M. and Smithers, S.R. (1984) The modulation of expression of polypeptide surface antigens on developing schistosomula of *Schistosoma mansoni*. *Journal of Immunology*, **133**, 2725–2730.

Skelly, P. J., and Alan Wilson, R. (2006) Making sense of the schistosome surface. *Advances in Parasitology*, **63**, 185-284.

Skelly, P. J., Da'dara, A., and Harn, D. A. (2003) Suppression of cathepsin B expression in *Schistosoma mansoni* by RNA interference. *International Journal for Parasitology*, **33**(4), 363-369.

Smithers, S. R., Terry, R. J., and Hockley, D. J. (1969) Host antigens in schistosomiasis. *Proceedings of the Royal Society of London. Series B. Biological Sciences*, **171**(1025), 483-494.

Smyth, J. D., and Halton, D. W. (1983) The physiology of trematodes. *Cambridge University Press, Cambridge*, **446**, 234-260.

Sohn U. D., Zoukhri, D., Dartt, D., Sergheraert, C., Harnett, K. M., Behar, J., and Biancani, P. (1997) Different protein kinase C isozymes mediate lower esophageal sphincter tone and phasic contraction of esophageal circular smooth muscle. *Molecular Pharmacology*, **51**,462–470

Sossin, W.S., Diaz-Arrastia, R., and Schwartz. J. H. (1993) Characterization of two isoforms of protein kinase C in the nervous system of *Aplysia californica*. *Journal Biological Chemistry*, *268*, 5763-5768.

Spiliotis, M., Konrad, C., Gelmedin, V., Tappe, D., Brückner, S., Mösch, U. and Brehm, A. (2006) Characterisation of EmMPK1, an ERK-like MAP kinase from *Echinococcus multilocularis* which is activated in response to human epidermal growth factor. *International Journal for Parasitology*, **36**, 1097-1112.

Spiliotis, M., Lechner, S., Tappe, D., Scheller, C., Krohne, G., and Brehm, K. (2008) Transient transfection of *Echinococcus multilocularis* primary cells and complete *in vitro* regeneration of meta-cestode vesicles. *International Journal for Parasitology*, **38**(8), 1025-1039.

Sponholtz, G.M and Short, R.B. (1976) *Schistosoma mansoni* miracidia: stimulation by calcium and magnesium. *Journal of Parasitology*, **62**(1), 155-157.

Sprague, G.F. (1998) Control of MAP kinase signalling specificity or how to not to go HOG wild. *Genes & Development*, **12**, 2817-2820.

Stefanic, S., Dvořák, J., Horn, M., Braschi, S., Sojka, D., Ruelas, D. S., and Caffrey, C. R. (2010) RNA interference in Schistosoma mansoni schistosomula: selectivity, sensitivity and operation for larger-scale screening. *PLoS Neglected Tropical Diseases*, **4**(10), e850.

Steinmann, P., Keiser, J., Bos, R., Tanner, M. and Utzinger, J. (2006) Schistosomiasis and water resources development: systematic review, meta-analysis, and estimates of people at risk. *Lancet Infect Diseases*, **6**, 411-425.

Sternberg, J. M., and Mcguigan, F. (1994) *Trypanosoma brucei*: Mammalian Epidermal Growth Factor Promotes the Growth of the African Trypanosome Bloodstream Form. *Experimental Parasitology*, **78**(4), 422-424.

Stirewalt, M. (1978) Quantitative collection and proteolytic activity of preacetabular gland enzyme (s) of cercariae of *Schistosoma mansoni*. *The American Journal of Tropical Medicine and Hygiene*, **27**(3), 548-553.

Stirewalt, M. A. (1973) *Schistosoma mansoni*: cercaria to schistosomule. *Advances in Parasitology*, **12**, 115-182.

Stirewalt, M. A., and Dorsey, C. H. (1974) *Schistosoma mansoni*: Cercarial penetration of host epidermis at the ultrastructural level. *Experimental Parasitology*, **35**(1), 1-15.

Stirewalt, M. A., and Walters, M. (1973) *Schistosoma mansoni*: Histochemical analysis of the postacetabular gland secretion of cercariae. *Experimental Parasitology*, **33**(1), 56-72.

Stricker, S. A., and Smythe, T. L. (2006) Differing mechanisms of cAMP-versus seawater-induced oocyte maturation in marine nemertean worms. The roles of serine/threonine kinases and phosphatases. *Molecular Reproduction and Development*, **73**(12), 1578-1590.

Sugano, T., Yanagita, T., Yokoo, H., Satoh, S., Kobayashi, H., and Wada, A. (2006) Enhancement of insulin-induced PI3K/Akt/GSK-3β and ERK signaling by neuronal nicotinic receptor/PKC-α/ERK pathway: up-regulation of IRS-1/-2 mRNA and protein in adrenal chromaffin cells. *Journal of Neurochemistry*, **98**(1), 20-33.

Sugden, P. H., and Clerk, A. (1998) Cellular mechanisms of cardiac hypertrophy. *Journal of Molecular Medicine*, **76**(11), 725-746.

Sukhdeo, M.V.K and Sukhdeo, S. C. (2004) Trematode behaviours and the perceptual worlds of parasites. *Canadian Journal of Zoology*, **82**, (2), 292-315.

Swierczewski, B. E., & Davies, S. J. (2009) A schistosome cAMP-dependent protein kinase catalytic subunit is essential for parasite viability. *PLoS neglected tropical diseases*, **3**(8), e505.

Tabuse, Y. (2002) Protein kinase C isotypes in *C. elegans*. *Journal of Biochemistry*, **132**(4), 519-522.

Takai, Y., Kishimoto, A., Iwasa, Y., Kawahara, Y., Mori, T. and Nishizuka, Y. (1979) Calcium-dependent activation of a multifunctional protein kinase by membrane phospholipids. *Journal of Biological Chemistry* **254**, (10), 3692-3695.

Tallima, H. and El Ridi, R. (2007) Praziquantel binds *Schistosoma mansoni* adult worm actin. *International Journal of Antimicrobiological Agents*, **29**, 570-575.

Tanoue, T., Adachi, M., Moriguchi, T., and Nishida, E. (2000) A conserved docking motif in MAP kinases common to substrates, activators and regulators. *Nature Cell Biology*, **2**(2), 110-116.

Tavernarakis, N., Wang, S. L., Dorovkov, M., Ryazanov, A., and Driscoll, M. (2000) Heritable and inducible genetic interference by double-stranded RNA encoded by transgenes. *Nature Genetics*, **24**(2), 180-183.

Tchuem Tchuenté, L. A., Southgate, V. R., Combes, C., and Jourdane, J. (1996) Mating behaviour in schistosomes: Are paired worms always faithful? *Parasitology Today*, **12**(6), 231-236.

Tchuem Tchuenté, L. T., Southgate, V. R., Imbert-Establet, D., and Jourdane, J. (1995) Change of mate and mating competition between males of *Schistosoma intercalatum* and *S. mansoni*. *Parasitology*, **110**, 45-52.

Teis, D., Wunderlich, W., & Huber, L. A. (2002) Localization of the MP1-MAPK scaffold complex to endosomes is mediated by p14 and required for signal transduction. *Developmental Cell*, **3**(6), 803-814.

Thornhill, J., Coelho, P.M., McVeigh, P., Maule, A., Jurberg, A.D. and Kusel, J.R. (2009) *Schistosoma mansoni* cercariae experience influx of macromolecules during skin penetration. *Parasitology*, **136**(11), 1257-67

Thornhill, J., Kusel, J., Oliviera, F.A., Ribeiro, F., Lima, S.F., Coelho, P.M., McVeigh, P. and Mattos, A.C. (2010) Uptake of macromolecules by cercariae during skin penetration and transformation to schistosomula (*Schistosoma mansoni*). *Memórias do Instituto Oswaldo Cruz*, **105**(4), 387-90.

Truscott, M., Evans, D. A., Gunn, M., and Hoffmann, K. F. (2013) *Schistosoma mansoni* Hemozoin Modulates Alternative Activation of Macrophages via Specific Suppression of Retnla Expression and Secretion. *Infection and Immunity*, **81**(1), 133-142.

Ullu, E., Tschudi, C., and Chakraborty, T. (2004) RNA interference in protozoan parasites. *Cellular Microbiology*, **6**(6), 509-519.

Valverde, A. M., Sinnett-Smith, J., Van Lint, J., and Rozengurt, E. (1994) Molecular cloning and characterization of protein kinase D: a target for diacylglycerol and phorbol esters with a distinctive catalytic domain. *Proceedings of the National Academy of Sciences*, **91**(18), 8572-8576.

van Balkom, B.W., van Gestel, R.A., Brouwers, J.F., Krijgsveld, J., and Tielens, A.G. (2005) Mass spectrometric analysis of the *Schistosoma mansoni* tegumental subproteome. *Journal of Proteome Research*, **4**, 958–966.

Verjovski-Almeida, S., DeMarco, R., and Martins E. A. L. (2003) Transcriptome analysis of the acoelomate human parasite *Schistosoma mansoni*, *Nature Genetics*, **35**(2), 148–157.

Verjovski-Almeida, S., DeMarco, R., Martins, E. A., Guimarães, P. E., Ojopi, E. P., Paquola, A. C., and Dias-Neto, E. (2003) Transcriptome analysis of the acoelomate human parasite *Schistosoma mansoni*. *Nature Genetics*, **35**(2), 148-157.

Vermeire, J.J., Osman, A., LoVerde, P.T. and Williams, D.L. (2003) Characterization of a Rho homologue of *Schistosoma mansoni*. *International Journal for Parasitology*, **33**, 721-731.

Vicogne, J., Cailliau, K., Tulasne, D., Browaeys, E., Yan, Y.T. Fafeur, V., Vilain, J.P., Legrand, D., Trolet, J., and Dissous, C. (2004) Conservation of epidermal growth factor receptor function in the human parasitic helminth *Schistosoma mansoni*. *Journal of Biological Chemistry*, **279** (36), 37407-37414.

Vicogne, J., Pin, J.P., Lardans, V., Capron, M., Noel, C. and Dissous, C. (2003) An unusual receptor tyrosine kinase of *Schistosoma mansoni* contains a Venus Flytrap module. *Molecular and Biochemical Parasitology*, **126**, 51-62.

Villareal, G., Li, Q., Cai, D., Fink, A. E., Lim, T., Bougie, J. K., and Glanzman, D. L. (2009) Role of protein kinase C in the induction and maintenance of serotonin-dependent enhancement of the glutamate response in isolated siphon motor neurons of *Aplysia californica*. *The Journal of Neuroscience*, **29**(16), 5100-5107.

Wada, T., and Penninger, J. M. (2004) Mitogen-activated protein kinases in apoptosis regulation. *Oncogene*, **23**(16), 2838-2849.

Walker, A. J. (2011) Insights into the functional biology of schistosomes. *Parasites and Vectors*, **4**, 203.

Walker, A. J. and Rollinson, D. (2008) Specific tyrosine phosphorylation induced in *Schistosoma mansoni* miracidia by haemolymph from schistosome susceptible, but not resistant, *Biomphalaria glabrata*. *Parasitology*, **135**, 337–345.

Walker, A. J. (2006) Do trematode parasites disrupt defence-cell signalling in their snail hosts? *Trends in Parasitology*, **22**(4), 154-159.

Wang, L., Yang, Z., Li, Y., Yu, F., Brindley, P.J., McManus, D.P., Wei, D., Han, Z. Feng, Z., Li, Y. and Hu, W. (2006) Reconstruction and in silico analysis of the MAPK signaling pathways in the human blood fluke, *Schistosoma japonicum*, *FEBS Letters*, **580**, 3677–3686.

Wang, T. P., Shrivastava, J., Johansen, M. V., Zhang, S. Q. and Wang, F. F. (2006) Does multiple hosts mean multiple parasites? Population genetic structure of *Schistosoma japonicum* between definitive host species. *International Journal for Parasitology*, **36**, 1317–1325.

Way, K. J., Chou, E., and King, G. L. (2000) Identification of PKC-isoform-specific biological actions using pharmacological approaches. *Trends in Pharmacological Sciences*, **21**(5), 181-187.

Whitfield, P.J., Bartlett, A., Brown, B. M. and Marriott, C. (2003) Invasion by schistosome cercariae: studies with human skin explants, *Trends in Parasitology*. **19**, 339–340.

Whitmarsh, A. J. (2010) A central role for p38 MAPK in the early transcriptional response to stress. *BMC Biology*, **8**(1), 47.

Wickner R. B. (1988) Host function of *MAK16*: G_1 arrest by a *mak16* mutant of *S. cerevisiae*. *Proceedings of the National Academy of Science*, **85**: 6007–6011.

Widmann, C., Gibson, S., Jarpe, M.B. and Johnson, G.L. (1999) Mitogen-Activated Protein Kinase: Conservation of a three-Kinase Module From Yeast to Human. *Physiology Reviews*. **79** (1), 143-180.

Wiest, P. M., Tartakoff, A. M., Aikawa, M., and Mahmoud, A. A. (1988) Inhibition of surface membrane maturation in schistosomula of *Schistosoma mansoni*. *Proceedings of the National Academy of Sciences*, **85**(11), 3825-3829.

Wiest, P.M., Burnham, D.C., Olds, R. and Bowen, W.D. (1992) Developmental expression of protein kinase C activity in *Schistosoma mansoni*. *American Journal Tropical Medicine Hygiene*. **46**, 358-365.

Wiest, P.M., Kunz, S.S. and Miller, K.R. (1994) Activation of protein kinase C by phorbol esters disrupts the tegument of *Schistosoma mansoni*. *Parasitology*, **109**, 461–468.

Wood. C., Thornton, M., Sabio, G., Davis, R.A., Rincon, M. (2009) Nuclear localization of p38 MAPK in response to DNA damage. *International Journal of Biological Sciences*, **5**,428-437.

Worden, M. K. (1998) Modulation of vertebrate and invertebrate neuromuscular junctions. *Current Opinion in Neurobiology*, **8**(6), 740-745.

World Health Organisation (WHO; 2005). Report on schistosomiasis.

World Health Organisation (WHO; 2007) Model list of essential medicines.

World Health Organisation (WHO; 2009) Strategy of schistosomiasis control.

Xu, Y. Z., & Dresden, M. H. (1986) Leucine aminopeptidase and hatching of Schistosoma mansoni eggs. *The Journal of Parasitology*, 507-511.

Xue, C., Hsueh, Y., Heitman, J. (2008) Magnificent seven: roles of G protein-coupled receptors in extracellular sensing in fungi. *FEMS Microbiology Reviews*, **32**, 1010–1032.

Yan, Y., Tulasne, D., Browaeys, E., Cailliau, K., Khayath, N., Pierce, R. J., Trolet, J., Fafeur, V., Younes, A., and Dissous, C. (2007) Molecular cloning and characterisation of SmSLK, a novel Ste20-like kinase in *Schistosoma mansoni*. *International Journal for Parasitology*, **37**(14), 1539-1550.

Yang, S. H., Sharrocks, A. D., and Whitmarsh, A. J. (2003) Transcriptional regulation by the MAP kinase signaling cascades. *Gene*, **320**, 3-21.

Yang, S. H., Whitmarsh, A. J., Davis, R. J., and Sharrocks, A. D. (1998) Differential targeting of MAP kinases to the ETS-domain transcription factor Elk-1. *The EMBO Journal*, **17**(6), 1740-1749.

Yarfitz S and Hurley JB. (1994) Transduction Mechanisms of Vertebrate and Invertebrate Photoreceptors. *The Journal of Biological Chemistry Minireview*, **269**, 14329-14332.

You, H., Zhang, W., Jones, M.K., Gobert, G.N., Mulvenna, J., Rees, G., Spanevello, M., Blair, D., Duke, M., Brehm, K. and McManus, D.P. (2010) Cloning and characterisation of *Schistosoma japonicum* insulin receptors. *PloS One*, **5**(3), e9868.

You, H., Zhang, W., Moertel, L., McManus, D.P. and Gobert, G.N. (2009) Transcriptional profiles of adult male and female *Schistosoma japonicum* in response to insulin reveal increased expression of genes involved in growth and development. *International Journal for Parasitology*, **39**(14),1551-9.

You, Y., Kim, J., Cobb, M. and Avery, L. (2006) Starvation activated MAP kinase through the muscarinic acetylcholine pathway in *Caenorhabditis elegans* pharynx. *Cell Metabolism*, **3**, 237-245

Young, N.D., Jex, A.R., Li, B., Liu, S., Yang, L., Xiong, Z. and Gasser, R.B. (2012) Whole-genome sequence of *Schistosoma haematobium*. *Nature Genetics*, **44**(2), 221-225.

Zahoor, Z., Davies, A. J., Kirk, R. S., Rollinson, D., and Walker, A. J. (2009) Nitric oxide production by Biomphalaria glabrata haemocytes: effects of Schistosoma mansoni ESPs and regulation through the extracellular signal-regulated kinase pathway. *Parasites and Vectors*, **2**(1), 18.

Zahoor, Z., Davies, A.J., Kirk, R.S., Rollinson, D. and Walker, A.J. (2008) Disruption of ERK signalling in *Biomphalaria glabrata* defence cells by *Schistosoma mansoni*: Implications for parasite survival in the snail host. *Developmental & Comparative Immunology*, **32**(12),1561–71.

Zhang, G., Kazanietz, M. G., Blumberg, P. M., & Hurley, J. H. (1995) Crystal structure of the Cys2 activator-binding domain of protein kinase Cδ in complex with phorbol ester. *Cell*, **81**(6), 917-924.

Zhang, K. Y., Card, G. L., Suzuki, Y., Artis, D. R., Fong, D., Gillette, S., and Bollag, G. (2004) A glutamine switch mechanism for nucleotide selectivity by phosphodiesterases. *Molecular Cell*, **15**(2), 279-286.

Zhou, Y., Zheng, H., Chen, Y., Zhang, L., Wang, K., Guo, J., and Yan, J. (2009) The *Schistosoma japonicum* genome reveals features of host–parasite interplay. *Nature*, **460**(7253), 345-351.

Appendix

Appendix A

Table 2.1 – Recipe for Basch's medium (adapted from Basch, 1981).

For 1 litre of Basch's Medium (store at 4^0C)	
50 ml	20X Lactalbumin hydrolysate/glucose: [2.5 g lactalbumin hydrolysate (Sigma, L9010), 2.5 g glucose (Sigma, G5400), 250 ml Basal Medium Eagle (Gibco, 21010046). Filter sterilize and store at 4°C]
0.5 ml	Hypoxanthine (1 mM) (-20°C) (Sigma, H9377)
1 ml	Serotonin (1 mM) (-20°C) (Sigma, H9523)
1 ml	Insulin (8mg/ml) (4°C) (Sigma, I0516)
1 ml	Hydrocortisone (1 mM) (-20°C) (Sigma, H0888)
1 ml	Triiodothyronine (0.2 mM) (-20°C) (Calbiochem, 64245)
5 ml	MEM Vitamins (100X) (-20°C) (Invitrogen, 11120-052)
50 ml	Schneiders Medium (Drosophila) (+4°C) (Invitrogen, 11720067)
10 ml	Hepes Buffer (+4°C)
100 ml	Human Serum (thaw at 37°C prior to use) (Gemini, 100-512)
20 ml	Antibiotic/Antimycotic (Invitrogen, 15240-062)
760.5ml	Basal Medium Eagle (Gibco, 21010046)

Appendix B

Table 4.1- Effects on egg output, pairing status and ventral sucker attachment observed in *S. mansoni* adult worms after exposure to GF109203X, PMA and U0126.

Physiological effects	Duration time (hours)	Treatments: RPMI	DMSO 0.5%	GF109203X 1µM	GF109203X 5µM	GF109203X 20µM	GF109203X 50µM	PMA 1µM	UO126 1µM	UO126 5µM	UO126 20µM	UO126 50µM
Detached V. S ± SEM (%)	1	-	-	3 ± 0.03	10 ± 0.05 *	94 ± 0.04 ***	97 ± 0.09 ***	22 ± 0.29 *	-	-	5 ± 0.05	100 ***
	24	-	-	27 ± 0.12 **	32 ± 0.07 ***	100 ***	100 ***	76 ± 0.17 ***	3 ± 0.03	3 ± 0.03	14 ± 0.05 *	98 ± 0.11 ***
	48	5 ± 0.08	4 ± 0.06	29 ± 0.12 **	53 ± 0.05 ***	100 ***	100 ***	81 ± 0.19 ***	4 ± 0.04	8 ± 0.05 *	34 ± 0.10 **	99 ± 0.08 ***
	72	7 ± 0.08	2 ± 0.04	33 ± 0.12***	90 ± 0.05 ***	100 ***	100 ***	82 ± 0.19 ***	8 ± 0.05 *	8 ± 0.05 *	42 ± 0.11 **	100 ***
	96	7 ± 0.10	2 ± 0.04	44 ± 0.12 ***	95 ± 0.04 ***	100 ***	100 ***	98 ± 0.05 ***	8 ± 0.05 *	50 ± 0.13 **	47 ± 0.11 **	100 ***
Paired ± SEM (%)	1	100	100	100	100	100	62 ± 0.14 **	45 ± 0.05 ***	100	100	100	4 ± 0.04 ***
	24	100	100	94 ± 0.04*	90 ± 0.04 **	26 ± 0.11 ***	-	1 ± 0.12 ***	100	96 ± 0.03	90 ± 0.05 **	-
	48	100	100	82 ± 0.16 ***	79 ± 0.09 ***	20 ± 0.07 ***	-	-	100	85 ± 0.05	77 ± 0.09 ***	-
	72	100	100	82± 0.16 ***	79 ± 0.09 ***	3 ± 0.09 ***	-	-	100	81 ± 0.05	77 ± 0.11 ***	-
	96	100	100	82 ± 0.16 ***	72 ± 0.13 ***	3 ± 0.09 ***	-	-	96 ± 0.04	74 ± 0.13	64 ± 0.09 ***	-
Eggs per pair ± SEM (n^{o})	24	106 ± 1.60	108 ± 1.33	73 ± 4.38 ***	6 ± 1.21 ***	1 ± 0.49 ***	1 ± 0.38 ***	7 ± 1.02 ***	82 ± 3.1 ***	82 ± 4.21***	74 ± 1.30 ***	7 ± 5.3 ***
	48	110± 5.81	119 ± 3.29	70 ± 4.42 ***	9 ± 2.05 ***	1 ± 0.33 ***	0 ± 0.34 ***	-	113 ± 1.88	133 ± 8.31	140 ± 4.13 *	-
	72	103 ± 2.94	111 ± 2.34	62 ± 6.38 ***	11 ± 2.63 ***	-	-	-	113 ± 2.29	104 ± 2.25	118 ± 0.97	-
	96	93± 2.19	109 ± 4.52	68 ± 4.57 ***	9 ± 2.60 ***	-	-	-	82 ± 3.41 *	84 ± 5.81 *	111 ± 5.48	-

Appendix B

Table 4.2 - Effects on sustained coiling observed in *S. mansoni* adult worms after exposure to Gf109203X, PMA and U0126.

Physiological effects		Treatments																																	
		RPMI			DMSO			GF109203X												PMA			UO126													
Coiling effect (%)					0.5%			1μM			5μM			20μM			50μM			1μM			1μM			5μM			20μM			50μM		
Duration treatment	Coil number	p	♂	♀	p	♂	♀	p	♂	♀	p	♂	♀	p	♂	♀	p	♂	♀	p	♂	♀	p	♂	♀	p	♂	♀	p	♂	♀	p	♂	♀
1 hours	0	97 ± 0.03	-	-	100	-	-	91 ± 0.06	-	-	52*** ± 0.10	-	-	26** ± 0.10	-	-	30** ± 0.09	-	-	67** ± 0.06	88 ± 0.06	60 ± 0.05	100	-	-	97 ± 0.03	-	-	100	-	-	43 ± 0.03	55 ± 0.04	92 ± 0.05
	1	3 ± 0.06	-	-	-	-	-	9 ± 0.06	-	-	23*** ± 0.08	-	-	15** ± 0.06	-	-	22*** ± 0.09	-	-	23** ± 0.06	12* ± 0.06	37 ± 0.04	-	-	-	3 ± 0.03	-	-	-	-	-	46 ± 0.05	39 ± 0.03	6 ± 0.05
	2	-	-	-	-	-	-	-	-	-	14** ± 0.06	-	-	35*** ± 0.10	-	-	19*** ± 0.09	-	-	10** ± 0.03	-	-	-	-	-	-	-	-	-	-	-	11 ± 0.04	16 ± 0.07	-
	≥ 3	-	-	-	-	-	-	-	-	-	1 ± 0.06	-	-	24*** ± 0.08	-	-	29*** ± 0.10	-	-	-	-	4 ± 0.3	-	-	-	-	-	-	-	-	-	-	-	-
24 hours	0	97 ± 0.03	-	-	82 ± 0.08	-	-	84 ± 0.07	-	-	76** ± 0.06	-	-	89 ± 0.01	36 ± 0.01	36 ± 0.01	-	83 ± 0.01	71 ± 0.02	-	58 ± 0.05	54 ± 0.08	96 ± 0.03	-	-	77* ± 0.07	100	98 ± 0.01	100	100	100	-	33 ± 0.04	100
	1	3 ± 0.08	-	-	9** ± 0.04	-	-	15* ± 0.07	-	-	19** ± 0.06	-	-	4 ± 0.02	1 ± 0.03	2 ± 0.02	-	11 ± 0.05	5 ± 0.07	-	30 ± 0.3	11 ± 0.05	4 ± 0.09	-	-	23 ± 0.07	-	1 ± 0.01	-	-	-	-	54 ± 0.04	-
	2	-	-	-	3 ± 0.02	-	-	1* ± 0.01	-	-	2 ± 0.02	-	-	6 ± 0.05	-	6 ± 0.06	-	7 ± 0.04	18 ± 0.03	-	12 ± 0.3	26 ± 0.05	-	-	-	-	-	1 ± 0.01	-	-	-	-	15 ± 0.03	-
	≥ 3	-	-	-	-	-	-	-	-	-	3 ± 0.02	-	-	1 ± 0.01	-	0.1 ± 0.01	-	-	6 ± 0.03	-	-	9 ± 0.03	-	-	-	-	-	-	-	-	-	-	-	-
48 hours	0	95 ± 0.04	-	-	78 ± 0.11	-	-	72 ± 0.10	-	-	76* ± 0.07	-	-	63** ± 0.05	98 ± 0.02	70 ± 0.3	-	66 ± 0.05	72 ± 0.06	-	58 ± 0.08	52 ± 0.3	100	-	-	84 ± 0.05	100	96 ± 0.01	74 ± 0.09	96 ± 0.05	92 ± 0.04	-	100	98 ± 0.02
	1	5 ± 0.10	-	-	20** ± 0.13	-	-	10* ± 0.09	-	-	14** ± 0.05	-	-	13** ± 0.05	-	10 ± 0.04	-	30 ± 0.04	24 ± 0.03	-	29 ± 0.05	52 ± 0.3	-	-	-	16 ± 0.05	-	2 ± 0.02	16 ± 0.16	4 ± 0.04	8 ± 0.03	-	-	2 ± 0.02
	2	-	-	-	2 ± 0.02	-	-	18** ± 0.07	-	-	8* ± 0.04	-	-	16** ± 0.04	-	13 ± 0.03	-	4 ± 0.01	2 ± 0.01	-	10 ± 0.05	52 ± 0.3	-	-	-	-	-	2 ± 0.02	-	-	-	-	-	-
	≥ 3	1 ± 0.08	-	-	-	-	-	-	-	-	2 ± 0.02	-	-	9* ± 0.03	2 ± 0.02	7 ± 0.02	-	-	2 ± 0.01	-	3 ± 0.02	52 ± 0.3	-	-	-	-	-	-	-	-	-	-	-	-
72 hours	0	87 ± 0.05	-	-	72 ± 0.09	-	-	86 ± 0.12	-	-	55** ± 0.11	-	-	70** ± 0.04	81 ± 0.04	89 ± 0.02	-	59 ± 0.05	52 ± 0.05	-	81 ± 0.05	100	96 ± 0.05	-	-	96 ± 0.05	100	96 ± 0.05	87 ± 0.15	92 ± 0.13	90 ± 0.04	-	100	93 ± 0.05
	1	13 ± 0.05	-	-	20 ± 0.14	-	-	14 ± 0.08	-	-	27* ± 0.10	-	-	17 ± 0.06	17 ± 0.06	-	-	28 ± 0.03	24 ± 0.04	-	18 ± 0.05	-	4 ± 0.09	-	-	4 ± 0.05	-	4 ± 0.05	10 ± 0.24	4 ± 0.13	10 ± 0.04	-	-	8 ± 0.05
	2	-	-	-	8 ± 0.07	-	-	-	-	-	18** ± 0.10	-	-	11* ± 0.04	2 ± 0.04	9 ± 0.04	-	6 ± 0.3	8 ± 0.3	-	1 ± 0.01	-	-	-	-	-	-	-	3 ± 0.07	-	-	-	-	-
	≥ 3	-	-	-	-	-	-	-	-	-	-	-	-	2 ± 0.02	-	2 ± 0.02	-	-	2 ± 0.3	-	-	-	-	-	-	-	-	-	-	-	-	-	-	-
96 hours	0	90 ± 0.04	-	-	77* ± 0.09	-	-	71 ± 0.08	-	-	43 *** ± 0.08	-	-	86 ± 0.06	95 ± 0.3	91 ± 0.03	-	63 ± 0.3	66 ± 0.3	-	66 ± 0.3	100	88 ± 0.06	-	-	100	100	99 ± 0.02	70 ± 0.35	100	100	-	67 ± 0.06	90 ± 0.05
	1	10 ± 0.07	-	-	23** ± 0.18	-	-	26 ± 0.07	-	-	36*** ± 0.07	-	-	7 ± 0.06	4 ± 0.02	3 ± 0.02	-	16 ± 0.3	10 ± 0.3	-	26 ± 0.3	-	12 ± 0.14	-	-	-	-	1 ± 0.02	23 ± 0.13	-	-	-	34 ± 0.06	10 ± 0.05

Appendix B

Table 4.3- Effects on movement observed in *S. mansoni* adult worms after exposure to Gf109203X, PMA and U0126

Physiological effects	Treatments																														
	RPMI			DMSO			GF109203X												PMA			UO126										
speed (mm/sec)				0.5%			1μM			5μM			20μM			50μM			1μM			1μM			5μM			20μM			50μM		
Duration treatment	p	♂	♀	p	♂	♀	p	♂	♀	p	♂	♀	p	♂	♀	p	♂	♀	p	♂	♀	p	♂	♀	p	♂	♀	p	♂	♀	p	♂	♀
1 hours	3.26 ± 0.33	-	-	3.54 ± 0.25	-	-	3.95 ± 0.83	-	-	6.76 *** ± 0.76	-	-	2.85* ± 0.26	1.87 ± 0.49	1.36 ± 0.79	1.85* ± 0.23	0.22 ** ± 0.05	2.14 ** ± 0.48	1.82 ** ± 0.68	2.05 ± 0.45	1.51 ± 0.37	9.37 *** ± 0.16	-	-	7.62 *** ± 0.46	-	-	8.87 *** ± 0.65	-	-	10.7 *** ± 1.27	9.74 ± 1.76	8.55 ± 0.20
24 hours	3.47 ± 0.36	-	-	2.84 ± 0.29	-	-	4.48 ± 0.86	-	-	3.94 ± 0.68	-	-	-	0.57 *** ± 0.09	1.28 *** ± 0.12	-	0.72 ± 0.20	0.86 ± 0.20	0.63 ** ± 0.1	1.31 ± 0.5	0.16 ± 0.35	7.60 *** ± 0.72	-	-	8.89 *** ± 0.90	-	-	5.96 ** ± 0.99	-	-	-	4.54 ± 0.98	4.01 ± 0.47
48 hours	3.58 ± .0.36	-	-	3.53 ± 0.29	-	-	4.78 ± 0.71	-	-	4.17 ± 0.38	1.80* ± 0.26	0.38* ± 0.15	-	0.67 ** ± 0.08	1.22 ** ± 0.14	-	0.44 ± 0.13	0.27 ± 0.13	-	3.42 * ± 0.3	2.01 * ± 0.39	5.46 ± 0.52	-	-	5.09 * ± 0.78	-	-	4.82 * ± 0.65	-	-	-	5.81 ** ± 0.34	1.86 ** ± 0.48
72 hours	3.69 ± 0.41	-	-	3.77 ± 0.25	-	-	6.20 *** ± 0.69	-	-	2.97 ± 0.22	1.60 ± 0.28	0.78 ± 0.28	-	0.06 *** ± 0.04	0.52 *** ± 0.10	-	0.38 ± 0.16	0.45 ± 0.16	-	5.98 ** ± 1.11	2.32 ** ± 1.1	5.65 ** ± 0.42	-	-	3.9 ± 0.40	-	-	4.97 ± 0.61	-	-	-	4.26 *** ± 0.57	0.50 *** ± 0.17
96 hours	3.98 ± 0.56	-	-	3.49 ± 0.21	-	-	4.73 * ± 0.77	6.48* ± 1.87	1.26* ± 0.41	3.47 ± 0.3	2.60* ± 0.47	0.97* ± 0.33	-	0.06 *** ± 0.02	0.3* ** ± 0.04	-	0.09 ± 0.11	0.17 ± 0.05	-	5.30 * ± 1.12	1.05 * ± 0.3	4.89 * ± 0.30	-	-	3.17 * ± 1.08	-	-	5.85 * ± 0.84	6.28 *** ± 0.78	0.71 *** ± 0.13	-	3.81 *** ± 0.81	1.11 *** ± 0.26

Appendix C

Screen shot of the "wrMTrck" plug-in parameters used for video analysis of *S. mansoni* schistosomules

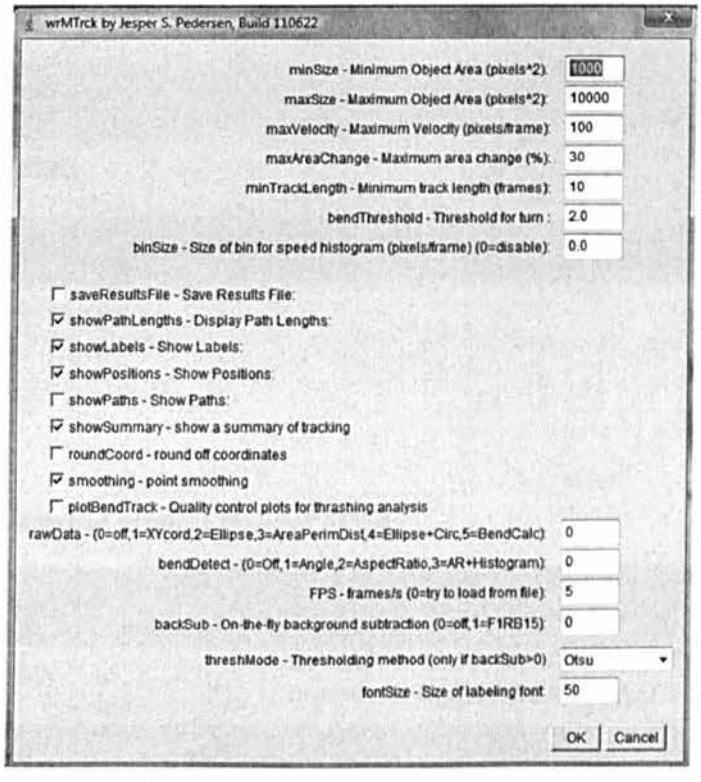

Table 8.1 – Sequences of siRNAs

Non-target negative control	sense	5' –CUUCUUCUGUUCUCUUGUGAdTdT–3'
	antisense	5' -UCACAAGAGAACAGAAGAAGdTdT–3'
Smp_128480 (PKC)	sense	5' -CCGCCAUUCAAACCUCGUAdTdT–3'
	antisense	5' –UACGAGGUUUGAAUGGCGGdTdT–3'
Smp_096310 (PKC)	sense	5' -GAACACGACCCUAUCGUUAdTdT–3'
	antisense	5' -UAACGAUAGGGUCGUGUUCdTdT–3'
Smp_131700 (PKC)	sense	5' -AUACAACGUGCACGACGAUdTdT–3'
	antisense	5' -AUACAACGUGCACGACGAUdTdT–3'
Smp_176360 (PKC)	sense	5' -GGAUCGUGAAUUACAUAGAdTdT–3'
	antisense	5' -UCUAUGUAAUUCACGAUCCdTdT–3'
Smp_142050 (ERK)	sense	5' -CCUUAAAGCUCGUGCCUAdTdT–3'
	antisense	5' -UAGGCACGAGCUUUAAGGdTdT–3'
Smp_047900 (ERK)	sense	5' -CACCGUUGAAGAAGCCUUAdTdT–3'
	antisense	5' -UAAGGCUUCUUCAACGGUGdTdT–3'
Smp_176360 (Moraes Mourão *et al.*)	sense	5' -CGCAAACCACCAUUUCUUGdTdT–3'
	antisense	5' -CAAGAAAUGGUGGUUUGCGdTdT–3'

Table 8.2– Sequences of primers used for qPCR

Smp_128480 (PKC)	forward	5'-GATACTGGGCCCGATACAGA–3'
	reverse	5'-GGTCCATTCCACAAAGTCGT–3'
Smp_096310 (PKC)	forward	5'-TAATGGGGTTCCAAGTGAGC–3'
	reverse	5'-GTCTGGCAGCAAACTGATGA–3'
Smp_131700 (PKC)	forward	5'-ATTCATGTTCCGTCCACTCC–3'
	reverse	5'-GAATGAGAACGGGTTGGAGA–3'
Smp_176360 (PKC)	forward	5'-CTTGGCGCTTACTTTCCAC–3'
	reverse	5'-TTCCGGTGAGGTTTTCAAAG–3'
Smp_142050 (ERK)	forward	5'-GTTGAATGCAGCGTGTGACT–3'
	reverse	5'-TTTCTGGTGCACGATACCAA–3'
Smp_047900 (ERK)	forward	5'-AGGAGCGTATGGAATGGTTG–3'
	reverse	5'-CATGGGAAAATCCAAGGAGA–3'
Alpha-tubulin	forward	5'-CAAATGGGAAATGCTTGTTG–3'
	reverse	5'-TGAACGAGTCATCACCACCT–3'
GAPDH	forward	5'-TCGTTGAGTCTACTGGAGTCTTTACG–3'
	reverse	5'-AATATGAGCCTGAGCTTTATCAATGG-3'
Smp_176360 (Moraes Mourão *et al.*)	forward	5'-CTTGGATGTGGTTCAGATGG–3'
	reverse	5'-TCACGTGGTGATAAAGTAACTGG–3'